Title
Natural IgM Secreting Cells of the Mouse

Author
Smith, Fauna Leah

Publication Date
2022

Peer reviewed|Thesis/dissertation

Natural IgM Secreting Cells of the Mouse

By

FAUNA LEAH SMITH
DISSERTATION

Submitted in partial satisfaction of the requirements for the degree of

DOCTOR OF PHILOSOPHY

in

Integrative Pathobiology

in the

OFFICE OF GRADUATE STUDIES

of the

UNIVERSITY OF CALIFORNIA

DAVIS

Approved:

Nicole Baumgarth, Chair

Renèe Tsolis

Marcelo Kuroda

Committee in Charge

2022

ABSTRACT

B-1 cells are unique, fetal-origin, self-reactive, innate like B lymphocytes that give rise to a heterogeneous population of cells, including IgM secreting cells. IgM secretion by B-1 cells occurs both, at steady state, mostly in bone marrow (BM) and spleen in the absence of microbial stimuli, and as an early response to inflammation or infection, usually in the draining lymphoid tissues. In my dissertation, I aimed to further characterize the subpopulations of IgM secreting B-1 derived cells and the mechanisms that drive their differentiation into three types of antibody secreting cells: Blimp-1 dependent B-1 plasma cells (PC), Blimp-1 independent non-terminally differentiated B-1 cells ($B\text{-}1_{sec)}$ and inflammation/infection induced B-1 plasma blasts and plasma cells.

In Chapter 1, I review the role of B-1 cells and nIgM in the control of and response to infections. This includes outlining our current understanding of B-1 cell development and maintenance, as well as the events that regulate the activation of B-1 cells to become antibody secreting cells. I explore as yet unanswered questions about the role of innate versus antigen-specific signaling in the ability of B-1 cells to engage in tissue homeostasis and immune defense through their secretion of IgM.

In Chapter 2, I examine the developmental requirements and nIgM repertoire contributions of B-1PC. In particular, the data demonstrate that BM B-1PC development requires the presence of αβCD4 T cells, bucking the dogma that nIgM is always T independent. Additionally, I demonstrate that B-1PC generate a distinct, oligoclonal nIgM repertoire that has relatively little overlap with non-secreting B-1 cells. This B-1PC repertoire was dominated by short 7-8 amino

acids. It was encoded by various CDR3 variable immunoglobulin heavy chain genes that nonetheless generated a small number of distinct CDR3 motives, highly suggestive of convergent recombination and thus positive selection. Additionally, the data showed that in the absence of BM B-1PC a population of B-1_{sec} emerged that compensated for the loss B-1PC derived serum nIgM. This population was phenotypically less differentiated than B-1PC and was unable to be reconstituted from adult peritoneal B-1 cells.

In Chapter 3, I aimed to identify the B-1_{sec} by flow cytometry and further characterize their function and transcriptional profile. B-1_{sec} were identified as CD19+ CD23- $CD43^{var}$ intracytoplasmic IgM^{hi} and CD138+. Using a double-reporter mouse to identify the immunoglobulin joining (J)-chain and Blimp-1, the master transcriptional regulator of plasma cell differentiation, B-1_{sec} were further identified as J-chain+ Blimp-1^{neg}. Despite the lack of Blimp-1 expression, I demonstrated that these cells secrete significant amounts of IgM and have a transcriptional profile of an antibody secreting cell.

In Chapter 4, I examine the role of toll like receptor (TLR) and B cell receptor (BCR) signaling on both, steady state nIgM production and infection-induced secretion of IgM by B-1 cells. I found that both were reduced, when B-1 cells lack TLR expression. I further demonstrate that B-1 cells do not use the same level of BCR and TLR signaling coordination to enhance their activation and differentiation as we see in B-2 cells. Instead, B-1 cells were exquisitely sensitive to TLR stimulation, but BCR signaling inhibited TLR-stimulated B-1 cell responses in contrast, while synergistic effects were noted in B-2 cells. Furthermore, when BCR signaling was blocked with a Syk inhibitor, the effects on TLR signaling were much more pronounced in B-2 than B-1

cells, suggesting that B-1 cells respond through a TLR pathway that is uncoupled from the MyD88-Syk axis previously shown to be present in B-2 cells.

Together my work adds to the understanding of how B-1 cells contribute to IgM production, and thus increase understanding of their integral role in early defense against pathogens and their role in connecting the innate and adaptive branches of the immune system.

PERSONAL ACKOWLEGMENT:

There are many people that I would like to thank for their contributions to my PhD work, but in particular the following people:

Zheng "Jean" Luo has been instrumental in helping complete the benchtop science that is presented here and in helping me develop my laboratory skills. Her patience and expertise drove the development and execution of the intracytoplasmic IgM staining protocol, optimization of cell culture conditions, and she diligently ensures that flow cytometry antibodies are made and tested for the lab.

Tracey Rourke has spent hours and hours with me sorting minuscule populations of finicky antibody secreting cells, even coming in out-of-hours or staying late to make sure that I could get my experiments done.

Hannah Savage, my predecessor on this project, whose meticulous notes and experimental records made my life much easier, a standard I likely will not live up to.

Kim Olsen for being the master manager of mice and always being willing to lend a hand when needed.

My lab mates for sharing the highs and lows of science; laughing and crying over lab and life.

My husband, Tamati Vanderbyl, for his encouragement, support, and patience with this endeavor, and agreeing to move 10,000K for me to chase my dreams.

Lastly, Nicole Baumgarth for being the most amazing mentor. I can never thank her enough for the time, energy, and effort that she put into training me as a graduate student. She is without a doubt one of the fiercest advocates for graduate students and graduate education that I know. Her dedication to her profession, to doing excellent science and to training good scientists are traits I hope to emulate in my future endeavors.

SCIENTIFIC ACKNOWLEDGMENT:

The science presented here represents a body of work that was contributed to a number of other scientists from across the globe and I would like to acknowledge their help and input:

Dr Stefan Keller, University of California, Davis for his expertise and input on the analysis of B-1PC repertoire.

Dr Ingvill Jensen, Norwegian College of Fishery Science, for spending her sabbatical working on the B-1 PC story with us in sunny California.

Dr Chris Tipton and Dr Eun-Hyung Lee, Emory University, for their assistance in running the BCR repertoire analysis.

Dr Anna Beaudin and her graduate students, April Apostol and Diego Lopez, University of Utah, for their help with the innate lymphocyte lineage tracing model.

Dr Blythe Durbin-Johnson, University of California, Davis, for her data processing and analysis of our RNAseq projects.

Dr Deepta Batthacharya, University of Arizona, for providing us with the J Chain reporter mice.

The following Fellowships that provide financial support for my PhD:

Herbert Kraft Fellowship - University of California, Davis

T32 OD011147 Training Grant – National Institute of Health

Graduate Student Support Program Stipend Award – University of California, Davis School of Veterinary Medicine

Simm Fellowship - University of California, Davis

UCD Research Fellowship - University of California, Davis

Table of Contents

Chapter 1:

Role of Natural IgM and B-1 cells in immune responses to infection

Fauna L Smith

***** This Chapter is published as:** Smith, F.L., and N. Baumgarth. 2019. **B-1 cell responses to infections.** *Curr. Opin. Immunol.* 57:23–31. doi:10.1016/j.coi.2018.12.001. ***

Abstract

B-1 cells represent an innate-like early-developing B cell population, whose existence as an independent lymphocyte subset has been questioned in the past. Recent molecular and lineage tracing studies have not only confirmed their unique origins and differentiation paths, they have also provided a rationale for their distinctive functionalities compared to conventional B cells. This review summarizes our current understanding of B-1 cell development, and the activation events that regulate B-1 cell responses to self and foreign antigens. We discuss the unresolved question to what extent BCR engagement, i.e. antigen-specificity versus innate signaling contribute to B-1 cell's participation in tissue homeostasis and immune defense as providers of "natural" and antigen-induced antibody responses, and as cytokine-producing immune regulators.

1.1 Introduction

The discovery of CD5+ (or Ly-1+) B-1 cells in mice in the early 1980's was followed by scientific inquiry that initially focused on the B-1 cell's developmental origins, their phenotypic resemblance to human CLL, and remarkable ability to continuously generate broadly self-reactive IgM antibodies in the steady-state, even in mice held under germfree conditions. We now understand B-1 cells to be mainly of fetal origin, selected during development for their ability to recognize self-antigens, and prevented from causing autoimmune disease through the expression of CD5, identified as an inhibitory component of the BCR complex. More recent studies have begun to reveal a protective and immune-regulatory role for B-1 cells in immune defense against pathogens. Because understanding the development of B-1 cells is critical for understanding the regulation of their functions, this review will first provide a brief summary of B-1 cell development, and then describes our current understanding of B-1 cell's contributions to immunity against infectious agents. As we discuss below, a challenge for the field remains gaining a more complete understanding of the mechanisms by which these self-reactive B-1 cells are regulated to contribute to immune host defense without causing autoimmune disease.

1.2 B-1 cell development and maintenance

Adoptive cell transfer studies initially showed that B-1 cells develop early in ontogeny, including prenatally from precursors residing in the embryonic splanchnopleura and in the fetal liver, as well as shortly after birth in bone marrow and spleen (reviewed in (Kantor & Herzenberg, 1993)). A series of recent studies have revealed the molecular basis for the ontogenically-restricted development of B-1 cells. A first critical step was the identification of distinct B cell precursors in fetal liver and bone marrow that developed into either only B-1 or B-2 cells

(Montecino-Rodriguez et al., 2006). Then, comparing gene expression by these distinct precursors, Lin 28b was identified as the master regulator of the genetic program that controls fetal but not adult hematopoiesis, including the development of B-1 cells(Yuan et al., 2012; Zhou et al., 2015). These studies are significant, as they identified B-1 cells independent of any phenotypic markers as distinct, fetal-derived lymphocyte populations that develop in multiple waves throughout early ontogeny (Montecino-Rodriguez & Dorshkind, 2012). Follow-up studies, consistent with the earlier adoptive transfer studies, confirmed that *de novo* B-1 cell development from the defined B-1 cell precursors cedes a few weeks after birth due to precursor-intrinsic changes (Barber et al., 2011) that correlate with the loss of Lin 28b expression (Yuan et al., 2012; Zhou et al., 2015). Studies with lethally-irradiated mice suggest that bone marrow B-1 precursors may be reactivated to a limited extend during lymphopenia and/or severe stress (Düber et al., 2009; Holodick et al., 2009).

For maturation into the peripheral B cell pools, B-1 cells require a positive selection step. Thwarting one of the major dogmas of immunology, central tolerance induction, which predicts the removal of all strongly self-reactive B cells, Hayakawa and colleagues demonstrated the presence of the self-antigen Thy-1 to be required for the development and/or expansion of Thy-1 specific B-1 cells (Hayakawa et al., 1999, 2003). The data not only explain the emergence of a B cell population that is self-reactive, they also explain why numerous genetic manipulations that alter the BCR-complex, or its downstream signaling cascade, usually also affect B-1 cell development (reviewed in(Kreslavsky et al., 2018)).

Self-reactive B cells must be regulated to avoid inappropriate activation. For B-1 cells this is likely achieved through the expression of CD5, a surface-expressed molecule, found mostly on T cells, that helped to first identify B-1 cells as distinct from conventional B cells(Hayakawa et al., 1983). CD5 is part of the antigen-receptor complex and acts as an inhibitor of both, TCR and BCR signaling. The level of CD5 expression by T cells correlated with the strength of TCR-signaling during positive selection of thymocytes(Azzam et al., 1998). On B cells, CD5 expression was identified not only on B-1 cells but also on anergic conventional B cells (Hippen et al., 2000). Consistent with a prominent inhibitory role for CD5 in BCR-stimulation, B-1 cells cannot proliferate in response to anti-IgM stimulation, unless taken from CD5-deficient mice, or otherwise lacking CD5 expression (Bikah et al., 1996). Thus, the induction of CD5 following positive selection of the B-1 cells appears to ensure suppression of responsiveness to BCR-mediated signals, i.e. responsiveness to self-antigens. Any regulation of CD5 surface expression therefore would be expected to greatly affect B-1 cell responsiveness.

Once *de novo* development of B-1 cells cedes, B-1 cell pools are maintained predominantly through self-renewal (reviewed in(Baumgarth, 2011)), a process that is largely unexplored. Given the dramatic and ongoing shifts in the BCR-repertoire of B-1 cells during the first 6 months of life, even in germfree mice (Yang et al., 2015), it is likely that interaction of the BCR with self-antigen contribute to this process. This is supported by findings that B-1 cells specific for phosphotidylcholine (PtC), encoding specificity for dead and dying cells, strongly clonally expand over the first 6 months of life(Prohaska et al., 2018; Yang et al., 2015). Thus, although CD5+ B-1 cell appear unresponsive to BCR-mediated stimulation, certain triggers must exist that can overcome their response block.

1.3 Tissue distribution and natural antibody production by B-1 cells

In steady state the highest frequencies, albeit not absolute numbers, of B-1 cells are found in the pleural and peritoneal cavities. Their presence at those sites is regulated by the local production of CXCL13 by macrophages(Ansel et al., 2002; Watanabe et al., 2000). Other tissues, including secondary and tertiary lymphoid tissue sites such as spleen, bone marrow, lymph node, pericardium, and mucosal associated lymphoid tissue, contain B-1 cell frequencies that are mostly below 1% (Choi et al., 2012; Choi & Baumgarth, 2008; Hayakawa et al., 1985; Jackson-Jones et al., 2016; Kawahara et al., 2003; Kroese et al., 1989; Yang et al., 2007).

In the body cavities, B-1 cells are identified easily as $CD19^{hi}$, $B220^{lo}$, $CD11b^{pos}$, $CD23^{neg}$, $CD43^{+}$ and either $CD5^{+}$ or $CD5^{lo/-}$(Wells et al., 1994). In response to insults, such as infections, body cavity B-1 cells are rapidly activated to migrate to lymph tissues where they differentiate to cytokine and antibody-secreting cells. Those cells rapidly lose CD11b expression (Waffarn et al., 2015), making them difficult to differentiate from activated B-2 cells at those sites. Most natural IgM production, however, occurs in bone marrow and spleen. These sites contain two types of spontaneous IgM-secreting B-1 cells: cells of similar phenotype than found in the body cavities, albeit lacking CD11b expression, and B-1-derived, Blimp-1+ CD138+ and mostly CD5- plasma cells (Savage et al., 2017). Natural IgM is produced at similar amounts in mice held under SPF and germ- and antigen-free conditions(Hooijkaas et al., 1985; Savage et al., 2017), but is altered in mice with changes to BCR-signaling and lack of Blimp-1 expression (Nguyen et al., 2017; Savage et al., 2017; Savitsky & Calame, 2006). Whether the repertoire of natural IgM antibodies is shaped by microbiota or other non-microbial antigens such as components of food, however, has not been studied systematically. Natural serum IgM levels are higher in female compared to

male mice, and recent studies suggested estrogen underlying this difference (Zeng et al., 2018). Thus, existing data indicate a role for self-antigen and sex-hormone-mediated B-1 cell activation and differentiation in the regulation of protective IgM.

The presence of B-1 cell-derived, constitutively-produced, self-reactive natural IgM serves as an important "first line of defense", providing immune protection against a wide variety of pathogens, and reducing the risk of sepsis (**Table 1**(Alugupalli et al., 2003; Baumgarth, Herman, et al., 2000; Briles et al., 1982; O'Brien et al., 1979; Ochsenbein et al., 1999; Zeng et al., 2018)). Knockout mice lacking the ability to secrete IgM (sIgM-/- mice) showed increased mortality following cecal ligation and puncture induced peritonitis, intranasal infection with influenza virus (Baumgarth, Herman, et al., 2000) and infection with the fungal pathogen *Cryptococcus neoformans*(Subramaniam et al., 2010). Conversely, reconstitution of mice deficient in CD5+ B-1 cells or sIgM production by B-1 cells were rescued from *Salmonella* LPS-induced endotoxemia and influenza infection via passive transfer of serum IgM from non-immune mice (Baumgarth, Chen, et al., 2000; Reid et al., 1997). Thus, while B-1 cells are selected for the binding to self-antigens, the antibodies produced by these cells appear to broadly bind to many pathogens. This suggests that natural IgM, similar to TLR and other innate receptors, binds conserved structures (reviewed in(Baumgarth et al., 2005)). The mechanisms of immune protection from natural IgM seem to be linked, at least in part, to their exquisite ability to activate the classical complement cascade. This was highlighted recently in two studies, one involving the role of IgM in protection from enteropathogenic E. coli(Zeng et al., 2018), the other demonstrating a role for complement-mediated lysis in inhibiting tumor-growth (Haro et al., 2019).

B-1 cells also provide class-switched antibodies, specifically IgA and IgG3(Kroese et al., 1989; Savage et al., 2017). Unlike production of natural IgM, however, mucosal IgA production by B-1 cells is dependent on host microbiota, to which these antibodies can bind (Koch et al., 2016; Zeng et al., 2018). Thus, in the strictest sense these antibodies are not "natural" antibodies, as they rely on foreign antigen for their production. Yet, what they have in common with natural IgM is their critical role in maintaining homeostasis between the host and its environment. For example, IgA acts primarily on mucosal surfaces to provide steady-state immune control of microbiota while avoiding tissue damage, as it cannot bind to and activate complement. Natural antibodies also seem to shape the development of a functional immune system in offspring following their passive transfer from the mother (Koch et al., 2016; Zeng et al., 2018). The mechanisms regulating the production of class-switched B-1 cell-derived antibodies, generally found to be induced independent of T cells, remain to be identified. However, recent studies suggest that they require TLR-mediated signals (Kreuk et al., 2019), raising questions about the relationship between B-1 cell activation and the antigen-specificity of their responses.

1.4 B-1 cell responses to infections

In addition to the provision of steady-state levels natural IgM, B-1 cells also actively respond with induced IgM production to infections to a variety of pathogens, including bacteria, viruses, fungi, and parasites (**Table 1**). For example, introduction of intestinal bacteria, or LPS, into the peritoneal cavity resulted in MyD88-dependent changes in surface expression of integrins, including CD9, and the subsequent migration of B-1 cells from the body cavity and their accumulation in omentum, mesenteric lymphoid tissues and spleen (Ha et al., 2006). Nematode infection of the pleural cavity resulted in the accumulation of B-1 cells in local mediastinal fat-

associated lymphoid tissues(Jackson-Jones et al., 2016), and following influenza infection, pleural cavity B-1 cells accumulated in the draining mediastinal lymph nodes (Waffarn et al., 2015).

The mechanisms controlling B-1 cell activation during infections are incompletely resolved. Existing data suggest that distinct innate signals control a stepwise B-1 cell activation process: i) egress from body cavities, ii) accumulation in lymphoid tissue and iii) differentiation to antibody secreting cells (**Fig. 1.1**). Egress may be regulated via chemokine/chemokine receptor expression, as LPS injection-induced egress of B-1 cells from the peritoneal cavity correlated with an up-regulation of CXCR4 and increased responsiveness of B-1 cells to CXCL12 (Moon et al., 2012). Accumulation of CD5+ B-1 cells in the draining lymph nodes after influenza infection was shown to be facilitated by, and depend on, the Type I IFN-induced conformational changes of CD11b on B-1 cells to a high-affinity state (Waffarn et al., 2015). Yet, the observed enhanced migration of CD5+ B-1 cells from the pleural cavity following influenza infection was independent of either Type I IFN or CD11b (Waffarn et al., 2015).

Once B-1 cells accumulate in regional lymph tissues, B-1 cell differentiation may be regulated at least in part by cytokine production. Recently this was shown for nematode infection, were the differentiation to IgM-producing cells depended on the local production of IL-5 (Jackson-Jones et al., 2016), consistent with other studies (McKay et al., 2017; Nisitani et al., 1995). Identifying the critical innate regulators of B-1 cell activation during infection is of importance, as it could help with their recruitment to vaccine responses.

1.5 Antigen-specific B-1 cell responses to infections

While chemokines and other innate signals are clearly critical for the regulation of B-1 cell responses, the question arises whether B-1 cells, most expressing CD5, can respond also in a BCR-mediated, antigen-specific manner. Emerging *in vivo* data provide some evidence of antigen-induced proliferation and possibly clonal expansion in response to encounter with foreign antigens. For example, using labeled antigen and identifying *Francisella tularensis* LPS-specific B-1 cells by their ability to bind such antigen, it was shown that administration of the non-mitogenic LPS resulted in increased frequencies of LPS-binding B-1 cells in spleen and peritoneal cavity (Cole et al., 2009). Neonatal, but not adult, intranasal exposure to cockroach allergens induced the local production of anti-alpha 1,3 glucan IgA antibodies that protected from induction of allergic reactions following challenge(Patel et al., 2016). That latter study is significant, as it provides support for the concept that the neonatal B-1 cell repertoire is not fixed, but is modulated significantly by subsequent microbial stimulation. It is currently unresolved, however, why the window for changing allergy resistance appears so short (reportedly to be about 9 days in the neonates used), while sequencing approaches suggested repertoire shaping of CD5+ B-1 cells to occur for at least 6 months after birth(Patel et al., 2016; Prohaska et al., 2018; Yang et al., 2015). Further support for antigen-specific responses by B-1 cells comes from reports of antigen-specific memory B-1 cell induction to various pathogens (Alugupalli et al., 2004; Haas et al., 2005). These memory B-1 cells were identified in the body cavities some time following antigen exposure by their enhanced ability to provide recall responses **(Fig. 1.1)** (Alugupalli et al., 2004; Yang et al., 2012).

The occurrence of antigen-specific B-1 cell responses is puzzling, given the *in vitro* data that have shown a clear inability of CD5+ B-1 cells to respond to BCR-mediated stimulation.

One potential explanation, suggested a number of years ago, is that only B-1 cells that lack expression of the inhibitor CD5 (so-called B-1b), can respond to antigenic stimulation (Alugupalli & Gerstein, 2005; Haas et al., 2005). However, only 25 – 30 % of body cavity B-1 cells express low/no CD5. Furthermore, studies with *F. tularensis* LPS identified CD5+ B-1 cells as responders (Cole et al., 2009; Yang et al., 2012), as did studies on influenza(Choi & Baumgarth, 2008). Interestingly, it was shown that the activation of *F. tularensis* specific memory B-1 cells into IgM-secreting cells required both antigen and TLR-mediated stimulation (Yang et al., 2012), consistent with studies on anti-microbial B-1 cell responses, which were shown also to require TLR signaling (Koch et al., 2016). Thus, innate signaling may act as co-stimulator to enhance or enables antigen-specific B-1 cell responses. Our ongoing work supports such conclusions. We recently showed that stimulation with TLR-agonists, but not with anti-IgM, led to the loss of CD5 and the reorganization of the BCR-complex on CD5+ B-1 cells, thus potentially "licensing" B-1 cells for responses to antigen (Savage et al., 2019) Furthermore, using proximal ligation assays we found that BCR-complex organization before and after stimulation differed significantly from that of B-2 cells. This is consistent with previous reports on differences between BCR stimulation by B-1 and B-2, most recently a study that analyzed the distinct roles of the Src-family kinase regulator CD148 in antigen-specific BCR signaling (Skrzypczynska et al., 2016) (**Fig. 1.2**).

1.6 B-1 cells are important for effective innate and adaptive responses to pathogens

Given the role of B-1 cell-derived natural IgM and IgA as first lines of defense, it seems surprising that following their activation body cavity B-1 cells migrate to lymphoid tissues, rather than to mucosal surfaces, where they could strengthen the immune barrier. The data

suggest that B-1 cells may have additional regulatory functions that go beyond simply providing pathogen-reactive antibodies.

Indeed, activated B-1 cells have been shown recently to secrete not only protective natural IgM during sepsis that can help the early control of bacterial dissemination, but also cytokines such as IL-3 and GM-CSF, which seem to play opposing roles in the control of inflammatory responses (Boes, Prodeus, et al., 1998; Rauch et al., 2012; Reid et al., 1997; Weber et al., 2015) and IL-10, which can control the extent of inflammation (Aziz et al., 2017; Leech et al., 2017). Little information exists about the interactions of B-1 cells with other cell types and the regulatory circuits that induce cytokine production by B-1 cells. However, for IL-10 production by B-1 cells, both in vitro and during sepsis in vivo, the induction of IL-10 required direct TLR4-mediated signaling (Aziz et al., 2017), while in a *Staphylococcus aureus* peritonitis model, B-1 cell-derived protective IL-10 was dependent on TLR-2 (Leech et al., 2017). Thus, B-1 cells represent one of a growing number of innate-like lymphocytes that respond to and in turn control the inflammatory process by generating cytokines.

B-1 cells do however, also generate increased amounts of IgM in secondary lymphoid tissues. This locally- secreted IgM was shown not to alter natural IgM titers in the serum following influenza infection (Baumgarth et al., 1999), indicating that IgM acts locally in the lymph nodes. IgM could act in multiple distinct ways. Due to its large size, the secreted IgM may be prevented from leaving the lymph tissue environment, thereby strengthening the barrier by containing pathogens in the draining lymph nodes, inhibiting their dissemination. Furthermore, earlier studies with mice lacking the ability to secrete IgM due to deletion of the μ_s splice region (Baumgarth, Herman, et al., 2000; Boes, Esau, et al., 1998; Ehrenstein et al., 1998; Gonzalez et al., 2008) showed that memory B cell as well as antigen-specific IgG responses

required IgM secretion for their optimal induction. A recent study expanded these findings by demonstrating that the lack of the IgM Fc-receptor (FcμR) on B cells resulted in similar reductions in IgG responses, and reduced numbers of antigen-specific B cells in the draining lymph nodes, as seen also in mice lacking secreted IgM. Thus, existing data suggest that B-1 cells migration to local lymph tissue can support maximal conventional B cell responses by secreting IgM(Nguyen et al., 2017). While the mechanism by which IgM-FcμR interactions enhance IgG responses remains to be identified, the data raise the interesting possibility that natural and polyreactive IgM facilitates the rapid uptake of antigen to B cells for antigen-processing and presentation, or may bring antigens in close contact with the BCR on the surface of the cell.

1.7 Conclusions

Recent studies have clarified the distinct molecular mechanism regulating the development of B-1 cells, supporting early conclusion about the distinct fetal/neonatal origin of B-1 cells that are selected to express a largely self-reactive BCR repertoire and then silenced to this antigen via expression of CD5. In-depths sequencing approaches, however, have revealed a much stronger shaping of the B-1 cell repertoire independent of microbial interactions over the first few months of life than previously anticipated. Thus, suggesting that B-1 cells remain responsive to BCR-stimulation *in vivo*, despite their inability to respond with proliferation to BCR-mediated stimulation *in vitro*. In addition, increasingly B-1 cells are shown to engage in antigen-driven responses to infections, but the mechanisms of their activation remain obscure. Existing data point to the stepwise activation of body cavity B-1 cells via various innate signals that result in their migration from the cavities to lymph tissues, where they can differentiate into antibody and

cytokine-producing cells. To what extent and how BCR-mediated antigen-specific responses regulate these cells remain a future target of investigation.

1.8 References

Alugupalli, K. R., & Gerstein, R. M. (2005). Divide and conquer: division of labor by B-1 B cells. *Immunity*, *23*(1), 1–2. https://doi.org/10.1016/J.IMMUNI.2005.07.001

Alugupalli, K. R., Gerstein, R. M., Chen, J., Szomolanyi-Tsuda, E., Woodland, R. T., & Leong, J. M. (2003). The resolution of relapsing fever borreliosis requires IgM and is concurrent with expansion of B1b lymphocytes. *Journal of Immunology (Baltimore, Md. : 1950)*, *170*(7), 3819–3827. https://doi.org/10.4049/JIMMUNOL.170.7.3819

Alugupalli, K. R., Leong, J. M., Woodland, R. T., Muramatsu, M., Honjo, T., & Gerstein, R. M. (2004). B1b lymphocytes confer T cell-independent long-lasting immunity. *Immunity*, *21*(3), 379–390. https://doi.org/10.1016/j.immuni.2004.06.019

Ansel, K. M., Harris, R. B. S., & Cyster, J. G. (2002). CXCL13 is required for B1 cell homing, natural antibody production, and body cavity immunity. *Immunity*, *16*(1), 67–76. https://doi.org/10.1016/S1074-7613(01)00257-6

Arcanjo, A. F., Nico, D., de Castro, G. M. M., da Silva Fontes, Y., Saltarelli, P., Decote-Ricardo, D., Nunes, M. P., Ferreira-Pereira, A., Palatnik-de-Sousa, C. B., Freire-de-Lima, C. G., & Morrot, A. (2017). Dependency of B-1 Cells in the Maintenance of Splenic Interleukin-10 Producing Cells and Impairment of Macrophage Resistance in Visceral Leishmaniasis. *Frontiers in Microbiology*, *8*(JUN), 978. https://doi.org/10.3389/fmicb.2017.00978

Aziz, M., Holodick, N. E., Rothstein, T. L., & Wang, P. (2017). B-1a Cells Protect Mice from Sepsis: Critical Role of cAMP-response Element Binding Protein (CREB). *Journal of Immunology (Baltimore, Md. : 1950)*, *199*(2), 750. https://doi.org/10.4049/JIMMUNOL.1602056

Azzam, H. S., Grinberg, A., Lui, K., Shen, H., Shores, E. W., & Love, P. E. (1998). CD5 expression is developmentally regulated by T cell receptor (TCR) signals and TCR avidity. *The Journal of Experimental Medicine*, *188*(12), 2301–2311. https://doi.org/10.1084/JEM.188.12.2301

Barbeiro, D. F., Barbeiro, H. V., Faintuch, J., Ariga, S. K. K., Mariano, M., Popi, A. F., de Souza, H. P., Velasco, I. T., & Soriano, F. G. (2011). B-1 cells temper endotoxemic inflammatory responses. *Immunobiology*, *216*(3), 302–308. https://doi.org/10.1016/J.IMBIO.2010.08.002

Barber, C. L., Montecino-Rodriguez, E., & Dorshkind, K. (2011). Reduced production of B-1-specified common lymphoid progenitors results in diminished potential of adult marrow to generate B-1 cells. *Proceedings of the National Academy of Sciences of the United States of America*, *108*(33), 13700–13704. https://doi.org/10.1073/PNAS.1107172108/SUPPL_FILE/PNAS.201107172SI.PDF

Barbosa, C. H. D., Lantier, L., Reynolds, J., Wang, J., & Re, F. (2021). Critical role of IL-25-ILC2-IL-5 axis in the production of anti-Francisella LPS IgM by B1 B cells. *PLOS Pathogens*, *17*(8), e1009905. https://doi.org/10.1371/JOURNAL.PPAT.1009905

Barbour, A. G., & Bundoc, V. (2001). In vitro and in vivo neutralization of the relapsing fever agent Borrelia hermsii with serotype-specific immunoglobulin M antibodies. *Infection and Immunity*, *69*(2), 1009–1015. https://doi.org/10.1128/IAI.69.2.1009-1015.2001

Baumgarth, N. (2011). The double life of a B-1 cell: Self-reactivity selects for protective effector functions. *Nature Reviews Immunology*, *11*(1), 34–46. https://doi.org/10.1038/nri2901

Baumgarth, N., Chen, J., Herman, O. C., Jager, G. C., & Herzenberg, L. A. (2000). The role of B-1 and B-2 cells in immune protection from influenza virus infection. *Current Topics in Microbiology and Immunology*, *252*, 163–169. https://doi.org/10.1007/978-3-642-57284-5_17

Baumgarth, N., Herman, O. C., Jager, G. C., Brown, L. E., Herzenberg, L. A., & Chen, J. (2000). B-1 and B-2 cell-derived immunoglobulin M antibodies are nonredundant components of the protective response to influenza virus infection. *J Exp Med*, *192*(2), 271–280. https://doi.org/10.1084/jem.192.2.271

Baumgarth, N., Herman, O. C., Jager, G. C., Brown, L., Herzenberg, L. A., & Herzenberg, L. A. (1999). Innate and acquired humoral immunities to influenza virus are mediated by distinct arms of the immune system. *Proceedings of the National Academy of Sciences of the United States of America*, *96*(5), 2250–2255. https://doi.org/10.1073/pnas.96.5.2250

Baumgarth, N., Tung, J. W., & Herzenberg, L. A. (2005). Inherent specificities in natural antibodies: a key to immune defense against pathogen invasion. *Springer Seminars in Immunopathology*, *26*(4), 347–362. https://doi.org/10.1007/S00281-004-0182-2

Bikah, G., Carey, J., Ciallella, J. R., Tarakhovsky, A., & Bondada, S. (1996). CD5-Mediated Negative Regulation of Antigen Receptor-Induced Growth Signals in B-1 B Cells. *Science*, *274*(5294), 1906–1909. https://doi.org/10.1126/SCIENCE.274.5294.1906

Binder, C. J., Hörkkö, S., Dewan, A., Chang, M. K., Kieu, E. P., Goodyear, C. S., Shaw, P. X., Palinski, W., Witztum, J. L., & Silverman, G. J. (2003). Pneumococcal vaccination decreases atherosclerotic lesion formation: molecular mimicry between Streptococcus pneumoniae and oxidized LDL. *Nature Medicine*, *9*(6), 736–743. https://doi.org/10.1038/NM876

Boes, M., Esau, C., Fischer, M. B., Schmidt, T., Carroll, M., & Chen, J. (1998). Enhanced B-1 cell development, but impaired IgG antibody responses in mice deficient in secreted IgM. *Journal of Immunology (Baltimore, Md. : 1950)*, *160*(10), 4776–4787. http://www.ncbi.nlm.nih.gov/pubmed/9590224

Boes, M., Prodeus, A. P., Schmidt, T., Carroll, M. C., & Chen, J. (1998). A critical role of natural immunoglobulin M in immediate defense against systemic bacterial infection. *The Journal of Experimental Medicine*, *188*(12), 2381–2386. https://doi.org/10.1084/JEM.188.12.2381

Briles, D. E., Forman, C., Hudak, S., & Latham Claflin, J. (1982). Anti-phosphorylcholine antibodies of the T15 idiotype are optimally protective against Streptococcus pneumoniae. *The Journal of Experimental Medicine*, *156*(4), 1177–1185. https://doi.org/10.1084/JEM.156.4.1177

Briles, D. E., Nahm, M., Schroer, K., Davie, J., Baker, P., Kearney, J., & Barletta, R. (1981). Antiphosphocholine antibodies found in normal mouse serum are protective against intravenous infection with type 3 streptococcus pneumoniae. *J Exp Med*, *153*(3), 694–705. https://doi.org/10.1084/jem.153.3.694

Choi, Y. S., & Baumgarth, N. (2008). Dual role for B-1a cells in immunity to influenza virus infection. *The Journal of Experimental Medicine*, *205*(13), 3053–3064. https://doi.org/10.1084/JEM.20080979

Choi, Y. S., Dieter, J. A., Rothaeusler, K., Luo, Z., & Baumgarth, N. (2012). B-1 cells in the bone marrow are a significant source of natural IgM. *Eur J Immunol*, *42*(1), 120–129. https://doi.org/10.1002/eji.201141890

Cole, L. E., Yang, Y., Elkins, K. L., Fernandez, E. T., Qureshi, N., Shlomchik, M. J., Herzenberg, L. A., Herzenberg, L. A., & Vogel, S. N. (2009). Antigen-specific B-1a antibodies induced by Francisella tularensis LPS provide long-term protect i on aga i nst F. tularensis LVS challenge. *Proceedings of the National Academy of Sciences of the United States of America*, *106*(11), 4343–4348. https://doi.org/10.1073/PNAS.0813411106/SUPPL_FILE/0813411106SI.PDF

Colombo, M. J., Abraham, D., Shibuya, A., & Alugupalli, K. R. (2011). B1b lymphocyte-derived antibodies control Borrelia hermsii independent of Fcα/μ receptor and in the absence of host cell contact. *Immunologic Research*, *51*(2–3), 249–256. https://doi.org/10.1007/S12026-011-8260-8

Colombo, M. J., & Alugupalli, K. R. (2008). Complement Factor H-Binding Protein, a Putative Virulence Determinant of Borrelia hermsii , Is an Antigenic Target for Protective B1b Lymphocytes . *The Journal of Immunology*, *180*(7), 4858–4864. https://doi.org/10.4049/jimmunol.180.7.4858

Cotte, C., & Szczepanek, S. M. (2017). Peritoneal B-1b and B-2 B-cells confer long-term protection from pneumococcal serotype 3 infection after vaccination with Prevnar-13 and are defective in sickle cell disease mice. *Vaccine*, *35*(28), 3520–3522. https://doi.org/10.1016/j.vaccine.2017.05.039

Crane, D. D., Griffin, A. J., Wehrly, T. D., & Bosio, C. M. (2013). B1a cells enhance susceptibility to infection with virulent Francisella tularensis via modulation of NK/NKT cell responses. *Journal of Immunology (Baltimore, Md. : 1950)*, *190*(6), 2756–2766. https://doi.org/10.4049/JIMMUNOL.1202697

Düber, S., Hafner, M., Krey, M., Lienenklaus, S., Roy, B., Hobeika, E., Reth, M., Buch, T., Waisman, A., Kretschmer, K., & Weiss, S. (2009). Induction of B-cell development in adult mice reveals the ability of bone marrow to produce B-1a cells. *Blood*, *114*(24), 4960–4967. https://doi.org/10.1182/BLOOD-2009-04-218156

Ehrenstein, M. R., O'Keefe, T. L., Davies, S. L., & Neuberger, M. S. (1998). Targeted gene disruption reveals a role for natural secretory IgM in the maturation of the primary immune response. *Proceedings of the National Academy of Sciences of the United States of America*, *95*(17), 10089–10093. https://doi.org/10.1073/PNAS.95.17.10089

Gonzaga, W. F. K. M., Geraldo, M. M., Vivanco, B. C., Popi, A. F., Mariano, M., Batista, W. L., & Xander, P. (2017). Evaluation of Experimental Infection with L. (L.) Amazonensis in X-Linked Immunodeficient Mice. *The Journal of Parasitology*, *103*(6), 708–717. https://doi.org/10.1645/16-145

Gonzalez, S. F., Jayasekera, J. P., & Carroll, M. C. (2008). Complement and natural antibody are required in the long-term memory response to influenza virus. *Vaccine*, *26 Suppl 8*(SUPPL. 8). https://doi.org/10.1016/J.VACCINE.2008.11.057

Ha, S. A., Tsuji, M., Suzuki, K., Meek, B., Yasuda, N., Kaisho, T., & Fagarasan, S. (2006). Regulation of B1 cell migration by signals through Toll-like receptors. *Journal of Experimental Medicine*, *203*(11), 2541–2550. https://doi.org/10.1084/jem.20061041

Haas, K. M., Poe, J. C., Steeber, D. A., & Tedder, T. F. (2005). B-1a and B-1b Cells Exhibit Distinct Developmental Requirements and Have Unique Functional Roles in Innate and Adaptive Immunity to S. pneumoniae. *Immunity*, *23*(1), 7–18. https://doi.org/10.1016/J.IMMUNI.2005.04.011

Harada, Y., Muramatsu, M., Shibata, T., Honjo, T., & Kuroda, K. (2003). Unmutated immunoglobulin M can protect mice from death by influenza virus infection. *The Journal of Experimental Medicine*, *197*(12), 1779–1785. https://doi.org/10.1084/JEM.20021457

Haro, M. A., Dyevoich, A. M., Phipps, J. P., & Haas, K. M. (2019). Activation of B-1 cells promotes tumor cell killing in the peritoneal cavity. *Cancer Research*, *79*(1), 159. https://doi.org/10.1158/0008-5472.CAN-18-0981

Hayakawa, K., Asano, M., Shinton, S. A., Gui, M., Allman, D., Stewart, C. L., Silver, J., & Hardy, R. R. (1999). Positive selection of natural autoreactive B cells. *Science (New York, N.Y.)*, *285*(5424), 113–116. https://doi.org/10.1126/SCIENCE.285.5424.113

Hayakawa, K., Asano, M., Shinton, S. A., Gui, M., Wen, L. J., Dashoff, J., & Hardy, R. R. (2003). Positive selection of anti-thy-1 autoreactive B-1 cells and natural serum autoantibody production independent from bone marrow B cell development. *Journal of Experimental Medicine*, *197*(1), 87–99. https://doi.org/10.1084/jem.20021459

Hayakawa, K., Hardy, R. R., Herzenberg, L. A., & Herzenberg, L. A. (1985). Progenitors for Ly-1 b cells are distinct from progenitors for other b cells. *Journal of Experimental Medicine*, *161*(6), 1554–1568. https://doi.org/10.1084/jem.161.6.1554

Hayakawa, K., Hardy, R. R., Parks, D. R., & Herzenberg, L. A. (1983). The "LY-1 B" cell subpopulation in normal, immunodefective, and autoimmune mice. *Journal of Experimental Medicine*, *157*(1), 202–218. https://doi.org/10.1084/jem.157.1.202

Hippen, K. L., Tze, L. E., & Behrens, T. W. (2000). CD5 maintains tolerance in anergic B cells. *Journal of Experimental Medicine*, *191*(5), 883–889. https://doi.org/10.1084/jem.191.5.883

Holodick, N. E., Repetny, K., Zhong, X., & Rothstein, T. L. (2009). Adult BM generates CD5+ B1 cells containing abundant N-region additions. *European Journal of Immunology*, *39*(9), 2383. https://doi.org/10.1002/EJI.200838920

Hooijkaas, H., Bos, N., Benner, R., Pleasants, J. R., & Wostmann, B. S. (1985). Immunoglobulin Isotypes and Antibody Specificity Repertoire of "Spontaneously" Occurring ("Background") Immunoglobulin-Secreting Cells in Germfree Mice Fed Chemically Defined Ultrafiltered "Antigen-Free" Diet. *Advances in Experimental Medicine and Biology*, *186*, 131–138. https://doi.org/10.1007/978-1-4613-2463-8_16

Jackson-Jones, L. H., Duncan, S. M., Magalhaes, M. S., Campbell, S. M., Maizels, R. M., McSorley, H. J., Allen, J. E., & Bénézech, C. (2016). Fat-associated lymphoid clusters control local IgM secretion during pleural infection and lung inflammation. *Nature Communications 2016 7:1*, *7*(1), 1–14. https://doi.org/10.1038/ncomms12651

Jayasekera, J. P., Moseman, E. A., & Carroll, M. C. (2007). Natural Antibody and Complement Mediate Neutralization of Influenza Virus in the Absence of Prior Immunity. *Journal of Virology*, *81*(7), 3487–3494. https://doi.org/10.1128/jvi.02128-06

Kantor, A. B., & Herzenberg, L. A. (1993). Origin of murine B cell lineages. In *Annual Review of Immunology* (Vol. 11, pp. 501–538). Annu Rev Immunol. https://doi.org/10.1146/annurev.iy.11.040193.002441

Kawahara, T., Ohdan, H., Zhao, G., Yang, Y. G., & Sykes, M. (2003). Peritoneal cavity B cells are precursors of splenic IgM natural antibody-producing cells. *J Immunol*, *171*(10), 5406–5414. https://doi.org/10.4049/jimmunol.171.10.5406

Koch, M. A., Reiner, G. L., Lugo, K. A., Kreuk, L. S. M., Stanbery, A. G., Ansaldo, E., Seher, T. D., Ludington, W. B., & Barton, G. M. (2016). Maternal IgG and IgA Antibodies Dampen

Mucosal T Helper Cell Responses in Early Life. *Cell*, *165*(4), 827–841. https://doi.org/10.1016/J.CELL.2016.04.055

Kreslavsky, T., Wong, J. B., Fischer, M., Skok, J. A., & Busslinger, M. (2018). Control of B-1a cell development by instructive BCR signaling. *Current Opinion in Immunology*, *51*, 24–31. https://doi.org/10.1016/J.COI.2018.01.001

Kreuk, L. S. M., Koch, M. A., Slayden, L. C., Lind, N. A., Chu, S., Savage, H. P., Kantor, A. B., Baumgarth, N., & Barton, G. M. (2019). B cell receptor and toll-like receptor signaling coordinate to control distinct B-1 responses to both self and the microbiota. *ELife*, *8*. https://doi.org/10.7554/eLife.47015

Kroese, F. G. M., Butcher, E. C., Stall, A. M., Lalor, P. A., Adams, S., & Herzenberg, L. A. (1989). Many of the IgA producing plasma cells in murine gut are derived from self-replenishing precursors in the peritoneal cavity. *International Immunology*, *1*(1), 75–84. https://doi.org/10.1093/INTIMM/1.1.75

Leech, J. M., Lacey, K. A., Mulcahy, M. E., Medina, E., & McLoughlin, R. M. (2017). IL-10 Plays Opposing Roles during Staphylococcus aureus Systemic and Localized Infections. *Journal of Immunology (Baltimore, Md. : 1950)*, *198*(6), 2352–2365. https://doi.org/10.4049/JIMMUNOL.1601018

Martin, F., Oliver, A. M., & Kearney, J. F. (2001). Marginal zone and B1 B cells unite in the early response against T-independent blood-borne particulate antigens. *Immunity*, *14*(5), 617–629. https://doi.org/10.1016/S1074-7613(01)00129-7

McKay, J. T., Haro, M. A., Daly, C. A., Yammani, R. D., Pang, B., Swords, W. E., & Haas, K. M. (2017). PD-L2 Regulates B-1 Cell Antibody Production against Phosphorylcholine through an IL-5-Dependent Mechanism. *J Immunol*, *199*(6), 2020–2029. https://doi.org/10.4049/jimmunol.1700555

Mi, Q. S., Zhou, L., Schulze, D. H., Fischer, R. T., Lustig, A., Rezanka, L. J., Donovan, D. M., Longo, D. L., & Kenny, J. J. (2000). Highly reduced protection against Streptococcus pneumoniae after deletion of a single heavy chain gene in mouse. *Proceedings of the National Academy of Sciences of the United States of America*, *97*(11), 6031–6036. https://doi.org/10.1073/pnas.110039497

Montecino-Rodriguez, E., & Dorshkind, K. (2012). B-1 B cell development in the fetus and adult. *Immunity*, *36*(1), 13–21. https://doi.org/10.1016/J.IMMUNI.2011.11.017

Montecino-Rodriguez, E., Leathers, H., & Dorshkind, K. (2006). Identification of a B-1 B cell-specified progenitor. *Nature Immunology*, *7*(3), 293–302. https://doi.org/10.1038/NI1301

Moon, H., Lee, J. G., Shin, S. H., & Kim, T. J. (2012). LPS-induced migration of peritoneal B-1 cells is associated with upregulation of CXCR4 and increased migratory sensitivity to

CXCL12. *Journal of Korean Medical Science*, *27*(1), 27–35. https://doi.org/10.3346/jkms.2012.27.1.27

Nguyen, T. T. T., Graf, B. A., Randall, T. D., & Baumgarth, N. (2017). sIgM-FcμR Interactions Regulate Early B Cell Activation and Plasma Cell Development after Influenza Virus Infection. *Journal of Immunology (Baltimore, Md. : 1950)*, *199*(5), 1635–1646. https://doi.org/10.4049/JIMMUNOL.1700560

Nisitani, S., Tsubata, T., Murakami, M., & Honjo, T. (1995). Administration of interleukin-5 or -10 activates peritoneal B-1 cells and induces autoimmune hemolytic anemia in anti-erythrocyte autoantibody-transgenic mice. *European Journal of Immunology*, *25*(11), 3047–3052. https://doi.org/10.1002/EJI.1830251110

O'Brien, A. D., Scher, I., Campbell, G. H., MacDermott, R. P., & Formal, S. B. (1979). Susceptibility of CBA/N Mice to Infection with Salmonella Typhimurium: Influence of the X-Linked Gene Controlling B Lymphocyte Function. *The Journal of Immunology*, *123*(2).

Ochsenbein, A. F., Fehr, T., Lutz, C., Suter, M., Brombacher, F., Hengartner, H., & Zinkernagel, R. M. (1999). Control of early viral and bacterial distribution and disease by natural antibodies. *Science*, *286*(5447), 2156–2159.

Ordoñez, C., Savage, H. P., Tarajia, M., Rivera, R., Weeks-Galindo, C., Sambrano, D., Riley, L., Fernandez, P. L., Baumgarth, N., & Goodridge, A. (2018). Both B-1a and B-1b cells exposed to Mycobacterium tuberculosis lipids differentiate into IgM antibody-secreting cells. *Immunology*, *154*(4), 613–623. https://doi.org/10.1111/IMM.12909

Patel, P. S., King, R. G., & Kearney, J. F. (2016). Pulmonary α-1,3-Glucan–Specific IgA-Secreting B Cells Suppress the Development of Cockroach Allergy. *The Journal of Immunology*, *197*(8), 3175–3187. https://doi.org/10.4049/jimmunol.1601039

Prohaska, T. A., Que, X., Diehl, C. J., Hendrikx, S., Chang, M. W., Jepsen, K., Glass, C. K., Benner, C., & Witztum, J. L. (2018). Massively Parallel Sequencing of Peritoneal and Splenic B Cell Repertoires Highlights Unique Properties of B-1 Cell Antibodies. *The Journal of Immunology*, *200*(5), ji1700568. https://doi.org/10.4049/jimmunol.1700568

Rauch, P. J., Chudnovskiy, A., Robbins, C. S., Weber, G. F., Etzrodt, M., Hilgendorf, I., Tiglao, E., Figueiredo, J. L., Iwamoto, Y., Theurl, I., Gorbatov, R., Waring, M. T., Chicoine, A. T., Mouded, M., Pittet, M. J., Nahrendorf, M., Weissleder, R., & Swirski, F. K. (2012). Innate response activator B cells protect against microbial sepsis. *Science*, *335*(6068), 597–601. https://doi.org/10.1126/SCIENCE.1215173/SUPPL_FILE/RAUCH.SOM.PDF

Reid, R. R., Prodeus, A. P., Khan, W., Hsu, T., Rosen, F. S., & Carroll, M. C. (1997). Endotoxin shock in antibody-deficient mice: unraveling the role of natural antibody and complement in the clearance of lipopolysaccharide. *Journal of Immunology (Baltimore, Md. : 1950)*, *159*(2), 970–975. http://www.ncbi.nlm.nih.gov/pubmed/9218618

Savage, H. P., Klasener, K., Smith, F. L., Luo, Z., Reth, M., & Baumgarth, N. (2019). TLR induces reorganization of the IgM-BCR complex regulating murine B-1 cell responses to infections. *ELife*, *8*. https://doi.org/10.7554/ELIFE.46997

Savage, H. P., Yenson, V. M., Sawhney, S. S., Mousseau, B. J., Lund, F. E., & Baumgarth, N. (2017). Blimp-1–dependent and –independent natural antibody production by B-1 and B-1–derived plasma cells. *The Journal of Experimental Medicine*, *214*(9), 2777–2794. https://doi.org/10.1084/jem.20161122

Savitsky, D., & Calame, K. (2006). B-1 B lymphocytes require Blimp-1 for immunoglobulin secretion. *Journal of Experimental Medicine*, *203*(10), 2305–2314. https://doi.org/10.1084/JEM.20060411

Skrzypczynska, K. M., Zhu, J. W., & Weiss, A. (2016). Positive Regulation of Lyn Kinase by CD148 Is Required for B Cell Receptor Signaling in B1 but Not B2 B Cells. *Immunity*, *45*(6), 1232–1244. https://doi.org/10.1016/J.IMMUNI.2016.10.013

Subramaniam, K. S., Datta, K., Quintero, E., Manix, C., Marks, M. S., & Pirofski, L. (2010). The Absence of Serum IgM Enhances the Susceptibility of Mice to Pulmonary Challenge with Cryptococcus neoformans . *The Journal of Immunology*, *184*(10), 5755–5767. https://doi.org/10.4049/jimmunol.0901638

Waffarn, E. E., Hastey, C. J., Dixit, N., Soo Choi, Y., Cherry, S., Kalinke, U., Simon, S. I., & Baumgarth, N. (2015). Infection-induced type I interferons activate CD11b on B-1 cells for subsequent lymph node accumulation. *Nature Communications*, *6*. https://doi.org/10.1038/NCOMMS9991

Watanabe, N., Ikuta, K., Fagarasan, S., Yazumi, S., Chiba, T., & Honjo, T. (2000). Migration and Differentiation of Autoreactive B-1 Cells Induced by Activated γ/δ T Cells in Antierythrocyte Immunoglobulin Transgenic Mice. *The Journal of Experimental Medicine*, *192*(11), 1577. https://doi.org/10.1084/JEM.192.11.1577

Weber, G. F., Chousterman, B. G., He, S., Fenn, A. M., Nairz, M., Anzai, A., Brenner, T., Uhle, F., Iwamoto, Y., Robbins, C. S., Noiret, L., Maier, S. L., Zönnchen, T., Rahbari, N. N., Schölch, S., Ameln, A. K. von, Chavakis, T., Weitz, J., Hofer, S., … Swirski, F. K. (2015). Interleukin-3 amplifies acute inflammation and is a potential therapeutic target in sepsis. *Science*, *347*(6227), 1260–1265. https://doi.org/10.1126/SCIENCE.AAA4268/SUPPL_FILE/AAA4268-WEBER-SM.PDF

Wells, S. M., Kantor, A. B., & Stall, A. M. (1994). CD43 (S7) expression identifies peripheral B cell subsets. *Journal of Immunology (Baltimore, Md. : 1950)*, *153*(12), 5503–5515. http://www.ncbi.nlm.nih.gov/pubmed/7989752

Wijburg, O. L. C., Uren, T. K., Simpfendorfer, K., Johansen, F. E., Brandtzaeg, P., & Strugnell, R. A. (2006). Innate secretory antibodies protect against natural Salmonella typhimurium

infection. *The Journal of Experimental Medicine*, *203*(1), 21–26. https://doi.org/10.1084/JEM.20052093

Yang, Y., Eid, E., Ghosn, B., Cole, L. E., Obukhanych, T. v, Sadate-Ngatchou, P., Vogel, S. N., Herzenberg, L. A., & Herzenberg, L. A. (2012). Antigen-specific memory in B-1a and its relationship to natural immunity. *PNAS*. https://doi.org/10.1073/pnas.1121631109

Yang, Y., Tung, J. W., Ghosn, E. E., Herzenberg, L. A., & Herzenberg, L. A. (2007). Division and differentiation of natural antibody-producing cells in mouse spleen. *Proc Natl Acad Sci U S A*, *104*(11), 4542–4546. https://doi.org/10.1073/pnas.0700001104

Yang, Y., Wang, C., Yang, Q., Kantor, A. B., Chu, H., Ghosn, E. E. B., Qin, G., Mazmanian, S. K., Han, J., & Herzenberg, L. A. (2015). Distinct mechanisms define murine B cell lineage immunoglobulin heavy chain (IgH) repertoires. *ELife*, *4*(September 2015). https://doi.org/10.7554/eLife.09083

Yuan, J., Nguyen, C. K., Liu, X., Kanellopoulou, C., & Muljo, S. A. (2012). Lin28b reprograms adult bone marrow hematopoietic progenitors to mediate fetal-like lymphopoiesis. *Science*, *335*(6073), 1195–1200. https://doi.org/10.1126/science.1216557

Zeng, Z., Surewaard, B. G. J., Wong, C. H. Y., Guettler, C., Petri, B., Burkhard, R., Wyss, M., le Moual, H., Devinney, R., Thompson, G. C., Blackwood, J., Joffe, A. R., McCoy, K. D., Jenne, C. N., & Kubes, P. (2018). Sex-hormone-driven innate antibodies protect females and infants against EPEC infection. *Nature Immunology*, *19*(10), 1100–1111. https://doi.org/10.1038/s41590-018-0211-2

Zhou, Y., Li, Y. S., Bandi, S. R., Tang, L., Shinton, S. A., Hayakawa, K., & Hardy, R. R. (2015). Lin28b promotes fetal B lymphopoiesis through the transcription factor Arid3a. *Journal of Experimental Medicine*, *212*(4), 569–580. https://doi.org/10.1084/JEM.20141510

1.9 Tables and Figures

Table 1.1: B-1 cells and B-1 cell derived antibodies protect from a variety of pathogens

Pathogen	B-1 Cell Response	References
Bacteria		
Sepsis	Natural IgM protects against endotoxemia. CD5+ B-1 derived IL-10 decreases mortality and multi-organ dysfunction. B-1 cell-derived GM-CSF and IL-3 regulate immunity to bacterial sepsis.	(Aziz et al., 2017; Barbeiro et al., 2011; Boes, Prodeus, et al., 1998; Rauch et al., 2012; Reid et al., 1997; Weber et al., 2015)
Borrelia hermsii	CD5- B-1 cells develop long lasting memory and produce *Borrelia*-binding IgM.	(Alugupalli et al., 2003; Barbour & Bundoc, 2001; Colombo et al., 2011; Colombo & Alugupalli, 2008)
Enteropathogenic E. coli (EPEC)	Natural IgM protects from EPEC infection via complement-mediated lysis of bacteria. Enhanced levels in females over males explains their increased resistance	(Zeng et al., 2018)
Francisella tularensis	*F. tularensis* LPS specific CD5+ B-1 cell populations expand and develop memory following exposure.	(Barbosa et al., 2021; Cole et al., 2009; Crane et al., 2013; Yang et al., 2012)
Listeria monocytogenes	Natural IgM protects against bacterial systemic dissemination.	(Ochsenbein et al., 1999; Ordoñez et al., 2018)
Mycobacterium spp.	CD5+ B-1 cells differentiation into CD138+ antibody secreting cells in response to mycobacterium lipids *in vitro*.	(Ordoñez et al., 2018)
Salmonella spp.	Natural IgM is protective. CD5- B-1 cells develop memory and secrete increased amounts antigen-specific protective antibodies following challenge.	(O'Brien et al., 1979; Wijburg et al., 2006)
Staphylococcus aureus	IL-10 production by CD5+ B-1 cells protects against bacterial dissemination.	(Leech et al., 2017)
Streptococcus pneumoniae	CD5+ B-1 cells produce natural antibodies to *S. pneumoniae.* CD5- B-1 cells produce antigen-specific antibodies and develop	(Binder et al., 2003; Briles et al., 1981, 1982; Cotte & Szczepanek, 2017; Haas et

	protective memory following vaccination with *S. pneumoniae* antigen.	al., 2005; Martin et al., 2001; Mi et al., 2000)
Fungi		
Cryptococcus neoformans	Natural IgM protects against death and dissemination to pulmonary infection.	(Subramaniam et al., 2010)
Altenaria alternata	Accumulation of B-1 cells in fat associated lymphoid clusters in the mediastinum and increase local production of IgM	(Jackson-Jones et al., 2016)
Viruses		
Influenza Virus	Natural IgM neutralizes virus early after infection. CD5+ B-1 cells migrate to MedLN and increase local production of polyreactive and influenza-binding IgM.	(Baumgarth et al., 1999; Baumgarth, Herman, et al., 2000; Choi & Baumgarth, 2008; Gonzalez et al., 2008; Harada et al., 2003; Jayasekera et al., 2007; Waffarn et al., 2015)
Lymphocytic Choriomengitis Virus (LCMV)	Natural IgM can bind to LCMV	(Ochsenbein et al., 1999)
Vesicular Stomatitis Virus (VSV)	Natural IgM neutralizes multiple strains of VSV. Natural IgM improves survival and prevents systemic dissemination.	(Ochsenbein et al., 1999)
Parasites		
Litomosoides sigmodontis	Accumulation in fat-associated lymphoid tissue; increased production of IgM	(Jackson-Jones et al., 2016)
Leishmania spp	IL-10 production by splenic B-1 cells impairs macrophage responses to visceral leishmaniasis. B-1 cells reduce parasite burden in subcutaneous infection.	(Arcanjo et al., 2017; Gonzaga et al., 2017)

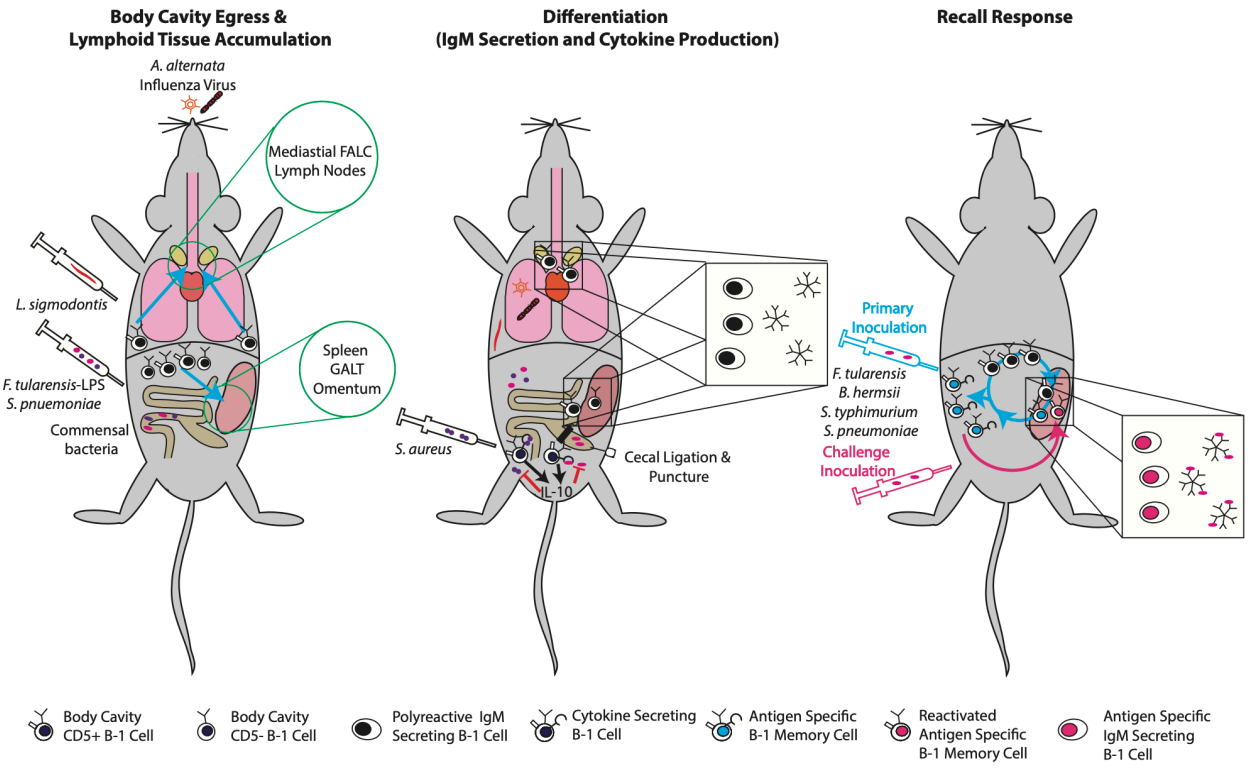

Figure 1.1 Outcomes of B-1 cell activation

Pleural cavity B-1 cells respond to microbial insults by migration to regional lymphoid tissue such as mediastinal lymph nodes and mediastinal fat-associated lymphocyte tissue, whereas peritoneal cavity B-1 cells will migrate to spleen, gut-associated lymphoid tissue and/or omentum. Although B-1 cells circulate continuously in and out of the body cavities, their migration seems enhanced after an insult (left panel). Following arrival in the lymphoid tissues B-1 cells were shown to differentiate into IgM-secreting cells. B-1 cells in the cavities may also spontaneously secrete cytokines, specifically IL-10, or GM-CSF and IL-3 following their arrival in lympmphoid tissues (middle panel). Weeks to months after foreign antigen exposure a higher frequency of antigen-binding B-1 cells accumulate in body cavities, which are otherwise

phenotypically indistinguishable from other B-1 cells. Following adoptive transfer of body cavity cells, these cell populations have been shown to provide increased immune protection, i.e. a memory function. It is unresolved whether antigen-stimulated B-1 cells have an enhanced ability to differentiate to antibody-secreting cells, or whether their higher frequencies alone can provide enhanced protection during challenge (right panel).

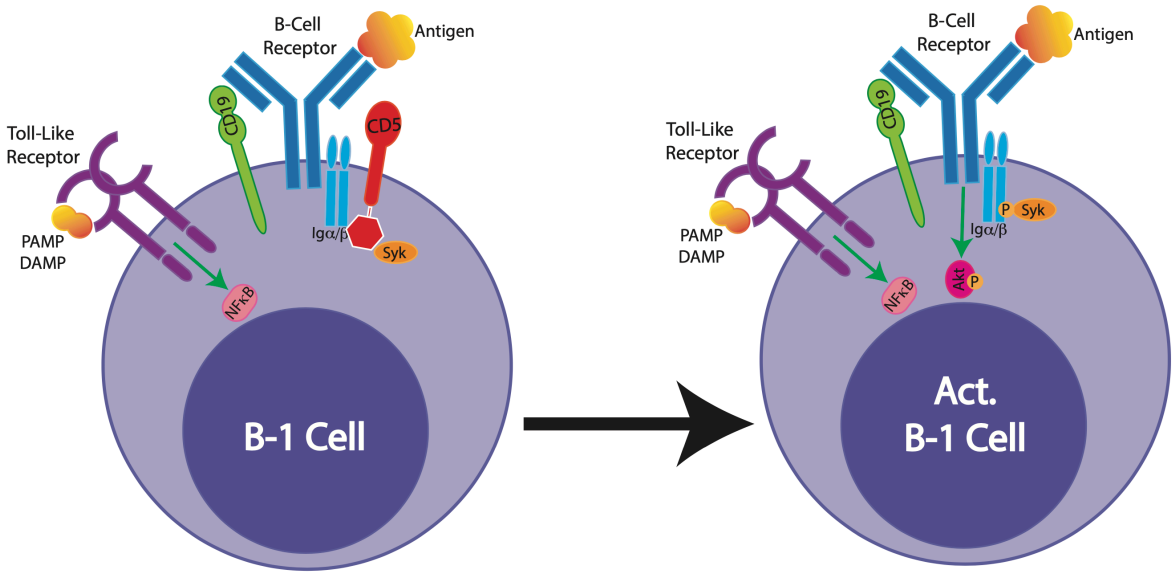

Figure 1.2 BCR complex reorganization following B-1 cell stimulation

B-1 cells express surface IgM- but little to no IgD-BCR. In the steady state their IgM-BCR closely associates with CD19 and with CD5. This complex is unable to signal via Igα/β following BCR-antigen stimulatik, however, B-1 cells vigoriously signal strongly following stimulation via TLR (left). Activation of B-1 cells via TLR alters their BCR complex, resulting in loss of CD5-mediated inhibition and BCR-downstream signaling (right). IgM-BCR complex reorganization may explain antigen-specific responses by self-reactive B-1 cells.

Chapter 2:

B-1 plasma cells require CD4 T cell help to generate a unique repertoire of natural IgM

This chapter is under revision: Smith FL, Savage HP, Luo Z, Tipton CM, Lee E-HF, Apostol A, Beaudin AE, Lopez D, Jensen I, Keller S, and Baumgarth N, **B-1 plasma cells require CD4 T cell help to generate a unique repertoire of natural IgM,** *J Exp Med*, 2022

Graphical Abstract

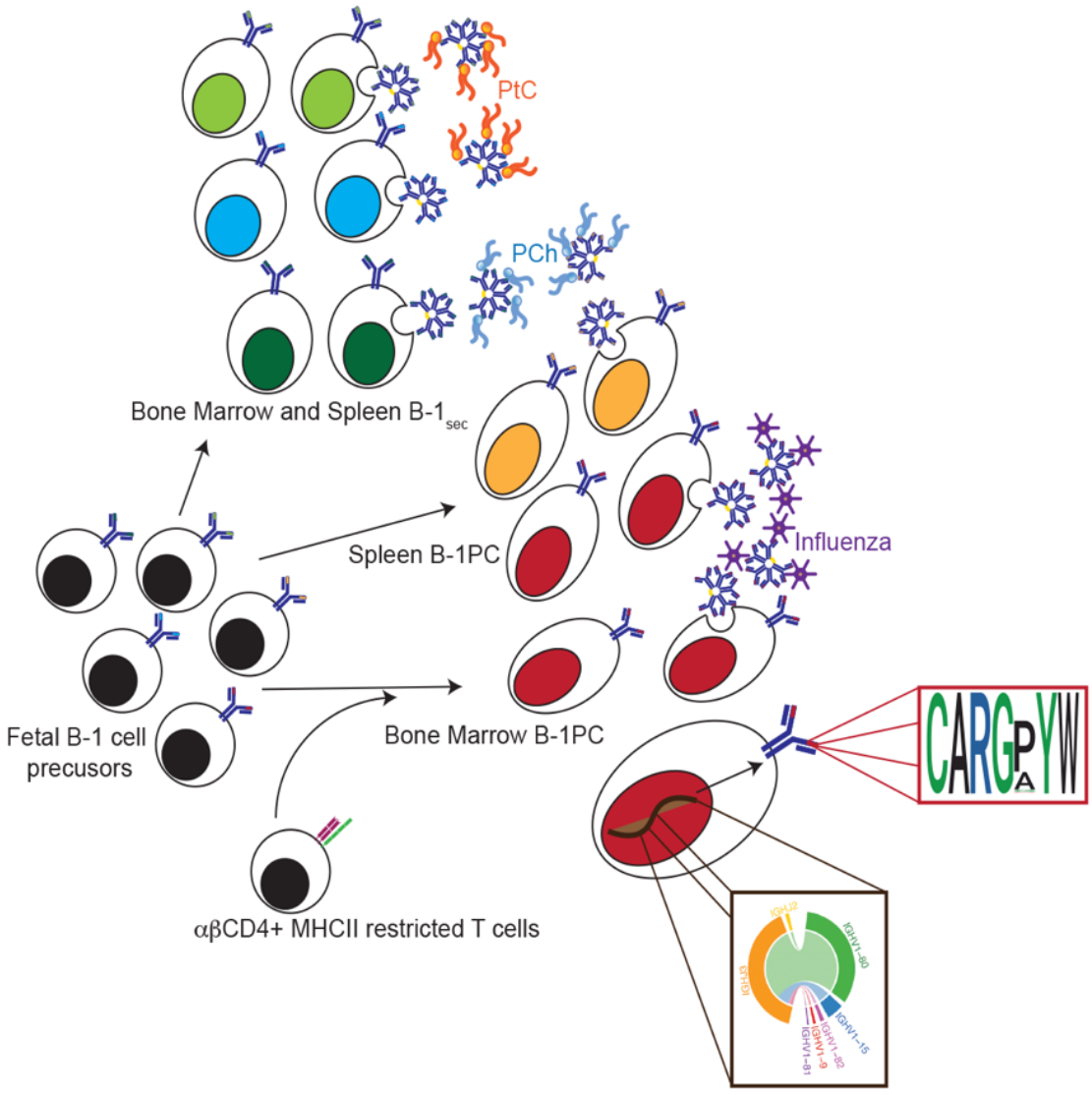

Abstract

Evolutionarily conserved, "natural" (n)IgM is broadly reactive to both self and foreign antigens. Its selective deficiency leads to increases in autoimmune diseases and infections. In mice, nIgM is secreted independent of microbial exposure by bone marrow and spleen B-1 cell-derived plasma cells (B-1PC), generating the majority of nIgM, or by B-1 cells that remain non-terminally differentiated ($B\text{-}1_{sec}$). Thus, it has been assumed that the nIgM repertoire is broadly reflective of the repertoire of body cavity B-1 cells. Studies here reveal, however, that B-1PC generate a distinct, oligoclonal nIgM repertoire, characterized by short CDR3 variable immunoglobulin heavy chain regions, 7-8 amino acids in lengths, some public, many arising from convergent rearrangements, while specificities previously associated with nIgM were generated by $B\text{-}1_{sec}$. Bone marrow but not spleen B-1PC, or $B\text{-}1_{sec}$ also required the presence of TCR$\alpha\beta$ CD4 T cells for their development from fetal precursors. Together the studies identify important previously unknown characteristics of the nIgM pool.

2.1 Introduction

Natural IgM (nIgM) are spontaneously generated, self-reactive, circulating antibodies that can be produced independent of foreign antigen exposure by antibody-secreting cells located primarily in bone marrow and spleen (Hayakawa et al., 1984; Savage et al., 2017; Choi et al., 2012; Forster and Rajewsky, 1987; Kawahara et al., 2003). Selective IgM deficiency, a rare human condition, leads to increased rates of infections and autoimmune disease. 30-45 % of human patients with selective IgM deficiency have higher incidences of asthma and allergic rhinitis (Goldstein et al., 2006), as well as systemic lupus erythematosus and Hashimoto's thyroiditis compared to the general population (Takeuchi et al., 2009; Gupta and Gupta, 2017). Also, humans with selective IgM deficiency are more likely to suffer from chronic and opportunistic infections (reviewed in Gupta and Gupta, 2017).

Mice with defects in secreted IgM show similar disease phenotypes to those observed in humans. They develop autoimmune diseases and have elevated levels of anti-nuclear, anti-dsDNA and anti-ssDNA antibodies (Boes et al., 2000; Ehrenstein et al., 2000; Notley et al., 2011; Nguyen et al., 2015). Mechanisms remain to be more fully explored but might involve reduced IgM-mediated opsonization and uptake of autoantigens (Ogden et al., 2009; Quartier et al., 2005; Chen et al., 2009), a failure to block the biological effects of oxidized phospholipids leading to chronic inflammation (Que et al., 2018) and/or alterations in central tolerance induction (Nguyen et al., 2015). Also, induction early after birth of phosphocholine (PCh)-specific IgM, germline-encoded by the T15 idiotype, by exposure to *Streptococcus pneumoniae* (Briles et al., 1981; Mi et al., 2000), was shown to reduce the development of PCh-specific IgE in response to PCh-containing house dust mite challenge later in life (Kearney et al., 2015; Patel and Kearney, 2015).

nIgM also protects again replication and dissemination of many bacterial, fungal and viral pathogens, (Baumgarth et al., 2000; Haas et al., 2005; Wardemann et al., 2002; Ochsenbein et al., 1999; Smith and Baumgarth, 2019; Zeng et al., 2018; Jackson-Jones et al., 2016; Alugupalli and Gerstein, 2005). It can do so by directly neutralizing pathogens, such as *S. pneumoniae*, influenza virus and *Borrelia hermsii* (Alugupalli et al., 2003; Jayasekera et al., 2007; Ehrenstein and Notley, 2010) and by supporting the induction of maximal antigen-specific IgG responses by conventional B-2 (Baumgarth et al., 2000; Yuan et al., 2012; Boes et al., 1998; Nguyen et al., 2017; Heyman, 2000). The lack of nIgM was also shown to attenuate adaptive T cell responses to neoantigens during cancer development (Atif et al., 2018).

Although serum nIgM levels and frequencies of IgM-secreting cells in bone marrow and spleen are comparable between mice held under germfree/antigen-free conditions and those housed under SPF conditions (Savage et al., 2017; Bos et al., 1989; Haury et al., 1997), the nIgM repertoire appears to be shaped by both, extrinsic and intrinsic factors. For example, and as mentioned above, antibodies to PCh are induced following exposure to S. *pneumoniae* (Kenny et al., 1983). Also, titers of certain antibacterial nIgM specificities have been shown to increase by exposure to microbiota in an apparent TLR-dependent manner (Kreuk et al., 2019; New et al., 2020). Furthermore, B cell-intrinsic estrogen receptor signaling was shown to affect the production of anti-enteropathogenic *Echerishia coli* and was found at protective levels only in female mice (Zeng et al., 2018). A better understanding of the mechanisms regulating the repertoire of nIgM may allow future exploration of nIgM for therapeutic uses.

In mice, nIgM is secreted in large part by differentiated, self-reactive B-1 cells that escape negative selection during fetal and early neonatal life (Hayakawa et al., 2003, 1999). They appear to require no foreign antigen stimulation to induce nIgM secretion (Baumgarth et

al., 2000; Lalor et al., 1989; Choi et al., 2012; Kantor and Herzenberg, 1993). Consistent with previous studies identifying spleen and bone marrow as major sites of IgM production, we demonstrated that nIgM-secreting B-1 cells are located mainly in spleen and bone marrow (Choi et al., 2012; Savage et al., 2017). Furthermore, we demonstrated the presence of two distinct B-1 populations secreting nIgM: non-terminally differentiated B-1 cells ($B\text{-}1_{sec}$) that generated IgM even in the absence of the transcriptional regulator of plasma cell development, BLIMP-1 (Shapiro-Shelef et al., 2003), and terminally differentiated, BLIMP-1+ B-1-derived plasma cells (B-1PC). The studies further suggested that about two-thirds of the circulating serum nIgM is produced by the B-1PC (Savage et al., 2017).

nIgM is considered a product of T-independent, innate B-1 cell activation, as B-1PC differentiation can be induced *in vitro* by stimulating peritoneal cavity B-1 cells with TLR agonists alone (Genestier et al., 2007). Furthermore, the lack of all T cells, or of MHCII and thus functional CD4 T cells, did not seem to affect circulating nIgM levels (Hooijkaas et al., 1985; Van Oudenaren et al., 1984; Madsen et al., 1999). In addition, the best-known specificities of B-1 cells are against T-independent antigens, such as PCh, phosphatidylcholine (PtC), as well as other oxidized phospholipids (Bos et al., 1989; Briles et al., 1981; Mercolino et al., 1988; Tuominen et al., 2006). The presence of two distinct nIgM secreting cell types, with B-1PC sharing Blimp-1 expression with those expressed by B-2 cell-derived plasma cells, suggested that nIgM-secreting B-1PC and $B\text{-}1_{sec}$ might be induced by distinct activation pathways and may also differ from the non-secreting B-1 cells in the body cavities. Studies shown here demonstrate that bone marrow, but not spleen B-1PC require the presence of MHCII-restricted CD4 T cells for their development from fetal precursors and that they generate a highly oligoclonal repertoire

of nIgM with unique characteristics that differ sharply from those previously associated with B-1 cell-derived nIgM.

Results

2.2 nIgM secreting B-1PC appear in bone marrow and spleen over time

Most spontaneous IgM-secreting cells in the bone marrow and spleen of C57BL/6 mice are B-1 cell-derived and consisted of non-terminally differentiated B-1_{sec} and terminally differentiated B-1PC (Savage et al., 2017). These two cell populations are distinguished by their phenotype. B-1_{sec} are present in small frequencies among "classical" B-1 cells ($CD19^{+/int}$ IgM^{hi} IgD^{lo} $CD23^{-}$ $CD43^{+}$) in bone marrow and spleen, while B-1PC are distinguished from these cells as being $CD19^{lo/neg}$ IgM^{+} IgD^{lo} $CD138^{+}$ (Savage et al., 2017; Choi et al., 2012). Thus, B-1PC phenotypically resemble conventional, B-2 cell-derived PC. Like conventional PC, most B-1PC also expressed the transcriptional regulator Blimp-1, and virtually every cell spontaneously secreted IgM when deposited into an ELISPOT plate (**Fig. 2.1A, B** and (Savage et al., 2017)). Measuring the appearance of B-1 and B-1PC in ontogeny revealed that, as expected, B-1 cells were present in spleen and bone marrow at birth, with frequencies reaching those seen in adult mice by about postnatal day 18. In contrast, B-1PC were absent in neonates and did not emerge until mice reached 3-4 weeks of age (**Fig. 2.1A, C, D**). Their appearance correlated with a rapid increase in serum IgM (**Fig. 2.1E**), consistent with their previously noted significant contributions to nIgM production (Savage et al., 2017; Savitsky and Calame, 2006).The frequency and number of B-1PC in spleen and bone marrow of germ-free mice was similar to that of mice held under SPF conditions (**Fig. 2.1F**), consistent with previous data which showed

that serum IgM concentrations are similar in SPF-held and germfree mice (Bos et al., 1989; Haury et al., 1997), although microbiota may alter their specificity (Kreuk et al., 2019; New et al., 2020). This suggested it was unlikely that the delayed development of B-1PC was due to a need for microbial antigen and/or PAMP-induced B-1 cell differentiation.

Early adoptive cell transfer studies showed that B-1 cells develop predominantly during fetal and early neonatal life, relying on a transcriptional gene network profile epigenetically-regulated by Lin28/Let7 (Hayakawa and Hardy, 2000; Yuan et al., 2012; Li et al., 2015). Furthermore, use of an irreversible lineage tracing model, the FlkSwitch mouse, revealed the presence of two distinct fetal HSC populations, which gave rise to B-1 cells: a transient, developmentally-restricted (dr) HSC population in the fetal liver, which preferentially gave rise to innate lymphoid lineage cells and was found only during a distinct window in fetal development, and a population of long-term fetal liver and bone marrow HSCs that generate both innate-like and conventional lymphocytes (Beaudin et al., 2016). In this model, the fetal liver drHSC can be distinguished from the long-term reconstituting fetal-derived HSCs by their early Flk-induced expression of GFP, instead of Tomato Red (Tom) (Boyer et al., 2012, 2011). Although all daughter cells eventually express GFP due to induction of Flk later in B cell differentiation (Boyer et al., 2011). We used this lineage tracing model to determine whether the later appearance of B-1PC was due to B-1PC precursors emerging only from the later appearing HSCs, studying lethally irradiated adult recipients that were reconstituted with either of the two purified HSC populations. The results demonstrated that both HSC populations could reconstitute the B-1PC compartment (**Fig. 2.1G, H**). Indeed, when compared to the development of granulocytes, both B-1 and B-1PC compartments were preferentially reconstituted by the

early-arising drHSC (**Fig. 2.1H**). Thus, while B-1PC precursors are present already in the fetus and the neonate, B-1PC differentiation is delayed until around the time of weaning.

2.3 The development of bone marrow B-1PC requires the presence of T cells

Although natural antibody production is widely reported to occur independent of T cells, adoptive transfer of B-1 cells into B and T cell-deficient RAG-/- mice showed relatively poor reconstitution of bone marrow IgM production and total serum IgM levels (Moon et al., 2004; Reynolds et al., 2015b). In contrast, adoptive transfer of B-1 cells into B cell-deficient, but T cell-sufficient neonates resulted in robust nIgM reconstitution (Savage et al., 2017; Baumgarth et al., 1999; Stall et al., 1992). We therefore reconsidered the role of T cells in nIgM production and B-1PC development and studied B-1PC populations in adult T cell-deficient TCRβ/$\delta^{-/-}$ mice (Mombaerts et al., 1992). Indeed, these mice showed a near complete lack of bone marrow B-1PC (**Fig. 2.2A, B**), while the splenic B-1PC compartment appeared largely unaffected (**Fig. 2.2C**).

Despite the absence of bone marrow B-1PC, and consistent with previously studies (Hooijkaas et al., 1985; Van Oudenaren et al., 1984; Madsen et al., 1999), the number of nIgM ASC in the bone marrow of adult TCRβ/$\delta^{-/-}$ mice and their serum IgM levels were comparable to T cell containing control mice (**Fig. 2.2D, E**). This was explained by a striking increase in the frequency and number of B-1 cells in both bone marrow and spleen of TCRβ/$\delta^{-/-}$ mice (**Fig. 2.2B, C lower panels**), the subset that contains nIgM-secreting B-1_{sec} cells (Savage et al., 2017). Furthermore, measuring serum IgM concentrations during early life showed that TCRβ/$\delta^{-/-}$ mice had transiently reduced IgM concentrations between 3-5 weeks of age compared to controls (**Fig. 2.2E**), thus the age at which the bone marrow B-1PC compartment rapidly expanded (**Fig. 2.1A,**

B). Serum IgM concentrations in the TCRβ/δ$^{-/-}$ mice reached levels comparable to that of controls by about 8 weeks of age (**Fig. 2.2E**). The data suggests that nIgM-secreting bone marrow B-1PC, but not spleen B-1PC or B-1$_{sec}$ require the presence of T cells for development. The apparent normal nIgM concentrations in the serum of TCRβ/δ$^{-/-}$ mice seemed to be restored, at least in part, via compensatory increases in bone marrow B-1$_{sec}$ cell differentiation and/or maintenance.

2.4 Establishment of bone marrow B-1PC but not their maintenance requires CD4+ T cells

Long-lived conventional B cell-derived Blimp-1+ plasma cells require costimulatory signals from CD4 T cells (Gershon, 1974; Keightley et al., 1976). Consistent with those findings, depletion of CD4+ cells from newborn C57BL/6 mice via anti-CD4 mAb treatment (GK1.5) resulted in greatly reduced numbers of IgM+ bone marrow B-1PC (**Fig. 2.3A)** but did not significantly affect serum IgM concentrations (**Fig. 2.3B**). We also depleted T cells from neonatal Ig-allotype chimeras, by treating Igha-expressing C57BL/6 mice via anti-CD4 treatment. In addition, these neonatal chimeras were rendered temporarily host-B cell deficient from birth until 6 weeks of age via treatment with allotype-specific anti-IgM (Igh-a). To replace their B-1 cell compartment, these mice were reconstituted, also at birth, with body cavity B-1 cells from allotype-disparate (Igh-b) but congenic adult C57BL/6 mice. These cells can reconstitute the Igh-a expressing host, as the anti-IgMa treatment does not affect their presence (Lalor et al., 1989) and enables tracing of B-1 cell-derived IgM via their expressed Ig-allotype (Baumgarth et al., 1999). Antibody-mediated CD4 cell-depletion greatly reduced the numbers of bone marrow Igh-b+ B-1PCs compared to control Ig-allotype chimeras that had received PBS

only (**Figs. 2.3C, D**). The data further confirmed the B-1 cell origin of the bone marrow IgM+ PC and demonstrated their dependence on CD4 T cells for development.

The compensatory increases in bone marrow and spleen B-1 cell numbers seen in the TCRβ/δ$^{-/-}$ mice were not seen in the CD4-depleted neonatal Ig-allotype chimeras. In fact, a significant drop in bone marrow B-1 cell frequency and total numbers were seen (**Fig. 2.3D**), a population that contains nIgM secreting B-1$_{sec}$ (Savage et al., 2017). Consistent with reductions of both nIgM-secreting B-1 cell populations, CD4-depleted Ig-allotype chimeras had severely reduced concentrations of serum IgM compared to the controls (**Fig. 2.3E**). This failure to compensate for the depletion of bone marrow B-1PC by B-1$_{sec}$ in chimeras in which all B-1 cells are reconstituted by adult-type body cavity B-1 cells may suggest that this functionality is restricted to fetal/neonatal B-1 cells and/or B-1 cells that reside outside the body cavities. The data indicate that functional heterogeneity exists within the B-1 cell compartment, which requires future exploration. In contrast to neonatal anti-CD4 treatment, when fully reconstituted adult Ig-allotype chimeras were treated for over two months with anti-CD4, no effect on the frequency or number of bone marrow B-1PC, nor of B-1 cell-derived serum IgM levels were noted (**Fig. 2.3F, G**), suggesting that CD4 T cells are required for the induction but not maintenance of the bone marrow IgM+ B-1PC pool.

2.5 CD4+ T cells are sufficient to rescue bone marrow B-1PC development

Reconstitution of T and B cell-deficient Rag1-/- mice with either peritoneal cavity B-1 cells alone or with splenic CD4+ T cells and peritoneal cavity B-1 cells demonstrated that CD4 T cells were both necessary and sufficient for B-1PC development (**Fig. 2.4A, B**). Additionally, mice reconstituted with B-1 cells alone had significantly lower numbers IgM secreting cells in the

bone marrow (**Fig. 2.4C, D**) as well as lower concentrations serum IgM (**Fig. 2.4E**) than mice reconstituted with CD4+ T cells and B-1 cells. This is consistent with results in the Ig-allotype chimeras (**Fig. 2.3E**), where the transfer of adult peritoneal cavity B-1 cells was unable to compensate for reduced serum IgM production due to the lack of B-1PC. The results are consistent also with a previous study, which demonstrated enhanced IgM secretion by bone marrow plasma cells after transfer of total peritoneal cavity cells, compared to transfer of B-1 cells alone (Reynolds et al., 2015a).

Conventional B cells receive T cell help from CD4+ TCRαβ+ MCH II-restricted T cells to generate long-lived bone marrow PC (Noelle et al.) while glycolipid-specific CD1d-restricted invariant (i)NKT cells as well as TCRγδ+ T cells were shown to provide cytokine-mediated "help" to B-1 cells in inflammation and infection (Campos et al., 2006; Wang et al., 2016). Yet, mice deficient in TCRαβ+ cells and neonatal Ig-allotype chimeras depleted of all TCRαβ+ T cells via treatment with an anti-pan-TCRαβ mAb (H57-597.1), had greatly reduced B-1PC compartments (**Fig. 2.5A, B**), similar to those seen after anti-CD4 treatment (**Fig. 2.5D**). Similarly, MHCII-deficient mice, lacking TCRαβ+ CD4 T cells, showed strong reductions in bone marrow B-1PC numbers (**Fig. 2.5E**), while the frequencies and absolute numbers of B-1PC were normal in mice lacking either TCRγδ+ cells or CD1d-restricted iNKT cells, respectively (**Fig. 2.5C, D**). Together, the data demonstrate that bone marrow B-1PC accumulation and nIgM secretion by these cells is dependent on the presence of MHCII-restricted, TCRαβ+ CD4 T cells.

2.6 B-1 and B-1PC express Ig of distinct specificities

We next asked whether B-1PC and B-1_{sec} differed in the nIgM specificities they generate. Previous studies had shown that a large number, roughly 5-15%, of peritoneal cavity CD5+ B-1

cells and 1-10% of spleen B-1 cells can bind to liposomes that contain phosphatidyl choline ((PtC; (Carmack et al.; Mercolino et al., 1988; Hayakawa et al., 1992)). The relative concentration of anti-PtC specific serum IgM, however, was found to be very low (Goodridge et al., 2014). Thus, the repertoires of the nIgM secreting bone marrow and spleen B-1-derived cells does not seem to reflect those of the non-secreting body cavity B-1 cells, nor the overall splenic $CD5^+$ B-1 cell compartment. Indeed, while about 0.4% of B-1 cells in bone marrow and 5% of spleen B-1 cells bound to PtC liposomes in our studies, a small fraction of which may include B-1_{sec}, (Savage et al., 2017), B-1PC in both spleen and bone marrow showed no binding to these liposomes, despite their high levels of surface IgM expression (**Fig. 2.6A, B**). Additionally, flow cytometric depletion of B-1 cells ($CD19^{int/hi}$ IgM^{hi}), but not B-1PC ($CD19^{lo/neg}$, IgM^+, $CD138^+$, Blimp-1^+) from $CD43^+$ IgM^+ bone marrow B cells resulted in significant reductions in anti-PtC IgM secreting cells (**Fig. 2.6C, D**). Thus, indicating that anti-PtC nIgM secreting cells belong to the non-terminally differentiated B-1_{sec} cells, but not to the B-1PC.

BCR encoded by Ig heavy chain variable regions VH11 and VH12 are largely restricted to the B-1 cell compartment and include cells with specificity for PtC (Conger et al., 1991; Arnold and Haughton, 1992). Consistent with the distribution of the PtC-binders among B-1_{sec} but not B-1PC (**Fig. 2.6A, B**), the frequencies of VH11 and VH12-expressing cells were higher among peritoneal cavity B-1 cells compared to splenic or bone marrow B-1 cells, and almost completely absent from spleen and bone marrow B-1PC (**Fig. 2.6E**). Similarly, B-1 cell-derived nIgM to phosphorylcholine (PCh), which is protective against infections with *S. pneumoniae* (Briles et al., 1981), was mostly secreted by B-1_{sec} in the spleen, but not the bone marrow, with some secretion by splenic B-1PC (**Fig. 2.6F**). Consistent with a lack of PCh-specific IgM production by bone marrow B-1PC, PCh-specific IgM levels were comparable between control

and TCRβδ-/- mice (**Fig. 2.6G**). This is consistent also with previous reports on the T cell independence of anti-PCh antibodies (Haas et al., 2005). In contrast, influenza virus-binding nIgM was secreted almost exclusively by B-1PC in both spleen and bone marrow (**Fig. 2.6 H, I**) and their levels were significantly reduced in TCRβδ-/- mice, consistent with the noted T cell-dependence of the B-1PC compartment (**Fig. 2.6J**). Autoantigen-specific serum IgM levels measured against a broad array of autoantigens showed no difference between wild type control mice and various mice that lacked T cell-dependent bone marrow B-1PC: TCRβ/δ-/- mice, CD4+ depleted Ig-allotype chimeras, and B-1 cell reconstituted Rag1-/- mice (**Suppl Fig. 2.1**). The data indicate that B-1PC do not contribute significantly to the production of strongly auto-reactive nIgM.

2.7 B-1PC express a unique and public repertoire

A comprehensive BCR Ig-heavy chain (Igh) repertoire analysis was conducted by sequencing Ig-heavy chains from bulk RNA of purified spleen and bone marrow CD5+ and CD5- B-1 cells, B-1PC as well as CD23+ mature, naive conventional B cells obtained from four individual mice. The data further supported the conclusion that B-1_{sec} and B-1PC secrete nIgM of distinct and mostly non-overlapping specificities. B-1PC showed little Igh-repertoire overlap with either CD5+ B-1, CD5- B-1 or conventional B cells isolated from the same tissue (**Fig. 2.7 A, B, Suppl Fig. 2.2).** Among all B-1 cell subsets studied, bone marrow and spleen B-1PC from the same mouse, but not between mice, were the only populations to consistently show a level of relatedness as assessed by calculating the Morisita overlap index (0.13-0.68; **Suppl Fig. 2.2**).

B-1PC were uniformly marked by a high degree of Igh-repertoire oligoclonality. About 70% of the Igh variable repertoire of bone marrow B-1PC encoded by between 1-10 unique

CDR3 Igh sequences per mouse (**Fig. 2.7A, Suppl Fig 3**). Among spleen B-1PC about half of the CDR3 regions were encoded by between 1-20 unique sequences (data no shown). Thus, extensive clonal expansion seemed to have preceded B-1PC differentiation. Furthermore, the level of oligoclonality exceeded that of both, the CD5+ and CD5- B-1 cells (**Fig. 2.7A, Suppl Fig 3**), which had been shown previously to contain expanded clones and a repertoire that is less diverse than that of conventional B cells (Yang et al., 2015; Prohaska et al., 2018; Upadhye et al., 2019).

In contrast to the other B cell populations studies, B-1PC contained a predominance of clones with short junctional length (7-8 aa) (**Fig. 2.7C, D**). Furthermore, these junctional sequences encoding the antigen-binding CDR3 regions were dominated by a small number of distinct motifs and these motifs were shared between different mice, thus encode many "public" clones (**Fig. 2.7E-G**). In addition, many motifs with unique junctional sequences were encoded by different V/J gene combinations, suggestive of convergent recombination (**Fig. 2.7H**). Thus, B-1PC generates a unique, highly selected and public nIgM repertoire characterized by short junctional sequences, revealing new features of the secreted nIgM repertoire that are distinct from those previously associated with B-1 cells (Yang et al., 2015; Prohaska et al., 2018; Upadhye et al., 2019).

2.8 Discussion

It has been well documented that B-1 cells generate much of the circulating, broadly self-reactive nIgM in mice, and that they do so seemingly independent of prior exposure to foreign antigens, including microbiota (Savage et al., 2017; Haury et al., 1997; Bos et al., 1989). The distinct developmental path of B-1 cells explains their unique capability of producing self-

reactive nIgM. These cells arise mainly from fetal HSC and bypass the need for pre-BCR assembly and hence selection, while requiring self-antigen reactivity for selection and/or expansion of immature B-1 into the mature B cell pool (Hayakawa et al., 1999; Wasserman et al., 1998; Wong et al.; Hayakawa et al., 2003). The broad and seemingly polyreactive specificities of nIgM are reminiscent of pattern recognition receptors (PRRs), which recognize broad classes of foreign antigens/pathogens as well as "altered self" in form of DAMPS. Like PRRs, the presence of nIgM is critical for the maintenance of both, immune homeostasis as well as host defense (Baumgarth, 2011). Here we identify the antigen-binding motives of the IgH-chains expressed by a major source of nIgM, B-1PC. The repertoire of B-1PC differs from that of B-1 cells sorted from the same tissues, and from that previously reported for B-1 cells from body cavities and spleen (Yang et al., 2015; Prohaska et al., 2018; Upadhye et al., 2019). Some of the repertoire's motifs expressed by B-1PCs have, however, been noted previously in BCR repertoire analyses conducted on total spleen cells (Rettig et al., 2018), further underscoring the abundance and presumably large contributions of these B-1PC to the nIgM pool.

The dominance of the B-1PC repertoire encoded by predominantly short Igh-CDR3 regions is distinct from the repertoire of previously identified, broadly neutralizing antibodies to HIV and influenza, which tend to be both highly mutated and to contain very long CDR3 regions (Yu and Guan, 2014; Ekiert et al., 2012), suggesting distinct origins of these types of antibodies. Instead, the repertoire is reminiscent of that reported for B cells in human cord blood, which showed a preference for shorter CDR3 regions and the presence of more public clones, compared to B cells in adult blood (Guo et al., 2016) This is interesting, as it provides a tangible link between nIgM generated by B-1PC in mice and fetal-derived B-1 cells in humans, where the presence of B-1 orthologs have long been debated (Rothstein et al., 2013). It is of course also

further support for the abundance of evidence that has linked B-1 cell development to fetal developing precursors, as the enzyme facilitating N-region editing, TdT, is not expressed until after birth (Feeney, 1990).

The development of the B-1PC-derived nIgM repertoire appears to be shaped by extensive selection and expansion resulting in the formation of a highly oligoclonal B-1PC pool, consistent with our findings that B-1PC development is delayed until a few weeks after birth. As expected from the PRR-like nIgM, the Igh-repertoire of B-1PC is broadly shared between individual mice, thus representing "public" clones. Their repertoire is restricted even further through convergent recombination, making it highly dominated by a handful of Igh-CDR3 region motifs.

Although the complete analysis of the B-1PC repertoire awaits single-cell sequencing of these rare cells and assessment of their light chains, the study demonstrates that the B-1 cell compartment provides at least two very distinct repertoires of nIgM, one generated by cells that terminally differentiate into B-1PC, and the other by B-1_{sec}, the latter providing an estimated 25-30% of the circulating nIgM (Savage et al., 2017), but seemingly encoding much of what has been associated previously with B-1 cell-derived nIgM. Bone marrow B-1PC generated the presumably broadly reactive nIgM that can bind to influenza virus. This is a natural-occurring specificity we have shown previously to be B-1 cell-derived and capable of suppressing viral replication early after virus infection, and not requiring infection for its presence (Baumgarth et al., 1999, 2000; Choi and Baumgarth, 2008; Waffarn et al., 2015). However, other previously identified specificities associated with B-1 cells, such as those to PhC or PtC-containing liposomes, were found to be generated by B-1_{sec} rather than B-1PC, even though both populations arise predominantly from fetal HSCs. B-1PC showed little expression of VH11 or

VH12, did not bind to PtC-containing liposomes, and did not secrete anti-PtC or anti-PCh IgM, previously identified hallmarks of B-1 cells in spleen and body cavity (Carmack et al.; Hardy et al., 1989; Conger et al., 1991; Briles et al., 1981).

The abundance of PtC-binding and VH11/VH11-expressing peritoneal cavity and spleen B-1 cells (Conger et al., 1991; Carmack et al.; Hardy et al., 1989; Yang et al., 2015; Prohaska et al., 2018), and their absence among B-1PC suggests that most PtC-binding B-1 cells require signals distinct from those causing B-1PC differentiation into nIgM-secreting cells and differentiate into B-1_{sec}. In support, we demonstrate here that bone marrow B-1PC, but not B-1_{sec}, required the presence of CD4 T cells for differentiation. With regards to the PtC-binding body cavity CD5+ B-1 cells, it is also noteworthy that previous studies suggested them less likely to differentiate into IgM secreting cells compared to non-PtC-binding CD5+ B-1 cells (Wang et al., 2012). This could thus also suggest that that PtC-binding B-1 cells fulfill functions that are distinct from those and/or in addition to those involving IgM secretion.

Innate activation leads to the differentiation of body cavity B-1 cells into IgM secreting cells *in vitro* as well as *in vivo*, where these signals drive CD5+ B-1 cells from the body cavity into secondary lymphoid tissues prior to their differentiation (Waffarn et al., 2015; Savage et al., 2019; Kawahara et al., 2003). While this could suggest a precursor-product relationship between the non-secreting body cavity B-1 cells and the nIgM-secreting B-1 cells in spleen and bone marrow, these events represent responses to changes to immune homeostasis, and may not reflect the mechanisms by which steady-state nIgM secretion is induced and/or regulated.

The T cell-dependence of bone marrow B-1PC differentiation was unexpected, given that depletion of T cells, or T cell-deficiency has not been reported previously to cause obvious reductions in serum IgM concentrations (Madsen et al., 1999; Hooijkaas et al., 1985; Van

Oudenaren et al., 1984). Our data provide an explanation for this apparent discrepancy by demonstrating that only the development of bone marrow B-1PC, but not of spleen B-1PC or B-1_{sec} required CD4 T cells. Making up for the lack of bone marrow B-1PC in the absence of CD4 T cells was an expansion in the number of bone marrow B-1_{sec}, which seem to reconstitute, at least in magnitude, nIgM production. However, nIgM to influenza remained at serum concentrations lower than those in wild type controls, further supporting the differences in the repertoire of nIgM produced by B-1PC and B-1sec. The compensatory increases in B-1_{sec} differentiation appear restricted to a subset of fetal/neonatal-derived B-1 cells, however, as body cavity-derived B-1 cells from adult mice did not differentiate into B-1_{sec} following their adoptive transfer, even when transferred into a neonatal environment. The latter is consistent with two previous studies that had noted reduced nIgM levels in mice reconstituted with adult B-1 cells when transferred into an adult T cell deficient environment (Moon et al., 2004; Reynolds et al., 2015a). This is significant, as it suggests different functionalities between B-1 cells arising from various waves of fetal and neonatal development and also suggests the loss of certain B-1 cell types as mice age (Montecino-Rodriguez and Dorshkind, 2012; Holodick and Rothstein, 2015; Holodick et al., 2016).

The exact nature of the help being provided for bone marrow B-1PC development by TCR$\alpha\beta$+ CD4+ MHC class II-restricted T cells remains to be more fully explored but required classical TCRα/β MHCII-restricted CD4 T cells, as deletion of TCRα/β and MHCII, but not of TCRγ/δ or CD1 affected bone marrow B-1PC numbers. The data indicate that CD4 T cell-mediated help might be needed for the differentiation but not maintenance of bone marrow B-1PC, as depletion of CD4 T cells in adulthood had no effect bone marrow B-1PC numbers or serum IgM levels. Given that spleen B-1PC development does not require T cell help and thus B-

1PC differentiation per se can occur without T cells, it remains possible that B-1PC reside in a particular bone marrow niche that requires CD4 T cells for its development, but once established is maintained without further need for T cells.

Alternatively, signals provided by CD4 T cells directly to B-1 cells allows their differentiation into bone marrow B-1PC. Although B-1 cells express relatively high levels of CD86 and were shown previously to activate T cells in both, an antigen-specific and non-specific manner (Hsu et al., 2014; Margry et al., 2013; Zimecki and Kapp, 1994), yet very little is known about what impact these interactions have on B-1 cells. NKT cells and TH17 cells have been implicated in activation of B-1 cells during active infection or inflammation (Campos et al., 2006; Wang et al., 2016)., but as we show here, depletion of CD1 does not affect bone marrow B-1PC, and IL-17 is unlikely responsible for regulating steady state nIgM production. T cell derived IL-5 can promote PCh specific nIgM (McKay et al., 2017), but anti-PCh nIgM does not appear to come from bone marrow, but rather from spleen B-1PC and B-1_{sec}. Furthermore, although IL5R deficiency has been shown to reduce serum IgM levels, it did so in a T independent manner (Moon et al., 2004) and more recent studies have shown ILCs to be a source for IL-5 mediated B-1 cell activation (Jackson-Jones et al., 2016; Barbosa et al., 2021).

In summary, our data demonstrate the presence of multiple distinct differentiation pathways that shape the pool of nIgM. The hallmarks of nIgM generated by B-1PC are their short CDR3 regions and the presence of but a handful of distinct Igh-CDR3 region motifs, not previously associated with B-1 cells. This leaves specificities such as phospholipids, PCh and PtC previously associated with B-1 cells (Arnold and Haughton, 1992; Conger et al., 1991; Briles et al., 1981) to the small pool of non-terminally differentiated B-1_{sec}, whose development appears restricted in ontogeny.

2.9 Materials and Methods:

Mice

7-8 week old male and female C57BL/6J (control), B6.129S6-Del(3Cd1d2-Cd1d1)1Sbp/J(CD1d-/-), B6.129P2-*Tcrd*^{tm1Mom}/J(TCRβ-/-)and B6.129P2-*Tcrd*^{tm1Mom}/J(TCRδ-/-) mice and breeding pairs of C57BL/6J, B6.129S2-H2$^{dlAb1\text{-}Ea}$/J (MHCII-/), B6.129P2-*Tcrb*^{tm1Mom} *Tcrd*^{tm1Mom}/J(TCRβδ-/-), B6.129S7-*Rag1*^{tm1Mom}/J (Rag-1-/-) and B6.Cg-Gpi1^{a} Thy1^{a} Igh^{a} /J (Igha) were purchased from The Jackson Laboratory. Six-week-old male and female SPF Swiss Webster mice were ordered from Taconic. Breeding pairs of B6.Cg-Tg(Prdm1-EYFP)1Mnz/J (Blimp-1 YFP) were generously provided by Michel Nussenzweig (The Rockefeller University, NY). Germ-free Swiss Webster mice, age and sex matched to the SPF controls, were generously maintained and provided by Andreas Bäumler (University of California, Davis).

Neonatal chimeras were generated as described previously (Baumgarth et al., 1999). Briefly, neonatal Igha mice were treated twice weekly with intra-peritoneal injections of DS-1.1 (anti-IgMa) in PBS beginning on day one after birth for a total of 2.3 mg over 42 day. Between days 2-4, mice were given also 5x10^{6} donor cells from the peritoneal cavity washout of C57BL/6J (IgMb) mice. Mice were rested for at least 42 days before use in experiments. Reconstituted Rag-1-/- mice were generated by intra-peritoneal injection of 1x10^{6} *auto*MACS sorted peritoneal B-1 cells +/- 1x10^{6} *auto*MACS sorted splenic CD4+ T cells at 3-6 days of age. They were kept for at least 12 weeks before use. Mice were used between 8-14 weeks of age for Blimp-1YFP, Swiss Webster, TCRβδ-/-, TCRδ-/-, CD1d-/-, MHCII-/-, and control (B6, Igha) mice, between 12 weeks-6 months of age for neonatal chimeras and between 12-16 weeks of age for reconstituted Rag-1-/- mice. All mice used for experiments were female unless otherwise

indicated. All mice were maintained in microisolator cages under SPF conditions, were provided mouse chow and water supplied at lib by the UC Davis Animal Care staff and were euthanized by overexposure to CO_2. All procedures were approved by the UC Davis Institutional Animal Care and Use Committee.

B-1 cell magnetic cell separation

Single cell suspensions of peritoneal cavity washout and spleen cells were counted and blocked with anti-FcR (2.4.G2). For B-1 cell enrichment peritoneal cavity cells were labeled with biotinylated anti-F4/80 (F4/80), Gr1 (RA3.6C2), NK1.1(DX5), CD4 (GK1.5), CD8a (53-6.7.3.1), CD23 (B3B4) and CD90.2 (30H12.1) generated in-house and splenic CD4 T cells were enriched by labeling with biotinylated anti- F4/80, Gr-1, CD8a, TCRδ (GL-3), NK1.1, CD19 (ID3), and CD11b (MAC1.13) followed by staining with anti-biotin magnetic beads (Miltenyi Biotec). and passing over a magnetic column (*auto*-MACS, Miltenyi Biotec).

Generation of lineage tracing FlkSwitch chimeras

Recipient C57BL/6 mice (8-12 weeks) were either sub-lethally (750 cGy) or lethally irradiated (1000 cGy, split dose) using a Precision X-Rad 320. Transplantations were performed by FACS-sorting GFP+ developmentally restricted hematopoietic stem cells (drHSC), only present during fetal and neonatal development, and Tom+ HSC (CD150+ cKit+ Sca1+ Lin-) from fetal liver of FlkSwitch mice (Beaudin et al., 2016; Boyer et al., 2011). 200 sorted GFP+ drHSC or Tom+ HSC in 100-200 μL were transferred via retroorbital injection with (for lethally irradiated mice) or without $5x10^6$ whole bone marrow cells from C57BL/6 mice. At 18 weeks, recipients were euthanized, and cell populations were assessed for chimerism by flow cytometry. Long-term multilineage reconstitution was defined as >1% chimerism in all mature blood lineages.

Flow cytometry and FACS sorting

Bone marrow and spleen were processed as previously described (Rothaeusler and Baumgarth, 2006). Briefly, bone marrow was harvested by injecting staining media through the marrow cavity of a long bone, a single cell suspension was made by pipette agitation and filtering through a 70μm nylon mesh. A single cell suspension of spleen was made by grinding the tissue between the frosted ends of two microscope slides and filtered through a 70μm nylon mesh. All samples were then treated with ACK lysis buffer(Rothaeusler and Baumgarth, 2006), re-filtered through nylon mesh, and suspended in staining media. Peritoneal/pleural cavity cells were obtained using staining media flushed into and then aspirated from the peritoneal and pleural cavities with a glass pipet and bulb, or a plastic pipette (Molecular Bio Products Inc.). Trypan Blue exclusion dye was performed on all samples to identify live cells using a hemocytometer or an automated cell counter (Nexcelom Bioscience). Cells were blocked with anti-FcR (2.4.G2), washed and stained with fluorescent antibodies (**Supplemental Table 2.1**).

Phosphatidylcholine-containing liposomes were generously provided by Aaron Kantor (Stanford University, CA). Dead cells were identified using Live/Dead Fixable Aqua or Live/Dead Fixable Violet stain (Invitrogen). Fluorescently labeled cells were read on either a 4-laser, 22-paramter LSR Fortessa (BD Bioscience), or a 5-laser, 30-parameter Symphony (BD Bioscience). FACS-sorting was done using a 3-laser FACSAria (BD Bioscience). Data were analyzed using FlowJo software (FlowJo LLC, kind gift of Adam Treister). Peritoneal B-1 cells are identified as Dump- (CD4, CD8a, Nk1.1, F4/80, Gr-1), CD23-, CD19hi. Bone Marrow and Spleen B-1 cells are identified as Dump-, CD23- C43+, IgD-, IgM+, CD19hi and B-1PC are identified as Dump-, CD23- C43+, IgD-, IgM+, CD19lo/- and Blimp-1 and/or CD138+.

Enzyme-Linked ImmunoSpot (ELISPOT)

IgM antibody secreting cells were enumerated as described previously (Doucett et al., 2005). Briefly, 96-well ELISPOT plates (Multi-Screen HA Filtration, Millipore) were coated with 5μg/ml anti-IgM (331), whole killed Influenza PR8/34 A (400 HAU/ml, In house), Phosphorylcholine-BSA (Biosearch Technologies) (0.625 μg/ml), or 110nm 1,2-Dioleoyl-sn-Glycero-3-Phosphocholine liposomes (FormuMax, 10 mg/ml in 100% ethanol). Non-specific binding was blocked with 4% bovine serum albumin (BSA) in PBS. Tissues were processed as detail above and cells were plated in culture media (RPMI 1640, 10% fetal bovine serum, 292 μg/ml L-glutamine, 100 Units/ml penicillin, 100 μg/ml streptomycin, and 50 μM 2-mercaptoethanol). Cells were two-fold serially diluted and cultured overnight (~16hrs) at 37°C/5% CO_2. Deionized water was used to lyse the cells after which, IgM secretion was revealed with biotinylated anti-IgM (Southern Biotech), followed by streptavadin-horseradish peroxidase (Vector Labs), both diluted in 2% BSA in PBS. Last, substrate solution (3.3 mg 3-amino-9-ethylcarbazole (Sigma Aldrich) dissolved in dimethyl formamide and 0.015% hydrogen perioxide in 0.1M sodium acetate) was added, and the reaction was stopped with deionized water. Spots were enumerated and images captured with the AID EliSpot Reader System (Autoimmun Diagnostika).

Enzyme-Linked Immunosorbant Assay (ELISA)

Sandwich ELISA were performed as previously described(Rothaeusler and Baumgarth, 2006). ELISA plates (MaxiSorp 96 well plates, Thermofisher) were coated with unlabeled anti-IgM (Southern Biotech or mAb 331), whole killed Influenza PR8/34 A (400 HAU/ml, In house),

Phosphorylcholine-BSA (Biosearch Technologies) (0.625 μg/ml), or 110nm 1,2-Dioleoyl-sn-Glycero-3-Phosphocholine liposomes (FormuMax, 10 mg/ml in 100% ethanol). Non-specific binding was blocked with 1% newborn calf serum, 0.1% dried milk powder, and 0.05% Tween20 in PBS (ELISA blocking buffer). Serum and standards were added to the plate at previously determined predilutions and were two-fold serially diluted. Binding was revealed with biotinylated anti-IgM (Southern Biotech), anti-IgMa (BD Bioscience) or anti-IgMb (BD Bioscience), then streptavadin-horseradish peroxidase (Vector Labs), all diluted in ELISA blocking buffer and substrate (0.005% 3,3',5,5'-tetramethylbenzidine (TMB) in 0.05 M citric acid buffer and 0.015% hydrogen peroxide). The reaction was stopped with 1N sulfuric acid. Absorbance was measured at 450 nm (595 nm reference wavelength) on a spectrophotometer (SpectraMax M5, Molecular Devices). IgM concentrations in the samples were determined by comparison to curves generated by the isotype standards or hyperimmune serum (influenza). The PCh standard was a kind gift from Karen Haas (Wake Forest University, NC).

Autoantigen Array

Ten μl of serum from TCRβ/δ-/-, CD4+ depleted Ig-Allotype chimeras, and B-1 cell reconstituted Rag1 -/- mice, as well as their T cell sufficient controls were treated with DNAse1, diluted 1:50 and incubated with the autoantigen array chip. IgM binding to the autoantigens was detected with Cy5 labeled anti-IgM and the chips were read using GenePix® 4400A Microarray Scanner (Molecular Devices). The images were analyzed using GenePix7.0 software (Molecular Devices). The average net fluorescent intensity of each autoantigen was normalized to an internal IgM control.

BCR Sequencing and Repertoire Analysis

The following populations of cells from Blimp-1 YFP reporter mice were FACS sorted into RLT buffer (Qiagen) using FACSAria: BM CD5+ B-1 (Dump-, CD23- C43+, IgD-, IgM+, CD19hi, CD5+), BM CD5- B-1(Dump-, CD23- C43+, IgD-, IgM+, CD19hi, CD5-), BM B-1PC (Dump-, CD23- C43+, IgD-, IgM+, CD19lo/- and Blimp-1). Total cellular RNA was extracted using the RNeasy Mini kit by following the manufacturer's protocol (Qiagen). Approximately 20ng of RNA was used for reverse transcription using the iScript cDNA synthesis kit (BioRad). Mouse IGH V gene transcripts were amplified by two rounds of nested PCR starting from 2.5 µl of cDNA as template using the primers in **Supplemental Table 2.2**. Inner primers were appended to Illumina Nextera sequencing tags (F tag: 5′-TCGTCGGCAGCGTCAGATGTGTATAAGAGACAG-3′ R tag: 5′-GTCTCGTGGGCTCGGAGATGTGTATAAGAGACAG-3′).

All PCR reactions were performed in 96-well plates in a total volume of 25 µl containing 200 nM of each primer. In brief, 200nM of 5' oligo and equimolar mixture of 3' oligos (final concentration 200nM) were used for nested PCRs (sequences listed key resource table as Nested PCR1 primers and Nested PCR2 primers), using High-Fidelity Platinum PCR Supermix (Invitrogen). Nested PCR1 was performed as follows: Denaturation at 94 °C for 15 min followed by 50 cycles of 94°C for 30s, 60°C for 30s, 72°C for 55s, and final incubation at 72°C for 10 min. Nested PCR2 was performed using with 0.5 µl of unpurified first-round PCR product as template. Conditions were as follows: 94°C for 15 min followed by 50 cycles of 94°C for 30s, 68 °C for 30s, 72°C for 45s, and final incubation at 72°C for 10 min.

Nextera (Illumina) indices were added via PCR described earlier (Tipton et al., 2015). Final purified PCR products were analysed, pooled and denatured before running on a MiSeq

(Illumina) using the 300bp×2 v3 kit with a depth of approximately 500,000 sequences per sample.

Sequences were quality filtered using length thresholds of 200-600bp and eliminating any sequences with more than 15bp less than Q30, more than 5bp less than Q20, and any bp less than Q10. Sequences were aligned with IMGT/HighVquest (Alamyar et al., 2012) and were then analyzed for V region mutations and clonality using programs developed in-house and made previously available for public use. All clonal assignments were based on matching V and J regions, matching CDR3 length, and 85% CDR3 homology. Matlab or R scripts were used for visualization (Tipton et al., 2015). BCR sequences are deposited in the Sequences Read Archive (SRA), accession # PRJNA781755.

Quantification and Statistical Analysis

All statistics were done with the help of Prism software (GraphPad Software) or the R software version 4.0.3 (R Core Team (2020). R: A language and environment for statistical computing. R Foundation for Statistical Computing, Vienna, Austria. URL https://www.R-project.org/) with packages ggseqlogo (Omar Wagih (2017). ggseqlogo: A 'ggplot2' Extension for Drawing Publication-Ready Sequence Logos. R package version 0.1. https://CRAN.R-project.org/package=ggseqlogo) and circlize (Gu et al., 2014).

Comparisons between two groups were done using a two-tailed student t test. For more than two groups, a one-way ANOVA was performed with post hoc analysis for significant differences between individual groups using Tukey's correction for multiple comparisons. Time courses were analyzed using a two-way ANOVA with post hoc analysis for differences between

conditions at each time point using a Šidák correction for multiple correction. A $p < 0.05$ was considered statistically significant.

2.10 References

Alamyar, E., P. Duroux, M.P. Lefranc, and V. Giudicelli. 2012. IMGT® tools for the nucleotide analysis of immunoglobulin (IG) and t cell receptor (TR) V-(D)-J repertoires, polymorphisms, and IG mutations: IMGT/V-QUEST and IMGT/HighV-QUEST for NGS. *Methods Mol. Biol.* 882:569–604. doi:10.1007/978-1-61779-842-9_32.

Alugupalli, K.R., and R.M. Gerstein. 2005. Divide and conquer: division of labor by B-1 B cells. *Immunity*. 23:1–2. doi:10.1016/J.IMMUNI.2005.07.001.

Alugupalli, K.R., R.M. Gerstein, J. Chen, E. Szomolanyi-Tsuda, R.T. Woodland, and J.M. Leong. 2003. The resolution of relapsing fever borreliosis requires IgM and is concurrent with expansion of B1b lymphocytes. *J. Immunol.* 170:3819–3827. doi:10.4049/JIMMUNOL.170.7.3819.

Arnold, L.W., and G. Haughton. 1992. Autoantibodies to Phosphatidylcholine: The Murine Antibromelain RBC Response. *Ann. N. Y. Acad. Sci.* 651:354–359. doi:10.1111/j.1749-6632.1992.tb24635.x.

Atif, S.M., S.L. Gibbings, E.F. Redente, F.A. Camp, R.M. Torres, R.M. Kedl, P.M. Henson, and C. V Jakubzick. 2018. Immune surveillance by natural IgM is required for early neoantigen recognition and initiation of adaptive immunity. *Am. J. Respir. Cell Mol. Biol.* 59:580–591. doi:10.1165/rcmb.2018-0159OC.

Barbosa, C.H.D., L. Lantier, J. Reynolds, J. Wang, and F. Re. 2021. Critical role of IL-25-ILC2-IL-5 axis in the production of anti-Francisella LPS IgM by B1 B cells. *PLOS Pathog.* 17:e1009905. doi:10.1371/JOURNAL.PPAT.1009905.

Baumgarth, N. 2011. The double life of a B-1 cell: Self-reactivity selects for protective effector functions. *Nat. Rev. Immunol.* 11:34–46. doi:10.1038/nri2901.

Baumgarth, N., O.C. Herman, G.C. Jager, L. Brown, L.A. Herzenberg, and L.A. Herzenberg. 1999. Innate and acquired humoral immunities to influenza virus are mediated by distinct arms of the immune system. *Proc. Natl. Acad. Sci. U. S. A.* 96:2250–2255. doi:10.1073/PNAS.96.5.2250.

Baumgarth, N., O.C. Herman, G.C. Jager, L.E. Brown, L.A. Herzenberg, and J. Chen. 2000. B-1 and B-2 cell-derived immunoglobulin M antibodies are nonredundant components of the protective response to influenza virus infection. *J Exp Med*. 192:271–280. doi:10.1084/jem.192.2.271.

Beaudin, A.E., S.W. Boyer, J. Perez-Cunningham, G.E. Hernandez, S.C. Derderian, C. Jujjavarapu, E. Aaserude, T. MacKenzie, and E.C. Forsberg. 2016. A Transient Developmental Hematopoietic Stem Cell Gives Rise to Innate-like B and T Cells. *Cell Stem Cell*. 19:768–783. doi:10.1016/j.stem.2016.08.013.

Boes, M., C. Esau, M.B. Fischer, T. Schmidt, M. Carroll, and J. Chen. 1998. Enhanced B-1 cell development, but impaired IgG antibody responses in mice deficient in secreted IgM. *J. Immunol.* 160:4776–87.

Boes, M., T. Schmidt, K. Linkemann, B.C. Beaudette, A. Marshak-Rothstein, and J. Chen. 2000. Accelerated development of IgG autoantibodies and autoimmune disease in the absence of secreted IgM. *Proc Natl Acad Sci U S A*. 97:1184–1189. doi:10.1073/pnas.97.3.1184.

Bos, N.A., H. Kimura, C.G. Meeuwsen, H. De Visser, M.P. Hazenberg, B.S. Wostmann, J.R. Pleasants, R. Benner, and D.M. Marcus. 1989. Serum immunoglobulin levels and naturally occurring antibodies against carbohydrate antigens in germ-free BALB/c mice fed chemically defined ultrafiltered diet. *Eur J Immunol*. 19:2335–2339. doi:10.1002/eji.1830191223.

Boyer, S., A. Beaudin, and E. Forsberg. 2012. Mapping differentiation pathways from hematopoietic stem cells using Flk2/Flt3 lineage tracing. *Cell Cycle*. 11:3180–3188. doi:10.4161/CC.21279.

Boyer, S.W., A. V. Schroeder, S. Smith-Berdan, and E.C. Forsberg. 2011. All Hematopoietic Cells Develop from Hematopoietic Stem Cells through Flk2/Flt3-Positive Progenitor Cells. *Cell Stem Cell*. 9:64–73. doi:10.1016/J.STEM.2011.04.021.

Briles, D.E., M. Nahm, K. Schroer, J. Davie, P. Baker, J. Kearney, and R. Barletta. 1981. Antiphosphocholine antibodies found in normal mouse serum are protective against intravenous infection with type 3 streptococcus pneumoniae. *J Exp Med*. 153:694–705. doi:10.1084/jem.153.3.694.

Campos, R.A., M. Szczepanik, M. Lisbonne, A. Itakura, M. Leite-de-Moraes, and P.W. Askenase. 2006. Invariant NKT Cells Rapidly Activated via Immunization with Diverse Contact Antigens Collaborate In Vitro with B-1 Cells to Initiate Contact Sensitivity. *J. Immunol.* 177:3686–3694. doi:10.4049/JIMMUNOL.177.6.3686.

Carmack, C.E., S.A. Shinton, K. Hayakawa, and R.R. Hardy. Rearrangement and Selection of VH11 in the Ly-1 B Cell Lineage.

Chen, Y., Y.-B. Park, E. Patel, and G.J. Silverman. 2009. IgM Antibodies to Apoptosis-Associated Determinants Recruit C1q and Enhance Dendritic Cell Phagocytosis of Apoptotic Cells. *J. Immunol.* 182:6031–6043. doi:10.4049/JIMMUNOL.0804191.

Choi, Y.S., and N. Baumgarth. 2008. Dual role for B-1a cells in immunity to influenza virus infection. *J. Exp. Med.* 205:3053–3064. doi:10.1084/JEM.20080979.

Choi, Y.S., J.A. Dieter, K. Rothaeusler, Z. Luo, and N. Baumgarth. 2012. B-1 cells in the bone marrow are a significant source of natural IgM. *Eur J Immunol*. 42:120–129. doi:10.1002/eji.201141890.

Conger, J., H. Sage, S. Kawaguchi, and R. Corley. 1991. Properties of murine antibodies from different V region families specific for bromelain-treated mouse erythrocytes. *J. Immunol.* 146:1216–1219.

Doucett, V.P., W. Gerhard, K. Owler, D. Curry, L. Brown, and N. Baumgarth. 2005. Enumeration and characterization of virus-specific B cells by multicolor flow cytometry. *J. Immunol. Methods*. 303:40–52. doi:10.1016/j.jim.2005.05.014.

Ehrenstein, M.R., H.T. Cook, and M.S. Neuberger. 2000. Deficiency in serum immunoglobulin (Ig)M predisposes to development of IgG autoantibodies. *J Exp Med*. 191:1253–1258. doi:10.1084/jem.191.7.1253.

Ehrenstein, M.R., and C.A. Notley. 2010. The importance of natural IgM: Scavenger, protector and regulator. *Nat. Rev. Immunol.* 10:778–786. doi:10.1038/nri2849.

Ekiert, D.C., A.K. Kashyap, J. Steel, A. Rubrum, G. Bhabha, R. Khayat, J.H. Lee, M.A. Dillon, R.E. O'Neil, A.M. Faynboym, M. Horowitz, L. Horowitz, A.B. Ward, P. Palese, R. Webby, R.A. Lerner, R.R. Bhatt, and I.A. Wilson. 2012. Cross-neutralization of influenza A viruses mediated by a single antibody loop. *Nat. 2012 4897417*. 489:526–532. doi:10.1038/nature11414.

Feeney, A.J. 1990. Lack of N regions in fetal and neonatal mouse immunoglobulin V-D-J junctional sequences. *J. Exp. Med.* 172:1377. doi:10.1084/JEM.172.5.1377.

Forster, I., and K. Rajewsky. 1987. Expansion and functional activity of Ly-1+ B cells upon transfer of peritoneal cells into allotype-congenic, newborn mice. *Eur J Immunol*. 17:521–528. doi:10.1002/eji.1830170414.

Genestier, L., M. Taillardet, P. Mondiere, H. Gheit, C. Bella, and T. Defrance. 2007. TLR Agonists Selectively Promote Terminal Plasma Cell Differentiation of B Cell Subsets Specialized in Thymus-Independent Responses. *J. Immunol.* 178:7779–7786. doi:10.4049/jimmunol.178.12.7779.

Gershon, R.K. 1974. T cell control of antibody production. *Contemp. Top. Immunobiol.* 3:1–40. doi:10.1007/978-1-4684-3045-5_1.

Goldstein, M.F., A.L. Goldstein, E.H. Dunsky, D.J. Dvorin, G.A. Belecanech, and K. Shamir. 2006. Selective IgM immunodeficiency: retrospective analysis of 36 adult patients with review of the literature. *Ann. Allergy, Asthma Immunol.* 97:717–730. doi:10.1016/S1081-1206(10)60962-3.

Goodridge, A., T. Zhang, T. Miyata, S. Lu, and L.W. Riley. 2014. Antiphospholipid IgM antibody response in acute and chronic Mycobacterium tuberculosis mouse infection model. *Clin. Respir. J.* 8:137–144. doi:10.1111/CRJ.12049.

Gu, Z., L. Gu, R. Eils, M. Schlesner, and B. Brors. 2014. circlize implements and enhances

circular visualization in R. *Bioinformatics*. 30:2811–2812. doi:10.1093/BIOINFORMATICS/BTU393.

Guo, C., Q. Wang, X. Cao, Y. Yang, X. Liu, L. An, R. Cai, M. Du, G. Wang, Y. Qiu, Z. Peng, C. Wang, X. Wang, X. Ma, X. Liu, X. Wang, M. Du, Y. Qiu, X. Ma, J. Han, S. Ni, X. Tan, L. Jin, S. Yu, H. Wang, and C. Wang. 2016. High-Throughput Sequencing Reveals Immunological Characteristics of the TRB-/IgH-CDR3 Region of Umbilical Cord Blood. *J. Pediatr.* 176:69-78.e1. doi:10.1016/J.JPEDS.2016.05.078.

Gupta, S., and A. Gupta. 2017. Selective IgM Deficiency—An Underestimated Primary Immunodeficiency. *Front. Immunol.* 8:1056. doi:10.3389/FIMMU.2017.01056.

Haas, K.M., J.C. Poe, D.A. Steeber, and T.F. Tedder. 2005. B-1a and B-1b Cells Exhibit Distinct Developmental Requirements and Have Unique Functional Roles in Innate and Adaptive Immunity to S. pneumoniae. *Immunity*. 23:7–18. doi:10.1016/J.IMMUNI.2005.04.011.

Hardy, R.R., C.E. Carmack, S.A. Shinton, R.J. Riblet, and K. Hayakawa. 1989. A single VH gene is utilized predominantly in anti-BrMRBC hybridomas derived from purified Ly-1 B cells. Definition of the VH11 family. *J. Immunol.* 142.

Haury, M., A. Sundblad, A. Grandien, C. Barreau, A. Coutinho, and A. Nobrega. 1997. The repertoire of serum IgM in normal mice is largely independent of external antigenic contact. *Eur. J. Immunol.* 27:1557–1563. doi:10.1002/EJI.1830270635.

Hayakawa, K., M. Asano, S.A. Shinton, M. Gui, D. Allman, C.L. Stewart, J. Silver, and R.R. Hardy. 1999. Positive selection of natural autoreactive B cells. *Science*. 285:113–116. doi:10.1126/SCIENCE.285.5424.113.

Hayakawa, K., M. Asano, S.A. Shinton, M. Gui, L.J. Wen, J. Dashoff, and R.R. Hardy. 2003. Positive selection of anti-thy-1 autoreactive B-1 cells and natural serum autoantibody production independent from bone marrow B cell development. *J. Exp. Med.* 197:87–99. doi:10.1084/jem.20021459.

Hayakawa, K., C.E. Carmnack, S.A. Shinton, and R.R. Hardy. 1992. Selection of Autoantibody Specificities in the Ly-1 B Subseta. *Ann. N. Y. Acad. Sci.* 651:346–353. doi:10.1111/J.1749-6632.1992.TB24634.X.

Hayakawa, K., and R.R. Hardy. 2000. Development and function of B-1 cells. *Curr. Opin. Immunol.* 12:346–354. doi:10.1016/S0952-7915(00)00098-4.

Hayakawa, K., R.R. Hardy, and M. Honda. 1984. Ly-1 B cells: Functionally distinct lymphocytes that secrete IgM autoantibodies. *Proc. Natl. Acad. Sci. U. S. A.* 81:2494–2498. doi:10.1073/pnas.81.8.2494.

Heyman, B. 2000. Regulation of antibody responses via antibodies, complement, and Fc receptors. *Annu. Rev. Immunol.* 18:709–737.

doi:10.1146/ANNUREV.IMMUNOL.18.1.709.

Holodick, N.E., and T.L. Rothstein. 2015. B cells in the aging immune system: Time to consider B-1 cells. *Ann. N. Y. Acad. Sci.* 1362:176–187. doi:10.1111/nyas.12825.

Holodick, N.E., T. Vizconde, T.J. Hopkins, and T.L. Rothstein. 2016. Age-Related Decline in Natural IgM Function: Diversification and Selection of the B-1a Cell Pool with Age. *J. Immunol.* 196:4348–4357. doi:10.4049/jimmunol.1600073.

Hooijkaas, H., A.A. van der Linde-Preesman, S. Benne, and R. Benner. 1985. Frequency analysis of the antibody specificity repertoire of mitogen-reactive B cells and "spontaneously" occurring "background" plaque-forming cells in nude mice. *Cell Immunol*. 92:154–162. doi:10.1016/0008-8749(85)90073-5.

Hsu, L.-H., K.-P. Li, K.-H. Chu, and B.-L. Chiang. 2014. A B-1a cell subset induces Foxp3− T cells with regulatory activity through an IL-10-independent pathway. *Cell. Mol. Immunol. 2014 123*. 12:354–365. doi:10.1038/cmi.2014.56.

Jackson-Jones, L.H., S.M. Duncan, M.S. Magalhaes, S.M. Campbell, R.M. Maizels, H.J. McSorley, J.E. Allen, and C. Bénézech. 2016. Fat-associated lymphoid clusters control local IgM secretion during pleural infection and lung inflammation. *Nat. Commun. 2016 71*. 7:1–14. doi:10.1038/ncomms12651.

Jayasekera, J.P., E.A. Moseman, and M.C. Carroll. 2007. Natural Antibody and Complement Mediate Neutralization of Influenza Virus in the Absence of Prior Immunity. *J. Virol.* 81:3487–3494. doi:10.1128/JVI.02128-06/ASSET/8C94F051-B607-44FF-AF2E-5D2CA5E831DA/ASSETS/GRAPHIC/ZJV0070789240006.JPEG.

Kantor, A.B., and L.A. Herzenberg. 1993. Origin of murine B cell lineages. *Annu. Rev. Immunol.* 11:501–538. doi:10.1146/annurev.iy.11.040193.002441.

Kawahara, T., H. Ohdan, G. Zhao, Y.G. Yang, and M. Sykes. 2003. Peritoneal cavity B cells are precursors of splenic IgM natural antibody-producing cells. *J Immunol*. 171:5406–5414. doi:10.4049/jimmunol.171.10.5406.

Kearney, J.F., P. Patel, E.K. Stefanov, and R.G. King. 2015. Natural antibody repertoires: Development and functional role in inhibiting allergic airway disease. *Annu. Rev. Immunol.* 33:475–504. doi:10.1146/annurev-immunol-032713-120140.

Keightley, R.G., M.D. Cooper, and A.R. Lawton. 1976. The T Cell Dependence of B Cell Differentiation Induced by Pokeweed Mitogen. *J. Immunol.* 117.

Kenny, J.J., L.J. Yaffe, A. Ahmed, and E.S. Metcalf. 1983. Contribution of Lyb 5+ and Lyb 5- B cells to the primary and secondary phosphocholine-specific antibody response. *J. Immunol.* 130.

Kreuk, L.S.M., M.A. Koch, L.C. Slayden, N.A. Lind, S. Chu, H.P. Savage, A.B. Kantor, N. Baumgarth, and G.M. Barton. 2019. B cell receptor and toll-like receptor signaling coordinate to control distinct B-1 responses to both self and the microbiota. *Elife*. 8. doi:10.7554/eLife.47015.

Lalor, P.A., L.A. Herzenberg, S. Adams, and A.M. Stall. 1989. Feedback regulation of murine Ly-1 B cell development. *Eur J Immunol*. 19:507–513. doi:10.1002/eji.1830190315.

Li, Y.S., Y. Zhou, L. Tang, S.A. Shinton, K. Hayakawa, and R.R. Hardy. 2015. A developmental switch between fetal and adult B lymphopoiesis. *Ann. N. Y. Acad. Sci.* 1362:8–15. doi:10.1111/NYAS.12769.

Madsen, L., N. Labrecque, J. Engberg, A. Dierich, A. Svejgaard, C. Benoist, D. Mathis, and L. Fugger. 1999. Mice lacking all conventional MHC class II genes. *Proc Natl Acad Sci U S A*. 96:10338–10343. doi:10.1073/pnas.96.18.10338.

Margry, B., W.H. Wieland, P.J. van Kooten, W. van Eden, and F. Broere. 2013. Peritoneal cavity B-1a cells promote peripheral CD4+ T-cell activation. *Eur. J. Immunol.* 43:2317–2326. doi:10.1002/eji.201343418.

McKay, J.T., M.A. Haro, C.A. Daly, R.D. Yammani, B. Pang, W.E. Swords, and K.M. Haas. 2017. PD-L2 Regulates B-1 Cell Antibody Production against Phosphorylcholine through an IL-5-Dependent Mechanism. *J Immunol*. 199:2020–2029. doi:10.4049/jimmunol.1700555.

Mercolino, T.J., L.W. Arnold, L.A. Hawkins, and G. Haughton. 1988. Normal mouse peritoneum contains a large population of Ly-1+ (CD5) B cells that recognize phosphatidyl choline. Relationship to cells that secrete hemolytic antibody specific for autologous erythrocytes. *J Exp Med*. 168:687–698.

Mi, Q.S., L. Zhou, D.H. Schulze, R.T. Fischer, A. Lustig, L.J. Rezanka, D.M. Donovan, D.L. Longo, and J.J. Kenny. 2000. Highly reduced protection against Streptococcus pneumoniae after deletion of a single heavy chain gene in mouse. *Proc. Natl. Acad. Sci. U. S. A.* 97:6031–6036. doi:10.1073/pnas.110039497.

Mombaerts, P., A.R. Clarke, M.A. Rudnicki, J. Iacomini, S. Itohara, J.J. Lafaille, L. Wang, Y. Ichikawa, R. Jaenisch, M.L. Hooper, and S. Tonegawa. 1992. Mutations in T-cell antigen receptor genes α and β block thymocyte development at different stages. *Nature*. 360:225–231. doi:10.1038/360225a0.

Montecino-Rodriguez, E., and K. Dorshkind. 2012. B-1 B cell development in the fetus and adult. *Immunity*. 36:13–21. doi:10.1016/J.IMMUNI.2011.11.017.

Moon, B., S. Takaki, K. Miyake, and K. Takatsu. 2004. The Role of IL-5 for Mature B-1 Cells in Homeostatic Proliferation, Cell Survival, and Ig Production. *J. Immunol.* 172:6020–6029. doi:10.4049/jimmunol.172.10.6020.

New, J.S., B.L.P. Dizon, C.F. Fucile, A.F. Rosenberg, J.F. Kearney, and R.G. King. 2020. Neonatal Exposure to Commensal-Bacteria-Derived Antigens Directs Polysaccharide-Specific B-1 B Cell Repertoire Development. *Immunity*. 53:172-186.e6. doi:10.1016/j.immuni.2020.06.006.

Nguyen, T.T., R.A. Elsner, and N. Baumgarth. 2015. Natural IgM prevents autoimmunity by enforcing B cell central tolerance induction. *J Immunol*. 194:1489–1502. doi:10.4049/jimmunol.1401880.

Nguyen, T.T.T., B.A. Graf, T.D. Randall, and N. Baumgarth. 2017. sIgM-FcμR Interactions Regulate Early B Cell Activation and Plasma Cell Development after Influenza Virus Infection. *J. Immunol.* 199:1635–1646. doi:10.4049/JIMMUNOL.1700560.

Noelle, R., J. Ledbetter, A.A.-I. today, and undefined 1992. CD40 and its ligand, an essential ligand-receptor pair for thymus-dependent B-cell activation. *Elsevier*.

Notley, C.A., M.A. Brown, G.P. Wright, and M.R. Ehrenstein. 2011. Natural IgM is required for suppression of inflammatory arthritis by apoptotic cells. *J Immunol*. 186:4967–4972. doi:10.4049/jimmunol.1003021.

Ochsenbein, A.F., T. Fehr, C. Lutz, M. Suter, F. Brombacher, H. Hengartner, and R.M. Zinkernagel. 1999. Control of early viral and bacterial distribution and disease by natural antibodies. *Science (80-.).* 286:2156–2159.

Ogden, C.A., R. Kowalewski, Y. Peng, V. Montenegro, and K.B. Elkon. 2009. IGM is required for efficient complement mediated phagocytosis of apoptotic cells in vivo. *http://dx.doi.org/10.1080/08916930500124452*. 38:259–264. doi:10.1080/08916930500124452.

Van Oudenaren, A., J.J. Haaijman, and R. Benner. 1984. Frequencies of background cytoplasmic Ig-containing cells in various lymphoid organs of athymic and euthymic mice as a function of age and immune status. *Immunology*. 51:735–742.

Patel, P.S., and J.F. Kearney. 2015. Neonatal Exposure to Pneumococcal Phosphorylcholine Modulates the Development of House Dust Mite Allergy during Adult Life. *J. Immunol.* 194:5838–5850. doi:10.4049/JIMMUNOL.1500251/-/DCSUPPLEMENTAL.

Prohaska, T.A., X. Que, C.J. Diehl, S. Hendrikx, M.W. Chang, K. Jepsen, C.K. Glass, C. Benner, and J.L. Witztum. 2018. Massively Parallel Sequencing of Peritoneal and Splenic B Cell Repertoires Highlights Unique Properties of B-1 Cell Antibodies. *J. Immunol.* 200:ji1700568. doi:10.4049/jimmunol.1700568.

Quartier, P., P.K. Potter, M.R. Ehrenstein, M.J. Walport, and M. Botto. 2005. Predominant role of IgM-dependent activation of the classical pathway in the clearance of dying cells by murine bone marrow-derived macrophages in vitro. *Eur. J. Immunol.* 35:252–260. doi:10.1002/EJI.200425497.

Que, X., M.Y. Hung, C. Yeang, A. Gonen, T.A. Prohaska, X. Sun, C. Diehl, A. Määttä, D.E. Gaddis, K. Bowden, J. Pattison, J.G. MacDonald, S. Ylä-Herttuala, P.L. Mellon, C.C. Hedrick, K. Ley, Y.I. Miller, C.K. Glass, K.L. Peterson, C.J. Binder, S. Tsimikas, and J.L. Witztum. 2018. Oxidized phospholipids are proinflammatory and proatherogenic in hypercholesterolaemic mice. *Nature*. 558:301–306. doi:10.1038/s41586-018-0198-8.

Rettig, T.A., C. Ward, B.A. Bye, M.J. Pecaut, and S.K. Chapes. 2018. Characterization of the naive murine antibody repertoire using unamplified high-throughput sequencing. *PLoS One*. 13. doi:10.1371/JOURNAL.PONE.0190982.

Reynolds, A.E., M. Kuraoka, and G. Kelsoe. 2015a. Natural IgM is produced by CD5- plasma cells that occupy a distinct survival niche in bone marrow. *J Immunol*. 194:231–242. doi:10.4049/jimmunol.1401203.

Reynolds, A.E., M. Kuraoka, and G. Kelsoe. 2015b. Natural IgM Is Produced by CD5 − Plasma Cells That Occupy a Distinct Survival Niche in Bone Marrow. *J. Immunol.* 194:231–242. doi:10.4049/jimmunol.1401203.

Rothaeusler, K., and N. Baumgarth. 2006. Evaluation of intranuclear BrdU detection procedures for use in multicolor flow cytometry. *Cytom. Part A*. 69:249–259. doi:10.1002/cyto.a.20252.

Rothstein, T.L., D.O. Griffin, N.E. Holodick, T.D. Quach, and H. Kaku. 2013. Human B-1 cells take the stage. *Ann. N. Y. Acad. Sci.* 1285:97–114. doi:10.1111/NYAS.12137.

Savage, H.P., K. Klasener, F.L. Smith, Z. Luo, M. Reth, and N. Baumgarth. 2019. TLR induces reorganization of the IgM-BCR complex regulating murine B-1 cell responses to infections. *Elife*. 8. doi:10.7554/ELIFE.46997.

Savage, H.P., V.M. Yenson, S.S. Sawhney, B.J. Mousseau, F.E. Lund, and N. Baumgarth. 2017. Blimp-1–dependent and –independent natural antibody production by B-1 and B-1–derived plasma cells. *J. Exp. Med.* 214:2777–2794. doi:10.1084/jem.20161122.

Savitsky, D., and K. Calame. 2006. B-1 B lymphocytes require Blimp-1 for immunoglobulin secretion. *J. Exp. Med.* 203:2305–2314. doi:10.1084/JEM.20060411.

Shapiro-Shelef, M., K.I. Lin, L.J. McHeyzer-Williams, J. Liao, M.G. McHeyzer-Williams, and K. Calame. 2003. Blimp-1 is required for the formation of immunoglobulin secreting plasma cells and pre-plasma memory B cells. *Immunity*. 19:607–620.

Smith, F.L., and N. Baumgarth. 2019. B-1 cell responses to infections. *Curr. Opin. Immunol.* 57:23–31. doi:10.1016/j.coi.2018.12.001.

Stall, A.M., S. Adams, L.A. Herzenberg, and A.B. Kantor. 1992. Characteristics and Development of the Murine B-lb (Ly-1 B Sister) Cell Population. *Ann. N. Y. Acad. Sci.* 651:33–43. doi:10.1111/j.1749-6632.1992.tb24591.x.

Takeuchi, T., T. Nakagawa, Y. Maeda, S. Hirano, M. Sasaki-Hayashi, S. Makino, A. Shimizu, T. Takeuchi~, T. Nakagawa~, Y. Maeda~, S. Hirano~, M. Sasaki-Hayashia, S. Makinoa, and A. Shimizub. 2009. Functional Defect of B Lymphocytes in a Patient with Selective IgM Deficiency Associated with Systemic Lupus Erythematosus. *http://dx.doi.org/10.3109/08916930109001959*. 34:115–122. doi:10.3109/08916930109001959.

Tipton, C.M., C.F. Fucile, J. Darce, A. Chida, T. Ichikawa, I. Gregoretti, S. Schieferl, J. Hom, S. Jenks, R.J. Feldman, R. Mehr, C. Wei, F.E.H. Lee, W.C. Cheung, A.F. Rosenberg, and I. Sanz. 2015. Diversity, cellular origin and autoreactivity of antibody-secreting cell population expansions in acute systemic lupus erythematosus. *Nat. Immunol.* 16:755–765. doi:10.1038/ni.3175.

Tuominen, A., Y.I. Miller, L.F. Hansen, Y.A. Kesäniemi, J.L. Witztum, and S. Hörkkö. 2006. A natural antibody to oxidized cardiolipin binds to oxidized low-density lipoprotein, apoptotic cells, and atherosclerotic lesions. *Arterioscler. Thromb. Vasc. Biol.* 26:2096–2102. doi:10.1161/01.ATV.0000233333.07991.4A.

Upadhye, A., P. Srikakulapu, A. Gonen, S. Hendrikx, H.M. Perry, A. Nguyen, C. McSkimming, M.A. Marshall, J.C. Garmey, A.M. Taylor, T.P. Bender, S. Tsimikas, N.E. Holodick, T.L. Rothstein, J.L. Witztum, and C.A. McNamara. 2019. Diversification and CXCR4-Dependent Establishment of the Bone Marrow B-1a Cell Pool Governs Atheroprotective IgM Production Linked to Human Coronary Atherosclerosis. *Circ. Res.* 125:e55–e70. doi:10.1161/CIRCRESAHA.119.315786.

Waffarn, E.E., C.J. Hastey, N. Dixit, Y. Soo Choi, S. Cherry, U. Kalinke, S.I. Simon, and N. Baumgarth. 2015. Infection-induced type I interferons activate CD11b on B-1 cells for subsequent lymph node accumulation. *Nat. Commun.* 6. doi:10.1038/NCOMMS9991.

Wang, H., D.M. Shin, S. Abbasi, S. Jain, A.L. Kovalchuk, N. Beaty, S. Chen, I. Gonzalez-Garcia, and H.C. Morse. 2012. Expression of plasma cell alloantigen 1 defines layered development of B-1a B-cell subsets with distinct innate-like functions. *Proc. Natl. Acad. Sci. U. S. A.* 109:20077–20082. doi:10.1073/PNAS.1212428109/-/DCSUPPLEMENTAL.

Wang, X., K. Ma, M. Chen, K.-H. Ko, B.-J. Zheng, and L. Lu. 2016. IL-17A Promotes Pulmonary B-1a Cell Differentiation via Induction of Blimp-1 Expression during Influenza Virus Infection. *PLOS Pathog.* 12:e1005367. doi:10.1371/JOURNAL.PPAT.1005367.

Wardemann, H., T. Boehm, N. Dear, and R. Carsetti. 2002. B-1a B Cells that Link the Innate and Adaptive Immune Responses Are Lacking in the Absence of the Spleen. *J. Exp. Med.* 195:771. doi:10.1084/JEM.20011140.

Wasserman, R., Y.S. Li, S.A. Shinton, C.E. Carmack, T. Manser, D.L. Wiest, K. Hayakawa, and R.R. Hardy. 1998. A Novel Mechanism for B Cell Repertoire Maturation Based on Response by B Cell Precursors to Pre–B Receptor Assembly. *J. Exp. Med.* 187:259–264. doi:10.1084/JEM.187.2.259.

Wong, J.B., S.L. Hewitt, L.M. Heltemes-Harris, M. Mandal, K. Johnson, K. Rajewsky, S.B. Koralov, M.R. Clark, M.A. Farrar, and J.A. Skok. B-1a cells acquire their unique characteristics by bypassing the pre-BCR selection stage. doi:10.1038/s41467-019-12824-z.

Yang, Y., C. Wang, Q. Yang, A.B. Kantor, H. Chu, E.E.B. Ghosn, G. Qin, S.K. Mazmanian, J. Han, and L.A. Herzenberg. 2015. Distinct mechanisms define murine B cell lineage immunoglobulin heavy chain (IgH) repertoires. *Elife*. 4. doi:10.7554/ELIFE.09083.

Yu, L., and Y. Guan. 2014. Immunologic basis for long HCDR3s in broadly neutralizing antibodies against HIV-1. *Front. Immunol.* 5:250. doi:10.3389/FIMMU.2014.00250/BIBTEX.

Yuan, J., C.K. Nguyen, X. Liu, C. Kanellopoulou, and S.A. Muljo. 2012. Lin28b reprograms adult bone marrow hematopoietic progenitors to mediate fetal-like lymphopoiesis. *Science (80-.).* 335:1195–1200. doi:10.1126/science.1216557.

Zeng, Z., B.G.J. Surewaard, C.H.Y. Wong, C. Guettler, B. Petri, R. Burkhard, M. Wyss, H. Le Moual, R. Devinney, G.C. Thompson, J. Blackwood, A.R. Joffe, K.D. McCoy, C.N. Jenne, and P. Kubes. 2018. Sex-hormone-driven innate antibodies protect females and infants against EPEC infection. *Nat. Immunol.* 19:1100–1111. doi:10.1038/s41590-018-0211-2.

Zimecki, M., and J.A. Kapp. 1994. Presentation of antigen by B cell subsets. II. The role of CD5 B cells in the presentation of antigen to antigen-specific T cells. *Arch. Immunol. Ther. Exp. (Warsz).* 42:349–353.

Zimecki, M., P.J. Whiteley, C.W. Pierce, and J.A. Kapp. 1994. Presentation of antigen by B cells subsets. I. Lyb-5+ and Lyb-5- B cells differ in ability to stimulate antigen specific T cells. *Arch. Immunol. Ther. Exp. (Warsz).* 42:115–123.

2.11 Figures and Tables

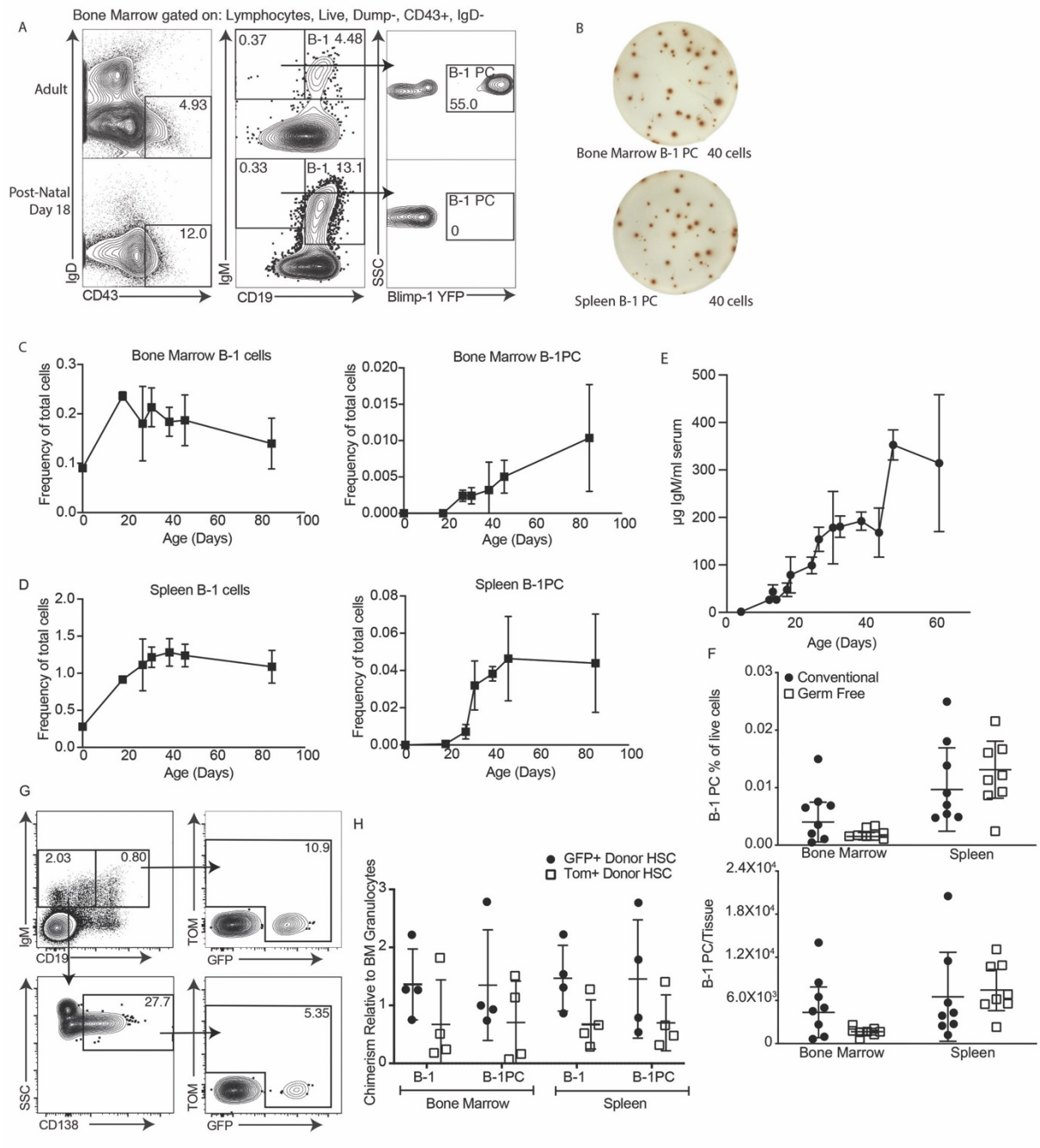

Figure 2.1: Natural IgM secreting B-1 PC in bone marrow (BM) and spleen appear over time. A) Representative FACS plots of BM from adult and post-natal day 18 Blimp-1 YFP reporter mice showing gating for B-1 cells (IgD-, CD43+, IgM+, CD19hi) and B-1 PCs (IgD-, CD43+, IgM+, CD19neg/lo Blimp-1 YFP+). **B**) Representative IgM ELISPOTs by B-1PC in BM and spleen of adult Blimp-1 YFP mice, number of cells sorted into each well are indicated. **C**) Mean percent ± SD B-1 cells and B-1PCs in BM and **D**) spleen of mice at indicated ages (n=2-4 mice per age group). **E**) Mean ± SD serum IgM (μg/ml), determined by ELISA (n = 2-5 per time point). **F**) Top, mean percent ± SD live and (bottom) total number B-1PC in BM and spleen of SPF versus germ free held mice (n=8 mice/group). Symbols are results from one mouse. Data are combined from two independent experiments. **G**) Representative FACS plots of HSC marker presence among B-1 and B-1 PCs in BM of mice reconstituted with FACS-purified transient fetal drHSC (GFP+) or conventional fetal (TdTomato +) HSC, respectively. **H**) Mean relative percent B-1 and B-1 PC in spleen and BM expressing HSC markers compared to BM granulocytes (n=4 GFP (drHSC), n=4 TdTomato (conventional fetal HSC). Values in (H) were compared using a one-way ANOVA. Values in (F) were compared by unpaired Student's t-test.

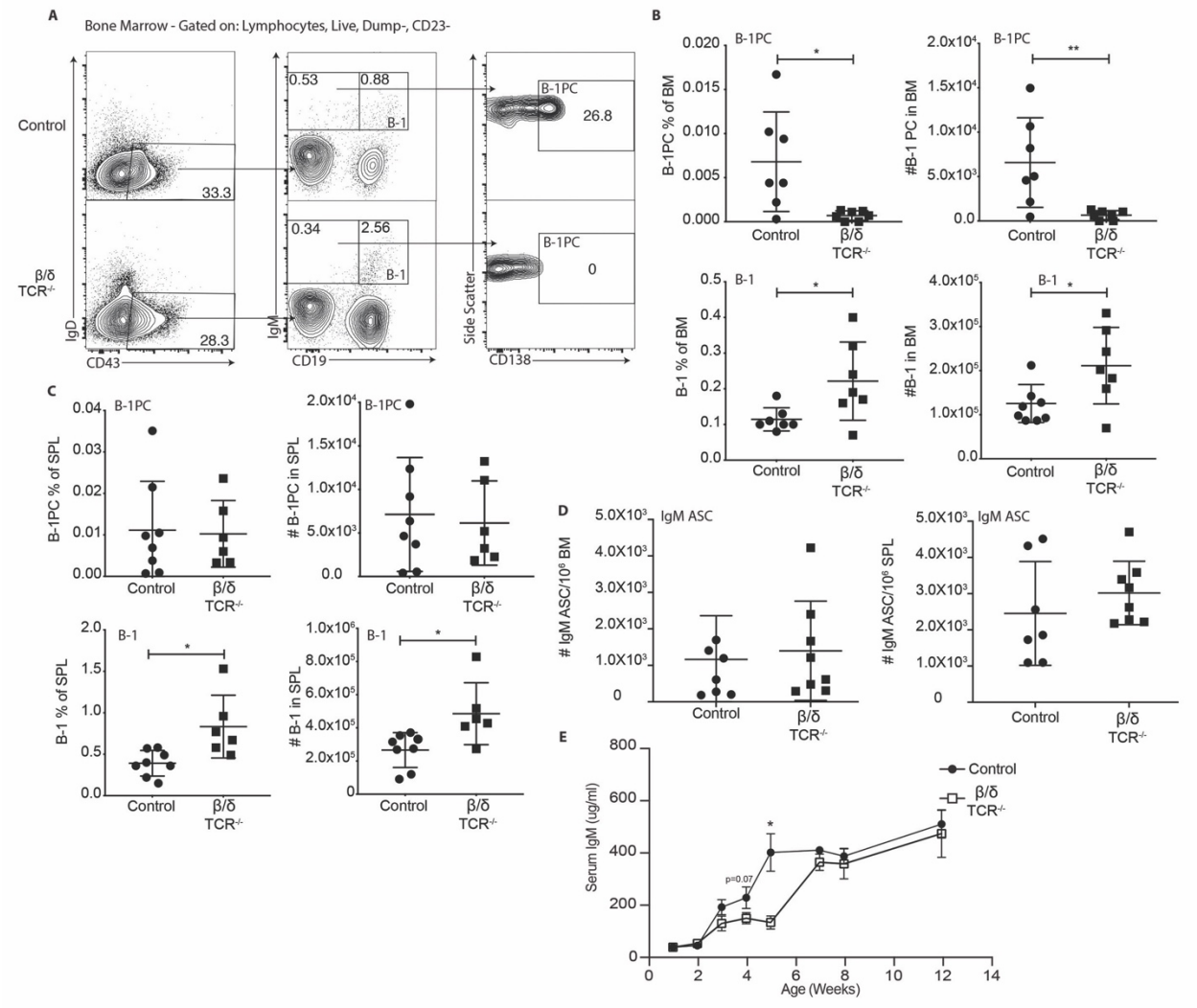
A
Bone Marrow - Gated on: Lymphocytes, Live, Dump-, CD23-
Control
β/δ TCR-/-
33.3
28.3
IgD
CD43
0.53
0.88
B-1
0.34
2.56
B-1
IgM
CD19
B-1PC
26.8
B-1PC
0
Side Scatter
CD138
B
B-1PC
B-1PC % of BM
#B-1 PC in BM
B-1
B-1 % of BM
#B-1 in BM
Control
β/δ TCR-/-
C
B-1PC % of SPL
B-1PC in SPL
B-1 % of SPL
B-1 in SPL
D
IgM ASC
IgM ASC/10^6 BM
IgM ASC/10^6 SPL
E
Serum IgM (ug/ml)
Age (Weeks)
p=0.07

Figure 2.2: BM B-1PC require T cells A) Representative FACS plots of live, singlet, Dump- BM from C57BL/6 (control) and complete β/δ TCR-/- mice. **B/C**) Left, mean percentage ± SD of live **C**) BM and **D**) spleen cells and right, total numbers B-1PCs (top) and B-1 cells (bottom). n= 6 - 8/group; Symbols represent data from individual mice. **D**) Mean number ± SD IgM ASC per 10^6 total cells in BM (left) and spleen (right); n = 7 - 8/group. **E**) Mean ± SD serum IgM (μg/ml) in control and β/δ TCR KO mice; n = 2 - 4 mice per time point). Data in B-D are combined from 2 independent experiments. Values in (B), (C), and (D) were compared by unpaired Student's t–test *$0.01 \leq p < 0.05$, ** $0.001 \leq p < 0.01$.

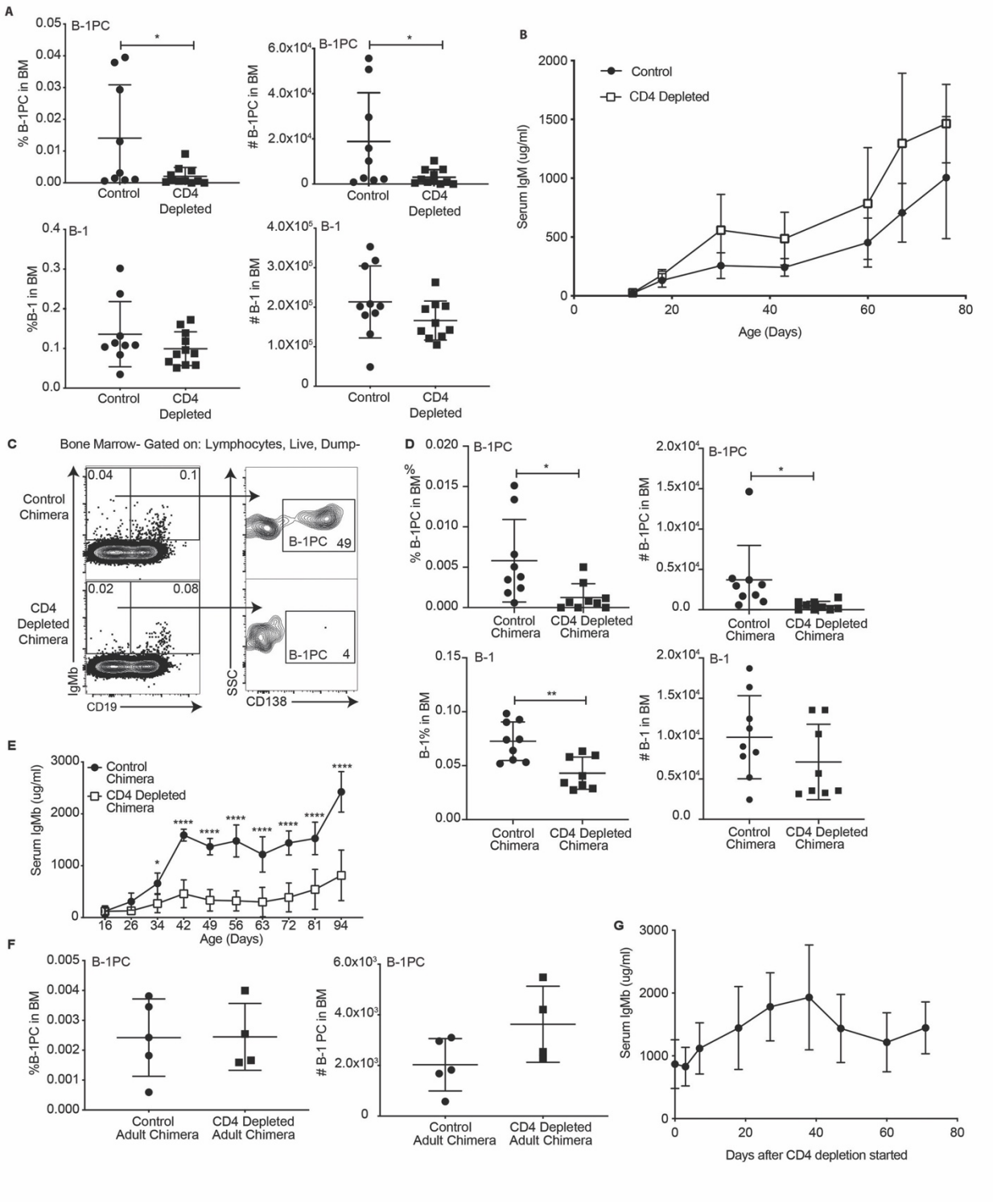
A
B-1PC
% B-1PC in BM
Control
CD4 Depleted
B-1PC in BM
B-1
%B-1 in BM
B-1 in BM
B
Control
CD4 Depleted
Serum IgM (ug/ml)
Age (Days)
C
Bone Marrow- Gated on: Lymphocytes, Live, Dump-
Control Chimera
CD4 Depleted Chimera
B-1PC 49
B-1PC 4
IgMb
CD19
SSC
CD138
D
B-1PC
% B-1PC in BM
# B-1PC in BM
B-1
B-1% in BM
B-1 in BM
Control Chimera
CD4 Depleted Chimera
E
Control Chimera
CD4 Depleted Chimera
Serum IgMb (ug/ml)
Age (Days)
F
B-1PC
%B-1PC in BM
B-1 PC in BM
Control Adult Chimera
CD4 Depleted Adult Chimera
G
Serum IgMb (ug/ml)
Days after CD4 depletion started

Figure 2.3: BM B-1 PC establishment but not maintenance requires CD4+ T cells. A) Left, mean percent ± SD live cells and right, total number BM B-1PCs (top) and B-1 cells (bottom) in C57BL/6 mice treated from birth with PBS (control) or anti-CD4 mAb (GK1.5; CD4 depleted); n = 9 – 11/group. Each symbol represents an individual mouse. B) Mean ± SD serum IgM (μg/ml) in control and CD4-depleted mice (n = 4 - 7 per time point). **C**) Representative gating strategy for B-1 PCs (IgMa-, IgMb+, CD19neg/lo, CD138+) and B-1 cells (IgMa-, IgMb+, CD19hi) in B cell Ig-allotype chimera treated from birth with PBS (control) or with anti-CD4 (CD4 depleted chimera). **D**) Left, mean percent ± SD live cells and right, total number of B-1PCs (top) and B-1 cells (bottom) in BM **E**) Mean ± SD serum IgM (μg/ml) in chimeras as in **C** (n=9 per time point, except D94 n=4). **F**) Left, mean percent ± SD of live cells and right, total number of B-1PCs (top) in BM of untreated or anti-CD4 treated adult allotype chimeras treated from age day 84 to analysis (n=4 – 5/group). **G**) Mean ± SD serum IgM (μg/ml) in adult treated chimeras from **F** (n = 4 per time point). Data in A and D are pooled from two experiments. Values in (A), (D), and (F) were compared by unpaired Student's t-test. Values in (B) and (E) were compared using a two-way repeats measure ANOVA,*$0.01 \leq p < 0.05$, **$0.001 \leq p < 0.01$, ****$0.00001 \leq p < 0.0001$.

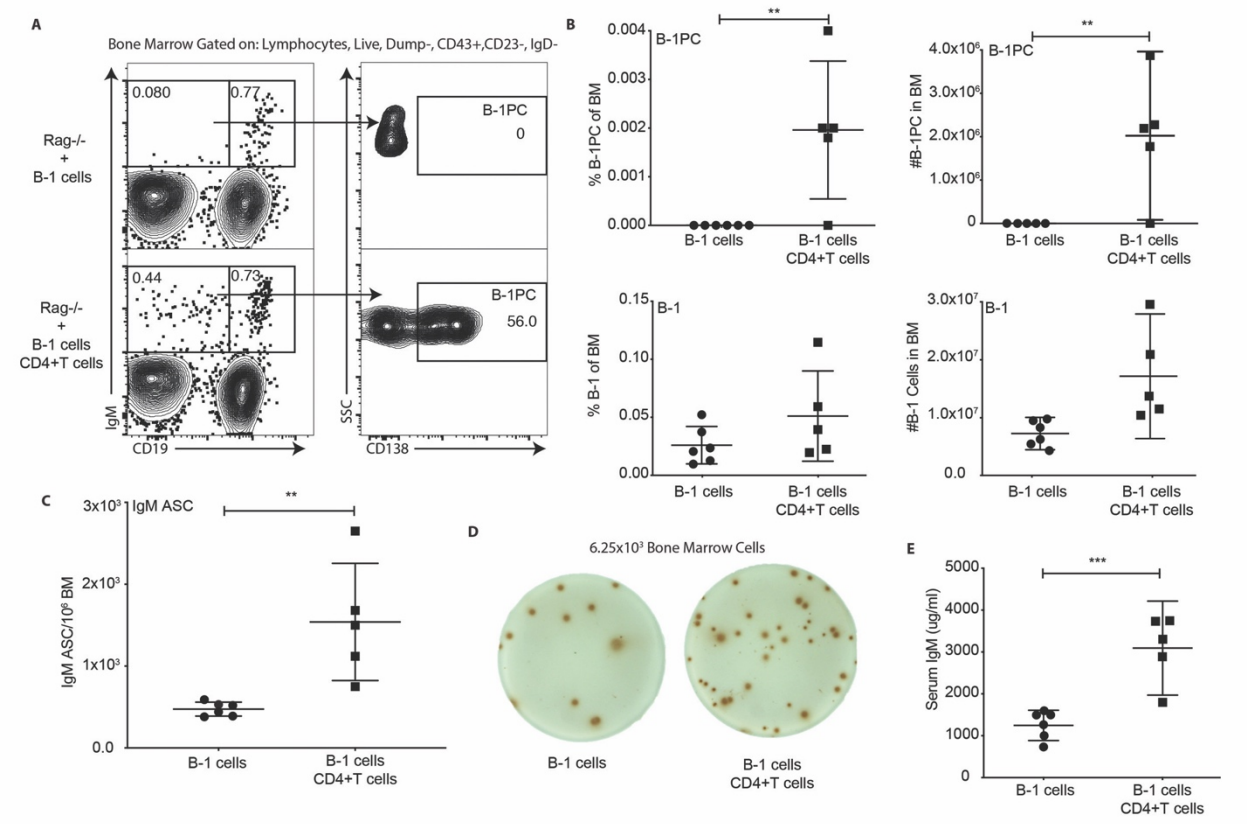

Figure 2.4: CD4+ T Cells are sufficient to rescue BM B-1 PC development. A) Representative FACS plots of BM from Rag1$^{-/-}$ mice reconstituted at postnatal day 2 with peritoneal B-1 alone or peritoneal B-1 and splenic CD4^{+} T cells. Gating identifies B-1 cells (IgD-, CD43+, IgM+, CD19hi) and B-1 PCs (IgD-, CD43+, IgM+, CD19neg/lo, CD138+). **B**) Left, mean percent ± SD live cells and right, total number B-1PCs (top) and B-1 cells (bottom) in BM in mice from **A** (n = 5-6/group). **C**) Mean number ± SD BM IgM ASC per 10^6 total cells (n = 5 - 6/group). **D**) Representative ELISPOTs of IgM ASC from BM. **E**) Mean ± SD serum IgM (μg/ml) at 16 weeks of age (n = 5 – 6/group). Values in (B), (C), and (E) were compared by unpaired Student's t–test. **0.001 ≤ p<0.01, ***0.0001 ≤p <0.001.

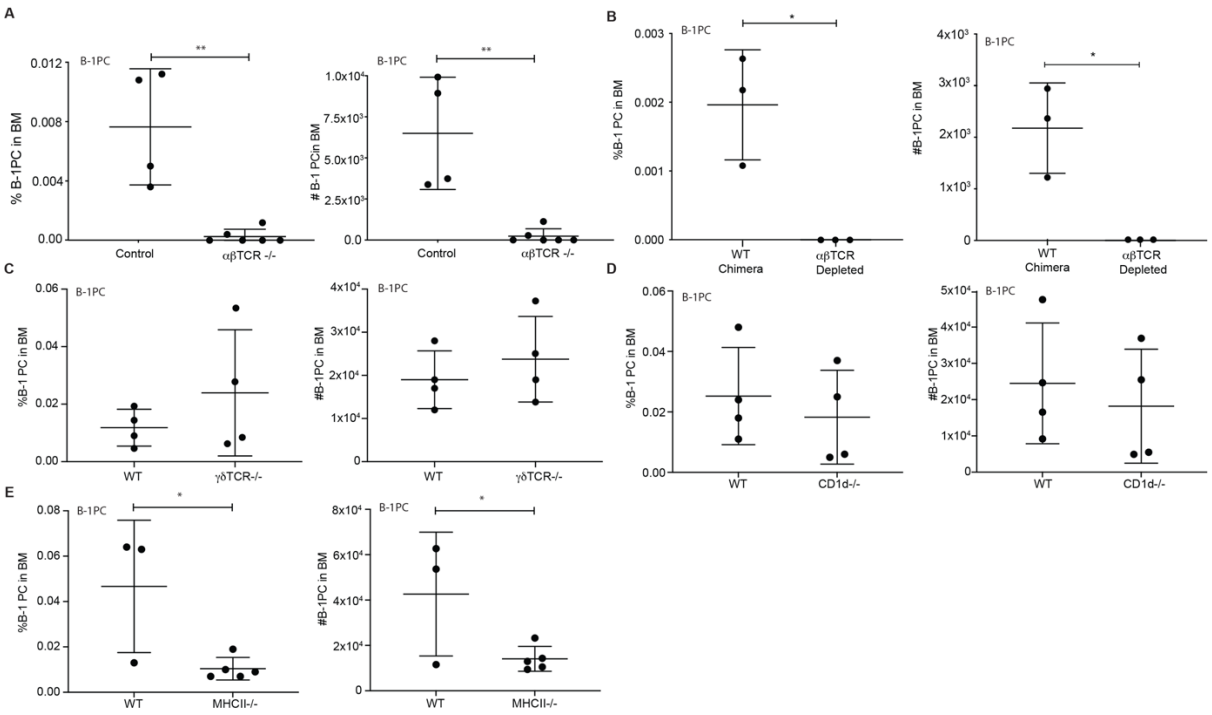

Figure 2.5: BM B-1PC require non-cognate CD4 T cell help. A-F) Left, mean percent ± SD live cells and right, total number B-1PC in BM of **A**) C57BL/6 and aβTCR -/- mice; n = 4-6/group, **B**) C57BL/6 mice treated from birth with PBS (control) or anti-βTCR mAb (H57-197); n = 3/group. **C**) C57BL/6 and δTCR -/- mice; n = 4/group, **D**) C57BL/6 and CD1d -/- mice; n = 4/group, **E**) C57BL/6 and MHCII -/- mice; n = 3 – 5/group. Values were compared by unpaired Student's t–test. ** $0.001 \leq p < 0.01$, * $0.01 \leq p < 0.05$.

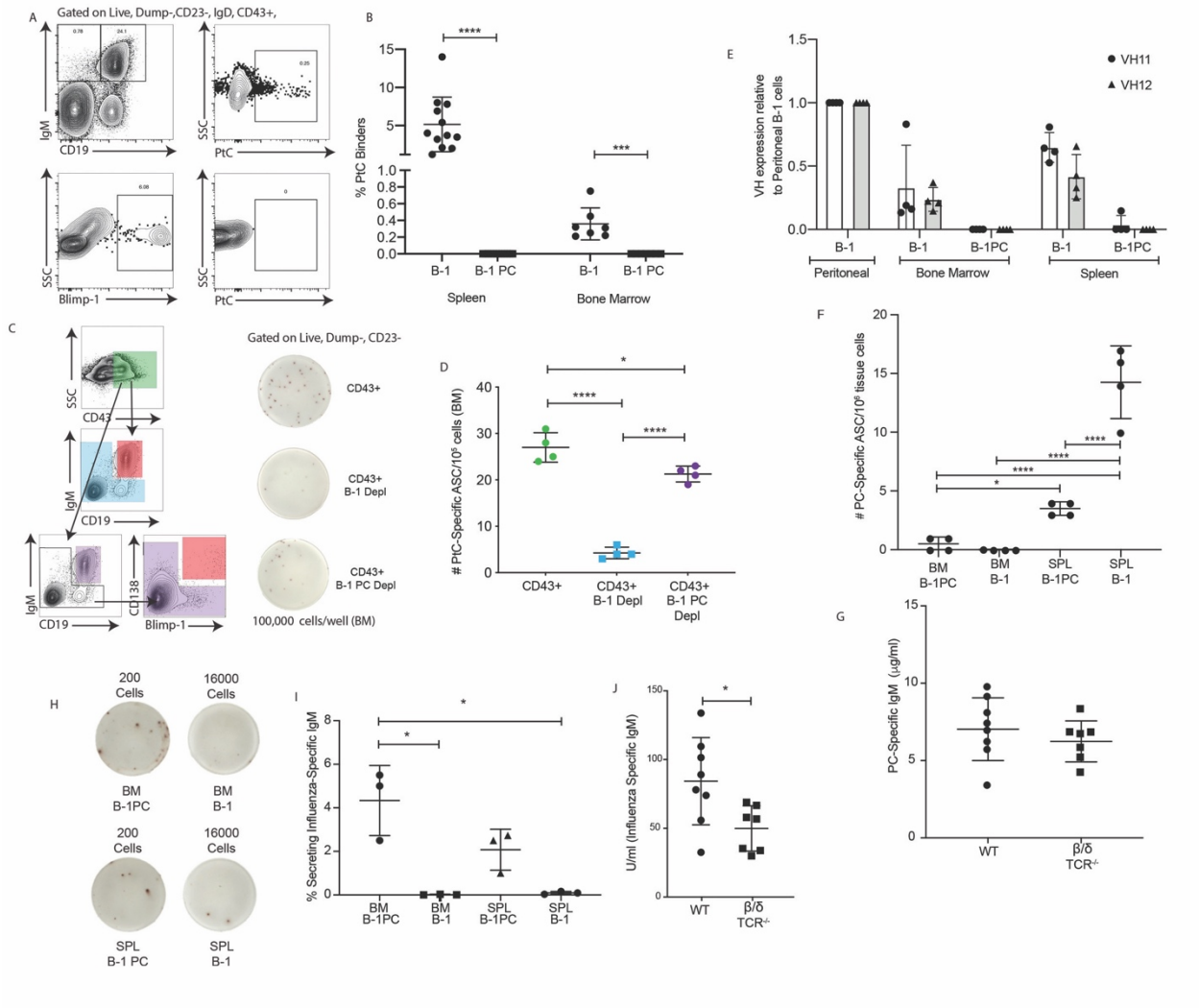
A
Gated on Live, Dump-,CD23-, IgD, CD43+,
IgM
CD19
SSC
PtC
SSC
Blimp-1
SSC
PtC
B
% PtC Binders
****
***
B-1
B-1 PC
B-1
B-1 PC
Spleen
Bone Marrow
E
VH expression relative to Peritoneal B-1 cells
VH11
VH12
B-1
B-1
B-1PC
B-1
B-1PC
Peritoneal
Bone Marrow
Spleen
C
Gated on Live, Dump-, CD23-
SSC
CD43
IgM
CD19
IgM
CD19
CD138
Blimp-1
CD43+
CD43+ B-1 Depl
CD43+ B-1 PC Depl
100,000 cells/well (BM)
D
PtC-Specific ASC/10^6 cells (BM)
CD43+
CD43+ B-1 Depl
CD43+ B-1 PC Depl
F
PC-Specific ASC/10^6 tissue cells
BM B-1PC
BM B-1
SPL B-1PC
SPL B-1
G
PC-Specific IgM (μg/ml)
WT
β/δ TCR-/-
H
200 Cells
16000 Cells
BM B-1PC
BM B-1
200 Cells
16000 Cells
SPL B-1 PC
SPL B-1
I
% Secreting Influenza-Specific IgM
BM B-1PC
BM B-1
SPL B-1PC
SPL B-1
J
U/ml (Influenza Specific IgM)
WT
β/δ TCR-/-

Figure 2.6: B-1 and B-1 PC differ in antigen binding. A) Representative FACS plots of Blimp-YFP mice showing gating for B-1 and B-1PC binding fluorescently labeled phosphatidylcholine (PtC) liposome. **B**) Mean percent ± SD B-1 cells or B-1PC binding to PtC liposomes (n=6-12 mice per group, combination of 3 independent experiments). **C**) Gating strategy for sorted populations of BM cells on to ELISPOT plates coated with PtC liposomes: CD43+ cells, CD43+ cells depleted of B-1 cells, CD43+ cells depleted of B-1 PC and corresponding representative ELISPOT wells. **D**) Mean number ± SD of anti-PtC IgM ASC per 10^6 cells from populations defined in (C) (n=4 replicates per group, combination of two independent experiments). **E)** Mean number $\pm$ SD of anti-PCh IgM ASC from each population per 10^6 bone marrow or spleen cells (n=4 replicates per group, combination of two independent experiments). **F)** Mean mg/ml ± SD of anti-PCh IgM in serum of control mice or mice lacking BM B-1 PC (TCR β/δ-/- mice) (n=6-8 per group) **G**) Representative ELISPOT of sorted B-1 and B-1PC from BM and spleen onto wells coated with Influenza A/Puerto Rico/8/34. Number represents total number of cells sorted into that well. **H)** Mean percentage ± SD of cells in each population in (G) secreting anti-influenza IgM (n=3 replicates per group). **I)** Mean relative units ± SD of anti-influenza IgM in serum of control mice or mice lacking BM B-1 PC (TCR β/δ-/- mice) (n=6-8 per group). Values were compared using a one-way ANOVA with post-hoc Tukey or unpaired Student's T test where appropriate (*=$0.01 \leq p < 0.05$, **=$0.001 \leq p < 0.01$, ***=$0.0001 \leq p < 0.001$, ****=$p < 0.0001$)

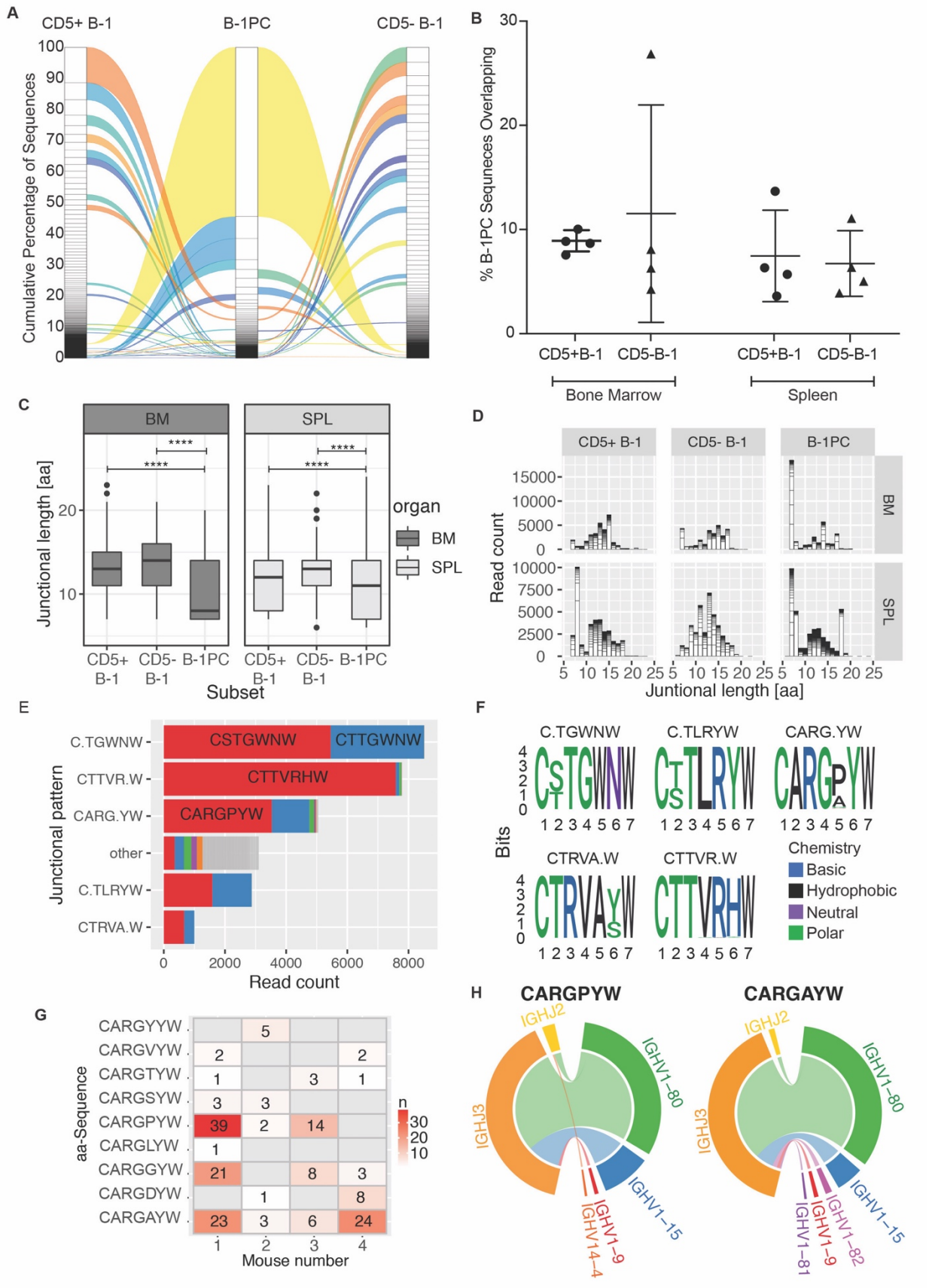
A
CD5+ B-1
B-1PC
CD5- B-1
Cumulative Percentage of Sequences
B
% B-1PC Sequneces Overlapping
CD5+B-1
CD5-B-1
Bone Marrow
Spleen
C
BM
SPL
Junctional length [aa]
organ
Subset
D
Read count
Juntional length [aa]
E
C.TGWNW
CTTVR.W
CARG.YW
other
C.TLRYW
CTRVA.W
CSTGWNW
CTTGWNW
CTTVRHW
CARGPYW
Junctional pattern
Read count
F
Bits
Chemistry
Basic
Hydrophobic
Neutral
Polar
G
aa-Sequence
Mouse number
n
H
CARGPYW
CARGAYW
IGHJ2
IGHJ3
IGHV1-80
IGHV1-15
IGHV1-9
IGHV14-4
IGHV1-82
IGHV1-81

Figure 2.7: B-1PC are highly oligoclonal with a unique Igh repertoire. A) Representative alluvial plot showing number of cumulative number of sequences and overlap of CDR3 regions of B cell subsets in bone marrow of mouse 3. **B)** Mean percent ± SD of overlapping sequences between B-1PC and CD5+ or CD5- B-1 cells in both bone marrow and spleen (n=4 mice). **C)** Mean junctional lengths among indicated B cell subsets in bone marrow and spleen. **D)** Distribution of junctional lengths by read count in indicated B cell subsets from bone marrow (top) and spleen (bottom). **E)** Distribution of 7 aa junctional sequences in B cell subsets. Each row identifies one pattern, the top 5 clonotypes are represented as colored slices. **F)** Position weight matrix for the 5 most abundant junctional patterns. **G)** Nine distinct clonotype encode the abundant 'CARG.YW' motif one indicated per row, and their distribution among the four individual mice studied (columns) reveal many shared public clones. Numbers identify unique occurrences. **H)** Depiction of different combinations of V and J genes that encode two identical shared sequences, suggestive of convergent recombination.


Rag1-/-
Control
βδTCR-/-
Control Chimera
CD4 Depl Chimera
B-1 Cell
B-1 cells CD4+ T cells
Low
High
Aggrecan
AGTR
alpha-actinine
Alpha Fodrin
Amyloid
AQP4
B2-microglobulin
B2 glycoprotein 1
BPI
Cardolipin
CENP-A
CENP-B
Chondroitin Sulfate C
Collagen I
Collagen II
Collagen III
Collagen IV
Collagen V
Collagen VI
complement C1q
complement C3
complement C3a
complement C4
complement C5
complement C6
complement C7
complement C8
complement C9
Core Histone
CRP
Cytochrome C
Decorin-bovine
DGPS
DNA Polymerase beta (POLB)
dsDNA
EBNA1
Elastin
Entaktin EDTA
Factor B
Factor D
Factor H
Factor I
Factor P
Fibrinogen IV
Fibrinogen S
Fibronectin
GBM
Genomic DNA
Gliadin
Glycated Albumin
GP2
GP210
Hemocyanin
Heparan sulfate proteoglycan
Heparan Sulphate
Heparin
Histone H1
Histone H2A
Histone H2B
Histone H3
Histone H4
Insulin
Intrinsic Factor
Jo-1
KU (P70/P80)
La/SSB
Laminin
LC1
LKM1
LPS
M2
Matrigel
MDA5
Mi-2
Mitochondrial antigen
MPO
Muscarinic receptor
Myelin basic protein (MBP)
Myosin
Nucleolin
Nucleosome antigen
Nup 62
PCNA
Peroxiredoxin 1
PL-7
PL-12
PM/Scl-75
PM/Scl 100
PR3
Proteoglycan
Prothrombin protein
Ribo Phosphoprotein P0
Ribo Phosphoprotein P1
Ribo Phosphoprotein P2
Ro/SSA (52 kda)
Ro/SSA (60 kda)
S100
Scl-70/Topoisomerase I
Sm
Sm/RNP
SmD
SmD1
SmD2
SmD3
SP100
Sphingomyelin
SRP54
ssDNA
ssRNA
T1F1 gama
Thyroglobulin
TNF-?
TPO
TTG
U1-snRNP 68/70
U1-snRNP A
U1-snRNP B/B'
U1-snRNP C
Vimentin
Vitronectin

Supplemental Figure 2.1: BM B-1PC do not contribute autoreactive IgM to the nIgM repertoire

Heatmap indicating the binding intensity of serum IgM against an array of indicated auto-antigens. Sera were taken from female T cell-deficient TCR β/δ-/- mice (n=6), control C57BL/6 (n=6) mice, B cell Ig-allotype chimera CD4-depleted via treatment with anti-CD4 mAb (n=4), B cell Ig-allotype chimera CD4, T cell sufficient (n=4), Rag1-/- mice reconstituted with B-1 cells only (n=5) and Rag1-/- mice reconstituted with B-1 cells and CD4+ T cells (n=5).

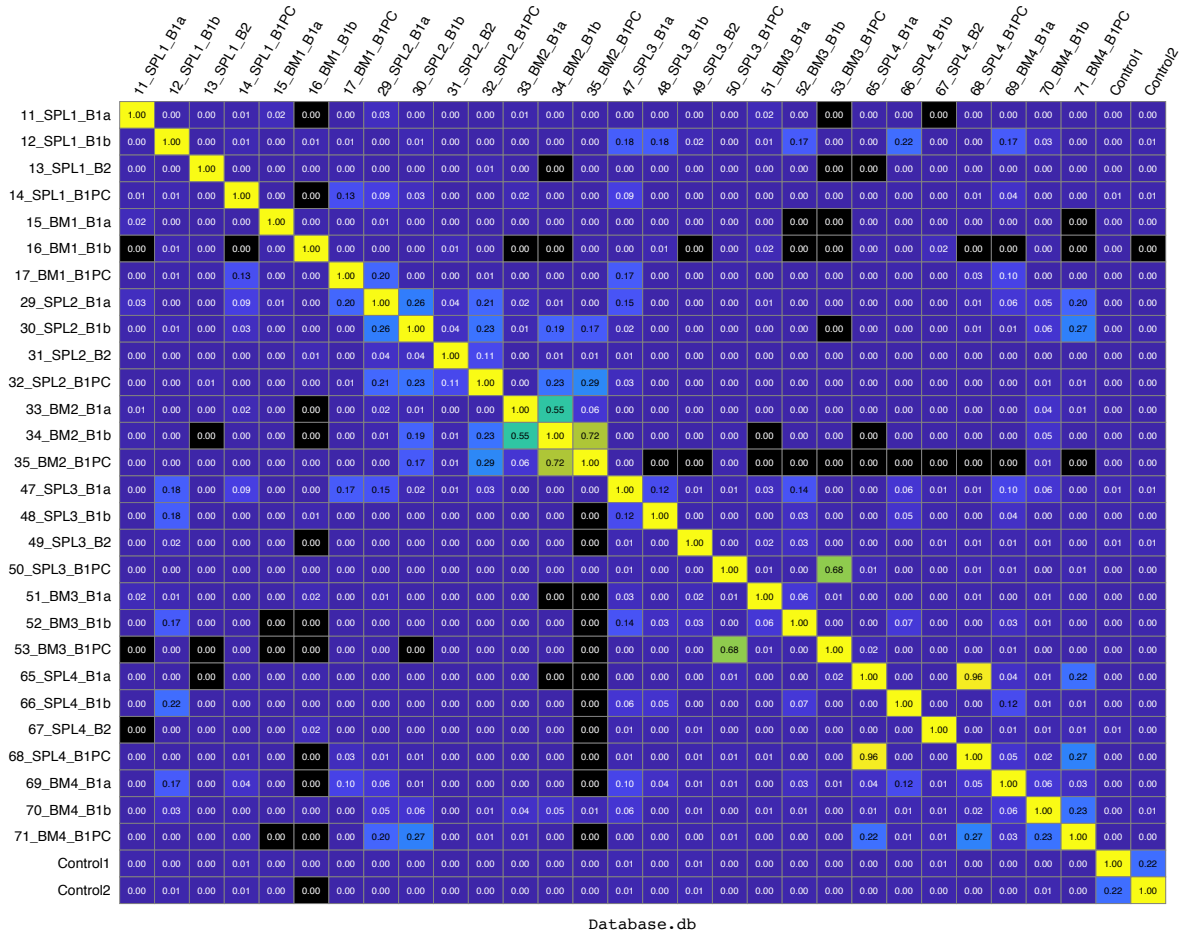

Supplemental Figure 2: B-1PC from spleen and bone marrow in the same mouse consistently have overlapping repertoire, but not with any other population of B cells

Morisita overlap index plot showing relatedness of Igh-chain sequences obtained by bulk RNA BCR-sequencing from FACS-purified populations of live, non-dump, CD19hi CD43+ IgM+ CD5+ B-1a; live, non-dump, CD19hi CD43+ IgM+ CD5- B-1b; live, non-dump CD23- IgM+ Blimp-1+ B-1PC from spleen and bone marrow and live, non-dump, CD19+ CD23+ follicular B cells (B-2) from spleen of four individual Blimp-1YFP reporter mice. Controls were mixed spleen cells from two C57BL/6 mice.

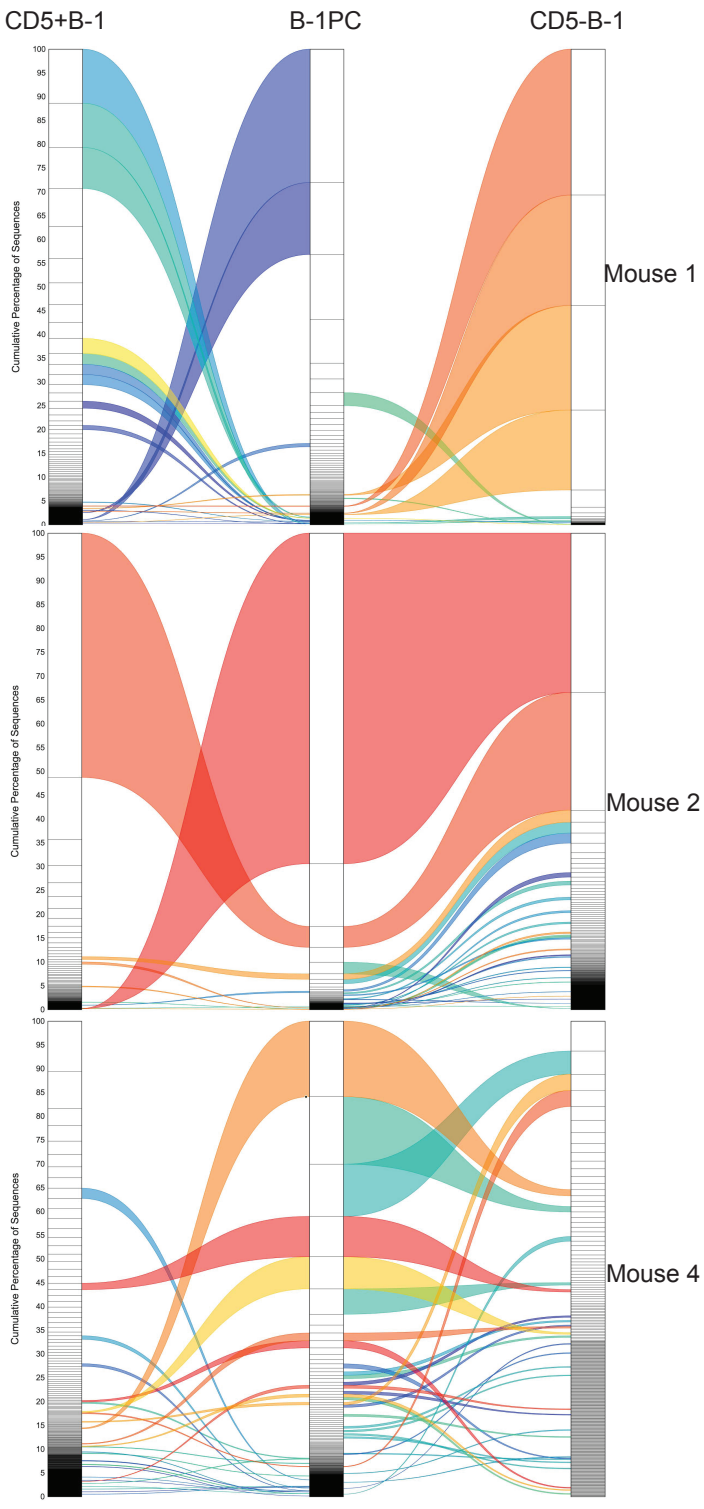
CD5+B-1
B-1PC
CD5-B-1
Cumulative Percentage of Sequences
Mouse 1
Mouse 2
Mouse 4

Supplemental Figure 2.3: Alluvial plots of mouse 1,2 and 4 demonstrating oligoclonality of B-1PC population and overlapping CDR3 sequences between B-1PC and CD5+ or CD5- B-1 cells in bone marrow.

Table 2.1: Antibodies and fluorescent reagents used for ELISA, ELISPOT, and flow cytometry

Antibodies	Source	Identifier
Anti-IgMa biotinylated (Clone: DS-1)	BD Bioscience	Cat#553515
Anti-IgMb biotinylated (Clone: AF6-78)	BD Bioscience	Cat#553519
Anti-IgM biotinylated (Clone: 331)	In House	N/A
Anti-IgM biotinylated (Pooled antisera from goats hyperimmunized with mouse IgM)	Southern Biotech	Cat#1020-08
Anti-IgM Efluor 750 (Clone: 331)	In house	N/A
Anti-IgM FITC (Clone:331)	In house	N/A
Anti-IgM APC-Cy7(Clone:331)	In house	N/A
Anti-IgD PE-Cy 7 (Clone:11-26C)	In house	N/A
Anti-F4/80 Pacific Blue (Clone:BM-8)	In house	N/A
Anti-F4/80 PE-Cy5 (Clone:BM-8)	In house	N/A
Anti-F4/80 Biotin (Clone:BM-8)	In house	N/A
Anti-Gr-1 Pacific Blue (Clone: RB6-8C5)	In house	N/A
Anti-Gr-1 eFluor 450 (Clone: RB6-8C5)	Invitrogen	Cat#48-5931-82
Anti-Gr-1 Biotin (Clone: RB6-8C5)	In house	N/A
Anti-Gr-1 PE-Cy5 (Clone: RB6-8C5)	In house	N/A
Anti-CD8a Pacific Blue (Clone: 53-6.7.3.1)	In house	N/A
Anti-CD8a Biotin (Clone: 53-6.7.3.1)	In house	N/A
Anti-CD8a eFluor 450 (Clone: 53-6.7)	Invitrogen	Cat#48-0081-82
Anti-CD4 unlabeled – depleting (Clone: GK1.5)	In house	N/A
Anti-CD4 Pacific Blue (Clone: GK1.5)	In house	N/A
Anti-CD4 Biotin (Clone: GK1.5)	In house	N/A

Anti-CD4 APC-EF780 (Clone: GK1.5)	Invitrogen	Cat#47-0041-82
Anti-CD3 Alexa Fluor 700 (Clone: 17A2)	Invitrogen	Cat#56-0032-82
Anti-CD19 Brilliant Violet 786(Clone: 1D3)	BD Bioscience	Cat#563333
Anti-CD19 PE (Clone: D3)	In house	N/A
Anti-CD19 Biotin (Clone: D3)	In house	N/A
Anti-CD19 PE CF594 (Clone: D3)	BD Bioscience	Cat#562329
Anti-CD43 APC (Clone: S7)	In house	N/A
Anti-CD43 Brilliant Violet 650 (Clone: S7)	BD Bioscience	Cat#740464
Anti-CD138 Brilliant Violet 605 (Clone: 281-2)	BD Bioscience	Cat#563147
Anti-CD23 Brilliant Violet 605 (Clone: B3B4)	BD Bioscience	Cat#747727
Anti-CD23 Brilliant Violet 711 (Clone: B3B4)	BD Bioscience	Cat#563987
Anti-CD23 Brilliant Biotin (Clone: B3B4)	In house	N/A
Anti-CD23 Brilliant eFluor 450 (Clone: B3B4)	Invitrogen	Cat#48-0232-82
Anti-TCRβ Unlabeled – depleting (Clone: H57-597)	In house	N/A
Anti-TCRβ Alexa Fluor 647 (Clone: H57-597)	Invitrogen	Cat#HM3621
Anti-TCRδ PE (Clone: GL-3)	Invitrogen	Cat#12-5711-82
Anti-TCRδ Biotin (Clone: GL-3)	Invitrogen	Cat#13-5711-82
Anti -NK1.1 Pacific Blue (Clone: PK136)	In house	N/A
Anti -NK1.1 Biotin (Clone: PK136)	In house	N/A
Anti-CD11b Biotin (Clone: M1/70)	In house	N/A
Anti-CD90.2 Biotin (Clone: 53-2.1)	In house	N/A

Anti-VH11 Biotin (Clone: VH11Id.6e9)	In house	N/A
Anti-VH12 Biotin (Clone: CH27Id.5c5)	In house	N/A
Anti-T15 idiotype Biotin (Clone: AB1-2)	In house	N/A
Anti-Sca-1 Pacific Blue (Clone: E13-161.7)	BioLegend	Cat#122520
Anti-CD150 PE-Cy7 (Clone:TC15-12F12.2)	BioLegend	Cat#115914
Anti-cKit APC/Fire 750 (Clone: 2B8)	BioLegend	Cat#105838
Other Fluorescent reagents		
Streptavidin-APC	Invitrogen	Cat#17-4317-82
Streptavidin-Qdot 605	Invitrogen	Cat#Q10101MP
PtC-liposome FITC	Aaron Cantor – Stanford University	N/A
PtC-liposome PE	Aaron Cantor – Stanford University	N/A

Table 2.2: PCR primers used for BCR sequencing of B-1 cell populations

Primers	IGH Nested PCR1	IGH Nested PCR2
5′ VH	GGGAATTCGAGGTGCAGCTGCAGGAGTCTGG	GGGAATTCGAGGTGCAGCTGCAGGAGTCTGG
3′ Cμ	outer: AGGGGGCTCTCGCAGGAGACGAGG	inner: AGGGGGAAGACATTTGGGAAGGAC
3′ Cγ1	outer: GGAAGGTGTGCACACCGCTGGAC	inner: GCTCAGGGAAATAGCCCTTGAC
3′ Cγ2c	outer: GGAAGGTGTGCACACCACTGGAC	inner: GCTCAGGGAAATAACCCTTGAC
3′ Cγ2b	outer: GGAAGGTGTGCACACTGCTGGAC	inner: ACTCAGGGAAGTAGCCCTTGAC
3′ Cγ3	outer: AGACTGTGCGCACACCGCTGGAC	inner: GCTCAGGGAAGTAGCCTTTGAC
3′ Cα	outer: GAAAGTTCACGGTGGTTATATCC	inner: TGCCGAAAGGGAAGTAATCGTGAAT

Chapter 3:

Characterization of B-1$_{sec}$: Unconventional Natural IgM secreting cells in the Bone Marrow

Fauna Leah Smith

ABSTRACT

B-1 cells are unique, fetal-origin, self-reactive, innate like B lymphocytes that give rise to a heterogeneous population of cells, including IgM secreting cells. The poly-reactive IgM produced by B-1cells is a first line of defense again invading pathogens and is essential for initiation of robust B-2 adaptive immune responses. Additionally, natural IgM aids protection from autoimmune diseases and neoplasia. I aimed to identify an important unique subset of B-1 cells that is responsible for significant contribution to the nIgM pool. B-1_{sec} by flow cytometry and further characterize their function and transcriptional profile. B-1_{sec} were identified as CD19+ CD23- $CD43^{var}$ intracytoplasmic IgM^{hi} and CD138+. Using a double-reporter mouse to identify the immunoglobulin joining (J)-chain and Blimp-1, the master transcriptional regulator of plasma cell differentiation, B-1_{sec} were further identified as J-chain+ Blimp-1^{neg}. Despite the lack of Blimp-1 expression, I demonstrated that these cells secrete significant amounts of IgM and have a transcriptional profile of an antibody secreting cell.

3.1 INTRODUCTION

B-1 cells are a heterogeneous population of innate like, fetal/neonatal B cells that develop from Lin28b+ precursor residing in the liver, fetal yolk sac and splanchnopleura during gestation and in the period shortly after birth (Beaudin et al., 2016; Montecino-Rodriguez and Dorshkind, 2012; Yuan et al., 2012). Subsequently they are maintained by self-renewal. B-1 derived cells residing in the BM and spleen produce the vast majority of natural antibodies, primarily immunoglobulin M (nIgM), while quiescent B-1 cells reside at high frequency in the body cavities (Baumgarth et al., 2000; Boes et al., 2000a; Choi et al., 2012; Holodick et al., 2014; Ochsenbein et al., 1999; Savage et al., 2017). Natural (n)IgM are spontaneously produced, broadly reactive antibodies that bind to both self and foreign antigens, generated in a manner that depends on self-antigen expression (Hayakawa et al., 1999, 2003), but are independent of exposure to foreign antigens, including the microbiota (Bos et al., 1989; Haury et al., 1997; Savage et al., 2017). nIgM aides in the control of autoimmune disease as well as tumor cell dispersal (Boes et al., 2000b; Haro et al., 2019; Nguyen et al., 2015). Additionally, they provide a first line of defense against a wide variety of pathogens by binding to and tagging antigens for removal, or by activating the classical complement cascade (Boes et al., 2000b; Ehrenstein et al., 2000; Nguyen et al., 2015; Notley et al., 2011).

Blimp-1, encoded by the gene prdm-1, is a master transcriptional regulator of plasma cell differentiation. Its induction is enhanced by another transcriptional regulator of the plasma cell fate, IRF4. Blimp-1 deficiency leads to an absence of antigen-specific plasma cells following immunization. However, we had shown previously that serum IgM was still present, albeit at reduced levels, in mice that lacked Blimp-1 due to a deletion of *prdm-1* exon 1A(PRDM1$^{\Delta Ex1A}$),

containing the NF-κB dependent promoter site required for B cell differentiation (Morgan et al., 2009). Consistent with that finding, we identified two B-1 cell types that actively secrete nIgM in BM and spleen of C57BL/6 mice: Blimp-1YFP+ IgM+ $CD19^{lo}$ CD138+ B-1 plasma cells (B-1PC), and non-terminally differentiated IgM+ $CD19^{int/hi}$ $Blimp\text{-}1^{neg}$ cells, we will call $B\text{-}1_{sec}$, that were contained within the population of "classical" non-secreting CD19+ IgM+ IgD- CD23- CD43+ $Blimp\text{-}1^{neg}$ B-1 cells, but were not further phenotypically differentiated from these non-secreting cells by flow cytometry (Savage et al., 2017). Thus $B\text{-}1_{sec}$ were present also in Blimp-1 deficient mice, suggesting their independence of Blimp-1 for induction of antibody secretion (Savage et al., 2017).

We recently showed that the presence of BM B-1PC, but not of all nIgM, is dependent on αβTCR+ CD4+ T cells (Smith et al. 2022 in revision, see Chapter 2). Given that the lack of all T cells, or of MHCII, and thus B-1PC, in adult gene targeted mice did not seem to affect circulating nIgM levels (Hooijkaas et al., 1985; Van Oudenaren et al., 1984), the data suggested the presence of another IgM-secreting B-1 cell population that can compensate for the lack of B-1PC. Furthermore, T cell deficient βδTCR-/- and thus BM B-1PC-deficient mice had increased numbers of BM B-1 cells, letting us to speculate that this populations includes increased numbers of the putative $B\text{-}1_{sec,}$ which we had shown previously to contribute to the circulating IgM levels in wild type mice.

In contrast to the normal IgM serum levels in T cell-deficient mice, reconstitution of neonatal mice depleted of B cells and CD4 T cells via mAb antibody treatment and reconstituted with peritoneal cavity cells as a source of B-1 cells, resulted in greatly reduced serum IgM

concentrations even after full reconstitution of the animals (Moon et al., 2004; Reynolds et al., 2015). This was in contrast to adult T-deficient mice, indicating a failure to induce compensatory nIgM production from the putative B-1sec, resulting in mice with reduced serum IgM levels. The data further indicate that B-1_{sec} derive from precursors not present in the peritoneal cavity of adult mice, or that they require stimuli other than those provided in an adult Rag-/- environment. This is significant, as it raises the possibility that B-1PC and the putative B-1_{sec} arise from distinct precursors and are activated to secrete nIgM by distinct mechanisms. The aim of this chapter was to unequivocally identify and characterize the nIgM secreting B-1_{sec} by phenotype, function, and transcriptional profile.

RESULTS

3.2 CD138 is a marker of nIgM secreting cells independent of Blimp-1 expression

Development and/or maintenance of BM B-1PC requires the presence of CD4 T cells, yet nIgM serum levels and the numbers of IgM ASCs in the BM of αβTCR -/- or CD4 depleted mice appeared similar to those of wild type mice (Smith et al. 2022 in revision, see Chapter 2). Because T-deficient mice had increased frequencies and numbers of BM CD19+ B-1 cells (Smith et al. 2022 in revision, see Chapter 2), we first determined the extent to which this population contained nIgM producing cells that may reconstitute nIgM production in the T-deficient mice. Flow cytometric analysis of αβTCR -/- mice demonstrated significant increased numbers of CD138+ cells among CD19+ CD23- IgD- IgM+ CD43+ B-1 cells (**Fig. 3.1A**). Syndecan-1 (CD138) is a transmembrane proteoglycan that is considered a canonical surface marker of antibody secreting cells (ASCs; (McCarron et al., 2017)), as its expression is upregulated over 1000-fold compared to resting B cells (Sanderson et al., 1989). Although its

function is still unknown, the cytokines IL-6 and APRIL enhance survival of conventional plasma cells in a CD138 dependent manner (McCarron et al., 2017). CD138 was identified previously as marker of B-1 derived ASCs in both BM and spleen at steady state (Holodick et al., 2014; Savage et al., 2017). Splenic CD19+ CD43+ CD138+ CD5+ B-1 cells secreted significantly more nIgM than their CD138- counterparts (Holodick et al., 2014). Expression of CD19 cells identifies conventional B cells, while their differentiation into ASCs results in CD19 downregulation and eventual loss of surface expression. Consistent with that, nIgM secreting B-1 cells were contained within the CD19+ B-1 cell pool, while B-1PC were $CD19^{lo/neg}$ (Holodick et al., 2014; Savage et al., 2017).

Mice lacking *prdm-1* in B cells also showed increased numbers of BM CD138+ B-1 cells among both the $CD19^{lo/neg}$ B-1PC and the $CD19^{int/hi}$ cells (**Fig. 3.1B**), consistent with nIgM-secretion by Blimp-1^{neg} CD19+ B-1 cells. To begin and identify nIgM-secreting cells among the Blimp-1^{neg} B-1 cells, we first developed flow cytometric staining panels to distinguish intracellular (ic)IgM from surface IgM, using high levels icIgM as an indicator for IgM-secretion. Blimp-1+ cells were distinguished from Blimp-1^{neg} cells via a Blimp-1 YFP reporter(Fooksman et al., 2010). Indeed, $icIgM^{hi}$ cells were present among both, Lin- CD23- CD43+ surface IgM+ and CD19+ and $CD19^{lo/neg}$ (**Fig. 3.1C**). As expected, $CD19^{lo/neg}$ surface IgM+ CD138+ Blimp-1+ (B-1PC) and the few Blimp-1+ CD138- cells we categorized here as B-1 plasmablasts (PB) were nearly uniformly $icIgM^{hi}$ (**Fig. 3.1C, D**), while cells expressing neither CD138 nor Blimp-1 had little icIgM (**Fig. 3.1C, D**). Among the CD19+ B-1 cells, the vast majority were $CD138^{neg}$ and Blimp-1^{neg} and showed no staining for icIgM i.e., were non-secreting B-1 cells. A small population of IgM+ CD19+ CD138+ Blimp-1^{neg} cells were present, however, of which about 25% expressed

high levels icIgM (**Fig. 3.1C, D**), thus had the expected phenotype of B-1_{sec} (Savage et al., 2017).

Consistent with the flow cytometric evaluation, most purified B-1PC and B-1PB spontaneously secreted IgM, as assessed by ELISPOT of cells isolated by flow cytometry (**Fig. 3.1E, F, Suppl Fig.3.1**). In addition, two populations of B-1 cells contained significant numbers IgM secretors: surface IgM+ CD23- CD43+ $CD19^{variable}$ CD138- Blimp-1+, which are more numerous in the spleen than the BM, and likely represent early or short-lived PC/PB (**Fig. 3.1E, F, Suppl Fig. 3.1**), and a population of surface IgM+ $CD19^{+}$ CD138+ Blimp-1^{neg} cells, i.e. cells with the phenotype of B-1_{sec} (**Fig. 3.1E, F, Suppl Fig. 3.1**). Together the data demonstrate both by phenotype and function the presence of distinct nIgM-secreting cells in both spleen and BM: Blimp-1^{+} B-1PC/PB and Blimp-1^{neg} B-1_{sec}. Blimp-1 and CD138 expression appeared not to be coordinately expressed in IgM ASC. Instead, expression of either Blimp-1 or CD138 was associated independently with IgM secretion, with IgM-secreting B-1 cells expressing at least one of these, while most mature B-1PC were double positive.

3.3 nIgM secreting B-1 cells are heterogeneous with regards to CD43 expression

Most nIgM produced at steady state in mice is B-1 derived ((Baumgarth et al., 1999a, 2000; Choi et al., 2012; Savage et al., 2017). Previous reports have considered nIgM secreting B-1 cells only among the CD43+ B cells (Holodick et al., 2014; Savage et al., 2017), as CD43 staining for the 115KDa isoform of CD43, identified by the monoclonal antibody S7 (Wells et al., 1994), is one of the few markers distinguishing B-1 from conventional B cells (Wells et al., 1994). Little is known about the function of CD43(S7) on B-1 cells, but in T cells it is constitutively expressed

and acts as a negative regulator of T cell activation and adhesion (Delon et al., 2001; Pedraza-Alva and Rosenstein, 2007; Tong et al., 2004). Regulatory B cell which share many characteristics of B-1 cells have been identified also as CD43+; yet the IL-10 secreting Bregs predominantly lack CD43 (Moore-Connors et al., 2014). Additionally, we previously showed that TLR-mediated activation/differentiation of B-1 cells resulted in the down regulations of another negative regulator of T and B cell activation, CD5 (Kreuk et al., 2019; Savage et al., 2019). Thus, it was possible that CD43 might be downregulated upon B-1 cell activation. which would have had us potentially miss significant numbers of nIgM producing cells. Indeed, sorting of CD43+ and CD43- live, Lin- CD23- surface IgM+ cells from spleen and BM into ELISPOT plates demonstrated approximately equal frequencies IgM-secreters among both the CD43+ and CD43- cells (**Fig. 3.2A, B**).

The original experiments that described CD43(S7) expression on B-1 cells used Ig-allotype chimeric mice made with BALB/c (Igha) and BAB25 (Ighb) (Wells et al., 1994). Using Ig-allotype chimeric mice generated with C57BL/6 -derived (Ighb) B-1 cell donors and congenic Igha recipients allowed us to unequivocally identify B-1 cells based on their expressed Ig-allotype. We observed that expression of CD43(S7) on IgMb-marked CD5+ B-1 cells was higher in the peritoneal cavity than in the spleen or BM, indicating that CD43 expression may vary also by tissue location (**Fig. 3.2 C, D**). Using CD138 as a marker of IgM ASCs (**Fig. 3.1**), we identified more CD43(S7) negative than positive IgM ASC in the BM (**Fig. 3.2E, F**). Only about half of BM B-1PC in Blimp-1 YFP reporter mice expressed CD43(S7) (**Fig. 3.2G**) while both populations expressed similarly high levels of icIgM (**Fig 3.2H, I**). Together the data

demonstrated that CD43(S7) expression is variable on B-1 derived nIgM secreting cells in C57BL/6 mice and thus that CD43 is not a marker of all IgM-secreting B-1 cells.

3.4 Blimp-1 independent, CD43-, J chain+ nIgM secreting B-1$_{sec}$ are major producers of BM derived nIgM

To functionally validate the icIgM^{hi} Blimp-1^{neg} CD138+ B-1$_{sec}$ as IgM secreting cells, we required a marker that would allow us to sort live cells. For that we generated a Blimp-1 YFP, Joining (J) chain Td Tomato double reporter mouse by crossing a Blimp-1 YFP reporter mouse (Fooksman et al., 2010) with a tamoxifen-inducible J chain reporter mouse (kind gift of Dr. Deepta Batthacharya, University of Arizona, (Wong et al., 2020)) (**Suppl. Fig. 3.2**). J chain is a 15KDa protein generated by ASCs that covalently binds to IgM monomers, creating the pentameric secreted IgM (Brandtzaeg, 1985; Castro and Flajnik, 2014; Koshland, 1985). Expression of the J chain, induced by 5 days of treatment with tamoxifen, strongly correlated with icIgM^{hi} staining (**Fig. 3.3A, B**). B-1$_{sec}$ were identified as small but discrete spleen and BM populations with the phenotype: surface IgM+, CD19var, Blimp-1-, CD138+, J chain+, icIgM^{hi}. Most B-1$_{sec}$ lacked CD43(S7) (**Fig. 3.3A**). CD43- BM B-1$_{sec}$ had higher levels icIgM than the CD43+ BM B-1$_{sec}$, indicating that they are secreting more IgM (**Fig. 3.3A, B**).

We then sorted various B cell subsets based on expression of Blimp-1YFP, Td Tomato J chain and surface CD138 staining and assessed IgM secretion by ELISPOT. The data demonstrated that CD138+ Blimp-1^{neg} CD138+ B-1$_{sec}$ indeed secreted nIgM. Frequencies of secreting cells among cells with this phenotype and IgM spot sizes were comparable to those seen by sorted Blimp-1+ nIgM secretors (**Fig. 3.3C, D**) further demonstrating that Blimp-1 expression is not

necessary for robust IgM production. Use of the J-chain reporter further enriched for IgM-secreting B-1_{sec}, as only the J-chain+ Blimp-1^{neg} CD138+ B-1 cells secreted IgM (**Fig. 3.3C, D**). The relative contribution of B-1_{sec} to nIgM production were greater in the BM than in the spleen (**Fig. 3.3E**). Consistent with their function as IgM secretors, histologic evaluation of B-1_{sec} showed them to have an expanded cytoplasm, similar to that of the Blimp-1+ B-1 cells (**Fig. 3.3F**). We conclude that B-1_{sec} are indeed IgM-secreting cells, expressing all the hallmarks of ASCs, such as CD138 and J-chain but show no detectable expression of Blimp-1YFP. The cells significantly contribute to spontaneous nIgM production in wild type mice, especially in the BM, and thus are likely to be responsible for IgM secretion in mice unable to generate B-1PC.

3.5 Genes associated with protein production are upregulated in B-1_{sec} compared to non-secreting B-1 cells.

To gain insight into the transcriptional state of B-1_{sec} we used the double reporter mice to isolate them as well as non-secreting B-1 cells and B-1PC from spleen, bone marrow and peritoneal cavity by flow cytometry for bulk RNA sequencing analysis (RNAseq) (**Suppl. Fig. 3.3A, B**). The top differentially expressed genes (DE) between BM B-1_{sec} and non-secreting BM B-1 cells were genes involved in protein transport, protein processing such as glycosylation, the activated unfolded protein response (UPR) and ER-associated degradation (ERAD) pathway (**Fig. 3.4A-C**). This is consistent with a cell that is making and transporting antibody. The UPR is induced in response to excessive accumulation of proteins in the endoplasmic reticulum, such as antibody in ASCs (Moore and Hollien, 2012). In conventional B-2 derived ASCs, the transcription factor X box binding protein 1 (XBP1) is critical for successful antibody secretion (Iwakoshi et al., 2003). Similarly, B-1_{sec} had significantly higher expression of *Xbp1* than non-secreting B-1 cells. ASCs

can secrete thousands of proteins per second (Moore and Hollien, 2012) that are folded and assembled in the ER before their transport via the Golgi to the cell surface for secretion. Misfolded/formed proteins are trapped in the ER for degradation via the ERAD pathway (Qi et al., 2017). Consistent with strong protein production and processing, the B-1_{sec} showed increased expression of genes of the ERAD machinery compared to non-secreting B-1 cells (Qi et al., 2017). Thus, as expected from the functional studies, the top identified GO terms and Pathways upregulated in B-1_{sec} compared to non-secreting B-1 cells identify B-1_{sec} as high protein secreting cells.

DE expression analysis between BM B-1_{sec} and peritoneal B-1 cells confirmed that B-1 cells in the peritoneal cavity do not secrete antibodies (**Fig. 3.4D, E**). The analysis also identified 12 candidate surface-expressed proteins that may help to further distinguish B-1_{sec} by phenotype (**Fig. 3.4F**). Among those, B cell receptor inhibitory molecules CD148 and Siglec G are known to be expressed on B-1 cells in the peritoneal cavity (Nitschke, 2015; Skrzypczynska et al., 2016). BM B-1 cells showed higher expression of *Cd148* and *Siglecg* compared to B-1_{sec} (**Fig. 3.4F**). Flow cytometry supported the RNAseq results and identified Siglec G as the more strongly differentially expressed surface marker of the two (**Fig. 3.4G**). Taken together the results further support the findings that the Blimp-1^{neg} B-1_{sec} are ASCs.

3.6 The transcriptional profile of B-1_{sec} identifies a non-terminally differentiated nIgM secreting B cell

Unsupervised clustering of the samples based on Ig heavy and light chain constant region genes resulted in the grouping of the non-secreting B-1 cells from BM and peritoneal cavity on the one

hand, and the secreting cells, i. e. BM B-1$_{sec}$ and B-1PCs, and spleen B-1$_{sec}$ on the other, with the non-secreting cells expressing higher levels of Ighd and lower levels of Ighm, as expected (Qian et al., 2015) (**Fig. 3.5A**). All cell populations showed preferential expression of Iglk as expected (**Fig. 3.5B**). The presences of isotypes other than IgM/IgD in a population sorted based on surface IgM positivity may indicate the presence of Ig-sterile transcripts. Alternatively, these populations may contain small numbers of contaminants, such as class-switched B cells to which soluble IgM bound to the cell surface, possibly via Fc□R (Blandino and Baumgarth, 2019; Kreuk et al., 2019; Liu et al., 2019).

When the entire set of |DE genes was used to perform clustering by multidimensional scaling, the cell populations clustered by cell type and by tissue of origin (**Fig. 3.5C**). It is possible that the differential clustering by tissue type is a reflection of contaminant cells specific to the tissue of origin. For example, granulocyte associated genes such as *Mpo, Epx, Elane, Ear6, Ms4a3* appeared increased in both BM populations compared to spleen B-1 cells (data not shown). Of note, these same genes appear to be present in publicly available databases from BM derived B cell samples, indicating the technical challenge in obtaining pure cell samples from these rare cell types (www.immgen.org). The ability of soluble IgM to bind to surface FcμR and/or the fact that we could not use a B cell lineage marker, such as CD19 or B220, due to low-level expression of this marker among the B-1PC, might further increase the likelihood of contamination.

Further comparative analysis was therefore focused on comparing BM B-1 cells (B-1PC, B-1$_{sec}$ and non-secreting B-1) and peritoneal cavity B-1 cells as another source of non-secreting cells.

Using expression of 12 genes that characterize the non-secreting from the secreting state showed clear clustering of cell types based on their ability to secrete IgM (**Fig. 3.5D**). As expected, B-1PC showed a plasma cell signature (**Fig. 3.5D**). The BM B-1_{sec} shared characteristic of both cell types, with expression levels of PC associated genes trending lower than seen in B-1PC, and those of B cell associated genes, including *Pax5, Bach2,* and *Cd19* trending higher than by the B-1PC, suggesting that these ASCs are not terminally differentiated (**Fig. 3.5D**). Consistent with the flow cytometric evaluation of Blimp-1 expression, B-1_{sec} had significantly lower transcript levels of *Prdm-1* than B-1PC. Nonetheless, and unexpectedly based on the Blimp-1YFP reporter, they had slightly higher *Prdm-1* transcript levels than the non-secreting B-1 cells populations, despite the fact that they were sorted using the same Blimp-1 YFP negative gate as the non-secreting BM B-1 (**Fig. 3.5D**).

Therefore, further analysis compared the relative expression of genes identified as being directly regulated by Blimp-1 (Minnich et al., 2016). A strong Blimp-1 driven signature was observed in the B-1PC but not in the non-secreting B-1 cells both for Blimp-1 enhanced as well as Blimp-1 repressed genes (**Fig. 3.5E**). B-1_{sec} showed a Blimp-1 signature that was intermediate between that of the B-1 and B-1PC, consistent with low but measurable levels of *Prdm-1* transcripts (**Fig. 3.5D, E**). Although differences in *Prdm-1* expression of the three groups reached statistical significance, transcript levels of *Irf4,* considered another master regulator of plasma cell differentiation (Ochiai et al., 2013), were highly variable between the various samples for each cell population and resulting in a lack of statistically significant differences in Irf4 expression between the populations (**Fig 3.5D**). In contrast, at the protein level all antibody secreting cell population, including the B-1_{sec} expressed uniformly high levels of IRF4 protein, whereas the

non-secreting populations were IRF4^{lo} (**Fig. 3.5F, G**). The data indicate that IRF4 drives the differentiation of both B-1PC and B-1$_{sec}$ towards antibody secretion. IRF4 and Blimp-1 have overlapping and non-redundant functions and positively enforce each other's expression (Low et al., 2019). The data further indicate a potential repression of this forward loop supporting induction of Blimp-1 in the B-1$_{sec}$ by mechanisms that remain to be determined.

3.7 Transcriptional regulators and genes regulating cell-cell interaction/adhesion are differentially expressed between B-1$_{sec}$ and B-1PC

Although B-1$_{sec}$ showed some differences in expression levels of Blimp-1 regulated genes (*Epcam, Sel1l*) compared to B-1PC (**Fig. 3.4E Fig. 3.6A, B**), B-1$_{sec}$ and B-1PC showed similar expression of genes associated with antibody production, such as protein trafficking, UPR, protein glycosylation, and ER stress response. Furthermore, *Ighm* and *J chain* were not differentially expressed between these two populations, supporting results from our functional studies that B-1$_{sec}$ and B-1PC produce similar amounts of total IgM (**Fig. 3.3C-E**). Most DE genes between B-1$_{sec}$ and B-1PC were Ig variable genes (43/69) suggesting that their repertoires are distinct (**Fig. 3.6A**). However, given the small numbers of cells that we were able to sort for analysis (**Suppl. Fig. 3.3B**), further studies are required to more fully compare their respective Ig-repertoires.

Some genes associated with transcriptional regulation were highly expressed in B-1$_{sec}$ compared to B-1PC. This included the small nuclear RNA 7SK and histone genes, *H2ac6* and *H2ac20* (**Fig. 3.6A, B**). The function of 7SK in lymphocytes is not fully resolved. However, it is known as an important regulator of positive transcription elongation factor b (P-TEFb), a protein

complex essential for the regulation of RNA polymerase II (Peterlin et al., 2012). Studies in activated cells suggest, however, that it may have functions unrelated to P-TEFb, such as cell survival (Haaland et al., 2003, 2005). Alterations in histone genes suggest differences in chromatin accessibility (**Fig. 3.6A, B**). H2ac6 was found to be elevated in B cells from human patients with chronic lymphocytic leukemia and in estrogen receptor (ER) positive breast cancers cells, where it mediates estrogen dependent oncogenes *myc* and *bcl2* (Espiritu et al., 2021). H2ac20 regulates cell proliferation and growth responses to hormone signaling such as epidermal growth factor (EGF) and estradiol (Espiritu et al., 2021). Estrogen signaling is required for the development of some nIgM specificities (Zeng et al., 2018), however, there was no difference in ER, *esr1,* expression between B-1_{sec} and B-1PC, nor in *myc* or *bcl2*. B-1_{sec} do have 2.8 log_2FC higher EGF expression than B-1PC, although the adjusted p-value was not significant (p=0.2). Collectively, the data suggest that transcriptional and epigenetic regulation may differ between B-1PC and B-1_{sec} but leaves unresolved how this may relate to their variant differentiation status.

Genes downregulated in B-1_{sec} compared to B-1PC included numerous that are involved in, or are predicted to be involved in cell-cell interaction/adhesion. Epcam,a Blimp-1 regulated adhesion molecule, that is expressed in conventional plasma cells (Minnich et al., 2016), is more strongly expressed in B-1PC **(Fig. 3.4F, 3.6B, Suppl. Table 3.1)** as are *Zfhx3* and *Sspo* **(Fig. 3.6B)**. Zinc-Finger homobox 3 transcription (ZFHX3) upregulates expression of cell adhesion molecules and extracellular matrix procollagens (Kim et al., 2010). Consistent with this, there were two collagen genes *Col2a1* and *Col11a* upregulated in B-1PC compared to B-1_{sec}. COL2a1 has been found in melanoma tumor repopulating cells, which are responsible for tumor seeding at secondary sites (Talluri et al., 2020) and COL11a1 modulates interactions between cancer

cells and stromal cells (Nallanthighal et al., 2021). This may suggest that these extracellular matrix proteins may play a role in interaction between B-1PC and the BM stroma. *Sspo* encodes for SCO-Spondin, an extracellular glycoprotein involved in neuronal cell aggregation during development (Gobron et al., 1996). Together, these data may suggest that B-1PC and B-1_{sec} reside in different BM niches that require differential interactions with surrounding cells.

3.8 Discussion

Here we identify and characterize a population of CD19var IgM+ CD43var J chain+ icIgM^{hi} CD138+ Blimp-1YFP^{neg}, IRF4^{hi} B-1_{sec} that contribute significantly to BM derived nIgM. They are very different from classical BM residing ASC, lacking strong expression of Blimp-1 and exhibiting characteristics of non-terminally differentiated but antibody secreting cells, both by phenotype and transcriptional profiling. Their levels of IgM secretion appeared comparable to that of B-1PC and functionally they seem to expand in T-deficient and Blimp-1-deficient mice lacking B-1PC, suggesting that they are not simply activation intermediates between B-1 cells and terminally-differentiated B-1PC, but are driven by distinct signals to differentiate into BM IgM-secreting cells.

The transcriptional profile of B-1_{sec} is consistent with that of other antibody secreting cells, showing high expression of genes associated with ER Stress, the UPR, protein transport, and the ERAD pathway. At the same time expression of *Prdm-1*, the gene encoding for the transcriptional regulator of B cell differentiation, Blimp-1, was expressed at levels intermediate between non-secreting B-1 and B-1PC, while we were unable to detect Blimp-1YFP reporter expression. Unfortunately, the low number of B-1_{sec} did not allow us to confirm protein

expression levels by Western Blotting and anti-Blimp-1 antibody staining by flow cytometry is not sufficiently sensitive to distinguish low expression from lack of expression (not shown). Despite their failure to express Blimp-1YFP, B-1_{sec} express high levels of IRF4 protein, although variable levels of its transcript. IRF4 is a transcription master regulator essential for differentiation and maintenance of plasma cells(Ochiai et al., 2013). IRF4 and Blimp-1 regulate each other through a positive feedback loop (Tellier et al., 2016)and thus seeing high levels IRF4 without Blimp-1 induction was unexpected. Using a published Blimp-1 dependent gene signature (Minnich et al., 2016)we found that the transcriptional profile of B-1_{sec} was intermediary between that of B-1PC and non-secreting B-1 cells, providing some evidence of Blimp-1 activity. However, given that IRF4 and Blimp-1 are co-expressed in conventional plasma cells and that the gene targets of IRF4 are not yet fully defined, it is conceivable that this profile is driven at least in part by IRF4 (Low et al., 2019), consistent evidence that IRF4 and Blimp-1 exert effects on some of the same genes. For example, *Xbp-1* expression relies on the non-redundant presence of both IRF4 and Blimp-1 in conventional plasma cells (Low et al., 2019).Thus, it remains to be determined to which extent the "Blimp-1 signature" of B-1_{sec} is actually regulated by IRF4.

Alternatively other transcriptional or epigenetic regulators may support B-1_{sec} antibody secretion, as may be suggested by their higher expression of histone genes, *H2ac6 and H2ac20* and a short nuclear RNA involved in transcriptional regulation. Another possibility is that B-1_{sec} use a different transcriptional start site of Blimp-1. Blimp-1 is essential for embryonic development so complete deletion of *Prdm-1* is embryonic lethal. Deletion of exon1A, however, removes the NF-κB dependent promoter site required for B cell differentiation, but embryonic expression of

Blimp-1 is maintained through use of an alternate promoter in exon 1 (Morgan et al., 2009). Additionally, there is another alternative promoter region located 5′ of *Prdm-1* exon 4 that generates a protein identical to classical *Prdm-1*, but lacking the PR/SET domain. The truncated protein is still capable of nuclear localization and DNA binding, but the repressive capacity for genes like *Pax5, c-myc, Ciita* and MHCII is around half that of classical *Prdm-1* (György et al., 2003). This splice form has been identified in human myeloma cells, which are spontaneous antibody secretors due to neoplastic transformation rather than normal differentiation (György et al., 2003). Use of an alternate promoter may explain the lack of YFP expression in the reporter mice, which use the classical NF-κB promoter site from exon 1 in a bacterial artificial chromosome to drive YFP expression (Fooksman et al., 2010).

IgM is a highly conserved Ig-isotype, expressed in all vertebrates and plays an important role in protection from infections and autoimmune diseases. It appears that the dichotomy of nIgM producing cells with regards to Blimp-1 expression in murine B-1_{sec} and B-1PC is conserved across species. In cartilaginous fish, both Blimp-1 positive and negative IgM secreting cells have been identified (Castro et al., 2013)

In T cell deficient mice that undergo normal B cell development, nIgM secretion in the BM is normal despite a lack of Blimp-1 dependent B-1PC (Smith et al. 2022 in revision see Chapter 2). It appears that B-1_{sec} are capable of compensating for lack of Blimp-1 dependent antibody production in the BM. However, characterization of mice with B-1 cells reconstituted from adult peritoneal cells but lacking CD4+ T cells and thus BM B-1PC, have a defect in total IgM and BM derived nIgM, suggesting that peritoneal B-1 cells may not directly differentiate into B-1_{sec}

(Smith et al. 2022 in revision see Chapter 2). Innate stimulation *in vitro* and *in vivo* of body cavity B-1 results in rapid differentiation to a classical plasma cell phenotype with down regulation of CD19, surface IgM and induction of Blimp and CD138 and IgM secretion (Barbosa et al., 2021; Genestier et al., 2007; Ochsenbein et al., 1999; Savage et al., 2019), suggesting that peritoneal B-1 cells and B-1PC may have precursor/effector relationship, additionally there is evidence that TLR expression can effect levels of some nIgM at steady state (Kreuk et al., 2019). This raises the question of whether the development of B-1_{sec} may differ in ontogeny from B-1PC. B-1 cells develop from multiple waves of precursors mostly from fetal and neonatal tissue of both hematopoietic and non-hematopoietic origins (Dzierzak and Bigas, 2018; Yoshimoto et al., 2011). The heterogeneity of the precursor populations suggests that different B-1 subsets could come from different precursors. It might also be expected that B-1 cells arising from different waves of precursors might express a different repertoire. The repertoire of B-1 derived nIgM is unique, made of oligoclonal, broadly reactive IgM that is generated through positive selection of self-reactive clones (Ferry et al., 2003; Hayakawa et al., 1999, 2003). It is possible that the self-antigens inducing B-1 development are different in the different tissues of origin. We found significant differential expression of many *Ighv* and *Igkv* genes between B-1_{sec} and B-1PC, however, the small number of cells used confounds any repertoire analysis of these populations. Studies utilizing lineage tracing techniques may be important to determine the origins of B-1_{sec} and their repertoire.

In conclusion B-1_{sec} are a subset of nIgM secreting cells that contribute significantly to BM derived serum nIgM. Their transcriptional profile is that of non-terminally differentiated B cells that are capable of maximal antibody secretion in an IRF4 dependent manner despite low levels

of *Prdm-1.* Their unique ability to secrete antibodies in the absence of terminal differentiation may support ongoing self-renewal and thus the maintenance of nIgM with unique specificity.

3.9 Materials and Methods

Mice

C57BL/6 mice and breeding pairs of B6.129P2-*Tcrb*^{tm1Mom} *Tcrd*^{tm1Mom}/J(TCRβδ-/-) and B6.Cg-Gpi1^{a} Thy1^{a} Igh^{a} /J (Igha) were purchased from The Jackson Laboratory. Breeding pairs of B6.Cg-Tg(Prdm1-EYFP)1Mnz/J (Blimp-1 YFP) were generously provided by Michel Nussenzweig (The Rockefeller University, NY) and breeding males of C57BL/6N-Jchain$^{em1(icre/ERT2)Deep}$/J X B6.Cg-Gt(ROSA)26Sor$^{tm14(CAG-tdTomato)Hze}$/J (J Chain TdTomato) heterozygotes were generously provided by Deepta Bhattacharya (University of Arizona). Female hemizygote Blimp-1 YFP mice were crossed with heterozygote male J Chain TdTomato mice until Blimp-1 YFP hemizygote and heterozygote or homozygote J Chain TdTomato (Blimp-1 YFP/J Chain TdTomato) mice were generated. Prior to experiments Blimp-1 YFP/J Chain TdTomato mice were treated with Tamoxifen at 75mg/kg intraperitoneally once daily for five days. They were then rested for 7 days before analysis. Mice were used between 8-16 weeks of age.

Neonatal Ig-allotype chimeras were generated as described previously (Baumgarth et al., 1999b). Briefly, neonatal Igha mice were treated twice weekly with intra-peritoneal injections of DS-1.1 (anti-IgMa) in PBS beginning on day one after birth for a total of 2.3 mg over 42 day. Between days 2-4, mice were given also $5x10^6$ donor cells from the peritoneal cavity washout of C57BL/6J (IgMb) mice. Mice were rested for at least 42 days after end of antibody treatment

before use in experiments. All mice used for experiments were female unless otherwise indicated. They were maintained in microisolator cages under SPF conditions, provided mouse chow and water supplied at lib by the UC Davis Animal Care staff and were euthanized by overexposure to CO_2. All procedures were approved by the UC Davis Institutional Animal Care and Use Committee.

Flow cytometry and FACS sorting

BM and spleen were processed as previously described (Rothaeusler and Baumgarth, 2006). Briefly, BM was harvested by injecting staining media through the marrow cavity of a long bone. Spleen was ground between the frosted ends of two microscope slides until dissociated. Peritoneal/pleural cavity cells were obtained using staining media flushed into and then aspirated from the peritoneal and pleural cavities with a plastic pipette (Molecular Bio Products Inc.). All samples were passed through a 70 mm to make a single cell suspension, treated with ACK lysis buffer (Rothaeusler and Baumgarth, 2006), re-filtered through nylon mesh, and resuspended in staining media. Trypan Blue exclusion dye was performed on all samples to identify live cells using a hemocytometer or an automated cell counter (Nexcelom Bioscience). Cells were blocked with anti-FcγR (2.4.G2), washed and stained with fluorescent antibodies (Supplemental Table 1). Dead cells were identified using Live/Dead Fixable Aqua or Live/Dead Fixable Violet stain (Invitrogen). Fluorescently labeled cells were read on either a 4-laser, 22-paramter LSR Fortessa (BD Bioscience), or a 5-laser, 30-parameter Symphony (BD Bioscience). FACS-sorting was done using a 3-laser FACSAria (BD Bioscience). Data were analyzed using FlowJo software (FlowJo LLC, kind gift of Adam Treister). Peritoneal B-1 cells are identified as Dump- (CD4, CD8a, Nk1.1, F4/80, Gr-1, CD93-), CD23-, CD19hi. BM and Spleen B-1 cells are identified as

Dump-, CD23- CD43var, IgM+, CD19varand B-1PC are identified as Dump-, CD23- C43+, IgD-, IgM+, CD19lo/- and Blimp-1 and/or CD138+.

IcIgM staining

Cells were processed and surface stained as for flow cytometry staining, including polyclonal fluorochrome-labeled anti-IgM (Table 1). Cells were washed and then incubated with unlabeled polyclonal anti-IgM in excess for 15 minutes on ice, fixed in 2% PFA (Thermo Fisher) for 15 minutes and permeabilized by washing twice in buffer containing 2% Saponin (Calbiochem) (Staining buffer for non-permeabilized controls). Cells were stained with anti-IgM (331) in 2% Saponin (non-perm control uses stain buffer) on ice for 15 minutes, washed and resuspended in staining media prior to being run on the flow cytometer.

Enzyme-Linked ImmunoSpot (ELISPOT)

IgM ASCs were enumerated following direct sorting of B-1 cells populations into ELISPOT plates. The number of cells sorted was optimized based on the frequency of the population and the frequency of IgM secretion in the population. In general, 10-20 cells were sorted from high antibody secreting population into a single well, 8,000-10,000 cells from populations with minimal antibody secretion, and 20,000 cells from the CD43+ an CD43- populations. 96-well ELISPOT plates (Multi-Screen HA Filtration, Millipore) were coated with 5µg/ml anti-IgM (331). Non-specific binding was blocked with 4% bovine serum albumin (BSA) in PBS. Tissues were processed as detail above and cells were plated in culture media (RPMI 1640, 10% fetal bovine serum, 292 µg/ml L-glutamine, 100 Units/ml penicillin, 100 µg/ml streptomycin, and 50 µM 2-mercaptoethanol). Cells were cultured overnight (~16hrs) at 37°C/5% CO_2. Deionized

water was used to lyse the cells after which IgM secretion was revealed with biotinylated anti-IgM (Southern Biotech), followed by streptavadin-horseradish peroxidase (Vector Labs), both diluted in 2% BSA in PBS. Last, substrate solution (3.3 mg 3-amino-9-ethylcarbazole (Sigma Aldrich) dissolved in dimethyl formamide and 0.015% hydrogen perioxide in 0.1M sodium acetate) was added, and the reaction was stopped with deionized water. Spots were enumerated and images captured with the AID EliSpot Reader System (Autoimmun Diagnostika).

Cytospin

Four populations of BM cells (CD138-, Blimp-1YFP-, Jchain Tom- Non-secreting B-1; CD138+, Blimp-1YFP-, JChain Tom+ B-1_{sec}; CD138-, Blimp-1YFP-+ Jchain Tom+ B-1; CD138+, Blimp-1YFP+, JChain Tom+ B-1PC) from Blimp-1 YFP/JChain TdTomato mice were FACS sorted into 1.5ml Eppendorf tubes containing culture media with 10% FBS. A minimum of 500 cells was sorted per population. Tubes were then filled to 1ml with culture medium and cells where pelleted at 1500 rpm for 5 minutes. All but 100µl of media was discarded. Cells were resuspended by gentle agitation and all 100µl were loaded into the cytofunnel. The slides were then place in the Cytospin and centrifuge at 1000 × g for 5 min. The cells were then stained with a hematoxylin & eosin staining kit per the manufacturers specifications (Abcam).

Bulk RNA sequencing

Five B-1 cell populations from 3 different mice were sorted using a 3-laser FACSAria with a 100mm nozzle (BD Bioscience). Cells were sorted directly into RNAase free Eppendorf tubes containing 75-300 µl of Norgen Buffer RL. The cell lysate was frozen at -80C until all samples

were collected. Total RNA from each population was extracted using Norgen Biotek single cell purification kit in single batch of 15 samples per manufacturer's instructions, unless otherwise noted. On column DNA digest was performed. In brief, 1ml superase (Thermo Fisher), 15 µl of DNAase and 100 µl of Enzyme incubation buffer A(Norgen) were run over every column, the flow through was collected and incubated on the column for 15 minutes before continuing extraction per manufacturers specifications. Samples from cell populations with under 10,000 cells were eluted in 15 µl of elution buffer, those with over 10,000 cells in 20 µl.
Quality control was performed on an Aligent bioanalyzer (Aligent) using a picochip. Libraries were made using SMARTer® Stranded Total RNA-Seq Kit v2 -Pico Input 5' sequencing. Illumina sequencing—30 million PE150 read-pairs per sample was then performed. The five populations sorted were as follows: Peritoneal B-1 (CD4-, CD8-, NK1.1-, Gr-1-, F4/80-, CD23-, CD93-, IgM+, CD19++), Spleen B-1_{sec} (CD4-, CD8-, NK1.1-, Gr-1-, F4/80-, CD23-,CD93-IgM+, CD19var, YFP-(Blimp-1-), CD138+, TdTomato+ (J-Chain+)), BM non secreting B-1 (CD4-, CD8-, NK1.1-, Gr-1-, F4/80-, CD23-, IgM+, CD19+, YFP-(Blimp-1-), CD138-, TdTomato-(J-Chain-)), BM B-1PC gated on CD4-, CD8-, NK1.1-, Gr-1-, F4/80-, CD23-, CD93-, IgM+, CD19var, YFP+ (Blimp-1+), CD138+, TdTomato+ (J-Chain+), BM B-$_{1sec}$ (CD4-, CD8-, NK1.1-, Gr-1-, F4/80-, CD23-,CD93-,IgM+, CD19var, YFP-(Blimp-1-), CD138+, TdTomato+ (J-Chain+)). Samples and cell numbers are found in Table 2.

Prior to differential gene expression analysis, sequence data were preprocessed using htstream, version 1.3.3 (https://github.com/s4hts/HTStream) and aligned to GRCm39, Gencode version M28, using STAR, version 2.7.9a (https://pubmed.ncbi.nlm.nih.gov/23104886/).

Differential expression analyses were conducted using limma-voom, using the model ~Group + NumCells + Mouse. Low expressed genes were filtered using the limma function filterByExpr, leaving 12749 genes.

Interpretation of DEG Data

Differentially expressed gene lists were input into DAVID (Huang et al., 2009b, 2009a) to identify associated Biologic Process GO terms. Only BP GO terms with Bonferroni adjust p value ≤ 0.05 were reported. Genes identified as the top BP GO term were then input into STRING (Szklarczyk et al., 2015) to further asses interactions between the proteins in that network and overlapping contributions to other networks or pathways. When DAVID did not return significant GO terms DEG were entered into NCBI Gene (https://www.ncbi.nlm.nih.gov/gene) and summary of function for each gene was assessed. When multiple genes were identified with similar functions a literature search for those genes, their corresponding proteins and their function was performed.

Quantification, Visualization and Statistical Analysis

All statistics were done with the help of Prism software (GraphPad Software). Comparisons between two groups were done using a two-tailed Student's t test. For more than two groups, a one-way ANOVA was performed with post hoc analysis for significant differences between individual groups using Tukey's correction for multiple comparisons. A $p < 0.05$ was considered statistically significant.

The R studio 2021.09.2 Build 382 (RStudio Team (2020). RStudio: Integrated Development for R. RStudio, PBC, Boston, MA URL http://www.rstudio.com/) was used for visualization of the RNAseq data via volcano plot and heat maps with packages tidyverse (v1. 3.0; Wickham et al., 2019), pheatmap (RRID:SCR_016418) and ggplot2 (Wickham, 2009).

3.10 References

Barbosa, C.H.D., Lantier, L., Reynolds, J., Wang, J., and Re, F. (2021). Critical role of IL-25-ILC2-IL-5 axis in the production of anti-Francisella LPS IgM by B1 B cells. PLOS Pathogens *17*, e1009905. https://doi.org/10.1371/JOURNAL.PPAT.1009905.

Baumgarth, N., Herman, O.C., Jager, G.C., Brown, L., Herzenberg, L.A., and Herzenberg, L.A. (1999a). Innate and acquired humoral immunities to influenza virus are mediated by distinct arms of the immune system. Proc Natl Acad Sci U S A *96*, 2250–2255. https://doi.org/10.1073/pnas.96.5.2250.

Baumgarth, N., Herman, O.C., Jager, G.C., Brown, L., Herzenberg, L.A., and Herzenberg, L.A. (1999b). Innate and acquired humoral immunities to influenza virus are mediated by distinct arms of the immune system. Proc Natl Acad Sci U S A *96*, 2250–2255. https://doi.org/10.1073/PNAS.96.5.2250.

Baumgarth, N., Herman, O.C., Jager, G.C., Brown, L.E., Herzenberg, L.A., and Chen, J. (2000). B-1 and B-2 cell-derived immunoglobulin M antibodies are nonredundant components of the protective response to influenza virus infection. J Exp Med *192*, 271–280. https://doi.org/10.1084/jem.192.2.271.

Beaudin, A.E., Boyer, S.W., Perez-Cunningham, J., Hernandez, G.E., Derderian, S.C., Jujjavarapu, C., Aaserude, E., MacKenzie, T., and Forsberg, E.C. (2016). A Transient Developmental Hematopoietic Stem Cell Gives Rise to Innate-like B and T Cells. Cell Stem Cell *19*, 768–783. https://doi.org/10.1016/j.stem.2016.08.013.

Blandino, R., and Baumgarth, N. (2019). Secreted IgM: New tricks for an old molecule. Journal of Leukocyte Biology *106*, 1021–1034. https://doi.org/10.1002/JLB.3RI0519-161R.

Boes, M., Schmidt, T., Linkemann, K., Beaudette, B.C., Marshak-Rothstein, A., and Chen, J. (2000a). Accelerated development of IgG autoantibodies and autoimmune disease in the absence of secreted IgM. Proc Natl Acad Sci U S A *97*, 1184–1189. https://doi.org/10.1073/pnas.97.3.1184.

Boes, M., Schmidt, T., Linkemann, K., Beaudette, B.C., Marshak-Rothstein, A., and Chen, J. (2000b). Accelerated development of IgG autoantibodies and autoimmune disease in the absence of secreted IgM. Proc Natl Acad Sci U S A *97*, 1184–1189. https://doi.org/10.1073/pnas.97.3.1184.

Bos, N.A., Kimura, H., Meeuwsen, C.G., Visser, H. De, Hazenberg, M.P., Wostmann, B.S., Pleasants, J.R., Benner, R., and Marcus, D.M. (1989). Serum immunoglobulin levels and naturally occurring antibodies against carbohydrate antigens in germ-free BALB/c mice fed chemically defined ultrafiltered diet. Eur J Immunol *19*, 2335–2339. https://doi.org/10.1002/EJI.1830191223.

Brandtzaeg, P. (1985). Role of J chain and secretory component in receptor-mediated glandular and hepatic transport of immunoglobulins in man. Scand J Immunol *22*, 111–146. https://doi.org/10.1111/J.1365-3083.1985.TB01866.X.

Castro, C.D., and Flajnik, M.F. (2014). Putting J chain back on the map: how might its expression define plasma cell development? Journal of Immunology (Baltimore, Md. : 1950) *193*, 3248–3255. https://doi.org/10.4049/JIMMUNOL.1400531.

Choi, Y.S., Dieter, J.A., Rothaeusler, K., Luo, Z., and Baumgarth, N. (2012). B-1 cells in the bone marrow are a significant source of natural IgM. Eur J Immunol *42*, 120–129. https://doi.org/10.1002/eji.201141890.

Delon, J., Kaibuchi, K., and Germain, R.N. (2001). Exclusion of CD43 from the immunological synapce is mediated by phosphorylation-regulated relocation of the cytoskeletal adaptor Moesin. Immunity *15*, 691–701. https://doi.org/10.1016/S1074-7613(01)00231-X.

Dzierzak, E., and Bigas, A. (2018). Blood Development: Hematopoietic Stem Cell Dependence and Independence. Cell Stem Cell *22*, 639–651. https://doi.org/10.1016/J.STEM.2018.04.015.

Ehrenstein, M.R., Cook, H.T., and Neuberger, M.S. (2000). Deficiency in serum immunoglobulin (Ig)M predisposes to development of IgG autoantibodies. J Exp Med *191*, 1253–1258. https://doi.org/10.1084/jem.191.7.1253.

Espiritu, D., Gribkova, A.K., Gupta, S., Shaytan, A.K., and Panchenko, A.R. (2021). Molecular Mechanisms of Oncogenesis through the Lens of Nucleosomes and Histones. Journal of Physical Chemistry B *125*, 3963–3976. https://doi.org/10.1021/ACS.JPCB.1C00694/SUPPL_FILE/JP1C00694_SI_001.PDF.

Ferry, H., Jones, M., Vaux, D.J., Roberts, I.S.D., and Cornall, R.J. (2003). The cellular location of self-antigen determines the positive and negative selection of autoreactive B cells. J Exp Med *198*, 1415–1425. https://doi.org/10.1084/JEM.20030279.

Fooksman, D.R., Schwickert, T.A., Victora, G.D., Dustin, M.L., Nussenzweig, M.C., and Skokos, D. (2010). Development and migration of plasma cells in the mouse lymph node. Immunity *33*, 118–127. https://doi.org/10.1016/J.IMMUNI.2010.06.015.

Genestier, L., Taillardet, M., Mondiere, P., Gheit, H., Bella, C., and Defrance, T. (2007). TLR Agonists Selectively Promote Terminal Plasma Cell Differentiation of B Cell Subsets Specialized in Thymus-Independent Responses. The Journal of Immunology *178*, 7779–7786. https://doi.org/10.4049/jimmunol.178.12.7779.

Gobron, S., Monnerie, H., Meiniel, R., Creveaux, I., Lehmann, W., Lamalle, D., Dastugue, B., and Meiniel, A. (1996). SCO-spondin: A new member of the thrombospondin family secreted by the subcommissural organ is a candidate in the modulation of neuronal aggregation. Journal of Cell Science *109*, 1053–1061. https://doi.org/10.1242/jcs.109.5.1053.

György, I., Fejér, G., Ghosh, N., Seto, E., and Wright, K.L. (2003). Identification of a functionally impaired positive regulatory domain I binding factor 1 transcription repressor in myeloma cell lines. J Immunol *170*, 3125–3133. https://doi.org/10.4049/JIMMUNOL.170.6.3125.

Haaland, R.E., Herrmann, C.H., and Rice, A.P. (2003). Increased association of 7SK snRNA with Tat cofactor P-TEFb following activation of peripheral blood lymphocytes. AIDS *17*, 2429–2436. https://doi.org/10.1097/00002030-200311210-00004.

Haaland, R.E., Herrmann, C.H., and Rice, A.P. (2005). siRNA depletion of 7SK snRNA induces apoptosis but does not affect expression of the HIV-1 LTR or P-TEFb-dependent cellular genes. Journal of Cellular Physiology *205*, 463–470. https://doi.org/10.1002/jcp.20528.

Haro, M.A., Dyevoich, A.M., Phipps, J.P., and Haas, K.M. (2019). Activation of B-1 cells promotes tumor cell killing in the peritoneal cavity. Cancer Res *79*, 159. https://doi.org/10.1158/0008-5472.CAN-18-0981.

Haury, M., Sundblad, A., Grandien, A., Barreau, C., Coutinho, A., and Nobrega, A. (1997). The repertoire of serum IgM in normal mice is largely independent of external antigenic contact. Eur J Immunol *27*, 1557–1563. https://doi.org/10.1002/EJI.1830270635.

Hayakawa, K., Asano, M., Shinton, S.A., Gui, M., Allman, D., Stewart, C.L., Silver, J., and Hardy, R.R. (1999). Positive selection of natural autoreactive B cells. Science *285*, 113–116. https://doi.org/10.1126/SCIENCE.285.5424.113.

Hayakawa, K., Asano, M., Shinton, S.A., Gui, M., Wen, L.J., Dashoff, J., and Hardy, R.R. (2003). Positive selection of anti-thy-1 autoreactive B-1 cells and natural serum autoantibody production independent from bone marrow B cell development. Journal of Experimental Medicine *197*, 87–99. https://doi.org/10.1084/jem.20021459.

Holodick, N.E., Vizconde, T., and Rothstein, T.L. (2014). Splenic B-1a cells expressing CD138 spontaneously secrete large amounts of immunoglobulin in naïve mice. Frontiers in Immunology *5*. https://doi.org/10.3389/FIMMU.2014.00129.

Hooijkaas, H., van der Linde-Preesman, A.A., Benne, S., and Benner, R. (1985). Frequency analysis of the antibody specificity repertoire of mitogen-reactive B cells and “spontaneously” occurring “background” plaque-forming cells in nude mice. Cell Immunol *92*, 154–162. https://doi.org/10.1016/0008-8749(85)90073-5.

Huang, D.W., Sherman, B.T., and Lempicki, R.A. (2009a). Systematic and integrative analysis of large gene lists using DAVID bioinformatics resources. Nat Protoc *4*, 44–57. https://doi.org/10.1038/NPROT.2008.211.

Huang, D.W., Sherman, B.T., and Lempicki, R.A. (2009b). Bioinformatics enrichment tools: paths toward the comprehensive functional analysis of large gene lists. Nucleic Acids Res *37*, 1–13. https://doi.org/10.1093/NAR/GKN923.

Iwakoshi, N.N., Lee, A.H., and Glimcher, L.H. (2003). The X-box binding protein-1 transcription factor is required for plasma cell differentiation and the unfolded protein response. Immunological Reviews *194*, 29–38. https://doi.org/10.1034/j.1600-065X.2003.00057.x.

Kim, T.S., Kawaguchi, M., Suzuki, M., Jung, C.G., Asai, K., Shibamoto, Y., Lavin, M.F., Khanna, K.K., and Miura, Y. (2010). The ZFHX3 (ATBF1) transcription factor induces PDGFRB, which activates ATM in the cytoplasm to protect cerebellar neurons from oxidative stress. Disease Models & Mechanisms *3*, 752–762. https://doi.org/10.1242/DMM.004689.

Koshland, M.E. (1985). The coming of age of the immunoglobulin J chain. Annu Rev Immunol *3*, 425–453. https://doi.org/10.1146/ANNUREV.IY.03.040185.002233.

Kreuk, L.S.M., Koch, M.A., Slayden, L.C., Lind, N.A., Chu, S., Savage, H.P., Kantor, A.B., Baumgarth, N., and Barton, G.M. (2019). B cell receptor and toll-like receptor signaling coordinate to control distinct B-1 responses to both self and the microbiota. Elife *8*. https://doi.org/10.7554/eLife.47015.

Liu, J., Wang, Y., Xiong, E., Hong, R., Lu, Q., Ohno, H., and Wang, J.Y. (2019). Role of the IgM Fc receptor in immunity and tolerance. Frontiers in Immunology *10*, 529. https://doi.org/10.3389/FIMMU.2019.00529/BIBTEX.

McCarron, M.J., Park, P.W., and Fooksman, D.R. (2017). CD138 mediates selection of mature plasma cells by regulating their survival. Blood *129*, 2749. https://doi.org/10.1182/BLOOD-2017-01-761643.

Montecino-Rodriguez, E., and Dorshkind, K. (2012). B-1 B cell development in the fetus and adult. Immunity *36*, 13–21. https://doi.org/10.1016/J.IMMUNI.2011.11.017.

Moon, B., Takaki, S., Miyake, K., and Takatsu, K. (2004). The Role of IL-5 for Mature B-1 Cells in Homeostatic Proliferation, Cell Survival, and Ig Production. The Journal of Immunology *172*, 6020–6029. https://doi.org/10.4049/jimmunol.172.10.6020.

Moore, K.A., and Hollien, J. (2012). The Unfolded Protein Response in Secretory Cell Function. Http://Dx.Doi.Org/10.1146/Annurev-Genet-110711-155644 *46*, 165–183. https://doi.org/10.1146/ANNUREV-GENET-110711-155644.

Moore-Connors, J.M., Kim, H.S., Marshall, J.S., Stadnyk, A.W., Halperin, S.A., and Wang, J. (2014). CD43−, but not CD43+, IL-10-producing CD1dhiCD5+ B cells suppress type 1 immune responses during Chlamydia muridarum genital tract infection. Mucosal Immunology 2015 8:1 *8*, 94–106. https://doi.org/10.1038/mi.2014.45.

Morgan, M.A.J., Magnusdottir, E., Kuo, T.C., Tunyaplin, C., Harper, J., Arnold, S.J., Calame, K., Robertson, E.J., and Bikoff, E.K. (2009). Blimp-1/Prdm1 Alternative Promoter Usage during Mouse Development and Plasma Cell Differentiation. Molecular and Cellular Biology *29*, 5813–5827. https://doi.org/10.1128/MCB.00670-09/FORMAT/EPUB.

Nallanthighal, S., Heiserman, J.P., and Cheon, D.J. (2021). Collagen Type XI Alpha 1 (COL11A1): A Novel Biomarker and a Key Player in Cancer. Cancers (Basel) *13*, 1–22. https://doi.org/10.3390/CANCERS13050935.

Nguyen, T.T., Elsner, R.A., and Baumgarth, N. (2015). Natural IgM prevents autoimmunity by enforcing B cell central tolerance induction. J Immunol *194*, 1489–1502. https://doi.org/10.4049/jimmunol.1401880.

Nitschke, L. (2015). Siglec-G is a B-1 cell inhibitory receptor and also controls B cell tolerance. Ann N Y Acad Sci *1362*, 117–121. https://doi.org/10.1111/nyas.12826.

Notley, C.A., Brown, M.A., Wright, G.P., and Ehrenstein, M.R. (2011). Natural IgM is required for suppression of inflammatory arthritis by apoptotic cells. J Immunol *186*, 4967–4972. https://doi.org/10.4049/jimmunol.1003021.

Ochsenbein, A.F., Fehr, T., Lutz, C., Suter, M., Brombacher, F., Hengartner, H., and Zinkernagel, R.M. (1999). Control of early viral and bacterial distribution and disease by natural antibodies. Science (1979) *286*, 2156–2159. .

Van Oudenaren, A., Haaijman, J.J., and Benner, R. (1984). Frequencies of background cytoplasmic Ig-containing cells in various lymphoid organs of athymic and euthymic mice as a function of age and immune status. Immunology *51*, 735–742. .

Pedraza-Alva, G., and Rosenstein, Y. (2007). CD43 - One molecule, many tales to recount. Signal Transduction *7*, 372–385. https://doi.org/10.1002/SITA.200700140.

Peterlin, B.M., Brogie, J.E., and Price, D.H. (2012). 7SK snRNA: a noncoding RNA that plays a major role in regulating eukaryotic transcription. Wiley Interdiscip Rev RNA *3*, 92. https://doi.org/10.1002/WRNA.106.

Qi, L., Tsai, B., and Arvan, P. (2017). New Insights into the Physiological Role of Endoplasmic Reticulum-Associated Degradation. Trends in Cell Biology *27*, 430–440. https://doi.org/10.1016/j.tcb.2016.12.002.

Qian, Y., Ke, Q., Wang, Z., and Zhang, B. (2015). Regulation of IgD Expression and Its Role in B Cell Transformation. Blood *126*, 2230–2230. https://doi.org/10.1182/BLOOD.V126.23.2230.2230.

Reynolds, A.E., Kuraoka, M., and Kelsoe, G. (2015). Natural IgM is produced by CD5- plasma cells that occupy a distinct survival niche in bone marrow. J Immunol *194*, 231–242. https://doi.org/10.4049/jimmunol.1401203.

Rothaeusler, K., and Baumgarth, N. (2006). Evaluation of intranuclear BrdU detection procedures for use in multicolor flow cytometry. Cytometry Part A *69*, 249–259. https://doi.org/10.1002/cyto.a.20252.

Sanderson, R.D., Lalor, P., and Bernfield, M. (1989). B lymphocytes express and lose syndecan at specific stages of differentiation. Cell Regul *1*, 27–35. https://doi.org/10.1091/MBC.1.1.27.

Savage, H.P., Yenson, V.M., Sawhney, S.S., Mousseau, B.J., Lund, F.E., and Baumgarth, N. (2017). Blimp-1–dependent and –independent natural antibody production by B-1 and B-1–derived plasma cells. The Journal of Experimental Medicine *214*, 2777–2794. https://doi.org/10.1084/jem.20161122.

Savage, H.P., Klasener, K., Smith, F.L., Luo, Z., Reth, M., and Baumgarth, N. (2019). TLR induces reorganization of the IgM-BCR complex regulating murine B-1 cell responses to infections. Elife *8*. https://doi.org/10.7554/ELIFE.46997.

Skrzypczynska, K.M., Zhu, J.W., and Weiss, A. (2016). Positive Regulation of Lyn Kinase by CD148 Is Required for B Cell Receptor Signaling in B1 but Not B2 B Cells. Immunity *45*, 1232–1244. https://doi.org/10.1016/J.IMMUNI.2016.10.013.

Szklarczyk, D., Franceschini, A., Wyder, S., Forslund, K., Heller, D., Huerta-Cepas, J., Simonovic, M., Roth, A., Santos, A., Tsafou, K.P., et al. (2015). STRING v10: protein-protein interaction networks, integrated over the tree of life. Nucleic Acids Res *43*, D447–D452. https://doi.org/10.1093/NAR/GKU1003.

Talluri, B., Amar, K., Saul, M., Shireen, T., Konjufca, V., Ma, J., Ha, T., and Chowdhury, F. (2020). COL2A1 Is a Novel Biomarker of Melanoma Tumor Repopulating Cells. Biomedicines *8*. https://doi.org/10.3390/BIOMEDICINES8090360.

Tellier, J., Shi, W., Minnich, M., Liao, Y., Crawford, S., Smyth, G.K., Kallies, A., Busslinger, M., and Nutt, S.L. (2016). Blimp-1 controls plasma cell function through the regulation of immunoglobulin secretion and the unfolded protein response. Nat Immunol *17*, 323–330. https://doi.org/10.1038/ni.3348.

Tong, J., Allenspach, E.J., Takahashi, S.M., Mody, P.D., Park, C., Burkhardt, J.K., and Sperling, A.I. (2004). CD43 Regulation of T Cell Activation Is Not through Steric Inhibition of T Cell–APC Interactions but through an Intracellular Mechanism. Journal of Experimental Medicine *199*, 1277–1283. https://doi.org/10.1084/JEM.20021602.

Wells, S.M., Kantor, A.B., and Stall, A.M. (1994). CD43 (S7) expression identifies peripheral B cell subsets. J Immunol *153*, 5503–5515. .

Wong, R., Belk, J.A., Govero, J., Uhrlaub, J.L., Reinartz, D., Zhao, H., Errico, J.M., D'Souza, L., Ripperger, T.J., Nikolich-Zugich, J., et al. (2020). Affinity-Restricted Memory B Cells Dominate Recall Responses to Heterologous Flaviviruses. Immunity *53*, 1078-1094.e7. https://doi.org/10.1016/J.IMMUNI.2020.09.001.

Yoshimoto, M., Montecino-Rodriguez, E., Ferkowicz, M.J., Porayette, P., Shelley, W.C., Conway, S.J., Dorshkind, K., and Yoder, M.C. (2011). Embryonic day 9 yolk sac and intra-embryonic hemogenic endothelium independently generate a B-1 and marginal zone progenitor

lacking B-2 potential. Proc Natl Acad Sci U S A *108*, 1468–1473. https://doi.org/10.1073/PNAS.1015841108/-/DCSUPPLEMENTAL/PNAS.201015841SI.PDF.

Yuan, J., Nguyen, C.K., Liu, X., Kanellopoulou, C., and Muljo, S.A. (2012). Lin28b reprograms adult bone marrow hematopoietic progenitors to mediate fetal-like lymphopoiesis. Science (1979) *335*, 1195–1200. https://doi.org/10.1126/science.1216557.

Zeng, Z., Surewaard, B.G.J., Wong, C.H.Y., Guettler, C., Petri, B., Burkhard, R., Wyss, M., Le Moual, H., Devinney, R., Thompson, G.C., et al. (2018). Sex-hormone-driven innate antibodies protect females and infants against EPEC infection. Nature Immunology *19*, 1100–1111. https://doi.org/10.1038/s41590-018-0211-2.

Immunological Genome Project.

3.11 Figures and Tables

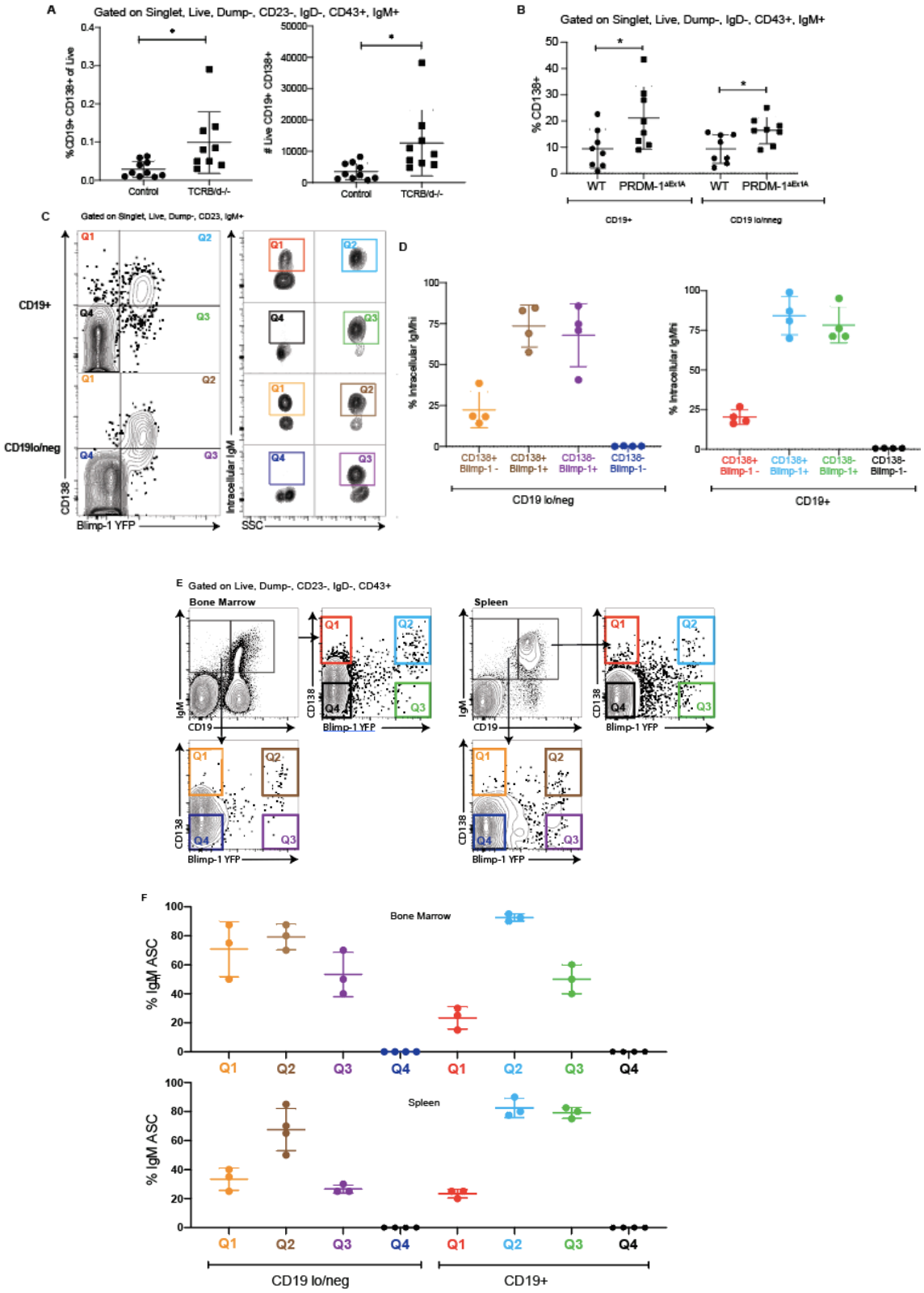

Figure 3.1: CD138 is marker of nIgM secreting cells independent of Blimp-1 expression

A) Mean percentage and cell number ± SD of CD138+, CD19+ B-1 cells in BM of βδTCR-/- mice, N=9-10 mice /group combination of 3 independent experiments **B)** Mean percentage ± SD of IgM+, IgD-, CD19lo/neg or CD19+ cells expressing CD138 in BM (top) and SPL (bottom) of control and PRDM-1$^{\Delta Ex1A}$ mice. N=8-9 mice per experiment, symbols represent data from individual mice. **C)** Representative FACS plots of BM from Blimp-1 YFP mice stained for ic IgM. **D)** Mean percentage± SD of cell populations identified in **(C)** with high ic IgM staining, n-4 mice. **E)** Gating strategy for sorting populations in to ELISPOT Plates. **F)** Mean percentage ± SD of cells secreting IgM per ELSPOT well for each sorted population. Each symbol represents a individual ELISPOT well n=3 per populations. Data are a combination of 3-4 independent experiments using 1 mouse per experiment. **G)** Representative IgM ELISPOTs by each sorted population in BM (top) and SPL (bottom) from Blimp-1 YFP mice, number of cells sorted into each well are indicated. Values in (A)and (B) were compared by unpaired Student's t-test.

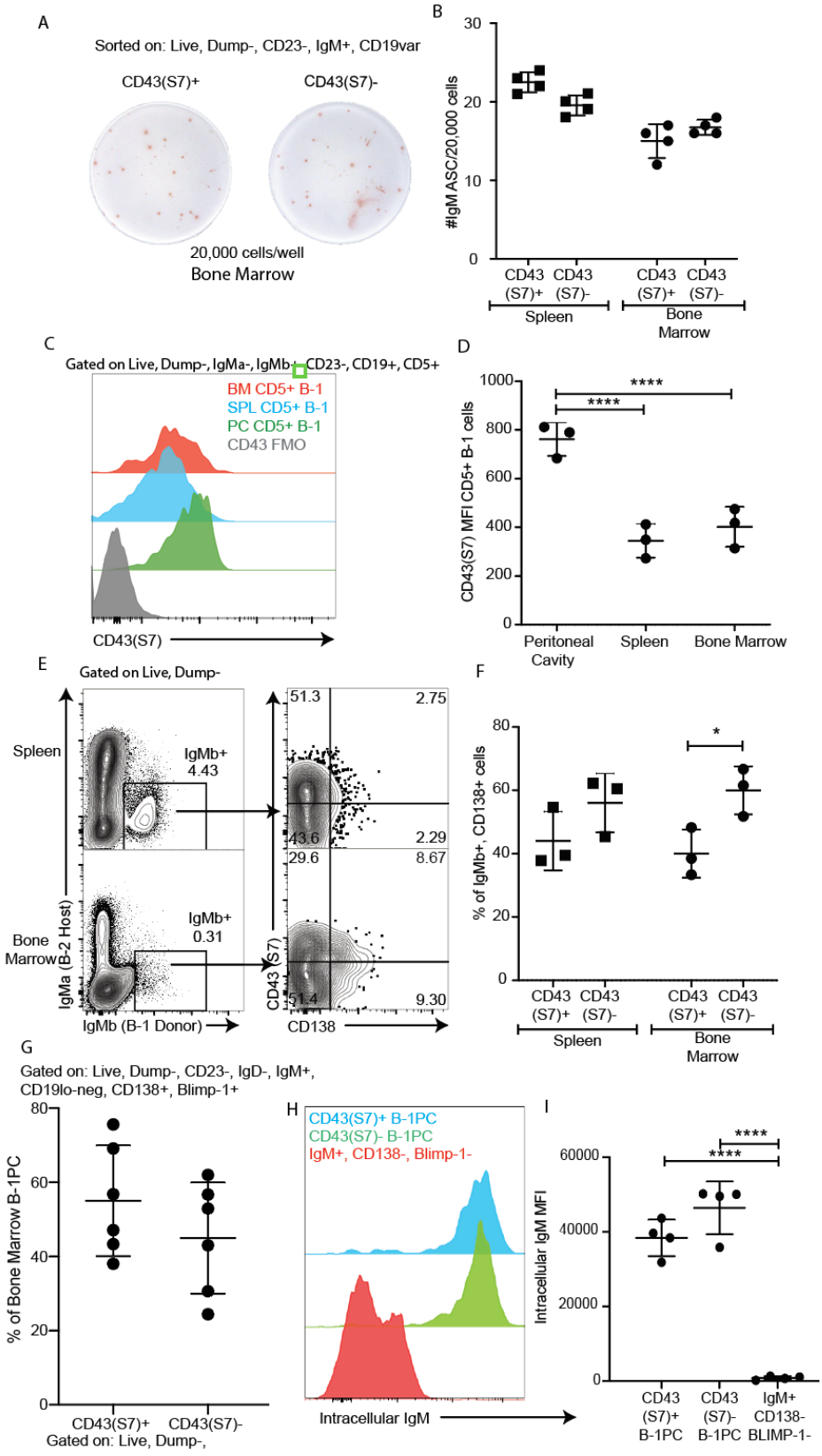
A
Sorted on: Live, Dump-, CD23-, IgM+, CD19var
CD43(S7)+
CD43(S7)-
20,000 cells/well
Bone Marrow
B
#IgM ASC/20,000 cells
CD43 (S7)+
CD43 (S7)-
Spleen
Bone Marrow
C
Gated on Live, Dump-, IgMa-, IgMb+, CD23-, CD19+, CD5+
BM CD5+ B-1
SPL CD5+ B-1
PC CD5+ B-1
CD43 FMO
CD43(S7)
D
CD43(S7) MFI CD5+ B-1 cells
****
Peritoneal Cavity
Spleen
Bone Marrow
E
Gated on Live, Dump-
Spleen
IgMb+ 4.43
Bone Marrow
IgMb+ 0.31
IgMa (B-2 Host)
IgMb (B-1 Donor)
51.3
2.75
43.6
2.29
29.6
8.67
51.4
9.30
CD43 (S7)
CD138
F
% of IgMb+, CD138+ cells
*
G
Gated on: Live, Dump-, CD23-, IgD-, IgM+, CD19lo-neg, CD138+, Blimp-1+
% of Bone Marrow B-1PC
CD43(S7)+
CD43(S7)-
Gated on: Live, Dump-,
H
CD43(S7)+ B-1PC
CD43(S7)- B-1PC
IgM+, CD138-, Blimp-1-
Intracellular IgM
I
Intracellular IgM MFI
IgM+ CD138- BLIMP-1-

Figure 3.2: nIgM secreting cells come from both CD43+a dn CD43- B-1 derived cells

A) Representative IgM ELISPOTs of sorted CD43+ or CD43- IgM+ cells from BM, number of cell sorted into each well is indicated. **B)** Mean number of IgM secreting cells ± SD/20,000 CD43+ or CD43- IgM+ cells from SPL and BM. N= 4 wells per condition, combination of 2 independent experiments. **C)** Representative histograms of CD43 expression on CD5+ B-1 in PC, SPL and BM of Ig allotype chimera mice **D)** Mean fluorescence intensity of CD43 ± SD of CD5+ B-1 cells in PC, SPL and BM of Ig allotype chimeras. N=3 mice, symbols represent data from individual mice. **E)** Representative FACS plots of BM (bottom) and SPL (top) from adult Ig allotype chimeric mice showing gating for CD43 expression amongst CC138+ B-1 derived cells. **F)** Mean percentage ± SD of CD43+ or CD43- CD138+ B-1 derived cells in SPL (left) and BM (right). N=3 mice per experiment, symbols represent data from individual mice. **G)** Mean percentage ± SD of CD43+ or CD43- B-1PC in BM. N=6 mice per experiment, symbols represent data from individual mice. **H)** Representative histograms of ic IgM staining in CD43+ B-1PC, CD43 B-1PC PC, and CD138-, Blimp-1-, IgM+ cells. **I)** Mean fluorescence intensity of ic IgM ± SD of CD43+ or CD43- B-1PC, or CD138-, Blimp-1-, IgM+ cells in BM.

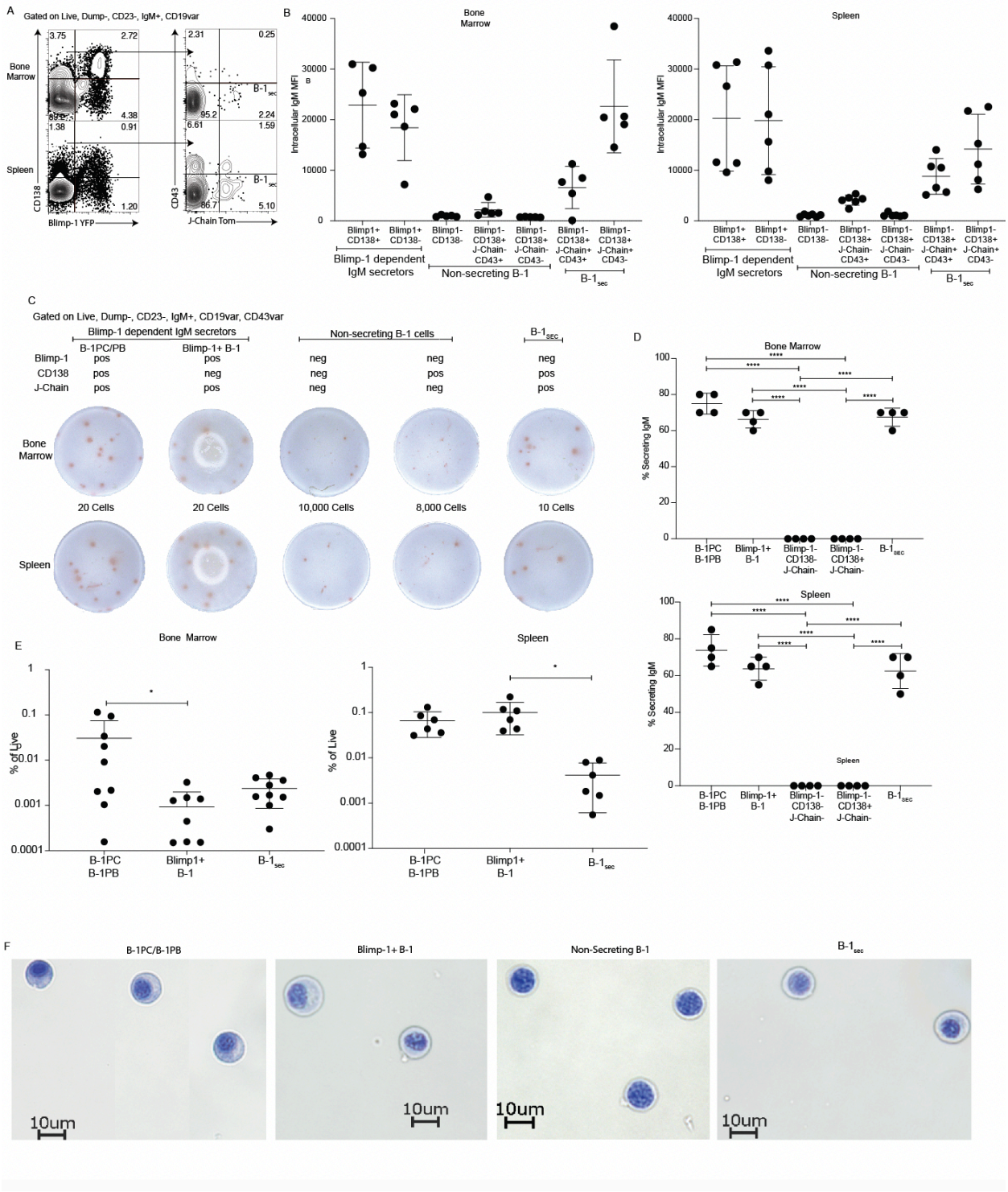
A
Gated on Live, Dump-, CD23-, IgM+, CD19var
Bone Marrow
Spleen
CD138
Blimp-1 YFP
CD43
J-Chain Tom
B
Bone Marrow
Spleen
Intracellular IgM MFI
Blimp1+ CD138+
Blimp1+ CD138-
Blimp1- CD138-
Blimp1- CD138+ J-Chain- CD43+
Blimp1- CD138+ J-Chain- CD43-
Blimp1- CD138+ J-Chain+ CD43+
Blimp1- CD138+ J-Chain+ CD43-
Blimp-1 dependent IgM secretors
Non-secreting B-1
B-1sec
C
Gated on Live, Dump-, CD23-, IgM+, CD19var, CD43var
Blimp-1 dependent IgM secretors
Non-secreting B-1 cells
B-1sec
B-1PC/PB
Blimp-1+ B-1
Blimp-1
CD138
J-Chain
Bone Marrow
Spleen
20 Cells
20 Cells
10,000 Cells
8,000 Cells
10 Cells
D
Bone Marrow
Spleen
% Secreting IgM
B-1PC B-1PB
Blimp-1+ B-1
Blimp-1- CD138- J-Chain-
Blimp-1- CD138+ J-Chain-
B-1sec
E
Bone Marrow
Spleen
% of Live
B-1PC B-1PB
Blimp1+ B-1
B-1sec
F
B-1PC/B-1PB
Blimp-1+ B-1
Non-Secreting B-1
B-1sec
10um

Figure 3.3: B-1$_{sec}$ are major producers of BM derived nIgM

A) Representative FACS plots and gating strategy to identify B-1$_{sec}$ in BM (top) and SPL (bottom) from Blimp-1 YFP, J-Chain-TdTomato reporter mice. **B)** Mean fluorescence intensity of ic IgM ± SD of B-1 cells population BM and SPL, n=5-6 per group, combination of two independent experiments. **C)** Representative IgM ELISPOTs by each sorted population in BM (top) and SPL (bottom) Blimp-1 YFP, J-Chain-TdTomato reporter mice, number of cells sorted into each well are indicated. **D)** Mean percentage ± SD of cells from each B-1 population in **(C)** secreting IgM in BM (left) and SPL (right). Each symbol represents an individual ELISPOT well. Data are a combination of 3-4 independent experiments using 1 mouse per experiment**. E)** Mean frequency ± SD of B-1 cell populations within BM and SPL. **F)** Hemotoxylin and Eosin staining of B-1 cells populations.

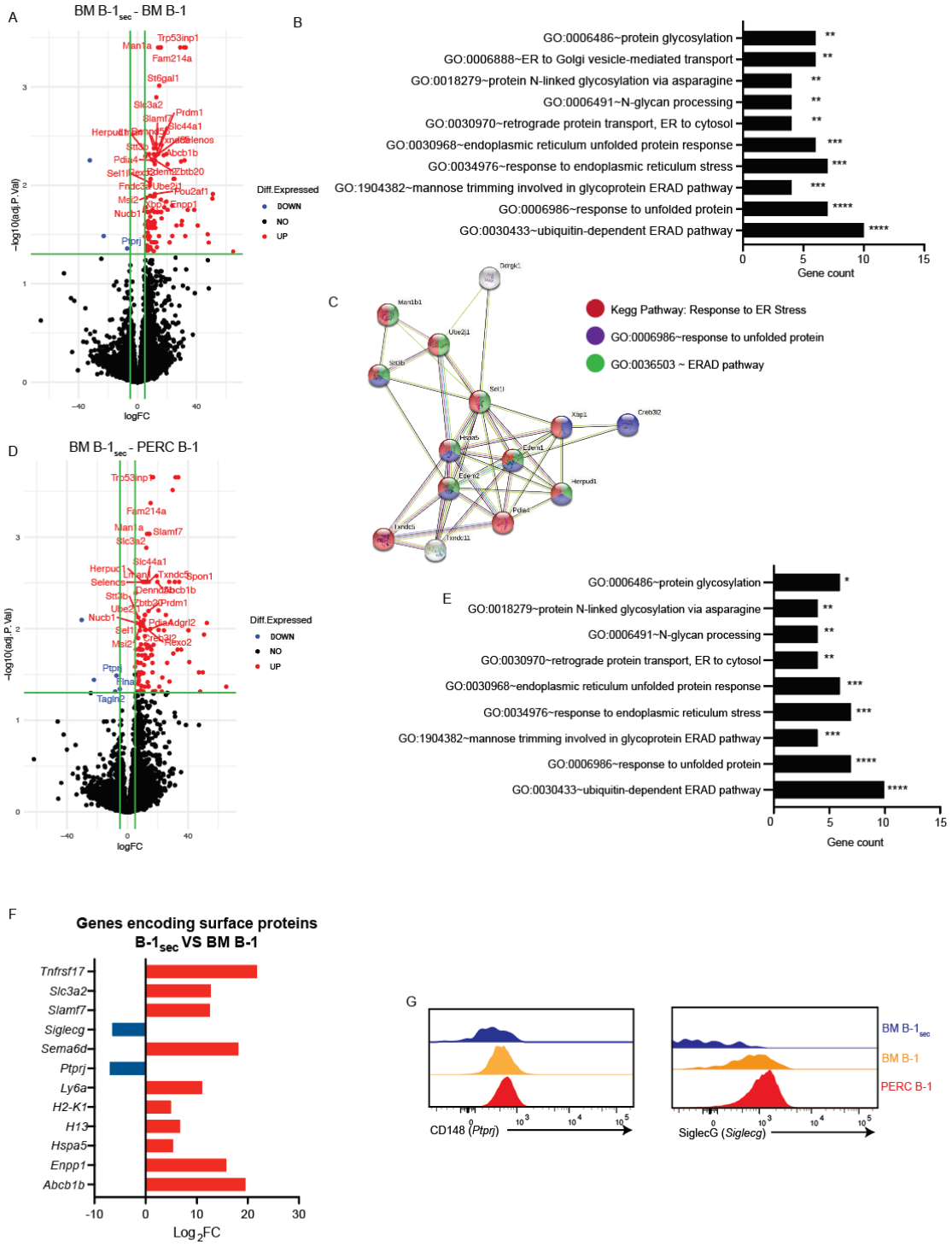
A
BM B-1sec - BM B-1
Trp53inp1
Man1a
Fam214a
St6gal1
Slc3a2
Slamf7
Prdm1
Slc44a1
Herpud1
Selenos
Abcb1b
Pdia4
Sel1l
Edem2
Zbtb20
Fndc3b
Ube2j1
Pou2af1
Msl2
Xbp1
Enpp1
Nucb1
Ptprj
−log10(adj.P.Val)
logFC
Diff.Expressed
DOWN
NO
UP
B
GO:0006486~protein glycosylation
GO:0006888~ER to Golgi vesicle-mediated transport
GO:0018279~protein N-linked glycosylation via asparagine
GO:0006491~N-glycan processing
GO:0030970~retrograde protein transport, ER to cytosol
GO:0030968~endoplasmic reticulum unfolded protein response
GO:0034976~response to endoplasmic reticulum stress
GO:1904382~mannose trimming involved in glycoprotein ERAD pathway
GO:0006986~response to unfolded protein
GO:0030433~ubiquitin-dependent ERAD pathway
Gene count
C
Kegg Pathway: Response to ER Stress
GO:0006986~response to unfolded protein
GO:0036503 ~ ERAD pathway
Dergic1
Man1b1
Ube2j1
Sel1l
Xbp1
Creb3l2
Hspa5
Edem1
Edem2
Herpud1
Pdia4
Tmtc1
Tmtc4
Tmtc3
Tmtc2
Tmtc1
Tmtc4
Tmtc3
Tmtc2
D
BM B-1sec - PERC B-1
Trp53inp1
Fam214a
Man1a
Slamf7
Slc3a2
Slc44a1
Herpud1
Txndc5
Spon1
Selenos
Dennd4c
Abcb1b
Stt3b
Zbtb20
Prdm1
Ube2j1
Pdia4
Adgrl2
Nucb1
Creb3l2
Rexo2
Sel1l
Msl2
Ptprj
Tln1
Tagln2
−log10(adj.P.Val)
logFC
Diff.Expressed
DOWN
NO
UP
E
GO:0006486~protein glycosylation
GO:0018279~protein N-linked glycosylation via asparagine
GO:0006491~N-glycan processing
GO:0030970~retrograde protein transport, ER to cytosol
GO:0030968~endoplasmic reticulum unfolded protein response
GO:0034976~response to endoplasmic reticulum stress
GO:1904382~mannose trimming involved in glycoprotein ERAD pathway
GO:0006986~response to unfolded protein
GO:0030433~ubiquitin-dependent ERAD pathway
Gene count
F
Genes encoding surface proteins
B-1sec VS BM B-1
Tnfrsf17
Slc3a2
Slamf7
Siglecg
Sema6d
Ptprj
Ly6a
H2-K1
H13
Hspa5
Enpp1
Abcb1b
Log2FC
G
BM B-1sec
BM B-1
PERC B-1
CD148 (Ptprj)
SiglecG (Siglecg)

Figure 3.4: Genes associated with protein production are upregulated in B-1$_{sec}$ as compared non-secreting B-1 cells.

A) Volcano plot highlighting genes significantly differentially expressed ($Log_2FC>5$, adj.p-value <0.05) between non secreting BM B-1 cells and B-1$_{sec}$. **B)** Top Biologic Process GO Terms returned after entering the upregulated differentially expressed genes from **(A)** into DAVID. **C)** STRING connectivity of proteins encoded for by genes identified by DAVID as Biologic Process GO term: 0030433 from **(B)** Proteins are color coded by the biologic go term or Kegg Pathways they are assigned to by STRING. **D)** Volcano plot highlighting genes significantly differentially expressed ($Log_2FC>5$, adj.P. value <0.05) between non secreting peritoneal B-1 cells and B-1$_{sec}$. **E)** Top Biologic Process GO Terms returned after entering the upregulated differentially expressed genes from **(D)** into DAVID. **E)** Log2 FC of genes encoding for surface markers that are differentially expressed in B-1$_{sec}$ and BM B-1 cells. **F)** Representative histograms of MFI of proteins CD148 and SiglecG in non-secreting BM and PerC B-1 cells and B-1$_{sec}$.

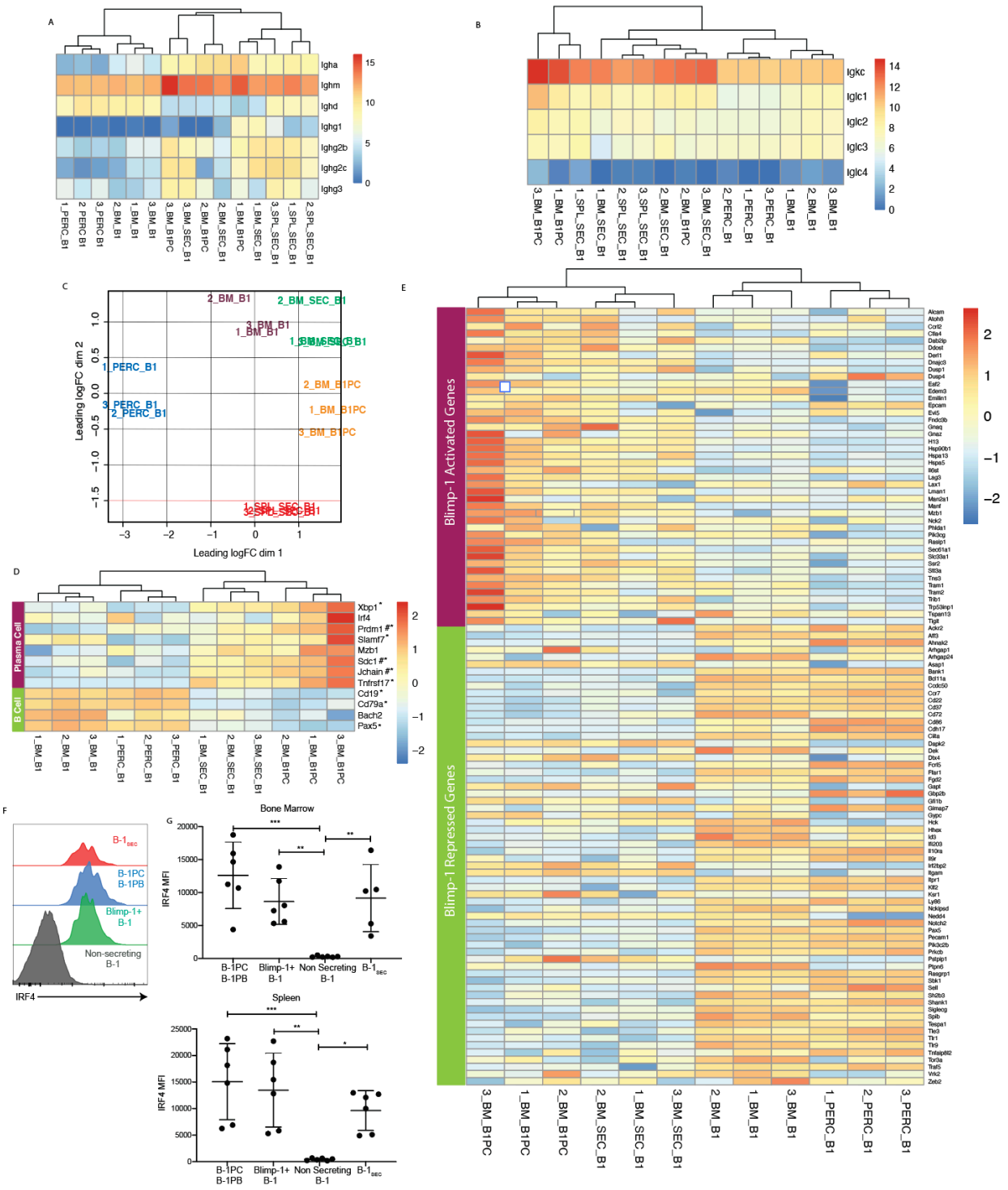
A
Ighm
Ighd
Ighg1
Ighg2b
Ighg2c
Ighg3
B
Igkc
Iglc1
Iglc2
Iglc3
Iglc4
C
Leading logFC dim 2
Leading logFC dim 1
D
Plasma Cell
B Cell
Xbp1*
Irf4
Prdm1 #*
Slamf7*
Mzb1
Sdc1 #*
Jchain #*
Tnfrsf17*
Cd19*
Cd79a*
Bach2
Pax5*
E
Blimp-1 Activated Genes
Blimp-1 Repressed Genes
F
B-1sec
B-1PC
B-1PB
Blimp-1+
B-1
Non-secreting
B-1
IRF4
G
Bone Marrow
Spleen
IRF4 MFI
B-1PC
B-1PB
Blimp-1+
B-1
Non Secreting
B-1
B-1sec

Figure 3.5: The transcriptional profile of B-1$_{sec}$ is consistent with a non-terminally differentiated nIgM secreting B cell.

A) Gating strategy for B-1 populations sorted for RNAseq. **B)** Heatmap comparing Ig-heavy chain constant region gene expression among the cell populations **C)** Heatmap comparing Ig-light chain constant region gene expression among the cell populations **D)** Multidimension scaling plot showing clustering of different B-1 cells population **E)** Heatmap showing clustering of BM and PerC B-1 cell populations basted on B-cell or Plasma cell associated genes, *- gene with adj. p-value of <0.05, # - proteins or reporters used to sort the analyzed populations. **F)** Heatmap of expression of Blimp-1 activated or repressed genes identified in (Tellier et al., 2016) **G)** Representative histograms of IRF-4 MFI by flow cytometry for secreting and non-secreting B-1 cell populations. **H)** Mean IRF-4 MFI ± SD for B-1 cell populations in BM and SPL.

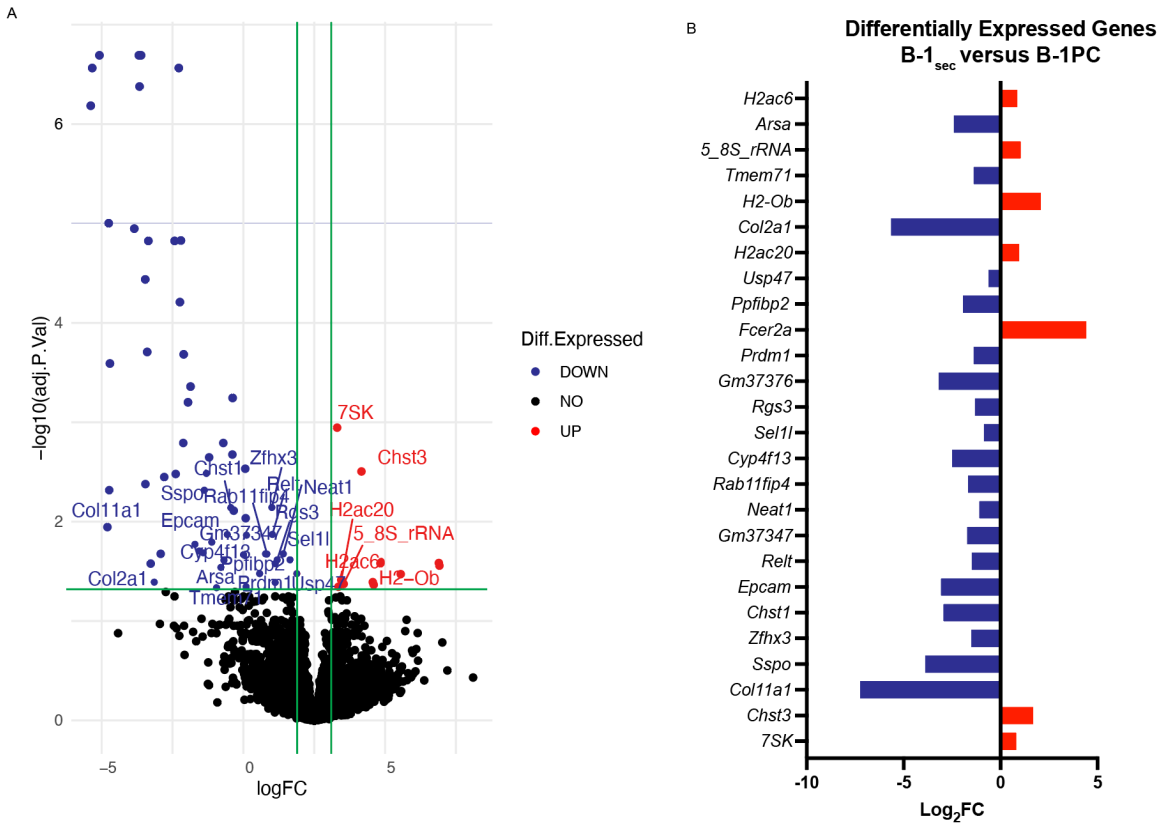

Figure 3.6: Transcriptional regulation genes and cell-cell interaction/adhesion genes are differentially expressed between B-1$_{sec}$ and B-1PC

A) Volcano plot highlighting genes significantly differentially expressed ($Log_2FC>1$, adj.p-value <0.05) between B-1$_{sec}$ and B-1PC. Unlabeled significantly differentially expressed genes are Ighv, Igkv or Iglv genes. **B)** Log_2FC of the 26 non-Ig variable genes significantly differentially expressed between B-1$_{sec}$ and B-1PC. Red bars/dots represented genes upregulated in B-1$_{sec}$. Blue bars/dots represent genes upregulated in B-1PC.

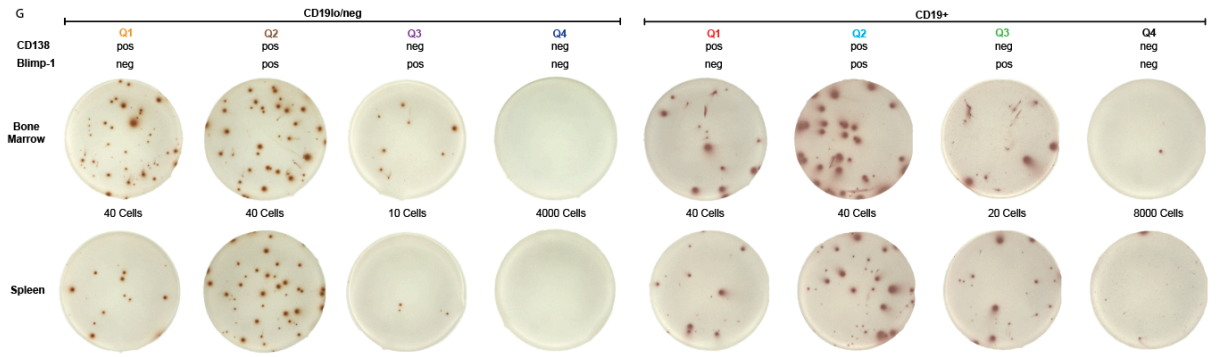

Supplemental Figgure 3.1:

A) Representative ELISPOTs of sorted B-1 cells populations based on expression of CD19, CD138 and Blimp-1YFP as defined in Figure 1C.

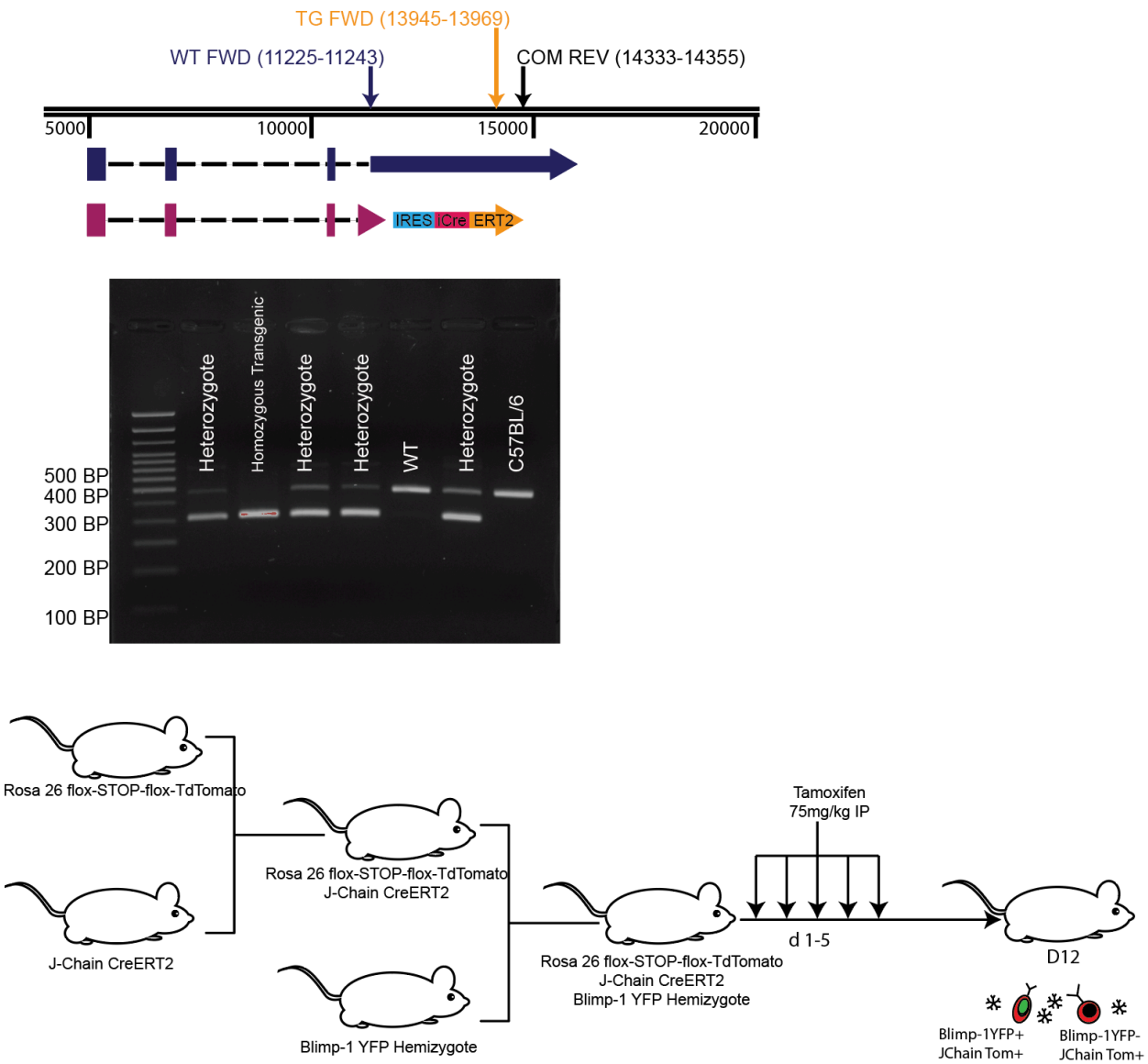

Supplemental Figure 3.2:

A) Diagram of genetic modification made to create to J Chain reporter mouse by inserting an ERT2-Cre in the *JChain* locus. **B)** Representative genotyping PCR gel showing mice of the three possible genotypes for the ERT2-Cre, includes C57BL/6 control. **C)** Breeding strategy employed to creat the double reporter, Blimp-1 YFP/JChain TdTomato, mouse.

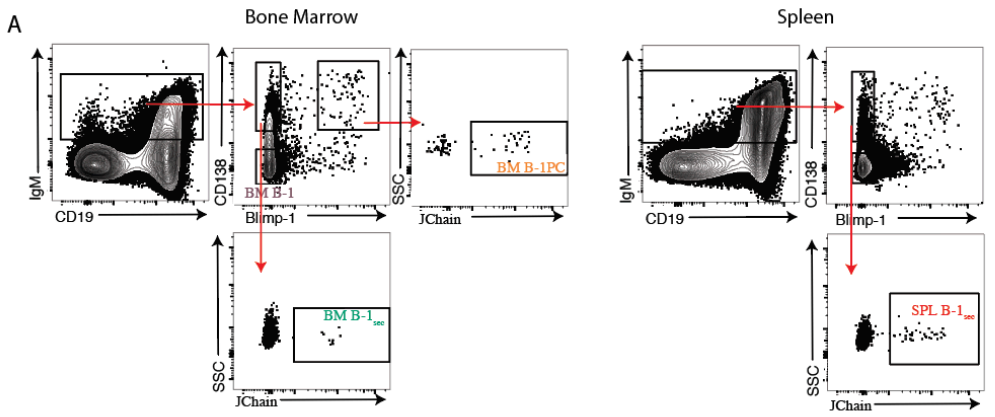

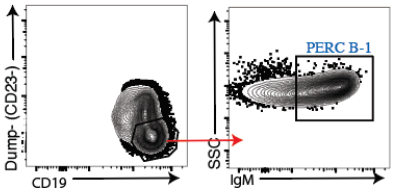

B

Mouse #	BM B-1$_{sec}$	BM B-1PB	BM B-1	PerC B-1	SPL B-1$_{sec}$
1	202	1063	50000	48000	1329
2	143	1352	50000	50125	1302
3	311	8369	50000	50000	1569

C

Comparison	Number of genes with adjusted P<0.05
BM B-1$_{sec}$ – BM B-1PC	69
BM B-1$_{sec}$ – BM B-1	109
BM B-1$_{sec}$ – PERC B-1	116
BM B-1$_{sec}$ – SPL B-1$_{sec}$	3265
BM B-1PC – BM B-1	178
BM B-1PC – PERC B-1	195
BM B-1PC – SPL B-1$_{sec}$	2413
BM B-1 - PERC B-1	2884
BM B-1 – SPL B-1$_{sec}$	157
PERC B-1 - SPL B-1$_{sec}$	159

Supplemental Figure 3.3:

A) Gating Strategy for RNAseq cell populations. **B)** Number of cells sorted for each population.

C) Number of differentially expressed genes between populations.

Table 3.1: Blimp-1 regulated genes from Figure 5F

Blimp-1 Activated Genes	*Blimp-1 Repressed Genes*
Pik3cg	*Ahnak*
Fndc3b	*Gbo2*
Dusp1	*Gap1*
Trib1	*Gbp1*
Dusp4	*Sbk1*
Nck2	*Shank1*
Tns3	*Tespa1*
Emilin1	*Dtx4*
Lax1	*Itpr1*
Evi5	*Arhgap24*
Gnaz	*Asap1*
Rasip	*Nedd4*
Dab2ip	*Fgd2*
Trp53inp1	*Traf5*
Ctla4	*Pik3c2b*
Lag3	*Ifi203*
Tmem66	*Hck*
Tigit	*Ksr1*
Enpp1	*Dapk2*
Ccr12	*Gimap7*
Alcam	*Ptpn6*
Atoh8	*Nckipsd*
Eaf2	*Arhgap17*
Gfi1	*Prkcb*
Ell2	*Tnfaip8l2*
Egr2	*Pstpip1*
Irf4	*Sh2b3*
Skil	*Bank1*
Lman1	*Vrk2*
Ddost	*Rasgrp1*
Ssr2	*Ccdc50*
Edem3	*Tlr9*
Sec61a1	*Ackr2*
Tram1	*Il10ra*
Man2af	*Itgam*
Hspa13	*Cdh17*
Hsp90b1	*Cd22*
Manf	*Fcrl5*
Hspa5	*Tir1*

Dnajc3	*Gypc*
Mzb1	*Ly38*
Slc33a1	*Sell*
Phida1	*Cd86*
Derf1	*Ccr7*
	Cd37
	Tor3a
	Notch2
	Spib
	Klf2
	Aff3
	Pax5
	Id3
	Dek
	Gfi1b
	Bcl11a
	Zeb2
	Tie3
	Ciita
	Hhex
	Irf2bp2

Table 3.2: Antibodies used for flow cytometry and ELISPOT

Antibodies	Source	Identifier
Anti-IgMa biotinylated (Clone: DS-1)	BD Bioscience	Cat#553515
Anti-IgMb biotinylated (Clone: AF6-78)	BD Bioscience	Cat#553519
Anti-IgM biotinylated (Clone: 331)	In House	N/A
Anti-IgM biotinylated (Pooled antisera from goats hyperimmunized with mouse IgM)	Southern Biotech	Cat#1020-08
Anti-IgM Efluor 750 (Clone: 331)	In house	N/A
Anti-IgM FITC (Clone:331)	In house	N/A
Anti-IgM APC-Cy7(Clone:331)	In house	N/A
Anti-IgD PE-Cy 7 (Clone:11-26C)	In house	N/A
Anti-F4/80 Pacific Blue (Clone:BM-8)	In house	N/A
Anti-F4/80 PE-Cy5 (Clone:BM-8)	In house	N/A
Anti-Gr-1 Pacific Blue (Clone: RB6-8C5)	In house	N/A
Anti-Gr-1 eFluor 450 (Clone: RB6-8C5)	Invitrogen	Cat#48-5931-82
Anti-Gr-1 PE-Cy5 (Clone: RB6-8C5)	In house	N/A
Anti-CD8a Pacific Blue (Clone: 53-6.7.3.1)	In house	N/A
Anti-CD8a eFluor 450 (Clone: 53-6.7)	Invitrogen	Cat#48-0081-82
Anti-CD4 Pacific Blue (Clone: GK1.5)	In house	N/A
Anti-CD4 Biotin (Clone: GK1.5)	In house	N/A
Anti-CD19 Brilliant Violet 786(Clone: 1D3)	BD Bioscience	Cat#563333
Anti-CD19 PE (Clone: D3)	In house	N/A
Anti-CD19 Biotin (Clone: D3)	In house	N/A
Anti-CD19 PE CF594 (Clone: D3)	BD Bioscience	Cat#562329

Anti-CD43 APC (Clone: S7)	In house	N/A
Anti-CD43 Brilliant Violet 650 (Clone: S7)	BD Bioscience	Cat#740464
Anti-CD138 Brilliant Violet 605 (Clone: 281-2)	BD Bioscience	Cat#563147
Anti-CD23 Brilliant Violet 605 (Clone: B3B4)	BD Bioscience	Cat#747727
Anti-CD23 Brilliant Violet 711 (Clone: B3B4)	BD Bioscience	Cat#563987
Anti-CD23 Brilliant Biotin (Clone: B3B4)	In house	N/A
Anti-CD23 Brilliant eFluor 450 (Clone: B3B4)	Invitrogen	Cat#48-0232-82
Anti -NK1.1 Pacific Blue (Clone: PK136)	In house	N/A
Other Fluorescent reagents		
Streptavidin-APC	Invitrogen	Cat#17-4317-82
Streptavidin-Qdot 605	Invitrogen	Cat#Q10101MP

Chapter 4:

B-1 and B-2 cells have distinct requirements for toll-like receptor and B cell receptor signaling to initiate differentiation of antibody secreting cells

Fauna Leah Smith

*** Portions of this Chapter are adapted from: Savage HP, Kläsener K, Smith FL, Luo Z, Reth M, Baumgarth N. **TLR induces reorganization of the IgM BCR complex regulating murine B-1 cell responses to infections.** eLife, 2019; 8: e46997. ***

Abstract

B-1 derived cells are unique innate-like B lymphocytes that provide broadly reactive IgM to aid the protection from both infectious and autoimmune dieases. Here we examine the role of toll-like receptor (TLR) and B cell receptor (BCR) signaling on both, steady state nIgM production and infection-induced secretion of IgM by B-1 cells. Both were reduced, when B-1 cells lack TLR expression. B-1 cells did not use the same level of BCR and TLR signaling coordination to enhance their activation and differentiation as we see in conventional B-2 cells. Instead, B-1 cells were exquisitely sensitive to TLR stimulation, but BCR signaling inhibited TLR-stimulated B-1 cell responses, while synergistic effects were noted in B-2 cells. Furthermore, when BCR signaling was blocked with a Syk inhibitor, the effects on TLR signaling were much more pronounced in B-2 than B-1 cells, suggesting that B-1 cells respond through a TLR pathway that is uncoupled from the MyD88-Syk axis previously shown to be critical in B-2 cells.

4.1 Introduction

B-1 cells, a unique population of fetal/neonatally derived B cells contribute natural antibodies in the absence of external antigenic stimulation, as total serum levels of natural (n)IgM and frequencies of IgM-secreting B-1 cells are similar in SPF and germ-free mice(Baumgarth et al., 2015; Ochsenbein et al., 1999; Savage et al., 2017). However, the repertoire selection of B-1 cells is not random, but rather driven by expression of self-antigens, resulting in a self-reactive repertoire. This was elegantly demonstrated using Thy-1-deficient mice that fail to produce any anti-Thy-1 self-reactive IgM antibodies (Hayakawa et al., 1999, 2003). Additionally, repertoire studies showed extensive clonal expansion of specific CD5+ B-1 cell clones during the first 6 months of life (Yang et al., 2015). Together this data demonstrate the need for B cell receptor (BCR) engagement for the selection/development of B-1 cells but does not address the mechanism by which B-1 cells differentiate into antibody secreting cells (ASCs).

CD5+ B-1 cells do not proliferate or expand *in vitro* in response to antigenic stimulation/BCR receptor signaling (Morris & Rothstein, 1993; Murakami et al., 1992; Savage et al., 2019; Sen et al., 1999). In the context of influenza infection clonal expansion of influenza specific B-1 was not observed in the draining lymph nodes or body cavities (Choi & Baumgarth, 2008). It has previously been shown that the lack of proliferative responses to antigen is related to B-1 cells' expression of BCR signaling inhibitors CD5 and Siglec G, as well as defective CD19 signaling, a coreceptor of the BCR (Berland & Wortis, 2002; Bikah et al., 1996; Nitschke, 2015; Sindhava & Bondada, 2012; Tarakhovsky et al., 1994). These strict controls of antigen specific activation of self-reactive B-1 cells are likely important for preventing induction of autoimmune diseases. Yet,

it is critical that some these cells differentiate into ASCs as they contribute broadly reactive circulating nIgM, which aids early control of infections, autoimmune disease and neoplasia(Alugupalli et al., 2004; Baumgarth et al., 2000; Haas et al., 2005; Haro et al., 2019; Jackson-Jones et al., 2016; Nguyen et al., 2015; Smith & Baumgarth, 2019).

While B-1 cells do not proliferate in response to BCR stimulation *in vitro,* they exhibit robust proliferation and rapid differentiation into ASC in response to toll-like receptors (TLR) stimulation(Genestier et al., 2007; Kreuk et al., 2019; Meyer-Bahlburg and Rawlings, 2012; Savage et al., 2019). TLR mediated stimulation results in rearrangement of the IgM-BCR signalosome of CD5+ B-1 cells, including the dissociation of CD5 from the IgM-BCR and eventually its loss from the cell surface, enhanced association between IgM-BCR and the co-stimulatory molecule CD19, as well as significant increases in CD79A:Syk interaction and phosphorylation of BCR downstream effectors (Savage et al., 2019). Consistent with these changes, the majority of B-1 derived ASCs, be it at steady state or during infection, have been characterized as CD5-/lo, even when the responding cells were initially CD5+. This is the case in influenza virus infection, where CD5+ B-1 cells migrate from the pleural cavity to the respiratory tract draining lymph nodes to differentiate into ASCs (Choi and Baumgarth, 2008; Savage et al., 2017, 2019). These findings lead to questions about how coordination between TLR and BCR signaling might regulate B-1 cell differentiation into nIgM secreting cells in BM and spleen at steady state and into IgM secreting cells in regional lymphoid tissues in response to infection. This chapter characterizes the effects of TLR signaling on the differentiation of B-1 cells into ASCs, both at steady state and during infection, and interrogates the responses of B-1

cells to innate (TLR) and antigen specific (BCR) stimulation to understand how they coordinate to regulate IgM secretion by B-1 cells.

4.2 nIgM production in steady state BM and spleen require intact TLR signaling in B-1 cells

The majority of nIgM at steady state is secreted by CD19+ CD5-, CD138+ B-1 ($B\text{-}1_{sec}$) and by $CD19^{lo/neg}$ CD5- CD138+ B-1 plasma cells (B-1PC), in both BM and spleen(Savage et al., 2017). Genetic deletion of TLR2 and TLR4 has been shown to result in reduced concentrations serum nIgM binding to microbiota, while deletion of Unc93, resulting in a functional loss of endosomal TLRs, led to decreased anti-phosphatidylcholine (PtC) nIgM, suggesting that intact TLR signaling is required for nIgM production at steady state(Kreuk et al., 2019). Consistent with these findings, *in vitro* stimulation of CD5+ peritoneal cavity B-1 cells resulted in their rapid differentiation to $CD5^{-/lo}$ CD138+ IgM antibody-secreting cells (ASCs) (Savage et al. 2019). Here I aimed to characterize further the extent to which TLR signaling affects B-1 cell activation and differentiation.

Studying mice lacking in all TLRs (TLR-/-), we observed that B-1 cells, identified as Dump-, CD23-, IgD-, IgM+ in the bone marrow (BM) and spleen appeared less differentiated compared to those in wild type control mice. They contained significantly more CD19+ and fewer $CD19^{lo/neg}$ cells (**Fig. 4.1A**), and fewer cells lacked CD5 and expressed the ASC marker CD138 **(Fig. 4.1B)**. Consistent with that finding, TLR-/- mice had significantly lower serum IgM levels than control mice at all ages sampled (**Fig. 4.1C**). Additionally, there were fewer IgM ASC in both the BM and spleen in TLR-/- mice **(Fig. 4.1D, E)**. To determine if the differences were due

to intrinsic TLR signaling in B-1 cells we used a neonatal Ig-allotype chimera model (Baumgarth et al., 1999a). This model uses adult peritoneal B-1 cells from control and TLR-/- mice to reconstitute the B-1 cell pool of neonatal wild type mice made temporarily B cell deficient by injection of anti-IgM antibodies. While seeding of the BM was not affected significantly by B-1 cell intrinsic TLR signaling, the spleens of adult fully reconstituted chimeras repopulated with TLR-/- B-1 cells had significantly lower numbers of B-1 cells than the control chimeras **(Fig. 4.1F)**. The lack of B-1 cell differentiation into ASCs was even more profound in the TLR-/- B-1 chimeras than in the total knockouts. The vast majority of B-1 cells maintained the classical, non-secreting CD5+ B-1 cell phenotype: CD19+, CD5+, CD138- **(Fig. 4.1G, H, I)** and these mice had 10 to 20-fold less serum IgM after reconstitution than chimeras made with TLR competent B-1 cells (**Fig. 4.1J)**.

We conclude that TLR signaling is required for B-1 cell differentiation into $CD19^{lo/neg}$ CD5- CD138+ B-1 plasma cells (PC) and optimal nIgM secretion during homeostasis. Given that these ASCs develop normally in germ-free mice (Savage, 2017), the data suggest that damage associated molecular patterns (DAMP) trigger differentiation of these nIgM secreting B-1 cells.

4.3 Local IgM production following influenza infection depends on TLR expression

We previously showed that CD5+ B-1 cells respond to influenza infection by migrating to the mediastinal lymph node (MedLN) in a type-1 interferon dependent manner, where they differentiate into CD5- ASCs, many of which were also $CD19^{lo}$, CD138+ (Choi and Baumgarth, 2008; Savage et al., 2019; Waffarn et al., 2015). Here we found that that TLR-/- mice had defective CD5+ B-1 cell responses to influenza infection (**Fig. 4.2).** It appeared that CD5+ B-1

cells in TLR-/-mice entered the MedLN but then failed to differentiate into ASC. This was shown by the B near complete loss of $CD19^{lo/-}$ IgM+ CD138+ B-1PC at day 5 of infection (**Fig 4.2A, B)** and correspondent significant reductions in IgM ASC in the MedLN of TLR-/- compared to control mice at that timepoint (**Fig. 4.2 C**). Generation of Ig-allotype chimeras in which only B-1 cells lacked TLR expression confirmed a B-1 cell-intrinsic requirement for TLR signaling in B-1 cell differentiation into IgM-secreting CD138+ ASCs on both day 5 and Day 7 of influenza infection (**Fig. 4.2D, E, F).** We previously showed that B-1 cells contribute significantly to virus-binding nIgM in the bronchoalveolar lavage fluid of mice (Choi & Baumgarth, 2008). Interestingly, chimeras lacking TLR on B-1 cells also showed higher viral load in their lungs on day 5 of infection (**Fig. 4.2G**), suggesting that local IgM production by B-1 cells in the lungs also requires TLR signaling. Taken together, the data demonstrate that TLR-mediated stimulation of B-1 cells is required for B-1 IgM ASC formation in the steady state as well as following a pathogenic insult.

4.4 B-1 cells fail to differentiate or proliferate in response BCR stimulation by membrane bound antigen

While B-1 cells vigorously respond to TLR agonism by proliferating and differentiating(Genestier et al., 2007; Kreuk et al., 2019; Meyer-Bahlburg and Rawlings, 2012; Savage et al., 2019), CD5+B-1 cells do not respond to BCR stimulation with soluble antigens with proliferation or differentiation (Alhakeem et al., 2015; Bikah et al., 1996; Morris and Rothstein, 1993; Murakami et al., 1992; Savage et al., 2019; Sen et al., 1999). Despite their hypo-responsiveness to antigen, B-1 cells can act as antigen presenting cells (APC) for CD4+ T cells, suggesting that they are capable of antigen internalization and its processing for

presentation in MHC class II. It has been proposed that B-1 cells are phagocytic, however, BCR-mediated antigen uptake by B-1 cells is likely the major mechanism leading to antigen-presentation (Gao et al., 2012). In fact, it has been shown that the checkpoint inhibitor CTLA-4 is important for maintaining B-1 cell homeostasis and, in its absence, quiescent B-1 cells internalized their BCR, presumably in response to self-antigen ligation, which induces activation of (self-reactive) Tfh and follicular B-2 cells, resulting in increased autoimmunity(Yang et al., 2021).

We confirmed by fluorescence microscopy that B-1 cells rapidly internalize the IgM-BCR in response to stimulation with soluble anti-IgM$(Fab)_2$ (αIgM; **Fig. 4.3A, B,)** and that antigen internalization likely occurs in a cognate manner, as only a portion of peritoneal, presumably VH11/12+ B-1 cells, internalized fluorescent PtC liposomes **(Fig. 4.3F).** During chronic infection atypical memory B cells (aMBC) develop, which express high levels of the inhibitory FCγRIIb and CD19. They do not respond to soluble antigen but respond to membrane bound antigens with upregulation of the transcriptional regulator of plasma cell development, IRF4. Given that B-1 cells express high levels of CD19, have multiple surface inhibitory molecules, and are autoreactive with specificities likely to be presented in a membrane bound context, we wanted to test whether they also can respond to membrane bound antigen. However, B-1 cells failed to proliferate and/or differentiate in response to αIgM bound to the surface of 10u beads to simulate surface-antigen. Overall, their responses to stimulation with surface-bound αIgM was comparable to that of soluble αIgM-induced stimulation (**Fig. 4.3C-E**), though one notable difference was an increase in CD86 expression (**Fig. 4.3D)**. They did not upregulate CD138 nor down-regulate CD5 (**Fig. 4.3E).**

Next we tested whether B-1 cells responses to a cognate antigen are similar to those following αIgM stimulation. For that we stimulated body cavity B-1 cells with fluorescent PtC liposomes, as a high proportion of these B-1 cells bind to PtC(Carmack et al.; Hardy et al., 1989). Flow cytometric analysis (**Fig. 4.3G**) showed that PtC-binding cells failed to proliferate and instead preferentially died in culture, compared to the non-PtC binders, suggesting that BCR stimulation resulted in increased B-1 cell death **(Fig. 4.3G, H and not shown).** This is in contrast to B-1 cell stimulation with the TLR agonist CpG, which resulted in increased survival of PtC+ B-1 cells (Savage et al., 2019). Following culture, the PtC+ B-1 cells expressed lower levels of the BCR stimulatory molecule, CD19, and higher levels CD5 compared to PtC non-binders (**Fig. 4.3I)**. CD138 expression was not induced in either antigen stimulated and non-stimulated cells (**Fig. 4.3I)**. We conclude that B-1 cells do not respond to membrane-bound or soluble antigen with proliferation or differentiation.

4.5 TLR mediated B-1 cell proliferation and differentiation is suppressed by BCR stimulation

It has been shown previously that BCR and TLR stimulation have opposite effects on the BCR signalosome of B-1 cells(Savage et al., 2019). TLR stimulation changed the BCR signalosome towards a more responsive state, as it decreased CD5-IgM BCR interaction and increased CD19-IgM BCR and Syk-CD79A interactions, as early as 24 hours after stimulation (Savage et al., 2019). In TLR-/- mice, surface expression of IgD- and IgM-BCR were both increased, suggesting that constitutive TLR-signaling also has some regulatory effect on BCR expression (**Fig 4.4)**. In contrast to TLR stimulation, BCR stimulation showed increased inhibition of BCR

signaling, as indicated by increased CD5-IgM BCR interaction, decreased CD19-IgM BCR and lack of Syk-CD79A interactions(Savage et al., 2019). However, *in vivo* it is unlikely that TLR or BCR stimulation occurs in isolation of each other. We therefore determined the effects of priming or co-stimulation of the BCR and TLR on B-1 cells.

In B-2 cells it has been well established that BCR priming before or co-stimulation with TLR have a synergistic effect on activation, proliferation and differentiation of B-2 cells (Chaturvedi et al., 2008; Pone et al., 2010). In contrast, priming of CD5+ B-1 cells for as little as 2 hours with αIgM resulted in significant reductions of cell survival and proliferation after subsequent stimulation with TLR compared to TLR stimulation alone **(Fig. 4.5 A, B)**. While TLR primed and BCR stimulated B-1 cells had slightly better survival than not stimulated, or BCR only stimulated cells, they did not proliferate **(Fig. 4.5 A, B).** All cells receiving TLR stimulation downregulated CD5, but only cells solely stimulated by TLRs upregulated CD138 expression (**Fig. 4.5 C, D).** Extending the pulse period of αIgM to 24 hours resulted in even greater inhibition of TLR induced proliferation, whereas in B-2 cells we continued to observe a synergistic enhancing effect (**Fig. 4.5 E)**. While proliferation was not observed until 72 hours of culture, our data suggest that the signals initiating proliferation occurred within the first 24 hours, as TLR stimulation of B-1 cells for 24 hours alone proliferated at the same rate as cells continuously cultured for 72 hours in the presence of TLR agonists (**Fig. 4.5 E)**. Our data also suggested that BCR stimulation of B-1 cells inhibited TLR induced proliferation even after the cells were activated, as B-1 cells stimulated for 24 hours with TLR agonists followed by 48 hours BCR stimulation proliferated less than cells receiving 24 hours stimulation with the TLR agonist followed by no further stimulation (**Fig. 4.5 E)**.

In contrast to B-1 cells, where stimulation through the BCR inhibited TLR-induced B cell proliferation, co-stimulation of B-2 cells with TLR and BCR agonists resulted in stronger proliferation **(Fig. 4.6A**). While CD19 expression was down regulated on B-1 cells under all stimulation condition **(Fig. 4.6B),** this appears to be the outcome of differentiation to CD138+ ASC fate in the TLR stimulated B-1 cells (**Fig. 4.6C** (Shaffer et al., 2002), and the inhibition of BCR-signalosome activity in BCR-stimulated cells, respectively (Savage et al., 2019). Co-stimulation of B-1 cells through BCR and TLR resulted in the upregulation of CD86, though not to the same degree as in B-2 cells stimulated through their BCR **(Fig. 4.6D)**. Frequencies of CD138+ B-1 cells were significantly lower during co-stimulation than after TLR stimulation alone **(Fig. 4.6C),** corresponding with a decrease in secreted IgM in these cultures **(Fig. 4.6E).** The data further demonstrate that TLR stimulation induces B-1 cell differentiation to ACS, but stimulation with antigen, likely self-antigens, generally constrain CD5+ B-1 cell activation and differentiation.

4.6 BCR and TLR9 expression in B-1 cells is not enhanced by reciprocal stimulation, but internalization of BCR enhances BCR/TLR colocalization

BCR stimulation of B-2 cells induces TLR9 expression (Bernasconi et al., 2003) and results in recruitment of TLR9 to the autophagosome, where TLR9 co-localizes with the internalized BCR inducing responsiveness to DNA containing antigens, potentially contributing to autoimmunity (Chaturvedi et al., 2008). In T1/immature B cells BCR and TLR7 co-localized following internalization of self-antigens containing DAMPs, resulting in high expression of AID and deletion of self-reactive B cells(Kuraoka et al., 2017). This suggests cooperation between TLR

and BCR that can determine B-2 cell fates. In vitro stimulation of B-1 cells reduced IgM-BCR expression and only CpG-mediated TLR9 stimulation induced further TLR9 expression in an apparent positive forward loop **(Fig. 4.7A, B).** In contrast, B-2 cells both TLR9 and BCR stimulation induced TLR9 expression, while TLR9 but not BCR stimulation induced expression of the IgM-BCR **(Fig. 4.7A, B).** In αIgM stimulated B-1 cells, intracellular co-localization of TLR9 and the BCR is readily observed (**Fig. 4.7C).** However, neither TLR nor BCR stimulation was significantly different from unstimulated cell, but TLR stimulated cells has significantly less colocalization than BCR stimulation suggesting uncoupling of BCR and TLR signaling in CpG stimulated cells **(Fig. 4.7 D-E)**. Thus B-1 and B-2 cells differ with regards to the stimulation-induced co-localization of BCR and TLR. Further work is needed to assess what interactions between BCR/TLR regulates the responsiveness of B-1 cells to antigen.

4.7 Syk signaling is required for optimal response to TLR stimulation

Both BCR and TLR signaling are initiated through ligand binding resulting in the activation of downstream signaling cascades. In B cells spleen tyrosine kinase (Syk) is most commonly associated with BCR signaling and has been implicated as an important signaling molecule in the interplay between BCR and TLR receptors(Jabara et al., 2012; Kremlitzka et al., 2015). In innate cells, however, the TLR-signaling molecule, MyD88, can directly activate Syk, which in turn initiates an inflammatory response through NF-κB activation(Yi et al., 2021). Syk is an essential component of the early BCR signaling cascade and was shown also to be essential for TLR9 mediated proliferation and activation of B-2 cells (Kremlitzka et al., 2015). Our previous work showed that stimulation of B-1 cells via TLR9 resulted in increased interaction between CD79A and Syk(Savage et al., 2019), which induces phosphorylation of Syk to its active state (pSyk; Pao

et al., 1998). Peritoneal cavity B-1 cells had higher levels of pSyk at steady state, suggesting a constitutive heightened state of activation compared to splenic B-2 cells **(Fig. 4.8A, B)**. pSyk was not seen in B-1 cells within 30 min of TLR or BCR stimulation, but was strongly increased following 24 hours in culture, even in the absence of TLR or BCR agonists (**Fig. 4.8C**). pSyk levels were increased most strongly following TLR, whereas cells receiving αIgM stimulation alone actually showed reduced pSyk levels compared to the unstimulated controls both with and without additional TLR stimulation **(Fig. 4.8C**). The data suggested that in B-1 cells pSyk was induced as a result of TLR not BCR stimulation. The latter may in fact inhibit pSyk. This is consistent with previous findings by us and others that an early marker of BCR activation, Nur77, constitutive expressed at higher levels in B-1 cells and has different kinetics to that reported in B-2 cells, increasing by 24 hours following TLR stimulation(Huizar et al., 2017; Savage et al., 2019)

To further investigate the role of Syk in TLR signaling by B-1 cells, we introduced the Syk inhibitor R406 into our *in vitro* culture system. Consistent with higher levels of constitutive pSyk, B-1 cells were more resistant to the effects of R406 than splenic B-2 cells, although we did see a decrease in survival and TLR induced proliferation at the highest dose (**Fig. 4.8D, E**). High-dose treatment of B-1 cells with R406 reduced survival significantly under all stimulation conditions (**Fig. 4.8E**). Despite the apparent unresponsiveness of B-1 cells to BCR stimulation, blockade of pSyk had the most profound effects when cells were stimulated through the BCR, similar to B-2 cells (**Fig. 4.8E**), while the effects on CpG-mediated increased survival and proliferation were affected less than seen in B-2 cells. TLR induced differentiation of B-1 cells

was also inhibited by Syk inhibition, including repression of CD5 and CD19 downregulation and modestly on CD138 upregulation (**Fig. 4.8F, G, H**).

4.8 Discussion

The central finding of this chapter and our understanding of B-1 cell biology is that these innate like B cells respond differently to TLR and BCR stimulation than conventional B-2 cells. In B-2 cells, optimal antibody responses require coordinated synergistic stimulation of TLR and BCR. This crosstalk occurs through Myd88 and Syk interaction leading to proliferation and differentiation(Schweighoffer et al., 2017). When this synergism is uncoupled, as done here experimentally by inhibiting Syk phosphorylation, it results in loss of responsiveness to both TLR and BCR. Conversely, in B-1 cells the interaction between TLR and BCR is antagonistic, with BCR activation repressing TLR activation in all conditions. Additionally, use of a Syk inhibitor has significantly less effect on the B-1 responses to TLR stimulation, but further suppresses responsiveness through the BCR. This suggests that TLR responses in B-1 cells are using a Syk-signaling independent pathway for activation leading to proliferation and differentiation into ASCs. This finding is supported by the dearth of B-1 derived antibodies in mice where B-1 cells are TLR deficient, demonstrating a requirement for TLR signaling in homeostatic nIgM production. While this homeostatic nIgM production requires TLR, it does not require microbiota, indicating that true homeostatic nIgM production is reliant on self-derived TLR agonists such as DAMPs. Enhanced local B-1 ASC responses required TLR stimulation also in the context of infection, indicating that exogenous TLR ligands can also be potent inducers of B-1 cell derived IgM production.

What our findings do not address is the apparent antigen-specific expansion of B-1 cell populations that have been reported. Work from Kreuk et al. indicated that anti-PtC nIgM production is dependent on expression of endosomal TLR by B-1 cells, whereas anti-microbiota nIgM required intact TLR2/4(Kreuk et al., 2019). This supports the idea of a cross-talk between TLR and BCR, as signaling of specific TLRs results in the activation and differentiation of B-1 cells expressing specific BCRs, suggesting that this process requires both antigen recognition by the BCR, and TLR stimulation by antigen associated molecular patterns (Kreuk et al., 2019). An explanation for this may be offered by work describing expansion of antigen specific CD5+ B-1 cells in the spleen following a *Francisella tularensis* glycolipid vaccination, where antigen-specific B-1 cells stimulated in the spleen then migrate to the peritoneal cavity, where they exist in a quiescent memory state(Yang et al., 2012). However, upon antigen-rechallenge, they failed to differentiate fully into an ASC, despite down regulation of B cell signature genes BCL-6 and Pax 5. However, additional stimulation of these memory B-1 cells with TLR agonists then induces their migration and rapid differentiation into antibody secreting cells in the spleen (Yang et al., 2012), causing them to speculate that peritoneal cavity B-1 cells are memory cells. This would be consistent also with studies by Allugupalli et al, who demonstrated accumulation of CD5- B-1 cells after *Borrelia hermsii* infection that provided immune protection following adaptive transfer(Alugupalli et al., 2003, 2004)Furthermore, during neonatal development, the spleen is required for B-1 cells accumulation in the peritoneal cavity, suggesting that recent B-1 cell emigrants from the fetal liver must first migrate to the spleen (Pedersen et al., 2018; Wardemann et al., 2002), perhaps only seeding the peritoneal cavity if they have experienced cognate antigen.

The most expansive clones in the peritoneal cavity are self-reactive VH11/12 PtC-binding CD5+ B-1 cells(Carmack et al.; Hardy et al., 1989; Prohaska et al., 2018; Yang et al., 2015). PtC is a major component of lipid droplets and cell membranes and is ubiquitous in most tissues(Moessinger et al., 2014). This still begs the question how B-1 cells expand in vivo in an antigen specific, thus BCR dependent manner, when *in vitro* B-1 cells do not respond to BCR stimulation with either soluble or membrane-bound antigen, and only TLR-mediated and thus antigen-non-specific stimulation results in ASC formation.

In summary, this chapter demonstrates that B-1 and B-2 cell responses to TLR and BCR stimulation are distinct. B-2 cells rely on BCR stimulation for efficient induction of pSyk and further downstream signaling events that trigger B cell proliferation and differentiation. In B-2 cells, TLR stimulation integrates with this BCR signaling pathways by enhancing pSyk, thus TLRs act as true co-stimulatory molecules. In contrast, although constitutive pSyk expression is higher in B-1 than B-2 cells, likely due to ongoing self-antigen-triggered BCR signaling, further BCR stimulation did not induce pSyk or enhanced B-1 cell survival, proliferation, and differentiation. Instead, B-1 cells rely on TLR-mediated signals for their activation and differentiation into ASC, in a manner independent of pSyk. Thus, the data suggest the presence of a novel TLR-mediated B cell activation axis not integrated with the BCR-pSyk signaling axis.

4.9 Materials and Methods

Mice

8-16 week old male and female C57BL/6J or female BALB/c mice and breeding pairs of B6.Cg-*Gpi1*^{a}*Thy1*^{a}*Igh*^{a}/J (Igh^{a}) mice were purchased from The Jackson Laboratory. Breeding pairs

of *Tlr2*$^{-/-}$ *x Tlr4*$^{-/-}$ *x Unc93b1*$^{3d/3d}$ (TLR-/-) mice were kindly provided by Greg Barton (University of California, Berkeley, CA). Mice were housed under SPF conditions in micro-isolator cages with food and water provided ad libitum. Mice were euthanized by overexposure to carbon dioxide. All procedures were approved by the UC Davis Animal Care and Use Committee. Neonatal Ig-allotype chimeras were generated as described previously (Baumgarth et al., 1999). Briefly, neonatal Igha mice were treated twice weekly with intra-peritoneal injections of DS-1.1 (anti-IgMa) in PBS beginning on day one after birth for a total of 2.3 mg/mouse over 42 days. Between days 2-4, mice were given also $5x10^6$ donor cells from the peritoneal cavity washout of C57BL/6J or TLR-/- (IgMb) mice. Mice were rested for at least 42 days after end of antibody treatment before use in experiments. All mice used for experiments were female unless otherwise indicated.

Sublethal Influenza infection

Influenza A/Puerto Rico/8/34 (A/PR/8) was grown and harvested as previously described (Doucett et al., 2005). Ten plaque forming units of A/PR/8 in 40 ul PBS was administered intranasally to mice anesthetized with isoflurane.

Flow cytometry

BM and spleen were processed as previously described (Rothaeusler and Baumgarth, 2006). Briefly, BM was harvested by injecting staining media through the marrow cavity of a long bone. Spleen was dissociated between the frosted ends of two microscope glass slides. Peritoneal/pleural cavity cells were obtained using staining media flushed into and then aspirated from the peritoneal and pleural cavities with a plastic pipette (Molecular Bio Products Inc.). All

single cell suspensions were passed through a 70 mm nylon mesh, treated with ACK lysis buffer (Rothaeusler and Baumgarth, 2006), re-filtered through nylon mesh, and resuspended in staining media. Trypan Blue exclusion dye was performed on all samples to identify live cells using a hemocytometer or an automated cell counter (Nexcelom Bioscience). Cells were blocked with anti-FcγR (2.4.G2), washed and stained with fluorescent antibodies (See **Supplemental Table 3.1** in Chapter 3).

Dead cells were identified using Live/Dead Fixable Aqua or Live/Dead Fixable Violet stain (Invitrogen). Fluorescently labeled cells were read on either a 4-laser, 22-paramter LSR Fortessa (BD Bioscience), or a 5-laser, 30-parameter Symphony (BD Bioscience). Data were analyzed using FlowJo software (FlowJo LLC, kind gift of Adam Treister).

Cell sorting/enrichment

Cells were sorted at pressures around 11psi using the FACSAria equipped with a 100µm nozzle. Single cell suspensions of peritoneal cavity washout and spleen cells were counted and blocked with anti-FcR (2.4.G2). Peritoneal cells were labeled with Live/Dead Fixable Aqua, antibodies against the following surface markers: F4/80 (F4/80), Gr1 (RA3.6C2), NK1.1(DX5), CD4 (GK1.5), CD8a (53-6.7.3.1), CD19 (Id.3), CD23 (B3B4) and CD90.2 (30H12.1) and then sorted on live, dump-, CD23-, $CD19^{hi}$ or $B220^{lo}$ to obtain B-1 cells. Spleen cells were labeled with anti-F4/80 (F4/80), Gr1 (RA3.6C2), NK1.1(DX5), CD4 (GK1.5), CD8a (53-6.7.3.1), CD19 (Id.3), CD23 (B3B4) and CD90.2 (30H12.1) and then sorted on live, dump-, CD23+, CD19+ or B220+ to obtain follicular (B-2) cells. Cells were sorted into 15 ml conical tubes containing RPMI based culture media with 50% FBS. Cells were rested for 2 hours after sorting prior to use for in vitro cultures.

For magnetic cell separation, single cell suspensions of peritoneal cavity washout and spleen cells were counted and blocked with anti-FcR (2.4.G2). For B-1 cell enrichment, peritoneal cavity cells were labeled with biotinylated antibodies to the following surface markers: F4/80 (F4/80), Gr1 (RA3.6C2), NK1.1(DX5), CD4 (GK1.5), CD8a (53-6.7.3.1), CD23 (B3B4) and CD90.2 (30H12.1). For splenic B-2 cell enrichment, cells were labeled with biotinylated antibodies against F4/80 (F4/80), Gr1 (RA3.6C2), NK1.1(DX5), CD4 (GK1.5), CD8a (53-6.7.3.1), CD9 (KMC8), CD138(281-2), CD5(53-7.3) and CD90.2 (30H12.1) generated in-house, followed by staining with anti-biotin magnetic beads (Miltenyi Biotec). Cells were passed over a magnetic column and separated using the DepleteS program (*auto*-MACS, Miltenyi Biotec). Purity was >90%.

Enzyme-Linked Immunosorbant Assay (ELISA)

Sandwich ELISAs were performed as previously described (Rothaeusler and Baumgarth, 2006). ELISA plates (MaxiSorp 96 well plates, Thermofisher) were coated with unlabeled anti-IgM (Southern Biotech). Non-specific binding was blocked with 1% newborn calf serum, 0.1% dried milk powder, and 0.05% Tween20 in PBS (ELISA blocking buffer). Serum and standards were added to the plate at previously determined optimal pre-dilutions and were two-fold serially diluted. Binding was revealed with biotinylated anti-IgM (Southern Biotech), anti-IgMa (BD Bioscience) or anti-IgMb (BD Bioscience), then streptavidin-horseradish peroxidase (Vector Labs), all diluted in ELISA blocking buffer. Finally, substrate (0.005% 3,3',5,5'-tetramethylbenzidine (TMB) in 0.05 M citric acid buffer and 0.015% hydrogen peroxide was added. The reaction was stopped with 1N sulfuric acid. Absorbance was measured at 450 nm

(595 nm reference wavelength) on a spectrophotometer (SpectraMax M5, Molecular Devices). IgM concentrations were determined by comparison to curves generated with the IgM standard.

Enzyme-Linked ImmunoSpot (ELISPOT)

96-well ELISPOT plates (Multi-Screen HA Filtration, Millipore) were coated with 5μg/ml anti-IgM (331) or anti-IgMb (AF6-78). Non-specific binding was blocked with 4% bovine serum albumin (BSA) in PBS. IgM ASCs were enumerated by plating 1.0 x10^6 MedLN, spleen or BM cells, processed as outlined above, into ELISPOT plates and then serially diluting samples seven times in culture media (RPMI 1640, 10% fetal bovine serum, 292 μg/ml L-glutamine, 100 Units/ml penicillin, 100 μg/ml streptomycin, and 50 μM 2-mercaptoethanol). Cells were cultured overnight (~16hrs) at 37°C/5% CO_2. Deionized water was used to lyse the cells after which IgM secretion was revealed with biotinylated anti-IgM (Southern Biotech), followed by streptavidin-horseradish peroxidase (Vector Labs), both diluted in 2% BSA in PBS. Last, substrate solution (3.3 mg 3-amino-9-ethylcarbazole (Sigma Aldrich) dissolved in dimethyl formamide and 0.015% hydrogen peroxide in 0.1M sodium acetate) was added, and the reaction was stopped with deionized water. Spots were enumerated and images captured with the AID EliSpot Reader System (Autoimmun Diagnostika).

Cell Culture

After isolation cells were labeled with Efluor670 by incubation at 37°C for 10 mins 125-250 ug/ml fluorochrome, washed three times with staining medium containing 10% neonatal calf serum and resuspended in Culture Media (RPMI 1640 with 10% heat inactivated fetal bovine serum, 292 μg/ml L-glutamine, 100 Units/ml penicillin, 100 μg/ml streptomycin, and 50 μM 2-

mercaptoethanol). Cells were plated at 1-2x10^5 cells/200µl well of 96-well U bottom tissue culture plates (BD Bioscience) and unless otherwise indicated, cultured at 37°C/5% CO_2 for 30 min - 3 days. When indicated, CpG ODN 7909 at 5 µg/ml, αIgM $(Fab)_2$ at 10 ug/ml, 10,000 αIgM-coated beads or 50µM PtC liposomes (source) were added to the wells. αIgM-coated beads were made using streptavidin (SA) coated particles according to the manufacturers (Spherotech, Inc.) specifications. In brief 1mg of SA coated beads were blocked with 0.1% BSA, washed, and then incubated with 10µg αIgM-biotin(331) at room temperature for hour, washed and resuspended. Bead were then titrated using splenic B cells to optimize for proliferation. After culture, culture plates were spun, and supernatant was collected and stored at −20°C. Cells were stained for FACS or imaging.

BCR internalization assay

Purified cells were incubated on ice for 30 minutes with 10 µg/ml αIgM$(Fab)_2$ αIgM-FITC or 50 µM PtC-FITC, washed three time in cold culture media at 4C, and then incubated in a 37C water bath for 30 minutes. Cells were then washed three times in ice cold staining buffer before being fixed in 2% PFA. Cells were imaged use BZ-X800 Keyence Florence Microscope, or they were permeabilized and stained with anti-TLR9-PE then anti-PE-Texas Red and imaged on a Leica TCS SP8 STED 3X confocal microscope.

Data Analysis and Visualization

All statistics and numerical representations were done with the help of Prism software (GraphPad Software). ImageJ with Coloc2 plugin was used to process images and quantify colocalization of TLR9 and IgM-BCR using Costes regression threshold(Costes et al., 2004).

Comparisons between two groups were done using a two-tailed Student's t test. For more than two groups, a one-way ANOVA was performed with post hoc analysis for significant differences between individual groups using Tukey's correction for multiple comparisons. A $p < 0.05$ was considered statistically significant.

4.10 References

Alhakeem, S. S., Sindhava, V. J., Mckenna, M. K., Gachuki, B. W., Byrd, J. C., Muthusamy, N., & Bondada, S. (2015). Role of B cell receptor signaling in IL-10 production by normal and malignant B-1 cells. *Annals of the New York Academy of Sciences*, *1362*(1), 239. https://doi.org/10.1111/NYAS.12802

Alugupalli, K. R., Gerstein, R. M., Chen, J., Szomolanyi-Tsuda, E., Woodland, R. T., & Leong, J. M. (2003). The resolution of relapsing fever borreliosis requires IgM and is concurrent with expansion of B1b lymphocytes. *Journal of Immunology (Baltimore, Md. : 1950)*, *170*(7), 3819–3827. https://doi.org/10.4049/JIMMUNOL.170.7.3819

Alugupalli, K. R., Leong, J. M., Woodland, R. T., Muramatsu, M., Honjo, T., & Gerstein, R. M. (2004). B1b lymphocytes confer T cell-independent long-lasting immunity. *Immunity*, *21*(3), 379–390. https://doi.org/10.1016/j.immuni.2004.06.019

Baumgarth, N., Herman, O. C., Jager, G. C., Brown, L. E., Herzenberg, L. A., & Chen, J. (2000). B-1 and B-2 cell-derived immunoglobulin M antibodies are nonredundant components of the protective response to influenza virus infection. *J Exp Med*, *192*(2), 271–280. https://doi.org/10.1084/jem.192.2.271

Baumgarth, N., Herman, O. C., Jager, G. C., Brown, L., Herzenberg, L. A., & Herzenberg, L. A. (1999). Innate and acquired humoral immunities to influenza virus are mediated by distinct arms of the immune system. *Proceedings of the National Academy of Sciences of the United States of America*, *96*(5), 2250–2255. https://doi.org/10.1073/pnas.96.5.2250

Baumgarth, N., Waffarn, E. E., & Nguyen, T. T. T. (2015). Natural and induced B-1 cell immunity to infections raises questions of nature versus nurture. *Annals of the New York Academy of Sciences*, *1362*(1), 188–199. https://doi.org/10.1111/NYAS.12804

Berland, R., & Wortis, H. H. (2002). Origins and functions of B-1 cells with notes on the role of CD5. *Annu Rev Immunol*, *20*, 253–300. https://doi.org/10.1146/annurev.immunol.20.100301.064833

Bernasconi, N. L., Onai, N., & Lanzavecchia, A. (2003). A role for Toll-like receptors in acquired immunity: up-regulation of TLR9 by BCR triggering in naive B cells and constitutive expression in memory B cells. *Blood*, *101*(11), 4500–4504. https://doi.org/10.1182/BLOOD-2002-11-3569

Bikah, G., Carey, J., Ciallella, J. R., Tarakhovsky, A., & Bondada, S. (1996). CD5-Mediated Negative Regulation of Antigen Receptor-Induced Growth Signals in B-1 B Cells. *Science*, *274*(5294), 1906–1909. https://doi.org/10.1126/SCIENCE.274.5294.1906

Carmack, C. E., Shinton, S. A., Hayakawa, K., & Hardy, R. R. (n.d.). *Rearrangement and Selection of VH11 in the Ly-1 B Cell Lineage*.

Chaturvedi, A., Dorward, D., & Pierce, S. K. (2008). The B cell receptor governs the subcellular location of Toll-like receptor 9 leading to hyperresponses to DNA-containing antigens. *Immunity*, *28*(6), 799–809. https://doi.org/10.1016/J.IMMUNI.2008.03.019

Choi, Y. S., & Baumgarth, N. (2008). Dual role for B-1a cells in immunity to influenza virus infection. *The Journal of Experimental Medicine*, *205*(13), 3053–3064. https://doi.org/10.1084/JEM.20080979

Costes, S. v., Daelemans, D., Cho, E. H., Dobbin, Z., Pavlakis, G., & Lockett, S. (2004). Automatic and Quantitative Measurement of Protein-Protein Colocalization in Live Cells. *Biophysical Journal*, *86*(6), 3993–4003. https://doi.org/10.1529/BIOPHYSJ.103.038422

Doucett, V. P., Gerhard, W., Owler, K., Curry, D., Brown, L., & Baumgarth, N. (2005). Enumeration and characterization of virus-specific B cells by multicolor flow cytometry. *Journal of Immunological Methods*, *303*(1–2), 40–52. https://doi.org/10.1016/j.jim.2005.05.014

Gao, J., Ma, X., Gu, W., Fu, M., An, J., Xing, Y., Gao, T., Li, W., & Liu, Y. (2012). Novel functions of murine B1 cells: active phagocytic and microbicidal abilities. *European Journal of Immunology*, *42*(4), 982–992. https://doi.org/10.1002/EJI.201141519

Genestier, L., Taillardet, M., Mondiere, P., Gheit, H., Bella, C., & Defrance, T. (2007). TLR Agonists Selectively Promote Terminal Plasma Cell Differentiation of B Cell Subsets Specialized in Thymus-Independent Responses. *The Journal of Immunology*, *178*(12), 7779–7786. https://doi.org/10.4049/jimmunol.178.12.7779

Haas, K. M., Poe, J. C., Steeber, D. A., & Tedder, T. F. (2005). B-1a and B-1b Cells Exhibit Distinct Developmental Requirements and Have Unique Functional Roles in Innate and Adaptive Immunity to S. pneumoniae. *Immunity*, *23*(1), 7–18. https://doi.org/10.1016/J.IMMUNI.2005.04.011

Hardy, R. R., Carmack, C. E., Shinton, S. A., Riblet, R. J., & Hayakawa, K. (1989). A single VH gene is utilized predominantly in anti-BrMRBC hybridomas derived from purified Ly-1 B cells. Definition of the VH11 family. *The Journal of Immunology*, *142*(10).

Haro, M. A., Dyevoich, A. M., Phipps, J. P., & Haas, K. M. (2019). Activation of B-1 cells promotes tumor cell killing in the peritoneal cavity. *Cancer Research*, *79*(1), 159. https://doi.org/10.1158/0008-5472.CAN-18-0981

Hayakawa, K., Asano, M., Shinton, S. A., Gui, M., Allman, D., Stewart, C. L., Silver, J., & Hardy, R. R. (1999). Positive selection of natural autoreactive B cells. *Science (New York, N.Y.)*, *285*(5424), 113–116. https://doi.org/10.1126/SCIENCE.285.5424.113

Hayakawa, K., Asano, M., Shinton, S. A., Gui, M., Wen, L. J., Dashoff, J., & Hardy, R. R. (2003). Positive selection of anti-thy-1 autoreactive B-1 cells and natural serum

autoantibody production independent from bone marrow B cell development. *Journal of Experimental Medicine*, *197*(1), 87–99. https://doi.org/10.1084/jem.20021459

Huizar, J., Tan, C., Noviski, M., Mueller, J. L., & Zikherman, J. (2017). Nur77 Is Upregulated in B-1a Cells by Chronic Self-Antigen Stimulation and Limits Generation of Natural IgM Plasma Cells. *ImmunoHorizons*, *1*(9), 188–197. https://doi.org/10.4049/immunohorizons.1700048

Jabara, H. H., McDonald, D. R., Janssen, E., Massaad, M. J., Ramesh, N., Borzutzky, A., Rauter, I., Benson, H., Schneider, L., Baxi, S., Recher, M., Notarangelo, L. D., Wakim, R., Dbaibo, G., Dasouki, M., Al-Herz, W., Barlan, I., Baris, S., Kutukculer, N., … Geha, R. S. (2012). DOCK8 functions as an adaptor that links Toll-like receptor–MyD88 signaling to B cell activation. *Nature Immunology*, *13*(6), 612. https://doi.org/10.1038/NI.2305

Jackson-Jones, L. H., Duncan, S. M., Magalhaes, M. S., Campbell, S. M., Maizels, R. M., McSorley, H. J., Allen, J. E., & Bénézech, C. (2016). Fat-associated lymphoid clusters control local IgM secretion during pleural infection and lung inflammation. *Nature Communications 2016 7:1*, *7*(1), 1–14. https://doi.org/10.1038/ncomms12651

Kremlitzka, M., Mácsik-Valent, B., & Erdei, A. (2015). Syk is indispensable for CpG-induced activation and differentiation of human B cells. *Cellular and Molecular Life Sciences*, *72*(11), 2223–2236. https://doi.org/10.1007/S00018-014-1806-X/FIGURES/7

Kreuk, L. S. M., Koch, M. A., Slayden, L. C., Lind, N. A., Chu, S., Savage, H. P., Kantor, A. B., Baumgarth, N., & Barton, G. M. (2019). B cell receptor and toll-like receptor signaling coordinate to control distinct B-1 responses to both self and the microbiota. *ELife*, *8*. https://doi.org/10.7554/eLife.47015

Kuraoka, M., Snowden, P. B., Nojima, T., Verkoczy, L., Haynes, B. F., Kitamura, D., & Kelsoe, G. (2017). BCR and Endosomal TLR Signals Synergize to Increase AID Expression and Establish Central B Cell Tolerance. *Cell Reports*, *18*(7), 1627. https://doi.org/10.1016/J.CELREP.2017.01.050

Meyer-Bahlburg, A., & Rawlings, D. J. (2012). Differential impact of Toll-like receptor signaling on distinct B cell subpopulations. *Frontiers in Bioscience*, *17*(4), 1499–1516. https://doi.org/10.2741/4000

Moessinger, C., Klizaite, K., Steinhagen, A., Philippou-Massier, J., Shevchenko, A., Hoch, M., Ejsing, C. S., & Thiele, C. (2014). Two different pathways of phosphatidylcholine synthesis, the Kennedy Pathway and the Lands Cycle, differentially regulate cellular triacylglycerol storage. *BMC Cell Biology*, *15*(1), 1–17. https://doi.org/10.1186/S12860-014-0043-3/FIGURES/6

Morris, D. L., & Rothstein, T. L. (1993). Abnormal transcription factor induction through the surface immunoglobulin M receptor of B-1 lymphocytes. *The Journal of Experimental Medicine*, *177*(3), 857–861. https://doi.org/10.1084/JEM.177.3.857

Murakami, M., Tsubata, T., Okamoto, M., Shimizu, A., Kumagai, S., Imura, H., & Honjo, T. (1992). Antigen-induced apoptotic death of Ly-1 B cells responsible for autoimmune disease in transgenic mice. *Nature 1992 357:6373*, *357*(6373), 77–80. https://doi.org/10.1038/357077a0

Nguyen, T. T., Elsner, R. A., & Baumgarth, N. (2015). Natural IgM prevents autoimmunity by enforcing B cell central tolerance induction. *J Immunol*, *194*(4), 1489–1502. https://doi.org/10.4049/jimmunol.1401880

Nitschke, L. (2015). Siglec-G is a B-1 cell inhibitory receptor and also controls B cell tolerance. *Annals of the New York Academy of Sciences*, *1362*(1), 117–121. https://doi.org/10.1111/nyas.12826

Ochsenbein, A. F., Fehr, T., Lutz, C., Suter, M., Brombacher, F., Hengartner, H., & Zinkernagel, R. M. (1999). Control of early viral and bacterial distribution and disease by natural antibodies. *Science*, *286*(5447), 2156–2159.

Pao, L. I., Famiglietti, S. J., & Cambier, J. C. (1998). *Signal Transduction Motif Tyrosines in B Cell Antigen Receptor Immunoreceptor Tyrosine-Based Activation Asymmetrical Phosphorylation and Function of*. http://www.jimmunol.org/content/160/7/3305

Pedersen, G. K., Li, X., Khoenkhoen, S., Ádori, M., Beutler, B., & Karlsson Hedestam, G. B. (2018). B-1a Cell Development in Splenectomized Neonatal Mice. *Frontiers in Immunology*, *9*, 1738. https://doi.org/10.3389/FIMMU.2018.01738/BIBTEX

Pone, E. J., Zan, H., Zhang, J., Al-Qahtani, A., Xu, Z., & Casali, P. (2010). Toll-Like Receptors and B-Cell Receptors Synergize to Induce Immunoglobulin Class-Switch DNA Recombination: Relevance to Microbial Antibody Responses. *Critical Reviews™ in Immunology*, *30*(1), 1–29. https://doi.org/10.1615/CRITREVIMMUNOL.V30.I1.10

Prohaska, T. A., Que, X., Diehl, C. J., Hendrikx, S., Chang, M. W., Jepsen, K., Glass, C. K., Benner, C., & Witztum, J. L. (2018). Massively Parallel Sequencing of Peritoneal and Splenic B Cell Repertoires Highlights Unique Properties of B-1 Cell Antibodies. *The Journal of Immunology*, *200*(5), ji1700568. https://doi.org/10.4049/jimmunol.1700568

Rothaeusler, K., & Baumgarth, N. (2006). Evaluation of intranuclear BrdU detection procedures for use in multicolor flow cytometry. *Cytometry Part A*, *69*(4), 249–259. https://doi.org/10.1002/cyto.a.20252

Savage, H. P., Klasener, K., Smith, F. L., Luo, Z., Reth, M., & Baumgarth, N. (2019). TLR induces reorganization of the IgM-BCR complex regulating murine B-1 cell responses to infections. *ELife*, *8*. https://doi.org/10.7554/ELIFE.46997

Savage, H. P., Yenson, V. M., Sawhney, S. S., Mousseau, B. J., Lund, F. E., & Baumgarth, N. (2017). Blimp-1–dependent and –independent natural antibody production by B-1 and B-1–

derived plasma cells. *The Journal of Experimental Medicine*, *214*(9), 2777–2794. https://doi.org/10.1084/jem.20161122

Schweighoffer, E., Nys, J., Vanes, L., Smithers, N., & Tybulewicz, V. L. J. (2017). TLR4 signals in B lymphocytes are transduced via the B cell antigen receptor and SYK. *The Journal of Experimental Medicine*, *214*(5), 1269–1280. https://doi.org/10.1084/JEM.20161117

Sen, G., Bikah, G., Venkataraman, C., & Bondada, S. (1999). *Negative regulation of antigen receptor-mediated signaling by constitutive association of CD5 with the SHP-1 protein tyrosine phosphatase in B-1 B cells*. https://doi.org/10.1002/(SICI)1521-4141(199910)29:10

Shaffer, A. L., Lin, K. I., Kuo, T. C., Yu, X., Hurt, E. M., Rosenwald, A., Giltnane, J. M., Yang, L., Zhao, H., Calame, K., & Staudt, L. M. (2002). Blimp-1 orchestrates plasma cell differentiation by extinguishing the mature B cell gene expression program. *Immunity*, *17*(1), 51–62.

Sindhava, V. J., & Bondada, S. (2012). Multiple Regulatory Mechanisms Control B-1 B Cell Activation. *Frontiers in Immunology*, *3*(DEC). https://doi.org/10.3389/FIMMU.2012.00372

Smith, F. L., & Baumgarth, N. (2019). B-1 cell responses to infections. In *Current Opinion in Immunology* (Vol. 57, pp. 23–31). https://doi.org/10.1016/j.coi.2018.12.001

Tarakhovsky, A., Müller, W., & Rajewsky, K. (1994). Lymphocyte populations and immune responses in CD5-deficient mice. *European Journal of Immunology*, *24*(7), 1678–1684. https://doi.org/10.1002/eji.1830240733

Waffarn, E. E., Hastey, C. J., Dixit, N., Soo Choi, Y., Cherry, S., Kalinke, U., Simon, S. I., & Baumgarth, N. (2015). Infection-induced type I interferons activate CD11b on B-1 cells for subsequent lymph node accumulation. *Nature Communications*, *6*. https://doi.org/10.1038/NCOMMS9991

Wardemann, H., Boehm, T., Dear, N., & Carsetti, R. (2002). B-1a B Cells that Link the Innate and Adaptive Immune Responses Are Lacking in the Absence of the Spleen. *The Journal of Experimental Medicine*, *195*(6), 771. https://doi.org/10.1084/JEM.20011140

Yang, Y., Eid, E., Ghosn, B., Cole, L. E., Obukhanych, T. v, Sadate-Ngatchou, P., Vogel, S. N., Herzenberg, L. A., & Herzenberg, L. A. (2012). Antigen-specific memory in B-1a and its relationship to natural immunity. *PNAS*. https://doi.org/10.1073/pnas.1121631109

Yang, Y., Li, X., Ma, Z., Wang, C., Yang, Q., Byrne-Steele, M., Hong, R., Min, Q., Zhou, G., Cheng, Y., Qin, G., Youngyunpipatkul, J. v., Wing, J. B., Sakaguchi, S., Toonstra, C., Wang, L.-X., Vilches-Moure, J. G., Wang, D., Snyder, M. P., … Herzenberg, L. A. (2021). CTLA-4 expression by B-1a B cells is essential for immune tolerance. *Nature Communications 2021 12:1*, *12*(1), 1–17. https://doi.org/10.1038/s41467-020-20874-x

Yang, Y., Wang, C., Yang, Q., Kantor, A. B., Chu, H., Ghosn, E. E. B., Qin, G., Mazmanian, S. K., Han, J., & Herzenberg, L. A. (2015). Distinct mechanisms define murine B cell lineage immunoglobulin heavy chain (IgH) repertoires. *ELife*, *4*(September 2015). https://doi.org/10.7554/eLife.09083

Yi, Y. S., Kim, H. G., Kim, J. H., Yang, W. S., Kim, E., Jeong, D., Park, J. G., Aziz, N., Kim, S., Parameswaran, N., & Cho, J. Y. (2021). Syk-MyD88 Axis Is a Critical Determinant of Inflammatory-Response in Activated Macrophages. *Frontiers in Immunology*, *12*, 5558. https://doi.org/10.3389/FIMMU.2021.767366/BIBTEX

4.11 Figures

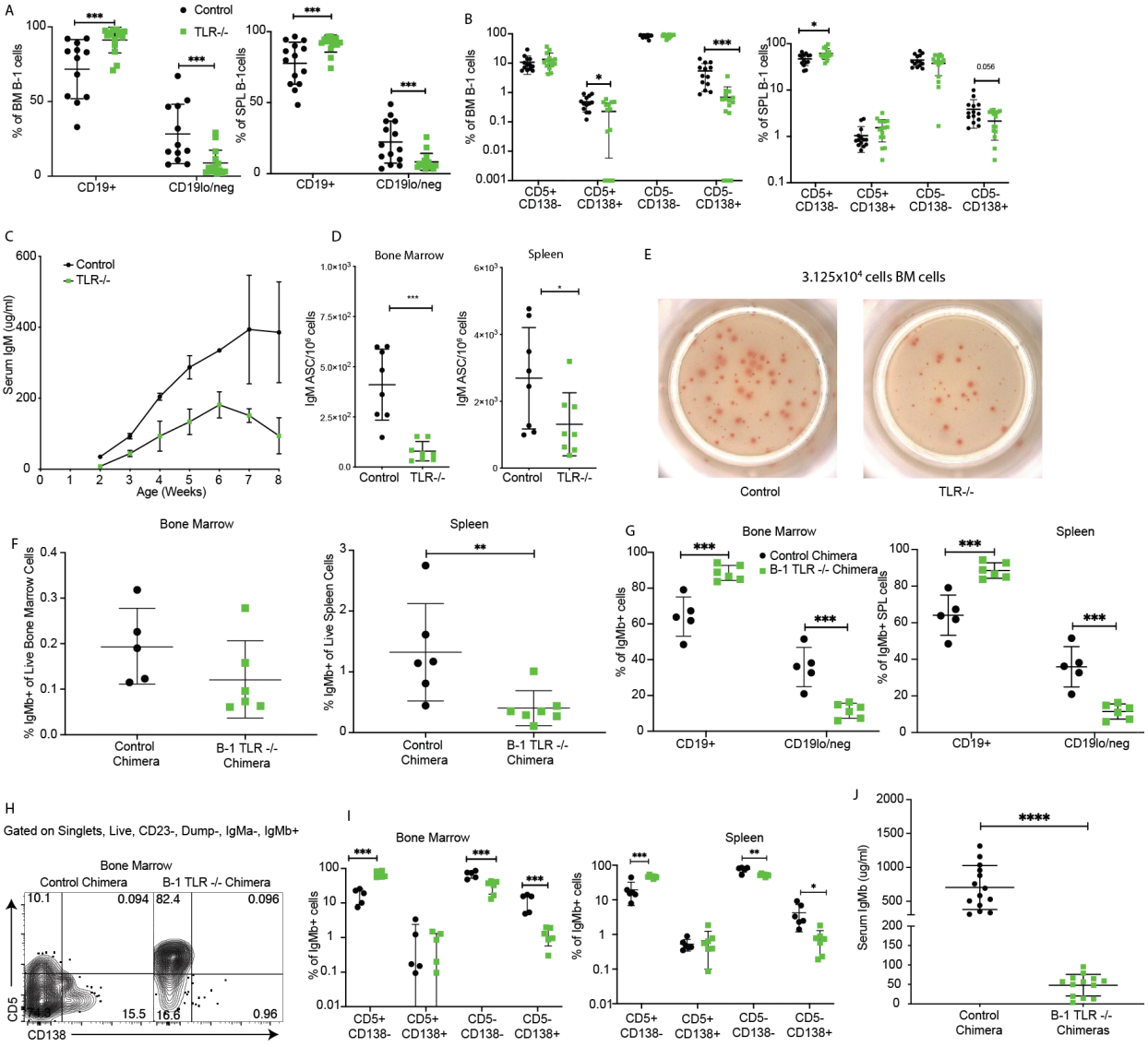
A
Control
TLR-/-
% of BM B-1 cells
% of SPL B-1cells
CD19+
CD19lo/neg
B
% of BM B-1 cells
% of SPL B-1 cells
CD5+ CD138-
CD5+ CD138+
CD5- CD138-
CD5- CD138+
0.056
C
Serum IgM (ug/ml)
Age (Weeks)
D
Bone Marrow
Spleen
IgM ASC/10⁶ cells
E
3.125x10⁴ cells BM cells
F
Bone Marrow
Spleen
% IgMb+ of Live Bone Marrow Cells
% IgMb+ of Live Spleen Cells
Control Chimera
B-1 TLR -/- Chimera
G
Bone Marrow
Spleen
Control Chimera
B-1 TLR -/- Chimera
% of IgMb+ cells
% of IgMb+ SPL cells
H
Gated on Singlets, Live, CD23-, Dump-, IgMa-, IgMb+
Bone Marrow
Control Chimera
B-1 TLR -/- Chimera
10.1
0.094
82.4
0.096
15.5
16.6
0.96
CD5
CD138
I
Bone Marrow
Spleen
% of IgMb+ cells
J
Serum IgMb (ug/ml)
Control Chimera
B-1 TLR -/- Chimeras

Figure 4.1: nIgM production in steady state BM and spleen require intact TLR signaling in B-1 cells

A, B) Mean percentage ± SD of (**A**) CD19+ (Dump- live CD23-, IgD-, IgM+) B-1 cells or $CD19^{lo/neg}$ B-1 cells and (**B**) CD5 and CD138 expression of B-1 cells in BM and spleen of C57BL/6 (control) and congenic total TLR-deficient (TLR-/-) mice, n=10-12 mice/group. **C)** Levels serum IgM (μg/ml) and **D**) mean number ± SD of BM and spleen cells secreting IgM as assessed by ELISPOT; n = 8 mice/group**. E)** Representative IgM ELISPOT wells**. F)** Mean percentage ± SD of IgMb+ (B-1) cells amongst live cells in BM and spleen from neonatal Ig-allotype chimeras with B-1 cells from control or TLR-/- mice, n=5 - 6 mice/group. **G)** Mean percentage ± SD of CD19+ IgMb+(B-1) cells or CD19lo/neg IgMb+(B-1) cells in BM and spleen of control and B-1 TLR-/- chimera mice, n=5-6 mice /group. **H** Representative flow plots of CD5 and CD138 expression in IgMb+(B-1) cells**. I)** Mean percentage ± SD of IgMb+ (B-1) cells based on CD5 and CD138 expression in BM and spleen of control and B-1 TLR-/- chimera mice, n=5-6 mice /group combination of 2 independent experiments. **J)** Serum IgM (μg/ml) as measured by ELISA in adult control and B-1 TLR-/- chimera mice, n=13-14 mice per group. Values were compared using an unpaired Student's t test or a one-way ANOVA with post-hoc analysis for multiple comparisons (*=$p < 0.05$, **=$p < 0.01$***=$p<0.001$, ****=$p<0.0001$). A, B data from 3 independent experiments; C, D, F, G, data combined from 2 independent experiments.

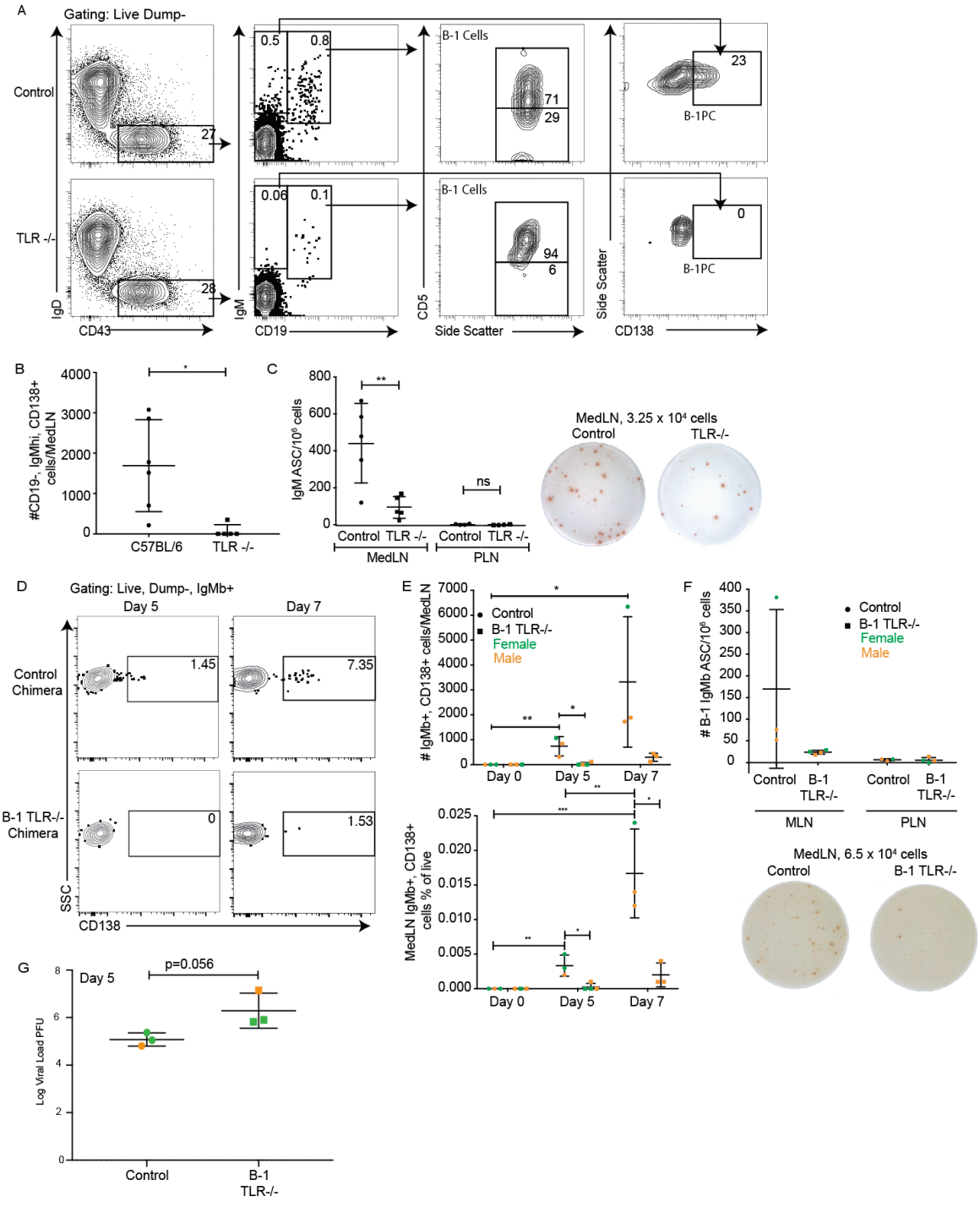
A
Gating: Live Dump-
Control
TLR -/-
IgD
CD43
IgM
CD19
CD5
Side Scatter
B-1 Cells
B-1PC
CD138
B
#CD19-, IgMhi, CD138+ cells/MedLN
C57BL/6
TLR -/-
C
IgM ASC/10⁶ cells
Control
TLR -/-
MedLN
PLN
ns
MedLN, 3.25 x 10⁴ cells
D
Gating: Live, Dump-, IgMb+
Day 5
Day 7
Control Chimera
B-1 TLR-/- Chimera
SSC
CD138
E
IgMb+, CD138+ cells/MedLN
B-1 TLR-/-
Female
Male
Day 0
Day 5
Day 7
MedLN IgMb+, CD138+ cells % of live
F
B-1 IgMb ASC/10⁶ cells
MLN
PLN
MedLN, 6.5 x 10⁴ cells
G
p=0.056
Log Viral Load PFU

Figure 4.2: Local IgM production following influenza infection depends on TLR expression

A) C57BL/6 and congenic total TLR-/- were infected with influenza A/Puerto Rico/8/34 for 5 days. Shown are representative FACS plots from control and TLR-/- mice FACS analysis of MedLN for the presence of B-1 and B-1PC (n=5 mice/group). **B**) Number of B-1PC per MedLN as assessed by FACS and **C**) number of IgM-secreting cells in MedLN as assessed by ELISPOT analysis. **D-F**) Similar analysis as for A-C but using allotype chimeras generated with Igha recipients and B-1 cells from either control or TLR-/- mice. **D**) Representative FACS analysis of CD138+ B-1PC pre-gated for live, dump-, B-1 donor (IgMb+) cells in MedLN on days 5 and 7 after influenza infection. **E**) Mean ± SD of data summarized from analysis shown in **D**. **F**) Mean ± SD of B-1 IgM-ASC in MedLN on day 7 after infection, as assessed by ELISPOT. **G) Log** Viral load PFU at day five in control and B-1 TLR-/- chimeras, n=3 per group. Each symbol represents results from one mouse with female mice shown as open symbols, males as closed symbols. Results are combined from two independent experiments. Values were compared using an unpaired Student's t test (*=$p < 0.05$, **=$p < 0.005$, n.s. not significant).

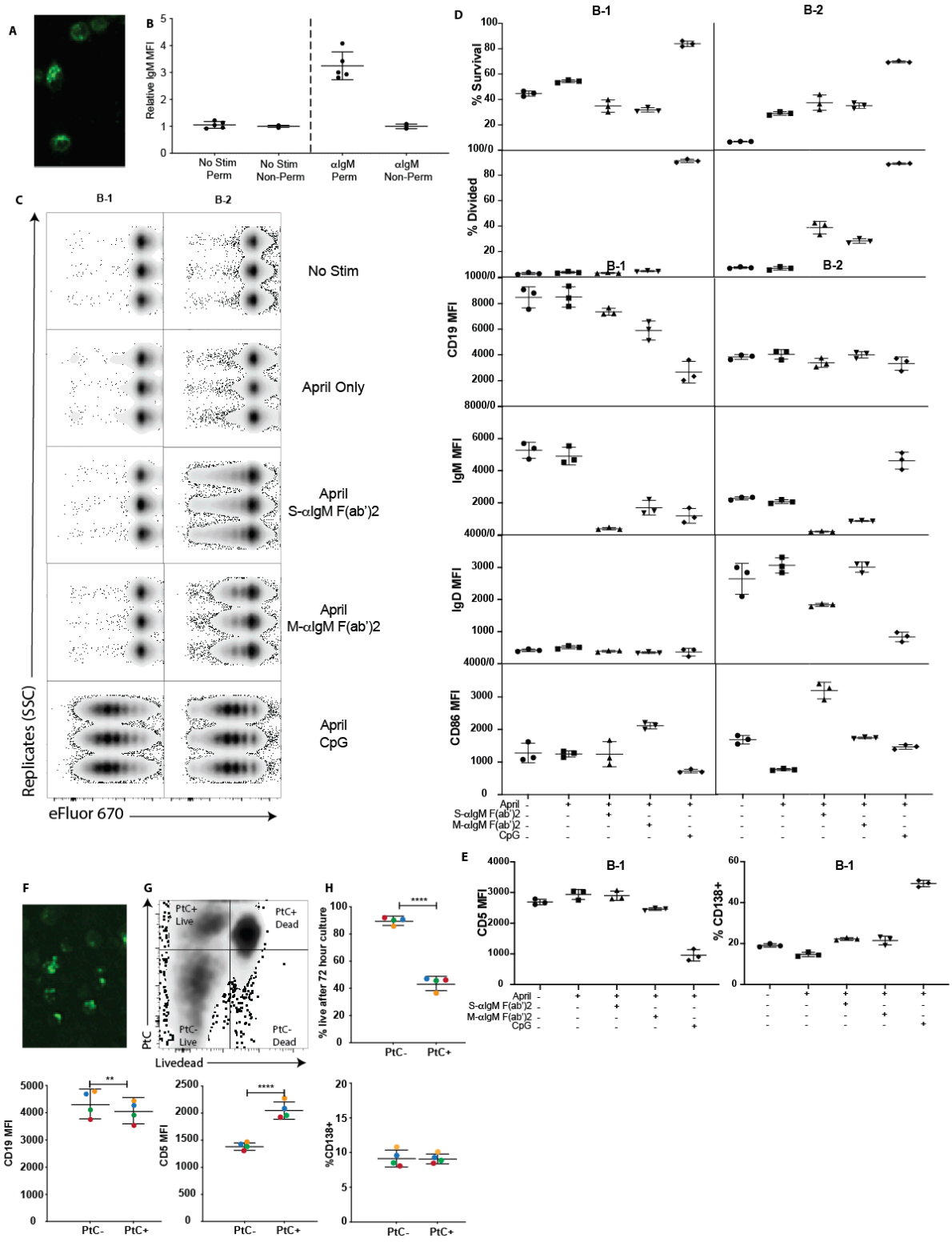
A
B
Relative IgM MFI
No Stim Perm
No Stim Non-Perm
αIgM Perm
αIgM Non-Perm
C
B-1
B-2
No Stim
April Only
April S-αIgM F(ab')2
April M-αIgM F(ab')2
April CpG
Replicates (SSC)
eFluor 670
D
B-1
B-2
% Survival
% Divided
CD19 MFI
IgM MFI
IgD MFI
CD86 MFI
April
S-αIgM F(ab')2
M-αIgM F(ab')2
CpG
E
B-1
CD5 MFI
% CD138+
F
G
PtC+ Live
PtC+ Dead
PtC- Live
PtC- Dead
PtC
Livedead
H
% live after 72 hour culture
PtC-
PtC+
I
CD19 MFI
CD5 MFI
%CD138+

Figure 4.3: B-1 cells internalize antigen, but do not differentiate in response to either soluble or membrane bound antigen

A, B) AutoMacs enriched peritoneal cavity B-1 cells from BALB/c mice were cultured for 30 min with αIgM F(ab')2 or left unstimulated (no stim). Staining for IgM with and without permeabilization identified surface and surface plus internalized IgM by flow cytometry. MFI, mean fluorescent intensity **A)** Representative image of αIgM treated cells permeabilized and stained for IgM. **B)** Relative MFI of permeabilized and non-permeabilized cells with/without stimulation. **C)** Representative flow plots showing proliferation dye (eFluor670) dilution of B-1 and splenic B-2 cells from BALB/c mice after culture for 72 hrs with the indicated stimuli. **D, E)** Flow cytometric analysis of cells after culture. **F)** Fluorescence microscopy, **G**) flow cytometry of peritoneal cavity B-1 cells from BALB/c mice after 30 min. culture with FITC-labelled PtC liposomes. **H, I)** Flow cytometric evaluation of PtC-binding and non-binding B-1 cells after 72 hrs stimulation with PtC liposomes. Values in were compared using an unpaired Student's t test (**B),** paired Student's t test **(H), (I)** or a one-way ANOVA **(D), (E)** followed by post hoc testing with correction for multiple comparison (*$p<0.05$, **$p<0.01$, ***$p<0.001$, ****$p<0.0001$).

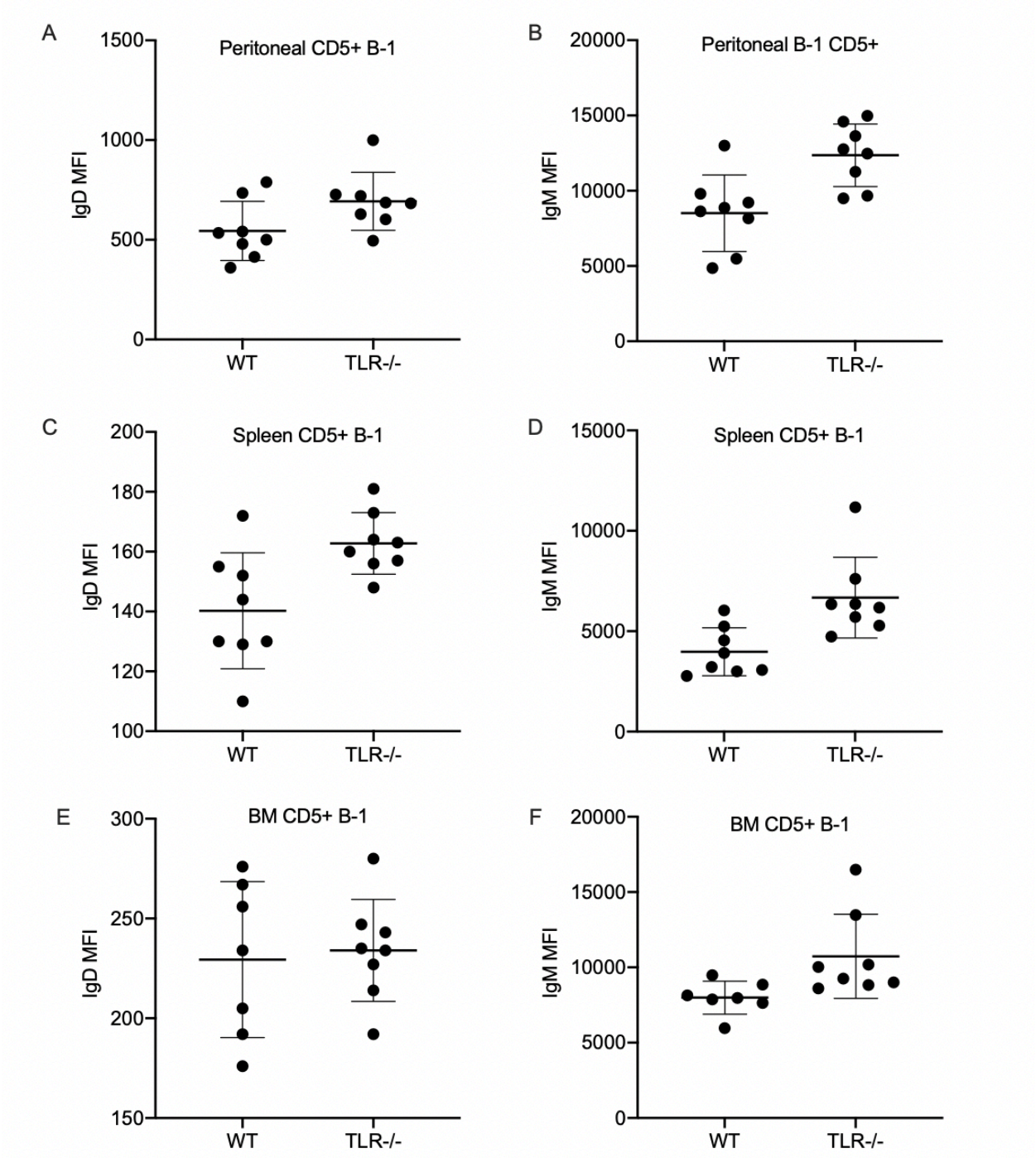
A
Peritoneal CD5+ B-1
IgD MFI
1500
1000
500
0
WT
TLR-/-
B
Peritoneal B-1 CD5+
IgM MFI
20000
15000
10000
5000
0
WT
TLR-/-
C
Spleen CD5+ B-1
IgD MFI
200
180
160
140
120
100
WT
TLR-/-
D
Spleen CD5+ B-1
IgM MFI
15000
10000
5000
0
WT
TLR-/-
E
BM CD5+ B-1
IgD MFI
300
250
200
150
WT
TLR-/-
F
BM CD5+ B-1
IgM MFI
20000
15000
10000
5000
0
WT
TLR-/-

Figure 4.4: Surface Ig Expresion by CD5+ B-1 cells is contrained by steady state TLR signaling *in vivo*.

A) Mean IgD MFI ± SD of unstimulated *ex vivo* peritoneal CD5+ B-1 from control and TLR-/-, n=8 mice/group **B**) Mean IgM MFI ± SD of unstimulated *ex vivo* peritoneal CD5+ B-1 from control and TLR-/-, n=8 mice/group **C**) Mean IgD MFI ± SD of unstimulated *ex vivo* splenic CD5+ B-1 from control and TLR-/-, n=8 mice/group **D**) Mean IgM MFI ± SD of unstimulated *ex vivo* splenic CD5+ B-1 from control and TLR-/-, n=8 mice/group **E**) Mean IgD MFI ± SD of unstimulated *ex vivo* bone marrow CD5+ B-1 from control and TLR-/-, n=7-8 mice/group **B**) Mean IgM MFI ± SD of unstimulated *ex vivo* bone marrow CD5+ B-1 from control and TLR-/-, n=7-8 mice/group

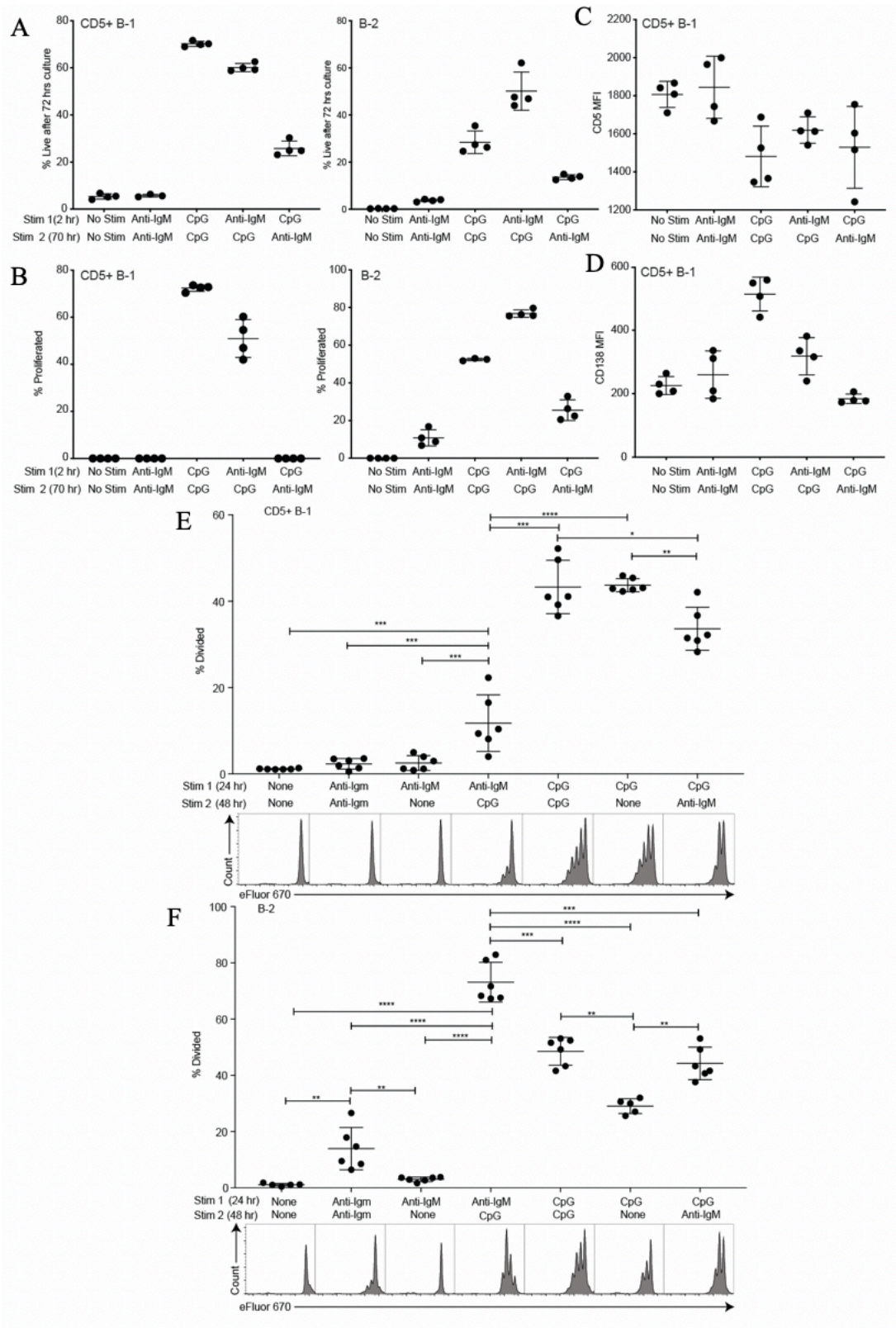
A
CD5+ B-1
% Live after 72 hrs culture
B-2
% Live after 72 hrs culture
Stim 1(2 hr) No Stim Anti-IgM CpG Anti-IgM CpG
Stim 2 (70 hr) No Stim Anti-IgM CpG CpG Anti-IgM
C
CD5+ B-1
CD5 MFI
B
CD5+ B-1
% Proliferated
B-2
% Proliferated
D
CD5+ B-1
CD138 MFI
E
CD5+ B-1
% Divided
Stim 1 (24 hr) None Anti-Igm Anti-IgM Anti-IgM CpG CpG CpG
Stim 2 (48 hr) None Anti-Igm None CpG CpG None Anti-IgM
Count
eFluor 670
F
B-2
% Divided
Stim 1 (24 hr) None Anti-Igm Anti-IgM Anti-IgM CpG CpG CpG
Stim 2 (48 hr) None Anti-Igm None CpG CpG None Anti-IgM
Count
eFluor 670

Figure 4.5: BCR priming inhibits TLR mediated responses in B-1 cells

A)Peritoneal cavity CD19^{hi}CD23- CD43+ CD5+ B-1 and splenic CD19+ CD23+ CD43 CD5- B-2 cells from BALB/C mice were labeled with eFluor 670, rested for 2 hr and then cultured for 2 with the indicated stimulus 1 (no stim, anti-IgM(10 μg/ml) or CpG ODN7909 (5 μg/ml), washed and recultured for 70 hr with stimulus 2 (no stim, anti-IgM anti-IgM(10 μg/ml) or CpG ODN7909 (5 μg/ml) prior to analysis for % live and **B)** efluor 670 staining. B-1 cells were assessed for **C)** CD5 and **D)** CD138 expression. **E)** Peritoneal B-1 and **F)** splenic B-2 cell from BALB/C mice were labeled in **(A)** and cultured with the indicated stimulus 1 (none, anti-IgM(10 μg/ml) or CpG ODN7909 (5 μg/ml), washed and recultured for 48 hr with stimulus 2 (none, anti-IgM anti-IgM(10 μg/ml) or CpG ODN7909 (5 μg/ml) prior to analysis for efluor 670 staining. Top panels show representative FACS histogram plots and bottom panels shows the % cells in each culture having undergone at least one cell division. Each symbol represents results from one culture well, horizontal line indicates mean for the group. Results are compiled from two independent experiments. Statistical analysis was done by one-way ANOVA, followed by an unpaired Student's t test with Holm-Sidak correction for multiple comparisons (*$p<0.05$, **$p<0.01$, ***$p<0.001$, ****$p<0.0001$).

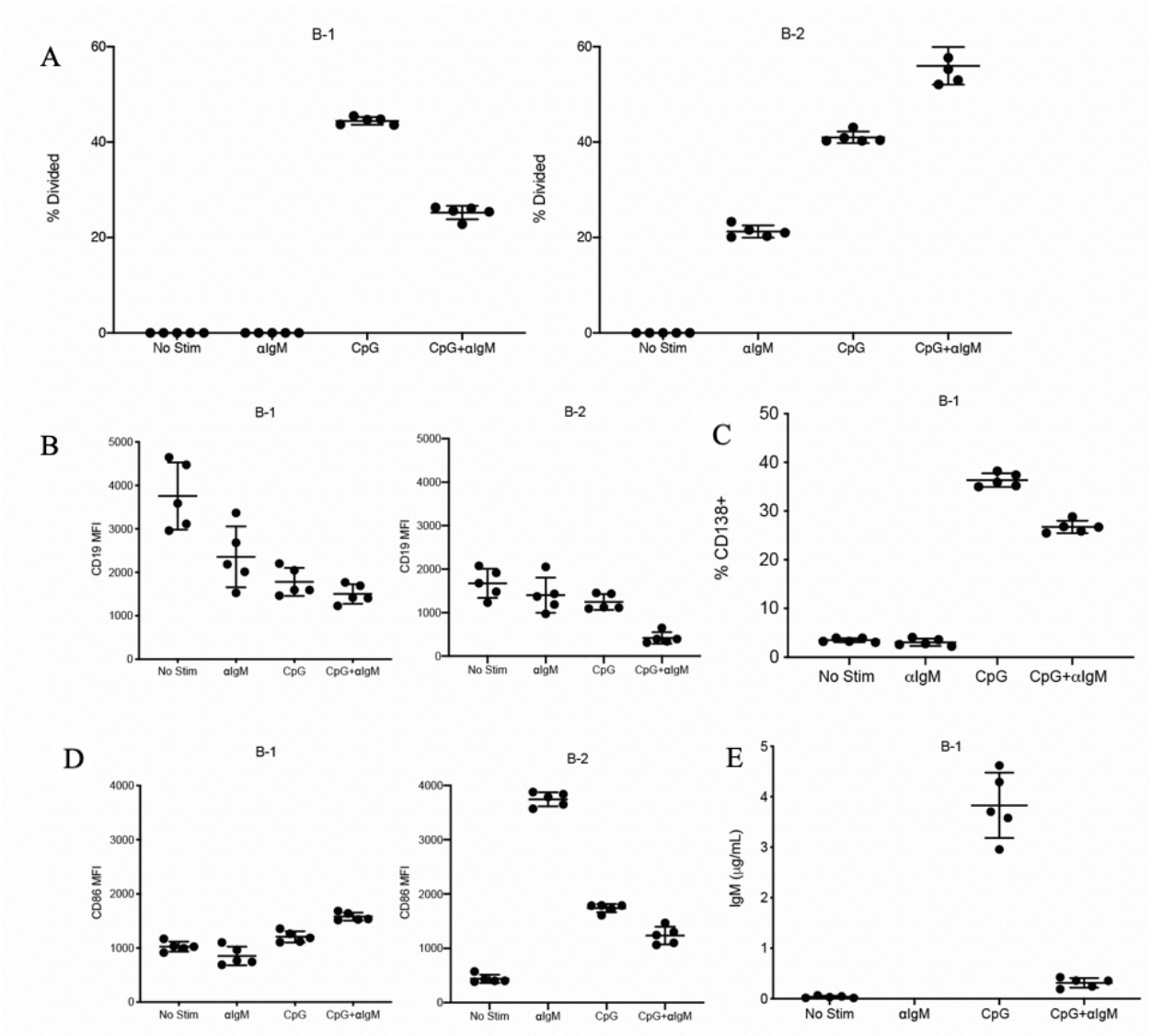
A
B-1
B-2
% Divided
No Stim
αIgM
CpG
CpG+αIgM
B
CD19 MFI
C
% CD138+
D
CD86 MFI
E
IgM (μg/mL)

Figure 4.6: Co-stimulation of BCR and TLR dampens activation and proliferation of B-1 cells

A) Peritoneal B-1 and splenic B-2 cell from BALB/C mice were labeled as in **(4A)** and cultured with the indicated stimulus for 72 hrs (no stim, αIgM(anti-IgM 10 μg/ml), CpG (ODN7909 5 μg/ml), or α IgM(10 μg/ml) & CpG (ODN7909 5 μg/ml) prior to analysis for efluor 670 staining. B-1 and B-2 cells were assessed for **B)** CD19 and **D)** CD86 expression. B-1 cells were assessed for **D)** expression of CD138 and **E)** IgM secretion in the supernatants of the cultures. Each symbol represents results from one culture well, horizontal line indicates mean for the group. Results are compiled from two independent experiments.

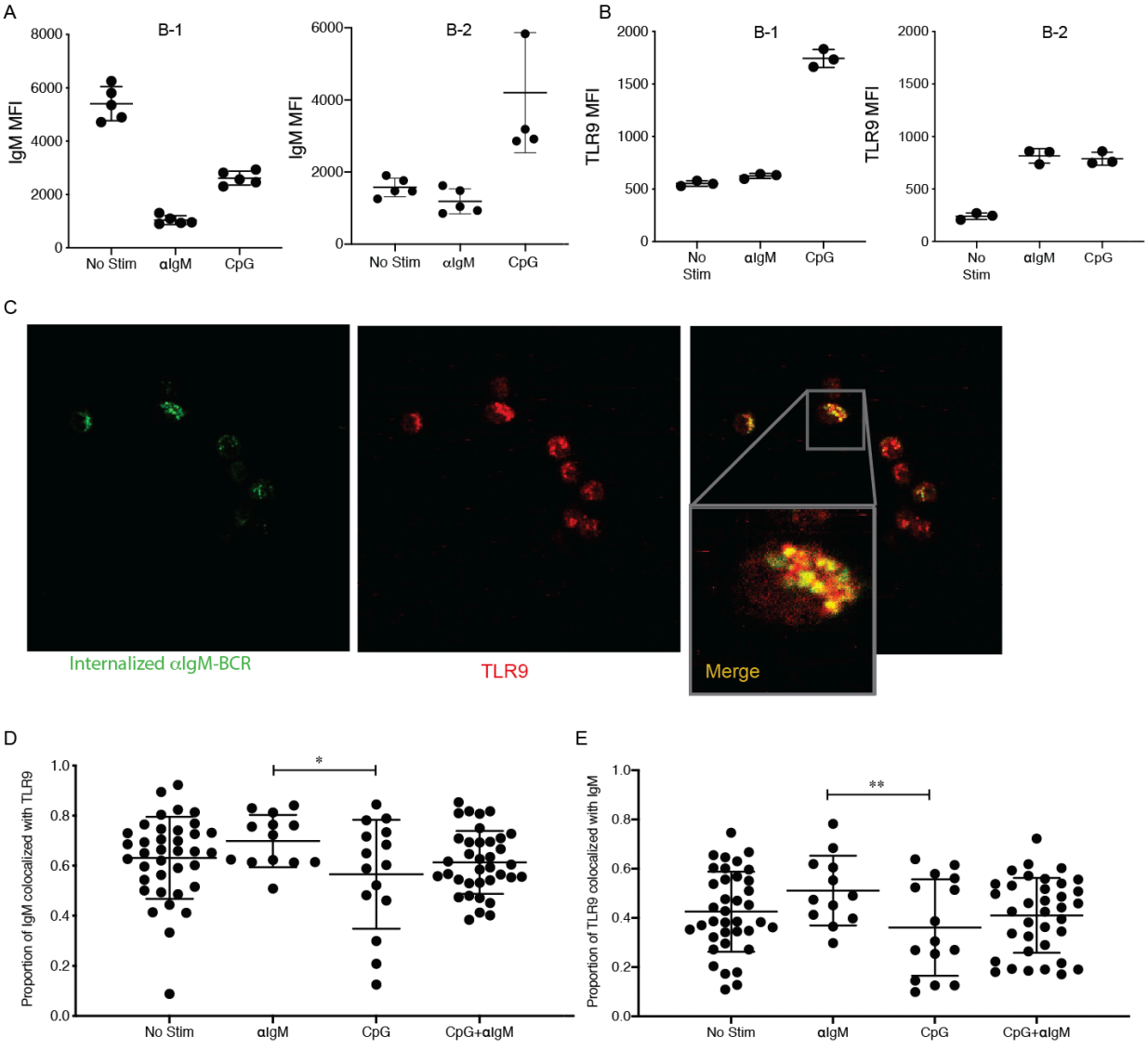
A
B-1
IgM MFI
8000
6000
4000
2000
0
No Stim
αIgM
CpG
B-2
6000
4000
2000
0
B
TLR9 MFI
2000
1500
1000
500
0
C
Internalized αIgM-BCR
TLR9
Merge
D
Proportion of IgM colocalized with TLR9
1.0
0.8
0.6
0.4
0.2
0.0
*
CpG+αIgM
E
Proportion of TLR9 colocalized with IgM
**

Figure 4.7: BCR stimulation enhances TLR/BCR colocalization, but BCR and TLR expression in B-1 cells is not driven by reciprocal stimulation

Peritoneal B-1 and splenic B-2 cell from BALB/c mice were cultured with the indicated stimulus for 24 hrs (no stim, αIgM(anti-IgM 10 μg/ml), CpG (ODN7909 5 μg/ml), prior to intracellular staining for **A)**IgM-BCR and **B)** TLR9. **C)** Peritoneal B-1 cells from BALB/c mice were cultured for 30 minutes with αIgM-FITC for 30 min at 37C. Cells were then fixed and permeabilized and stained for TLR9, cells were mounted and imaged using a Leica TCS SP8 STED 3X confocal microscope. **D)** Peritoneal B-1 and splenic B-2 cell from BALB/C mice were cultured with the indicated stimulus for 24 hrs (no stim, αIgM(anti-IgM 10 μg/ml), CpG (ODN7909 5 μg/ml), or α IgM(10 μg/ml) & CpG (ODN7909 5 μg/ml). Cells were then fixed and permeabilized and stained for IgM BCR and TLR9, cells were mounted and imaged using a Leica TCS SP8 STED 3X confocal microscope. Colocalization of IgM with TLR and TLR with IgM were then assessed on a cell-by-cell basis. Each dot represents an individual cell, n=11-37 cells per condition.

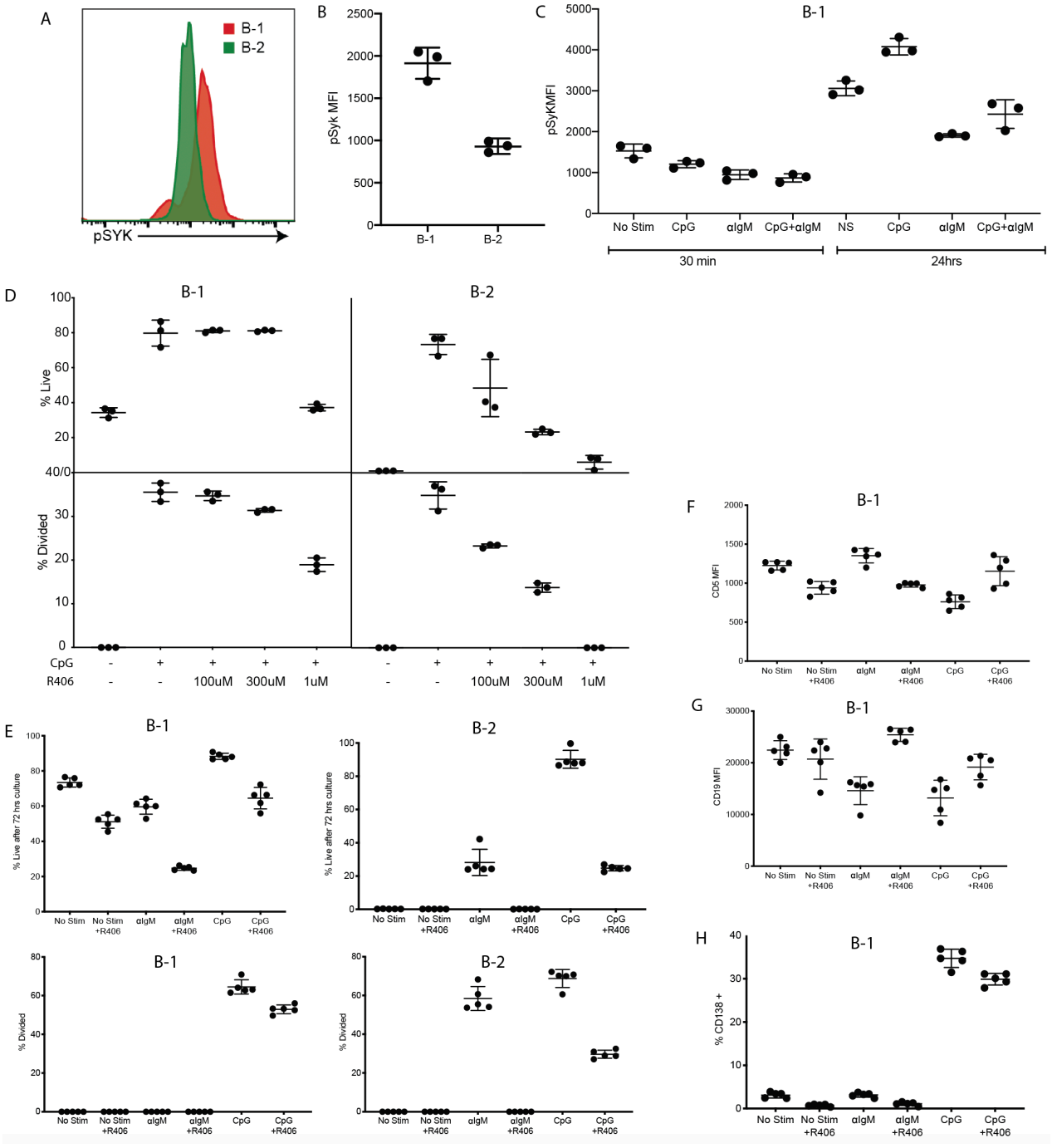
A
B-1
B-2
pSYK
B
pSyk MFI
B-1
B-2
C
B-1
pSykMFI
No Stim
CpG
αIgM
CpG+αIgM
NS
CpG
αIgM
CpG+αIgM
30 min
24hrs
D
B-1
B-2
% Live
% Divided
CpG
R406
100uM
300uM
1uM
E
B-1
B-2
% Live after 72 hrs culture
% Divided
No Stim
No Stim +R406
αIgM
αIgM +R406
CpG
CpG +R406
F
B-1
CD5 MFI
G
B-1
CD19 MFI
H
B-1
% CD138 +

Figure 4.8: Syk signaling is required for optimal B-1 cell responses to TLR stimulation

A) Representative histogram of phosphorylated Syk expression by phosphoflow *ex vivo* in peritoneal B-1 and splenic B-2 cell from BALB/c mice as described in **(Fig. 4A). B)** Mean pSyk MFI ± SD of unstimulated *ex vivo* peritoneal B-1 and splenic B-2 cell. **C)** Mean pSyk MFI ± SD of peritoneal B-1 from BALB/c mice as described in (**Fig. 4A)** cultured with the indicated stimulus for 30 min or 24 hrs (no stim, αIgM (anti-IgM 10 μg/ml), CpG (ODN7909 5 μg/ml), or α IgM(10 μg/ml) & CpG (ODN7909 5 μg/ml). **D)** Peritoneal B-1 and splenic B-2 cell from BALB/C mice were labeled as in **(Fig. 4A)** and cultured with no stimulus, CpG (ODN7909 5 μg/ml) or CpG with 100nm, 300nm or 1μm of Syk inhibitor, R406, for 72 hrs prior to analysis for percent live and efluor 670 staining. **E)** Peritoneal B-1 and splenic B-2 cell from BALB/C mice were labeled as in **(Fig. 4A)** and cultured with the indicated stimulus(no stim, αIgM(anti-IgM 10 μg/ml) or CpG (ODN7909 5 μg/ml) ± 1μm R406 for 72 hrs72 hrs prior to analysis for percent live and efluor 670 staining. B-1 cultures in **E)** we also assessed for **F)** CD5, **G)** CD19 and **H)** CD138 expression. Each symbol represents results from one culture well, horizontal line indicates mean for the group.